

Universiteit
Leiden
The Netherlands

The unique procoagulant adaptations of pseudonaja textilis venom factor V and factor X

Schreuder, M.

Citation
Schreuder, M. (2022, September 22). *The unique procoagulant adaptations of pseudonaja textilis venom factor V and factor X*. Retrieved from https://hdl.handle.net/1887/3464432

Version:	Publisher's Version
License:	Licence agreement concerning inclusion of doctoral thesis in the Institutional Repository of the University of Leiden
Downloaded from:	https://hdl.handle.net/1887/3464432

Note: To cite this publication please use the final published version (if applicable).

The Unique Procoagulant Adaptations of Pseudonaja Textilis Venom Factor V and Factor X

Mark Schreuder

The Unique Procoagulant Adaptations of Pseudonaja Textilis Venom Factor V and Factor X

The research described in this thesis was financially supported by the Bayer Hemophilia Awards Program (Special Project Award) and Landsteiner Foundation for Blood Transfusion (LSBR, grant. no. 1451).

Financial support by the Trombosestichting Nederland and VarmX for the publication of this thesis is gratefully acknowledged.

Provided by thesis specialist Ridderprint, ridderprint.nl
Printing: Ridderprint
Layout and design by: Jesse Haaksman, persoonlijkproefschrift.nl
Cover design: Mark Schreuder

The Unique Procoagulant Adaptations of Pseudonaja Textilis Venom Factor V and Factor X

Proefschrift

ter verkrijging van
de graad van doctor aan de Universiteit Leiden,
op gezag van rector magnificus prof.dr.ir. H. Bijl,
volgens besluit van het college voor promoties
te verdedigen op donderdag 22 september 2022
klokke 15.00 uur

door

Mark Schreuder
geboren te Amersfoort
in 1990

Promotor

Prof. dr. P.H. Reitsma

Copromotor

Dr. M.H.A. Bos

Leden promotiecommissie

Prof. dr. H.C.J. Eikenboom	
Prof. dr. K. Vanhoorelbeke	Katholieke Universiteit Leuven
Prof. dr. T. M. Hackeng	Universiteit Maastricht
Dr. C. van 't Veer	Universiteit van Amsterdam

Table of Contents

Chapter 1	General Introduction and Thesis Outline	7
Chapter 2	Blood Coagulation Factor Va's Key Interactive Residues and Regions for Prothrombinase Assembly and Prothrombin Binding	19
Chapter 3	ptFVa (Pseudonaja Textilis Venom-Derived Factor Va) Retains Structural Integrity Following Proteolysis by Activated Protein C	51
Chapter 4	Pseudonaja textilis Venom Factor Va Circumvents Natural Regulatory Mechanisms via a Unique A2 Domain Region	83
Chapter 5	Evolutionary Adaptations in Pseudonaja textilis Venom FX Induce Zymogen Activity and Resistance to the Intrinsic Tenase Complex	117
Chapter 6	Reversal Agents for the Direct Factor Xa Inhibitors: Biochemical Mechanisms of Current and Newly Emerging Therapies	145
Chapter 7	F174-Substituted Human Factor X as Bypassing Agent for the Direct FXa Inhibitors	173
Chapter 8	General Discussion and Summary	209
Chapter 9	Nederlandse Samenvattingen	237
	Nederlandse Samenvatting voor Leken	244
Appendix	Curriculum Vitae	250
	Scientific Publications	251
	Dankwoord	253

Chapter 1

General Introduction and Outline of the Thesis





Hemostasis

The cardiovascular system is responsible for the continuous flow of blood that delivers essential nutrients and oxygen to cells throughout the body and transports metabolic degradation products away from distal tissues. Upon vascular damage, a process known as blood coagulation is initiated, which acts to form a hemostatic plug at the site of injury to arrest bleeding and maintain hemostasis. This process consists of two main components known as primary and secondary hemostasis. In primary hemostasis, the loss of blood is initially limited by the contraction of smooth muscle cells underlining the vascular endothelium, resulting in a reduction of blood flow. Subsequently, platelets are activated and aggregate at the site of injury, forming a physical barrier known as the primary platelet plug[1]. Secondary hemostasis serves to stabilize and strengthen the blood clot by forming an insoluble mesh of fibrin in and around the platelet plug[2]. The deposition of fibrin is the result of a series of enzymatic reactions that take place on the surface of activated platelets and endothelial cells via a 'cascade' principle **(Figure 1)**. This so-called coagulation cascade traditionally consists of two different initiation pathways that both culminate into the common pathway with the activation of factor X (FX), the generation of thrombin, and ultimately the formation of fibrin.

Coagulation Cascade

In the coagulation cascade, the intrinsic pathway is triggered by negatively charged surfaces, such as kaolin or glass[3]. This results in the activation of factor XII (FXII), prekallikrein, and high molecular weight kininogen. Upon the activation of FXII, the coagulation proteins factor XI (FXI), factor IX (FIX), and FX are converted to their activated state via a series of concerted proteolytic reactions.

The extrinsic pathway starts upon the exposure of subendothelial tissue factor (TF) to blood and the subsequent binding of circulating factor VII(a) (FVII(a)) to TF. The resulting FVIIa-TF complex immediately initiates the common pathway by converting factor X to factor Xa (FXa). In addition, the TF-FVIIa complex activates part of the intrinsic pathway by proteolytic conversion of FIX to factor IXa (FIXa). The extrinsic pathway is activated by external trauma and is therefore considered as the most common trigger of the coagulation cascade.

Both the intrinsic and extrinsic pathways converge into the common pathway with the generation of FXa. FXa assembles into the prothrombinase complex by binding to its cofactor factor Va (FVa). The spatiotemporal assembly of the prothrombinase complex occurs exclusively on the surface of anionic membranes in the presence of calcium

ions. This complex rapidly converts prothrombin into the active protease thrombin, a key step in the formation of a blood clot. Subsequently, thrombin converts soluble fibrinogen into the insoluble fibrin which spontaneously polymerizes into long fibrin strands. In addition, thrombin initiates several positive feedback loops by activating FXI and the cofactors FVIII and FV in order to generate sufficient amounts of fibrin. The fibrin strands are cross-linked by factor XIIIa (FXIIIa) to create a strong and dense fibrin network resulting in the formation of a stable blood clot.

Coagulation Factor V

Coagulation FV circulates in plasma as a large single-chain procofactor of ~330 kDa, comprising an A1-A2-B-A3-C1-C2 domain structure **(Figure 2A)**. The B domain contains a basic and a complementary acidic region that interact with each other, thereby creating an autoinhibitory conformation that is assumed to prevent FXa binding[4,5]. Factor V is mainly synthesized by the liver and excreted in the plasma. The majority of the total FV pool circulates in plasma, whereas ~20% is stored in platelet α-granules and is secreted upon platelet activation[6].

The activation of factor V is facilitated by FXa and meizothrombin in the initiation phase and subsequently by thrombin in the propagation phase of coagulation[7-10]. Sequential cleavage at B domain residues Arg709, Arg1018, and Arg1545 results in the dissociation of the B domain and the generation of a heavy (A1-A2) and light (A3-C1-C2) chain that are non-covalently linked by divalent metal ions **(Figure 2A)**[11,12]. Once partially or fully activated, FVa is able to serve as a cofactor for FXa through assembly into the prothrombinase complex. This complex increases the catalytic rate of prothrombin activation by five-orders of magnitude relative to membrane-bound FXa[13], illustrating the physiological relevance of the prothrombinase complex in prothrombin activation.

Apart from its procoagulant function, thrombin fullfills an anticoagulant role by converting protein C to the protease activated protein C (APC) in the presence of thrombomodulin and the endothelial protein C receptor[14]. Activated protein C plays a crucial role in the downregulation of the procoagulant response by selective proteolysis and subsequent inactivation of FVa. It exerts this function by cleaving FVa at the A2 domain residues Arg306, Arg506, and Arg679, resulting in the dissociation of the A2 domain[15,16]. The kinetically rapid cleavage at Arg506 results in a partially active FVa intermediate, which is fully inactivated by the relatively slow proteolysis at Arg306[17]. The functional relevance of the Arg679 cleavage is currently not fully understood. The APC-induced inactivation of FVa is further stimulated by the nonenzymatic cofactor protein S, which specifically accelerates the cleavage at Arg306[18].

Coagulation Factor X

Coagulation FX is a vitamin-K dependent serine protease and one of the central components of the coagulation cascade **(Figure 2B)**. Factor X is composed of a heavy and light chain that are covalently linked via a disulfide bond. The light chain comprises a γ-carboxyglutamic acid-containing domain that is responsible for anionic phospholipid binding and two epidermal growth factor-like domains that have been implicated in macromolecular interactions[2,19-22]. The heavy chain consists of an activation peptide that prevents unwanted catalytic activity and the serine protease domain that comprises the active site which is hallmarked by the catalytic triad residues His^{95}, Asp^{102}, and Ser^{195} (chymotrypsinogen numbering).

Factor X circulates in plasma in a zymogen form and is converted into FXa **(Figure 2B)** by the intrinsic (factor VIIIa (FVIIIa) and FIXa) or extrinsic (TF and FVIIa) tenase complexes via proteolytic removal of the activation peptide upon cleavage of the highly conserved Arg^{15}-Ile^{16} scissile bond. The transition to a fully active protease requires conformational changes in the serine protease domain that realign the active site and exosite regions[23,24]. These conformational changes are induced when the newly formed heavy chain N-terminus (Ile^{16}) engages with the active site residue Asp^{194} to form a Ile^{16}-Asp^{194} salt bridge[23,24]. The matured FXa comprises the essential S1 and S4 subpockets which determine the substrate specificity[24,25].

The central negative regulators of FXa are the active site inhibitors tissue factor pathway inhibitor (TFPI) and antithrombin. TFPI is an anticoagulant protein that downregulates the early phases of the procoagulant response. Several alternatively spliced isoforms of TFPI are expressed; however, each splice variants comprises the Kunitz 1 and 2 domains. The Kunitz-1 domain of TFPI inhibits FVIIa that is complexed with TF, and the Kunitz-2 domain is responsible for FXa inhibition[26,27]. Since TFPI is a weak inhibitor of TF–FVIIa in the absence of FXa, TFPI is often described as a FXa-dependent inhibitor of TF–FVIIa. As a consequence, TFPI appears to simultaneously inhibit FXa and TF–FVIIa immediately after the activation of FX by the TF–FVIIa complex[28]. The other physiological relevant inhibitor of FXa is the serine protease inhibitor antithrombin. The inhibitory effect of antithrombin is relatively low but can be stimulated up to four-orders of magnitude in the presence of heparin. Antithrombin inhibits FXa via a substrate recognition sequence within its exposed reactive center loop[29,30]. This sequence acts as a bait region that is cleaved by FXa resulting in a covalent antithrombin-FXa complex[29,30]. Subsequently, this complex undergoes a major conformational change that stably traps and fully inactivates FXa[30,31].

Inhibition of Factor Xa and Thrombosis

A disruption of the hemostatic system can result in life-threatening bleeding disorders, such as hemophilia or pathological thrombosis. Because of its central role in the coagulation cascade, FXa has been a major drug target for antithrombotic therapy. Traditionally, oral vitamin K antagonists were used for the prevention and treatment of thrombosis, which effectively inhibit the hemostatic vitamin K-dependent proteases. However, their narrow therapeutic range and variable response to dosing provide several disadvantages that significantly affect their efficacy. In the past decades, the direct oral anticoagulants (DOACs) have been developed as an alternative anticoagulant treatment option for thrombosis-related disorders. The DOACs are small molecules that reversibly engage the active site of the key proteases FXa (apixaban, rivaroxaban, edoxaban, and betrixaban)[32-35] or thrombin (dabigatran)[36]. These drugs are characterized by a superior pharmacodynamic profile relative to the vitamin K antagonists, and as such these drugs are considered as the preferred anticoagulant therapy[37]. Currently, the DOACs have been clinically approved for the prevention of stroke in atrial fibrillation patients, the treatment of thromboembolism, and thromboprophylaxis following orthopedic surgery[38-42].

Pseudonaja textilis Venom Factor V and Factor X

The procoagulant venom of the Australian Elapid snakes comprises a powerful prothrombin-activating enzyme complex consisting of FV- and FX-like proteins that are specifically expressed in the venom gland[43-45]. These coagulation proteins have evolved into potent toxins due to some remarkable gain-of-function adaptations that enable this prothrombinase-like complex to initiate coagulation in an uncontrolled manner[46-48]. In contrast to human FV, the venom FV homolog from *Pseudonaja textilis* (v-ptFV) was found to be a constitutively active cofactor for the venom-derived FXa (v-ptFXa)[47]. Furthermore, both v-ptFV and v-ptFXa bypass the normal requirement of membrane binding by forming a high affinity complex in the absence of anionic phospholipids[47,49]. In addition, v-ptFV and v-ptFXa are functionally resistant or display a reduced sensitivity towards their natural inhibitors APC or antithrombin, respectively[45-47,49].

Outline of this Thesis

In this thesis, we focus on the unique evolutionary adaptations of the *P. textilis* venom-derived proteins v-ptFV and v-ptFX. By using biochemical approaches, we asssess the structure-function relationships of several uniquely modified structural elements.

Secondly, we address current and newly emerging reversal agents for FXa-inhibiting DOACs as therapeutic option for life-threatening bleeding complications.

Identification of the binding sites responsible for protein-protein interactions provides fundamental information on functional important regions and allows for a better understanding of the biology of the specific proteins involved. In **chapter 2**, we review the current literature on the interactive residues and regions of FVa that are essential for prothrombinase assembly and prothrombin binding, forming the basis for further studies on functionally important regions in FVa.

The functional APC resistance of v-ptFV was studied in **chapter 3**. Since v-ptFV does not comprise an Arg306-like cleavage site that is essential for mammalian FV inactivation, we hypothesized that introduction of the human Arg306 region would inactivate v-ptFV upon APC-mediated proteolysis.

Sequence analysis has shown that ptFV comprises a significantly extended A2 domain C-terminus (A2T) compared to other FV species. In human FV, this structural element has been implicated in the formation of the prothrombinase complex and the engagement of prothrombin. In **chapter 4** we examined the functional role of the extended A2T in ptFVa.

In **chapter 5,** we studied the functional relevance of a particular modification in v-ptFX. The activation peptide of v-ptFX is significantly shortened compared to the FX activation peptide of other known organisms. We hypothesize that this venom-derived activation peptide plays an important role in the unique procoagulant characteristics of v-ptFX.

The additional focus of this thesis is on the reversal agents for the direct FXa inhibitors. Bleeding complications associated with DOAC-use remain the main concern in clinical practice. Patients presenting with major bleeds may require rapid reversal of the anticoagulant DOAC activity. **Chapter 6** summarizes the antidotes and bypassing agents that are currently approved or in (pre)clinical development.

In **chapter 7** we characterized a novel FX-based bypassing agent for the direct FXa inhibitors. In this study, several FX variants were generated by substituting a single residue in the FX S4 subsite. The FX variants were characterized and tested for their ability to restore thrombin generation in the presence of the direct FXa inhibitors.

Finally, **chapter 8** provides a general summary and discussion of this thesis.

Figures

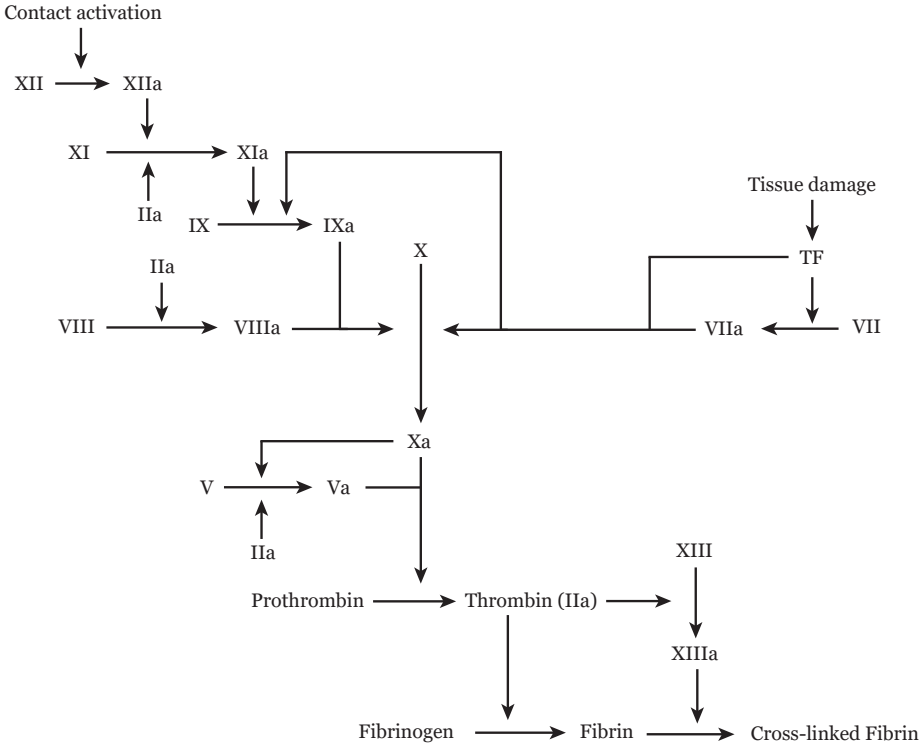


Figure 1. Schematic representation of the procoagulant reactions in the coagulation cascade. Coagulation is triggered by contact activation or tissue injury and activates the intrinsic or extrinsic pathway, respectively. The activation of factor Xa initiates the common pathway and ultimately results in the formation of a fibrin network. TF indicates tissue factor, and the blood coagulation factors are indicated by their Roman numerals.

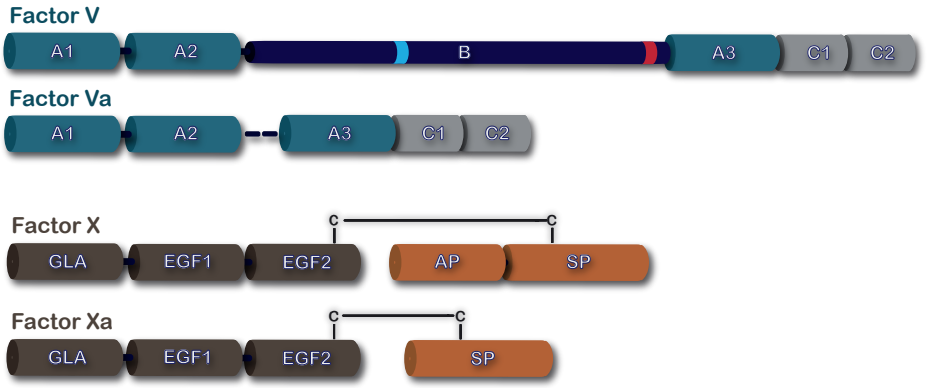


Figure 2. Schematic representation of precursor and activated forms of human coagulation factor V and factor X. (A) Factor V is composed of an A1-A2-B-A3-C1-C2 domain structure in which the A domains are involved in macromolecular interactions and the C domains interact with the lipid membrane layer. The B domain comprises the basic (blue) and acidic (red) regions that keep factor V in a precursor state. Upon activation of factor V, the B domain is proteolytically removed thereby generating factor Va. **(B)** Factor X comprises a lipid-binding γ-carboxyglutamic acid (GLA) domain, two epidermal growth factor (EGF) domains, an activation peptide (AP), and the serine protease (SP) domain. Factor X is converted to factor Xa upon cleavage and dissociation of the activation peptide.

References

1 Broos, K., Feys, H. B., De Meyer, S. F., Vanhoorelbeke, K. & Deckmyn, H. Platelets at work in primary hemostasis. *Blood Rev* **25**, 155-167, doi:10.1016/j.blre.2011.03.002 (2011).

2 Bos, M. H. A., Van 't Veer, C. & Reitsma, P. H. Molecular biology and biochemistry of the coagulation factors and pathways of hemostasis. *Williams Hematology* **9th edn.**, 1915–1948 (2016).

3 Wiggins, R. C., Bouma, B. N., Cochrane, C. G. & Griffin, J. H. Role of high-molecular-weight kininogen in surface-binding and activation of coagulation Factor XI and prekallikrein. *Proc Natl Acad Sci U S A* **74**, 4636-4640, doi:10.1073/pnas.74.10.4636 (1977).

4 Bos, M. H. & Camire, R. M. A bipartite autoinhibitory region within the B-domain suppresses function in factor V. *J Biol Chem* **287**, 26342-26351, doi:10.1074/jbc.M112.377168 (2012).

5 Bunce, M. W., Bos, M. H., Krishnaswamy, S. & Camire, R. M. Restoring the procofactor state of factor Va-like variants by complementation with B-domain peptides. *J Biol Chem* **288**, 30151-30160, doi:10.1074/jbc.M113.506840 (2013).

6 Tracy, P. B., Eide, L. L., Bowie, E. J. & Mann, K. G. Radioimmunoassay of factor V in human plasma and platelets. *Blood* **60**, 59-63 (1982).

7 Foster, W. B., Nesheim, M. E. & Mann, K. G. The factor Xa-catalyzed activation of factor V. *J Biol Chem* **258**, 13970-13977 (1983).

8 Monkovic, D. D. & Tracy, P. B. Activation of human factor V by factor Xa and thrombin. *Biochemistry* **29**, 1118-1128, doi:10.1021/bi00457a004 (1990).

9 Tans, G. *et al.* Activation of human factor V by meizothrombin. *J Biol Chem* **269**, 15969-15972 (1994).

10 Schuijt, T. J. *et al.* Factor Xa activation of factor V is of paramount importance in initiating the coagulation system: lessons from a tick salivary protein. *Circulation* **128**, 254-266, doi:10.1161/CIRCULATIONAHA.113.003191 (2013).

11 Dahlback, B. Human coagluation factor V purification and thrombin-catalyzed activation. *J Clin Invest* **66**, 583-591, doi:10.1172/JCI109890 (1980).

12 Nesheim, M. E. & Mann, K. G. Thrombin-catalyzed activation of single chain bovine factor V. *J Biol Chem* **254**, 1326-1334 (1979).

13 Mann, K. G., Nesheim, M. E., Church, W. R., Haley, P. & Krishnaswamy, S. Surface-dependent reactions of the vitamin K-dependent enzyme complexes. *Blood* **76**, 1-16 (1990).

14 Dahlback, B. & Villoutreix, B. O. The anticoagulant protein C pathway. *FEBS Lett* **579**, 3310-3316, doi:10.1016/j.febslet.2005.03.001 (2005).

15 Kalafatis, M., Rand, M. D. & Mann, K. G. The mechanism of inactivation of human factor V and human factor Va by activated protein C. *J Biol Chem* **269**, 31869-31880 (1994).

16 Mann, K. G., Hockin, M. F., Begin, K. J. & Kalafatis, M. Activated protein C cleavage of factor Va leads to dissociation of the A2 domain. *J Biol Chem* **272**, 20678-20683 (1997).

17 Kalafatis, M. & Mann, K. G. Role of the membrane in the inactivation of factor Va by activated protein C. *J Biol Chem* **268**, 27246-27257 (1993).

18 Rosing, J. *et al.* Effects of protein S and factor Xa on peptide bond cleavages during inactivation of factor Va and factor VaR506Q by activated protein C. *J Biol Chem* **270**, 27852-27858 (1995).

19 Valcarce, C., Holmgren, A. & Stenflo, J. Calcium-dependent interaction between gamma-carboxyglutamic acid-containing and N-terminal epidermal growth factor-like modules in factor X. *J Biol Chem* **269**, 26011-26016 (1994).

20 Hertzberg, M. S., Ben-Tal, O., Furie, B. & Furie, B. C. Construction, expression, and characterization of a chimera of factor IX and factor X. The role of the second epidermal growth factor domain and serine protease domain in factor Va binding. *J Biol Chem* **267**, 14759-14766 (1992).

21 Muller, M. P., Wang, Y., Morrissey, J. H. & Tajkhorshid, E. Lipid specificity of the membrane binding domain of coagulation factor X. *J Thromb Haemost* **15**, 2005-2016, doi:10.1111/jth.13788 (2017).
22 Huang, M. *et al.* Structural basis of membrane binding by Gla domains of vitamin K-dependent proteins. *Nat Struct Biol* **10**, 751-756, doi:10.1038/nsb971 (2003).
23 Huber, R. & Bode, W. Structural Basis of the Activation and Action of Trypsin. *Accounts of Chemical Research* **11**, 114-122 (1978).
24 Hedstrom, L. Serine protease mechanism and specificity. *Chem Rev* **102**, 4501-4524 (2002).
25 Hopfner, K. P. *et al.* Converting blood coagulation factor IXa into factor Xa: dramatic increase in amidolytic activity identifies important active site determinants. *EMBO J* **16**, 6626-6635, doi:10.1093/emboj/16.22.6626 (1997).
26 Mast, A. E. Tissue Factor Pathway Inhibitor: Multiple Anticoagulant Activities for a Single Protein. *Arterioscler Thromb Vasc Biol* **36**, 9-14, doi:10.1161/ATVBAHA.115.305996 (2016).
27 Broze, G. J., Jr. & Girard, T. J. Tissue factor pathway inhibitor: structure-function. *Front Biosci (Landmark Ed)* **17**, 262-280, doi:10.2741/3926 (2012).
28 Baugh, R. J., Broze, G. J., Jr. & Krishnaswamy, S. Regulation of extrinsic pathway factor Xa formation by tissue factor pathway inhibitor. *J Biol Chem* **273**, 4378-4386, doi:10.1074/jbc.273.8.4378 (1998).
29 Johnson, D. J., Li, W., Adams, T. E. & Huntington, J. A. Antithrombin-S195A factor Xa-heparin structure reveals the allosteric mechanism of antithrombin activation. *EMBO J* **25**, 2029-2037, doi:10.1038/sj.emboj.7601089 (2006).
30 Olson, S. T., Richard, B., Izaguirre, G., Schedin-Weiss, S. & Gettins, P. G. Molecular mechanisms of antithrombin-heparin regulation of blood clotting proteinases. A paradigm for understanding proteinase regulation by serpin family protein proteinase inhibitors. *Biochimie* **92**, 1587-1596, doi:10.1016/j.biochi.2010.05.011 (2010).
31 Huntington, J. A., Read, R. J. & Carrell, R. W. Structure of a serpin-protease complex shows inhibition by deformation. *Nature* **407**, 923-926, doi:10.1038/35038119 (2000).
32 Zhang, P. *et al.* Discovery of betrixaban (PRT054021), N-(5-chloropyridin-2-yl)-2-(4-(N,N-dimethylcarbamimidoyl)benzamido)-5-methoxybenz amide, a highly potent, selective, and orally efficacious factor Xa inhibitor. *Bioorg Med Chem Lett* **19**, 2179-2185, doi:10.1016/j.bmcl.2009.02.111 (2009).
33 Furugohri, T. *et al.* DU-176b, a potent and orally active factor Xa inhibitor: in vitro and in vivo pharmacological profiles. *J Thromb Haemost* **6**, 1542-1549, doi:10.1111/j.1538-7836.2008.03064.x (2008).
34 Roehrig, S. *et al.* Discovery of the novel antithrombotic agent 5-chloro-N-({(5S)-2-oxo-3-[4-(3-oxomorpholin-4-yl)phenyl]-1,3-oxazolidin-5-yl}methyl)thiophene- 2-carboxamide (BAY 59-7939): an oral, direct factor Xa inhibitor. *J Med Chem* **48**, 5900-5908, doi:10.1021/jm050101d (2005).
35 Pinto, D. J. *et al.* Discovery of 1-(4-methoxyphenyl)-7-oxo-6-(4-(2-oxopiperidin-1-yl)phenyl)-4,5,6,7-tetrahydro-1H -pyrazolo[3,4-c]pyridine-3-carboxamide (apixaban, BMS-562247), a highly potent, selective, efficacious, and orally bioavailable inhibitor of blood coagulation factor Xa. *J Med Chem* **50**, 5339-5356, doi:10.1021/jm070245n (2007).
36 Hauel, N. H. *et al.* Structure-based design of novel potent nonpeptide thrombin inhibitors. *J Med Chem* **45**, 1757-1766, doi:10.1021/jm0109513 (2002).
37 Cuker, A. & Siegal, D. Monitoring and reversal of direct oral anticoagulants. *Hematology Am Soc Hematol Educ Program* **2015**, 117-124, doi:10.1182/asheducation-2015.1.117 (2015).
38 Granger, C. B. *et al.* Apixaban versus warfarin in patients with atrial fibrillation. *N Engl J Med* **365**, 981-992, doi:10.1056/NEJMoa1107039 (2011).
39 Hokusai, V. T. E. I. *et al.* Edoxaban versus warfarin for the treatment of symptomatic venous thromboembolism. *N Engl J Med* **369**, 1406-1415, doi:10.1056/NEJMoa1306638 (2013).

40 Patel, M. R. *et al.* Rivaroxaban versus warfarin in nonvalvular atrial fibrillation. *N Engl J Med* **365**, 883-891, doi:10.1056/NEJMoa1009638 (2011).
41 Agnelli, G. *et al.* Oral apixaban for the treatment of acute venous thromboembolism. *N Engl J Med* **369**, 799-808, doi:10.1056/NEJMoa1302507 (2013).
42 Connolly, S. J. *et al.* Dabigatran versus warfarin in patients with atrial fibrillation. *N Engl J Med* **361**, 1139-1151, doi:10.1056/NEJMoa0905561 (2009).
43 Rao, V. S. & Kini, R. M. Pseutarin C, a prothrombin activator from Pseudonaja textilis venom: its structural and functional similarity to mammalian coagulation factor Xa-Va complex. *Thrombosis and haemostasis* **88**, 611-619 (2002).
44 Rao, V. S., Swarup, S. & Manjunatha Kini, R. The catalytic subunit of pseutarin C, a group C prothrombin activator from the venom of Pseudonaja textilis, is structurally similar to mammalian blood coagulation factor Xa. *Thrombosis and haemostasis* **92**, 509-521, doi:10.1160/TH04-03-0144 (2004).
45 Rao, V. S., Swarup, S. & Kini, R. M. The nonenzymatic subunit of pseutarin C, a prothrombin activator from eastern brown snake (Pseudonaja textilis) venom, shows structural similarity to mammalian coagulation factor V. *Blood* **102**, 1347-1354, doi:10.1182/blood-2002-12-3839 (2003).
46 Lechtenberg, B. C. *et al.* Crystal structure of the prothrombinase complex from the venom of Pseudonaja textilis. *Blood* **122**, 2777-2783, doi:10.1182/blood-2013-06-511733 (2013).
47 Bos, M. H. *et al.* Venom factor V from the common brown snake escapes hemostatic regulation through procoagulant adaptations. *Blood* **114**, 686-692, doi:10.1182/blood-2009-02-202663 (2009).
48 Bos, M. H. & Camire, R. M. Procoagulant adaptation of a blood coagulation prothrombinase-like enzyme complex in australian elapid venom. *Toxins (Basel)* **2**, 1554-1567, doi:10.3390/toxins2061554 (2010).
49 Verhoef, D. *et al.* Functional implications of the unique disulfide bond in venom factor V from the Australian common brown snake Pseudonaja textilis. *Toxin Reviews* **33**, 37-41, doi:10.3109/15569543.2013.844712 (2014).



Chapter 2

Blood Coagulation Factor Va's Key Interactive Residues and Regions for Prothrombinase Assembly and Prothrombin Binding

Mark Schreuder, Pieter H. Reitsma, Mettine H.A. Bos

Journal of Thrombosis and Haemostasis. 2019 17(8):1229-1239



Abstract

Blood coagulation factor Va serves an indispensable role in hemostasis as cofactor for the serine protease factor Xa. In the presence of an anionic phospholipid membrane and calcium ions, factors Va and Xa assemble into the prothrombinase complex. Following formation of the ternary complex with the macromolecular zymogen substrate prothrombin, the latter is rapidly converted into thrombin, the key regulatory enzyme of coagulation. Over the years, multiple binding sites have been identified in factor Va that play a role in the interaction of the cofactor with factor Xa, prothrombin, or the anionic phospholipid membrane surface. In this review, an overview of the currently available information on these interactive sites in factor Va is provided, and data from biochemical approaches and three-dimensional structural protein complex models are discussed. The structural models have been generated in recent years and provide novel insights into the molecular requirements for assembly of both the prothrombinase and the ternary prothrombinase-prothrombin complexes. The integrated knowledge on functionally important regions in factor Va will allow for a better understanding of factor Va cofactor activity.

Introduction

Factor Va (FVa) is a blood coagulation protein that is central to the formation of a blood clot following vascular injury. It is generated from its precursor or procofactor factor V (FV) by limited proteolysis and removal of the inhibitory B domain[1,2]; for a review on FV activation see Camire and Bos[3]. Once FV is activated, it is able to function as a cofactor to the serine protease factor Xa (FXa) in the so-called prothrombinase complex that is responsible for converting prothrombin to the key regulatory enzyme thrombin. Factor Va assembly with FXa into the prothrombinase complex occurs exclusively in the presence of Ca^{2+} and on a phosphatidylserine (PS)-exposing lipid membrane provided by activated platelets or endothelial cells. Although FXa is capable of activating prothrombin in the absence of its cofactor, assembly into the prothrombinase complex increases the conversion rate by five orders of magnitude[4], illustrating the essential role of FVa in coagulation. In this review, we will focus on the structural requirements of FVa to assemble into the prothrombinase complex and engage prothrombin, thereby forming the ternary complex. For this purpose, data from *in vitro* studies and three-dimensional structural protein complex models are discussed. The structural models have been generated in recent years and provide novel insights into the interactive sites in FVa that are involved in the assembly of the prothrombinase and the ternary complexes. Earlier reviews have focused on the general functionality of FV under normal conditions and in disease states, see Mann and Kalafatis[5] and Nicolaes and Dahlbäck[6].

The Factor V Protein Structure

Factor V circulates as a 330 kDa procofactor and comprises an A1-A2-B-A3-C1-C2 domain structure. The A domains of FV are ~30% identical to the copper-binding plasma protein ceruloplasmin, while the FV C domains share ~20% sequence homology with the discoidin I-like domain of phospholipid-binding lectins in slime mold[7,8]. The large B domain of FV is poorly conserved among species[3]. This domain comprises several tandem repeats, yet their role remains largely unknown[7,8]. The inhibitory effect of the B domain is maintained by a basic and a complementary acidic region, creating an autoinhibitory conformation which is considered to obscure FXa-interactive sites[9,10]. Proteolytic activation of FV is facilitated by FXa and meizothrombin in the initiation phase of coagulation and subsequently by thrombin in the propagation phase[11-14]. Sequential cleavage at the B domain sites Arg709, Arg1018, and Arg1545 results in dissociation of the B domain and generation of the non-covalently associated heavy (A1-A2) and light chains (A3-C1-C2) that form FVa[2,15,16].

Downregulation of the cofactor function of FVa is regulated by activated protein C (APC) and its cofactor protein S[17,18]. Activated protein C cleaves FVa at Arg306, Arg506, and Arg679 in the A2 domain[19,20]. The cleavage at Arg506 is kinetically preferred, causing a rapid loss of FVa cofactor activity, while the relatively slow cleavage at Arg306 is required for full FVa inactivation[19,21], the latter resulting from dissociation of the complete A2 domain[22].

The FV molecule contains a copper- and calcium-ion binding site, located between the A1 and A3 domains. Although the exact mechanism remains unclear, both ions likely stabilize the interaction between the FVa heavy and light chains and are crucial for the FVa cofactor activity[23-28]. Furthermore, FV undergoes multiple post-translational modifications including glycosylation, sulfation, and phosphorylation[5] (for a review on post-translational modifications in blood coagulation proteins see Hansson *et al.*[29]). The three-dimensional FV protein structure is further mediated by seven intradomain disulfide bridges in the A and C domains[30,31].

The Factor Va-Factor Xa Interaction

To gain insight into the molecular requirements of protein-protein interactions, the generation of crystal structures of proteins in combination with mutagenesis approaches has greatly contributed to unravel these characteristics. While crystal structures are available for both FVa and FXa, they are lacking for the human prothrombinase complex. As a result, the 3D structure of the human prothrombinase complex has been modelled based on (partial) crystal structures and guided by biochemical studies. The first 3D model of prothrombinase dates from 2006 and was based on the crystal structures of APC-inactivated bovine FVa and active site-inhibited human FXa[32]. Protein docking simulations revealed five representative prothrombinase structures, of which one proved consistent with most of the reported FVa-FXa binding data. A second prothrombinase model reported in 2008 by Lee *et al*. was generated from Molecular Dynamics simulations data[33]. Subsequently, the same group constructed the first ternary complex in 2011. By making use of the X-ray crystal structure of human prethrombin-1, the human prothrombin 3D structure was modelled and docked onto the prothrombinase complex[34]. In 2013, a crystal structure of a prothrombinase-like complex from the venom of the Australian Eastern Common Brown snake became available[35]. The components of this prothrombinase-like complex, known as Pseutarin C, associate with high affinity in the absence of a negatively charged lipid surface[36]. As Pseutarin C shares ~40-60% sequence identity with human FVa-FXa[35], this crystal structure provides a reliable blueprint for molecular modelling of human prothrombinase. Consequently, the latter was generated by Huntington and

co-workers[37]. More recently, a full human ternary complex was reported[38], thereby providing important new insights in the structural organization of the prothrombinase complex and prothrombin binding. In the following sections, we will review the molecular details of the FVa-FXa interactions, guided by the crystal structure of Pseutarin C, structural homology models, and biochemical studies.

The A2 Domain Arg306 region in Factor Va

The FVa A2 domain has been suggested to play a critical role in the interaction of FVa with FXa, as several distinct FXa binding sites have been identified of which an overview can be found in **Table S1**. One of these sites is a region in close proximity of the APC cleavage site Arg306 **(Figure 1)**. The first evidence for involvement of this region came from studies in which peptides of FV A2 domain sequences were assessed for their capacity to inhibit prothrombinase activity. In a screen of overlapping 15-residue peptides covering FVa region Thr271-Lys345, the peptide encompassing region Ile311-Phe325 was found to significantly inhibit prothrombin activation in the presence of FVa, while full activity was maintained in the absence of FVa[39]. These observations led Kojima *et al.* to conclude that this peptide competes for FXa binding. Supporting this finding, Kalafatis and Mann obtained evidence indicating that the FVa clotting activity was inhibited by a 42-amino acid peptide comprising residues Asn307-Arg348[40]. Further studies making use of both FV peptides and recombinant FV variants with targeted amino acid substitutions suggested amino acids Glu323, Tyr324, Glu330, Val331, Asp334, and Tyr335 as a FXa-binding cluster[41-43].

Interestingly, the crystal structure of Pseutarin C reveals that these residues are located at relative far distance from FXa (>20 Ångström). In Pseutarin C, only Met318, homologous to human Arg317, was found to interact with FXa[35] and similar observations were made for recent homology models of human prothrombinase[37,38] **(Figure 1; Table S1)**. It therefore seems unlikely that the A2 domain Arg306 region in FVa is directly contributing to FXa binding, but rather seems to be involved in the interaction with prothrombin (see also the 'The factor Va-prothrombin interaction' section). This would be in agreement with the findings by Norstrøm and colleagues, who reported that the Arg306 cleavage site is not protected by FXa[44], suggesting that APC and FXa do not share the Arg306 region in FVa as binding site.

The A2 Domain Arg506 Region in Factor Va

In contrast to the Arg306 region in the FVa A2 domain, the Arg506 cleavage site is known to be protected from APC-dependent proteolysis by FXa[17,44], indicating that this region harbors a competitive binding site for FXa and APC. Several other studies have provided further evidence for a FXa-binding site in the Arg506 region of the FVa A2

domain **(Figure 2; Table S1)**. For instance, a Gly493-Arg506 FV peptide was found to inhibit prothrombin activation[45]. In addition, a FVa variant in which residues Lys499-Arg505 were swapped for the homologous FVIIIa residues Tyr555-Gln561 revealed a significantly reduced FXa affinity, while Arg506 cleavage by APC was unaffected[46]. Further evidence was provided by site-directed glycosylation studies, demonstrating that introduction of N-glycosylation sites at FVa residues Glu467 and Ala511 attenuated FXa binding, while the affinity for prothrombin remained unaffected[47]. Still, these results could potentially be caused by steric hindrance rather than disrupting direct interactions between FVa and FXa. A direct assessment approach in which several charged residues were mutated to neutral amino acids revealed that four out of the fifteen FVa variants exhibited a markedly reduced FXa binding and cofactor activity, thereby identifying an A2 domain binding cluster of Arg501, Arg510, Ala511, Asp513, Asp577, and Asp578[48]. Structural analysis confirms that these residues are all located on the A2 domain surface in close proximity of FXa (<4 Ångström) **(Figure 2)**. Furthermore, these residues and their homologs in Pseutarin C have been implicated as FXa contact residues[35,37,38].

The A2 Domain C-terminus (A2T) in Factor Va

During the activation of FV, the B domain is cleaved and dissociates, resulting in a non-covalently linked FVa heavy and light chain[3]. The resulting A2 domain C-terminus (A2T) forms a long negatively charged tail that has been implicated as a FXa-interactive site **(Figure 3; Table S1)**. Initial evidence came from a study in which FVa was treated with a protease from the venom of the snake *Naja naja oxiana*, which resulted in the cleavage of a 27-amino acid peptide (Asp683-Arg709) from the FVa A2T[49]. The resulting cofactor, FVa_{NO}, displayed a markedly reduced affinity for both FXa and prothrombin, while the catalytic efficiency of prothrombinase-assembled FVa_{NO} was comparable to that of FVa. This finding indicates that the A2T plays a role in the assembly of the ternary complex rather than affecting its cofactor activity.

Although no crystal structure is available and only structural models exist of the complete A2T, part of the structural interactions (up to Glu683) were revealed by the Pseutarin C structure[35]. In this crystal structure, the A2T residues Asn656, Tyr657, and Asp671-Glu683 interact with the highly basic heparin-binding site of FXa. Interestingly, similar interactions have been reported for human FXa in studies in which potential FVa-binding residues were identified using inhibitory peptides or a mutagenesis approach[50,51]. The A2T may therefore function as a FXa recognition site and is as such important to prothrombinase complex assembly. However, the exact contribution of the A2T region to the interaction with FXa remains to be determined.

The Factor Va A3 Domain

The FVa light chain has been implicated in prothrombinase assembly through the FVa A3 domain-FXa EGF domain interaction **(Figure 4; Table S2)**. Most data on the FVa residues involved in this interaction has been derived from structural models, and few biochemical studies have provided evidence for the involvement of the A3 domain in FXa binding. A monoclonal antibody recognizing the FVa region Asp1537-Lys1752 was found to drastically reduce FXa binding and prothrombin conversion[52]. Further data uncovered a possible role for the region surrounding His1683, as introduction of a glycan at this position fully abrogated FXa binding and greatly decreased thrombin formation[48]. Furthermore, alanine substitution of residues Arg1551, Glu1650, Trp1665, and His1683 in FVa resulted in a minor reduction in FXa affinity[48]. The aforementioned residues have also been identified as FXa contact residues in several prothrombinase structures[37,38]. Within the Pseutarin C FV sequence Thr789-Gln922 (equivalent to human FV Ser1546-His1683), seven residues were found to be directly involved in FXa binding, while sixteen other amino acids were considered as contact residues[35]. Similar observations were made for the human homology models, revealing tight connections between the FXa EGF domains and the A3 domain of FVa[37,38]. Together, these studies highlight a role for the FVa A3 domain in prothrombinase complex assembly. These interactions might be important for the initial docking of the complex, allowing for subsequent productive interactions between the FVa A2 domain and FXa. As the structure of Pseutarin C comprises a truncated FXa molecule that lacks the EGF1 domain[35], structural data on the interaction with the EGF1 domain is currently provided by prothrombinase models only.

The Factor Va–Prothrombin Interaction

Upon assembly of the prothrombinase complex, the ternary complex is formed following docking of the macromolecular substrate prothrombin. Efficient docking of prothrombin is crucial for its conversion to thrombin that requires limited proteolysis by FXa at cleavage sites at Arg271 and Arg320[53]; for a review on prothrombin activation see Krishnaswamy[54]. Both molecular models that have been generated for the human ternary complex provide a template for prothrombin binding[34,38]. In addition, several experimental studies have provided evidence for prothrombin binding sites on the FVa heavy and light chains. In the next sections, we will describe the interactive sites in FVa for prothrombin that have been identified based on biochemical studies and the structural models of the ternary complex.

The A2 Domain Arg306 and Arg506 Region in Factor Va

As described in previous sections, the regions surrounding positions 306 and 506 in the FVa A2 domain have been implicated in FXa binding based on results from both structural models and *in vitro* studies. In most *in vitro* studies, a reduction in FVa cofactor activity was linked to an impaired interaction of FVa with either FXa or prothrombin. However, an exact determination of the affected binding partner would require analysis of direct protein-protein interactions. As a consequence, the regions that have been implicated in FXa binding could function as prothrombin-binding sites and vice versa. In support of this, several prothrombin binding residues that are in close proximity of the Arg306 region (Arg313, Arg316, and Arg317) or Arg506 region (Arg503, Arg505, and Arg506) have been identified following assessment of the ternary structural models **(Figures 1, 2; Table S3)**[34,38]. Interestingly, while FXa has been found to compete for APC-dependent cleavage at Arg506 only[44], prothrombin is capable of protecting both Arg306 and Arg506 from cleavage by APC[55]. This suggests that the Arg506 region in FVa interacts with both FXa and prothrombin, while the FVa Arg306 region acts solely as prothrombin binding site. Considering these observations, we conclude that those FXa-binding sites in the FVa Arg306 region that have been identified based on prothrombinase and/or clotting activity analyses might in fact be responsible for the interaction with prothrombin.

The A2 Domain C-terminus (A2T) in Factor Va

Apart from its role in the interaction with FXa, the FVa A2T may also serve an important role in prothrombin binding **(Figure 5; Table S3)**. For instance, FVa cleaved at Arg679 by a venom protease found in *Naja nigricollis nigricollis* exhibited a 60-80% reduced clotting activity[56]. The study further revealed that a synthetic peptide comprising residues Asp697-Arg709 was found to competitively inhibit prothrombinase activity by interfering with prothrombin binding, while the FVa-FXa binding remained unaffected. Similarly, the Asp697-Arg709 peptide was found to directly interact with thrombin-agarose, suggestive of a role in prothrombin rather than FXa binding. Next, a FV peptide encompassing region Asp695-Gln699 (DYDYQ) was observed to interfere with the incorporation of prothrombin and impaired prothrombin conversion[57]. In FVa region Asp695-Gln698, both tyrosines (Tyr696, Tyr698) are sulphated and have been suggested to facilitate the initial binding of prothrombin, thereby securing the position of prothrombin and its cleavage sites Arg271 and Arg320 close to the FXa active site[38]. This notion was further supported by alanine substitution of residues Asp695-Gln698, which resulted in a surprising ~20% increase in k_{cat} for the activation of prothrombin, while ,in contrast, an accumulation of meizothrombin and subsequent delay in prothrombin activation was observed[58]. Similar results were obtained for FVa variants in which residues Asp659-Asp663 were either mutated or deleted[59], or in

which residues Asn700-Arg701 were replaced for the bovine homologs Asp-Glu[60]. These results indicate that the A2T plays a prominent role in both the incorporation and catalysis of prothrombin.

Despite the fact that multiple studies have shown the involvement of the A2T in prothrombin binding and conversion, contradictory studies have also been reported. For example, a 13-residue C-terminal peptide of the FV A2 domain (residues Asp697-Arg709) was not able to inhibit the FVa clotting activity[40]. Furthermore, recombinant truncation of the FVa heavy chain between Thr679-Arg709 did not affect the FVa clotting activity, prothrombin conversion kinetics, nor FXa binding[61]. Conversely, truncation at Pro658 resulted in a markedly reduced clotting activity and FXa binding, although this variant showed normal prothrombinase kinetics when fully saturated with FXa and anionic membranes[61]. Although prothrombin time-based clotting assays may not be sufficiently sensitive to detect small functional differences in FVa cofactor activity, the observation that truncation of the FVa A2 domain C-terminus failed to affect the interaction with FXa and/or prothrombin might suggest that this region contributes minimally towards the assembly of the ternary complex.

The findings described above have thus far not been supported by mechanistic insights derived from crystal structures, as the FVa A2T has not been fully resolved in the available X-ray structures of the FV A2 domain. Currently, only an X-ray structure of active site-inhibited thrombin bound to FVa residues Glu666-Glu672 has been reported[62], revealing that these FVa residues interact with exosite I in thrombin. Interestingly, in addition to the reported X-ray structure, the authors modeled the complete A2T (Ile657-Arg709) as a peptide wrapping around thrombin, thereby covering a large surface of productive interactions. Similarly modeled interactions of the FVa A2T were obtained from the ternary model created by Shim *et al.*[38]. In this model, the A2T first interacts with the heparin-binding site of FXa and subsequently binds prothrombin, hereby acting as a long arm grasping prothrombin and assisting in its assembly into the ternary complex **(Figure 3)**. Collectively, these structural studies indicate a dual role for the A2T, being involved in both FXa and prothrombin binding. Based on the available data, we suggest that the N-terminal segment of the A2T may interact with FXa thereby contributing to prothrombinase formation. Subsequently, the remaining C-terminal part of the A2T region might interact with prothrombin to facilitate efficient substrate docking onto the prothrombinase complex. However, until high resolution X-ray structures of the ternary complex will become available, the exact molecular interactions facilitating the interaction of the FVa A2T with both FXa and prothrombin remain undefined.

The A3 and C1-C2 Domains in Factor Va

Currently, direct evidence supporting binding of prothrombin and the FVa light chain is absent. Yet, interactions between the Kringle domains of prothrombin and FVa have been reported. Characterization of prothrombin mutants in which either the Kringle 1 or Kringle 2 domain was deleted suggested that the Kringle 2, but not the Kringle 1 domain, interacts with FVa[63]. In contrast, in a later study both Kringle domains of prothrombin were found to contribute to FVa binding[64]. It is generally acknowledged that the Kringle 1 domain is located close to the membrane layer as it is separated via a small linker from the Gla domain[65], the latter facilitating phospholipid binding. Given the structural orientation of prothrombin and the Kringle 1 domain, the Kringle 1 domain could have the potential to interact with the FVa A3 domain and/or with the lipid-binding C domains. Such interactions were observed in the two ternary models, revealing significant interactions between the Kringle 1 and Gla domain of prothrombin and the A3 and C1 domains of FVa[34,38]. Thus far, support for this has come from one *in vitro* study in which a peptide comprising the sequence of prothrombin's Gla domain (residues 1-46) was demonstrated to inhibit prothrombinase activity and to directly interact with FVa [66]. While the binding site in FVa is likely located in the lipid-binding light chain, the contribution of the FVa A3-C1-C2 domains to prothrombin assembly remains largely unclear. Collectively, the current models and sparse *in vitro* data suggest that interactive regions are located in the A3 and C1 domains **(Figure 6; Tables S4-S5)**. Nevertheless, future studies focused on providing solid evidence for the contribution of the FVa A3-C1 domains to prothrombin binding are required.

The Factor Va–Anionic Membrane Interaction

A negatively charged membrane surface comprising PS is essential for the formation of the ternary prothrombinase-prothrombin complex. This anionic phospholipid layer provides a binding surface for the ternary complex assembly and is mainly provided by the membranes of activated platelets and endothelial cells. The interaction of FVa with the PS-rich membrane is facilitated by its C1 and C2 domains. These domains contain several protruding spikes that are orientated towards the lipid layer. Hydrophobic and positively charged residues are located at the apex of these spikes and have been implicated as the lipid-binding sites[67,68]. Here, we will review the studies providing evidence for these membrane binding sites and describe our current understanding of the key residues facilitating such interactions.

The C1 Domain of Factor Va

Interaction of FVa with the negatively charged membrane surface is, together with contributions of the C2 domain, mediated by the immersion of hydrophobic C1 domain

spikes into the phospholipid bilayer **(Figure 7; Table S6)**. The FVa C1 domain was initially considered to facilitate phospholipid binding due to the observation that FVa comprised a higher membrane affinity relative to the isolated FVa C2 domain[69]. Using alanine-scanning mutagenesis, several membrane binding residues were identified in the C1 domain[70]. Out of twenty generated FVa variants, alanine substitution of the residue pairs Lys1954 and His1955, Tyr1956 and Leu1957, and Arg2023 and Arg2027 revealed an impaired binding to immobilized PS. Further characterization showed a significantly reduced prothrombinase activity of the Tyr1956 and Leu1957, and Arg2023 and Arg2027 substituted variants, although this was only observed at limiting phospholipid concentrations. Conversely, the Lys1954 and His1955 mutated FVa variant displayed a similar prothrombinase activity compared to wild-type FVa[70], suggesting that these residues might be involved in FVa-lipid binding but are not essential for prothrombinase assembly. Later studies demonstrated that the binding site for a soluble form of PS (C6PS) was lost upon alanine substitution of the hydrophobic residues Tyr1956 and Leu1957[71,72]. Binding of FVa to soluble PS has been shown to increase the affinity of FVa for FXa[73,74]. Interestingly, substitution of Tyr1956 and Leu1957 resulted in an approximately 200-fold decreased affinity for FXa in the presence of soluble C6PS[71] and a ~4-fold reduced affinity was observed on PS membranes[70]. Still, at saturating concentrations of FVa, FXa, and PS membranes, the maximal rate of prothrombin activation was indistinguishable from wild-type FVa. Therefore, mutating residues Tyr1956 and Leu1957 seems to affect the assembly of FVa and prothrombinase on lipid membranes rather than affecting the activity while assembled. This might suggest that binding of the C1 domain to the lipid surface induces conformational changes in FVa, resulting in an enhanced affinity for FXa. It has been proposed that these changes may induce rearrangements in the A2 domain, the main binding region for FXa[71,75]. Alternatively, the conformational changes may also result in the presentation of a FXa binding site on the FVa C1 and/or C2 domain, although no interactions between the C domains and FXa have been identified in recent structural models[37,38].

The C2 Domain of Factor Va

The C2 domain plays a pivotal role in the binding of FVa to the lipid membrane layer, which involves both hydrophobic and electrostatic interactions **(Figure 7; Table S7)**. The first studies demonstrating C2 domain binding to the lipid surface revealed an impaired PS-binding upon either deletion of the C2 domain or by making use of specific inhibitory antibodies directed against the C2 domain[76-78]. Subsequently, chimeric FV variants generated by exchange of exon-size sequences for the corresponding FVIII regions revealed that the N-terminal region of the C2 domain (residues Gly2037-Lys2087) was involved in PS binding[79]. In 1998, the first models of the FV C1 and C2 domains were reported, based on the crystal structure of the homologous D1 domain of galactose

oxidase[80]. A cluster of hydrophobic/aromatic residues (Lys2060, Lys2061, Trp2063, and Trp2064) was identified in a solvent-exposed loop in the C2 domain, suggesting a role in membrane binding[80]. This suggestion was strengthened by the crystal structure of the C2 domain of FV, which revealed three protruding spikes containing hydrophobic and polar residues, with Trp2063, Trp2064 (spike 1), and Leu2116 (spike 3) suggested as particular candidates for membrane immersion[81]. Subsequent alanine-scanning revealed a critical role for Trp2063 and Trp2064 in PS binding[72,82-86]. Mutating both residues resulted in a markedly reduced membrane binding affinity in addition to an attenuated prothrombinase activity. However, the attenuated activity was only observed in conditions with limiting PS concentrations (<10%) and was restored in the presence of 25% PS membranes with saturating concentrations of FVa and FXa. Therefore, these results indicate that Trp2063 and Trp2064 are important for PS-membrane binding, but do not affect the intrinsic activity of FVa. The fact that FVa variants comprising mutations at key lipid-binding residues fail to show abrogated prothrombinase activity on membranes containing >20% PS may suggest the involvement of other regions in FVa-membrane binding. However, given that physiological concentrations of PS are considered to be in the range of 5-10%[87,88], the contribution of individual binding sites should be assessed employing relevant compositions of negatively charged phospholipids and direct membrane-binding assessments.

Two FV isoforms, FV1 and FV2, exist in plasma that display different FVa cofactor activities and slightly different molecular weights as a result of heterogeneity in the light chain caused by partial glycosylation at Asn2181[89-91]. The Asn2181-glycosylated FVa1 displays an impaired lipid binding and FVa cofactor activity compared to the non-glycosylated form FVa2. Yet, the reduced prothrombin conversion could only be detected in the presence of limiting PS concentrations; once assembled, FVa1 and FVa2 exhibit comparable catalytic efficiencies[89]. These results indicate that although Asn2181 does not directly contribute to membrane binding, glycosylation of Asn2181 interferes with the binding of FVa to PS-membranes.

Interestingly, the crystal structure of the FVa C2 domain revealed two distinct conformations referred to as an 'open form' and 'closed form' that correspond to a membrane binding state and a circulating state, respectively[81]. In the open form, the three protruding spikes create a deep groove lined by hydrophobic and polar residues that are ideally arranged to interact with the PS head groups. The hydrophobic residues located at the apex of the spikes could thereby facilitate the initial binding and immersion into the membrane layer. This allows for the formation of additional interactions between the interior of the groove (residues Trp2064, Trp2068, Met2120, and Leu2116) and the PS head groups. An additional PS-binding site might be localized

between the second and third spikes consisting of residues Gln2078, Gly2079, Asn2082, Lys2114, and Arg2187[81]. This basic region would be more accessible for acidic phospholipids, explaining the preference of FVa for acidic membranes[92]. In the closed form, the first and third spikes are slightly tilted and as a result the interior of the groove is covered by the side chains of Trp2063, Trp2064, and Leu2116, leading to a markedly reduced hydrophobic exposed surface.

The C1 and C2 Domains of Factor Va

A mechanistic model describing the FVa C1-C2-lipid interaction has been proposed[69,71]. The C2 domain, and perhaps also the C1 domain, circulate in a closed state preventing phospholipid binding and prothrombinase assembly. The basic and polar residues surrounding the binding spikes facilitate the approach to the negatively charged PS-membrane. The subsequent PS-membrane binding triggers the open state of the C domains, resulting in membrane insertion of hydrophobic residues Tyr1956 and Leu1957 (C1 domain), Trp2063 and Trp2064 (C2 domain), and subsequent interactions between the lipid-binding groove and PS head groups. Initial membrane binding may be facilitated by the C2 domain[71], and subsequent anchoring of FVa to the phospholipid layer allows the C1 membrane to interact, establishing FVa-membrane binding. This proposed mechanism is in agreement with Molecular Dynamics simulations studies on the homologous FVIII C domains, in which the FVIII C2 domain is the first to interact with the membrane layer, followed by membrane immersion of the C1 spikes[93].

Summary

In this review, we have evaluated the regions in FVa that are responsible for the interaction with FXa, prothrombin, and the negatively charged lipid membrane. As FVa plays a central role in hemostasis, the binding sites in FVa are essential functional regions that mediate full prothrombinase activity. Important interactive regions for FXa are mainly located within the A2 domain of FVa. The two main FXa-binding sites within this domain are the A2T and the region surrounding Arg506. Although the Arg306-surrounding region has previously been implicated as a FXa-binding site, the Pseutarin C structure and homology models of the ternary prothrombinase-prothrombin complex reveal that this region is likely involved in prothrombin binding rather than FXa binding. Instead, the Arg506 and A2T regions were found to play a dual role, as they contribute to both FXa and prothrombin binding. While the exact contribution of the A2T remains to be elucidated, current observations suggest a role in the initial binding of prothrombin and its positioning close to the FXa active site to facilitate efficient proteolytic conversion to thrombin. Lastly, we summarized the interaction of FVa with the lipid membrane layer. Membrane binding is facilitated by both C domains, in

which the hydrophobic residues of several protruding spikes insert into the membrane layer. These membrane interactions may result in conformational changes within the C domains that have been suggested to induce structural rearrangements that allow for assembly of the ternary complex.

Collectively, this review has provided an overview of the essential binding sites in FVa for incorporation into the prothrombinase and functional ternary complexes. Unfortunately, X-ray structures of the complete prothrombinase or ternary complexes are lacking, limiting our knowledge to available structural models and biochemical data. Nevertheless, in the last decades considerable knowledge has been gained, as a crystal structure of the prothrombinase-like Pseutarin C complex has been generated and several structural models of the prothrombinase and ternary complexes have become available. While some issues concerning the molecular details and mechanisms of FVa binding still remain, the current overview will provide a framework for future research and novel approaches to uncover details on binding sites and functional regions in FVa.

Acknowledgements

This work was financially supported by the Bayer Hemophilia Awards Program (Special Project Award) and Landsteiner Foundation for Blood Transfusion (LSBR, grant. no. 1451). The funding agencies had no role in the preparation, review, or approval of the manuscript.

Figures

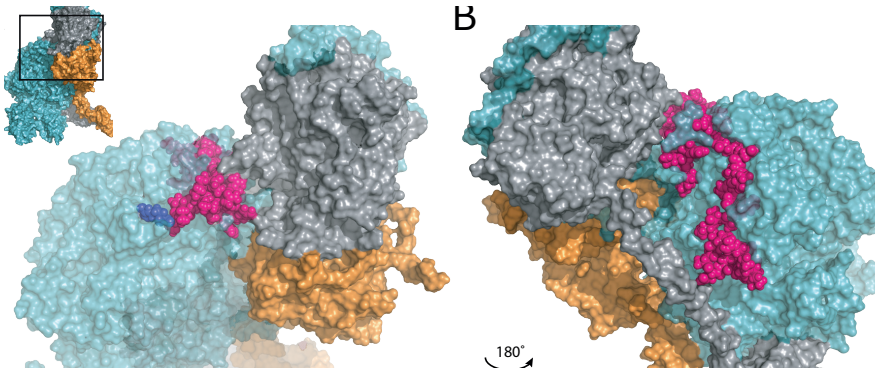


Figure 1. Interface between the factor Va A2 domain Arg306 region and factor Xa or prothrombin. A zoomed-in region of the human ternary model by Shim *et al.* is shown[38]; the insert in panel A outlines the specific region depicted. Panel B displays the same region after a 180° rotation around the Y-axis. The region (Asn307-Lys386, specified in Tables S1 and S3) surrounding the Arg306 site (indicated in blue) is in close proximity to prothrombin, suggesting that this specific region is a binding site for prothrombin rather than for FXa. FVa amino acids implicated as contact residues are highlighted in pink; FVa (teal), FXa (orange), and prothrombin (gray) are indicated. See Movie S1 for a 3D overview. Abbreviations: FVa, factor Va; FXa, factor Xa.

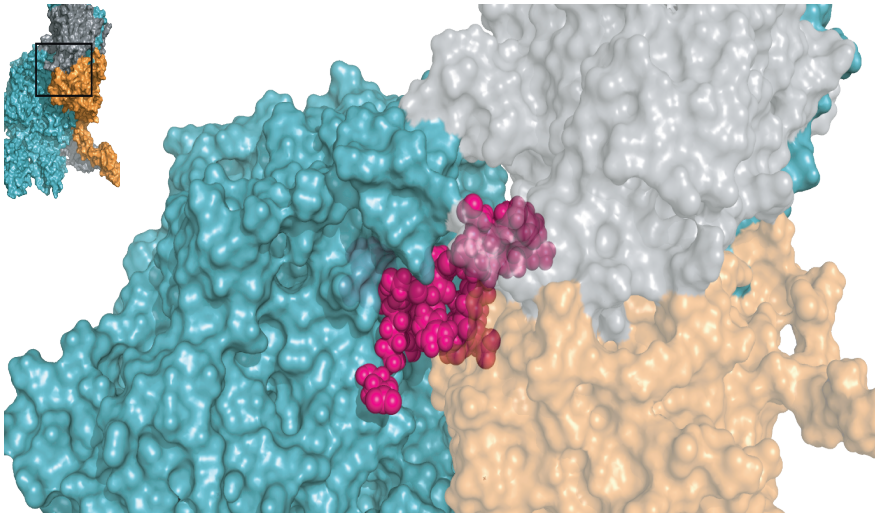


Figure 2. The factor Va A2 domain Arg506 region functions as a binding site for both factor Xa and prothrombin. A zoomed-in region of the human ternary model by Shim *et al.* is shown[38]; the insert outlines the specific region depicted. A cluster of amino acids between Glu467-Ile514, specified in Tables S1 and S3, forms a binding site for factor Xa, while residues Leu503, Arg505, and Arg506 interact with both FXa and prothrombin. FVa amino acids implicated as contact residues are indicated in pink; FVa (teal), FXa (orange), and prothrombin (gray) are indicated. See Movie S2 for a 3D overview. Abbreviations: FVa, factor Va; FXa, factor Xa.

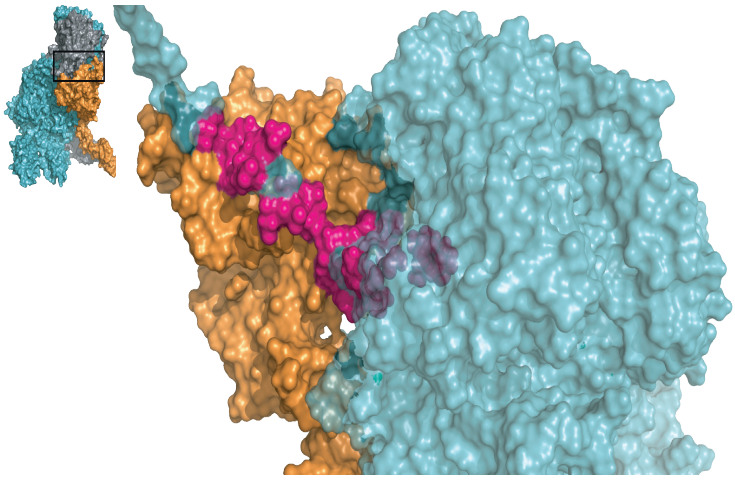


Figure 3. The factor Xa binding region in the A2 domain C-terminus of factor Va. A zoomed-in region of the human ternary model by Shim *et al.* is shown[38]; the insert outlines the specific region depicted. Several residues in the A2-domain C-terminus, spanning from Cys575 to Pro670, as specified in Table S1, are involved in the assembly of the prothrombinase complex by interacting with the heparin-binding site of FXa. FVa amino acids implicated as contact residues are indicated in pink; FVa (teal) and FXa (orange) are indicated; prothrombin has been removed for clarity. See Movie S3 for a 3D overview. Abbreviations: FVa, factor Va; FXa, factor Xa.

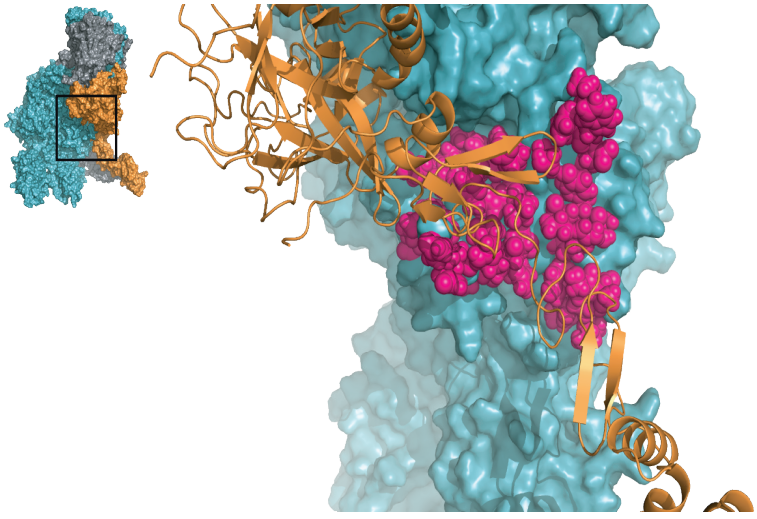


Figure 4. The factor Va A3 domain interacts with the serine protease and EGF domains of factor Xa. A zoomed-in region of the human ternary model by Shim *et al.* is shown[38]; the insert outlines the specific region depicted. All highlighted residues (pink spheres) in FVa, spanning from Asn1547 to Lys1725 (specified in Table S2), are located close to FXa and may be directly involved in the formation of the prothrombinase complex. FVa (teal) and FXa (orange cartoon) are indicated; prothrombin has been removed for clarity. See Movie S4 for a 3D overview. Abbreviations: FVa, factor Va; FXa, factor Xa.

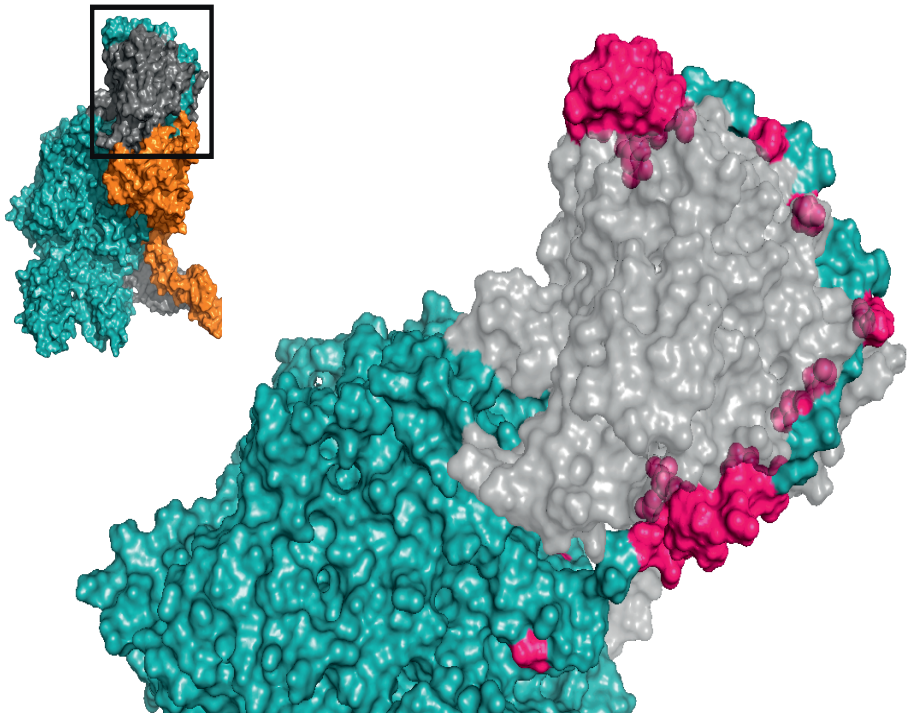


Figure 5. The factor Va A2 domain C-terminus is predicted to wrap around the serine protease domain of prothrombin. A zoomed-in region of the human ternary model by Shim *et al.* is shown[38]; the insert outlines the specific region depicted. Asp628-Arg709 (highlighted in pink, specified in Table S3) within the A2 domain C-terminus has been implicated to function as a prothrombin binding site. This region forms an extended arm that likely facilitates the docking of prothrombin onto the prothrombinase complex. FVa (teal) and prothrombin (gray) are indicated; FXa has been removed for clarity. See Movie S5 for a 3D overview. Abbreviations: FVa, factor Va; FXa, factor Xa.

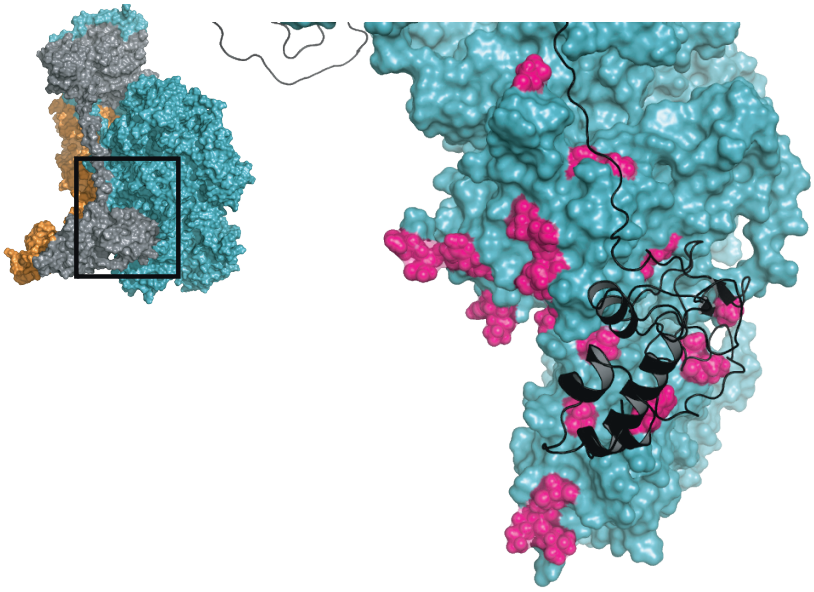


Figure 6. The interaction of the factor Va A3 and C1 domains with prothrombin. A zoomed-in region of the human ternary model by Shim *et al.* is shown[38]; the insert outlines the specific region depicted. Several prothrombin-interactive regions have been suggested for the FVa A3 and C1 domains (highlighted in pink, specified in Tables S4 and S5) and are proposed to interact with the Kringle 2 and Gla domains of prothrombin. FVa (teal) and prothrombin (black cartoon) are indicated; FXa has been removed for clarity. See Movie S6 for a 3D overview. Abbreviations: FVa, factor Va; FXa, factor Xa.

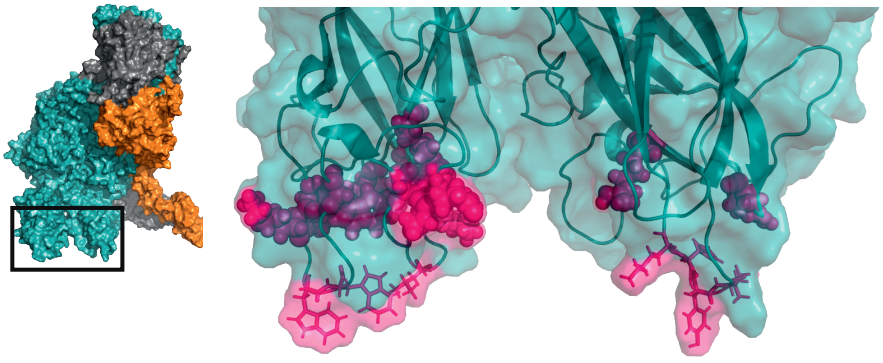


Figure 7. The factor Va C1 and C2 domains facilitate interaction with the anionic lipid membrane surface. A zoomed-in region of the human ternary model by Shim *et al.* is shown[38]; the insert outlines the specific region depicted. The hydrophobic protruding spikes of the C1 and C2 domains (shown in stick configuration) insert into the anionic lipid membrane layer. Additional interactions are provided by the groove between the C domains (residues spanning Lys1954-Arg2027 and Lys2060-Arg2187, specified at Tables S6 and S7). FVa amino acids implicated as contact residues are indicated in pink, FVa is indicated in teal. See Movie S7 for a 3D overview. Abbreviations: FVa, factor Va; FXa, factor Xa.

Supplemental Tables

Regions				
Regions FVa				**Reference**
Glu323-Val331				[41]
Ile311-Phe325				[39]
Asn307-Arg348				[40]
Gly493-Arg506				[45]
Lys499-Arg505				[46]
Asp683-Arg709				[49]
Asp697-Arg709				[56]

Residues				
Residue FVa	**Residue FXa**	**Chymptrypsin numbering**	**Bindingtype**	**Reference**
Arg317	Ser355	Ser173	Hydrogen Bond/ Buried surface	[37]
Lys320	Asp346	Asp164		[33]
Arg321	Asn348	Asn166	Hydrogen Bond	[33, 34]
Trp322	Arg347	Arg165	Hydrogen Bond	[33, 34]
Glu323	Asn348/Lys351	Asn166/Lys169	Hydrogen Bond	[33-34, 42]
Glu323	Lys351	Lys169	Salt-bridge	[33]
Tyr324				[42]
Phe325	Lys351	Lys169	Cation-Pi interaction	[33]
Glu330				[42]
Val331				[42]
Asp334				[43]
Tyr335				[43]
Glu372	Lys351	Lys169	Salt-bridge	[34]
Phe376	Thr278/Thr275/ Glu277/ Phe356/ Ile357	Thr98//Thr95/Glu97/ Phe174/Ile175	Hydrophobic interaction	[33, 34]
His379	Glu277/Asp280	Glu97/Asp100	Salt-bridge	[33, 34]
Thr380	Arg273	Arg93		[33]
Met385	Gln360	Gln178		[33]
Glu467			Buried surface	[37, 47]
Gln471			Buried surface	[39]
Arg501	Leu352	Leu170	Hydrogen Bond/ Buried surface	[37, 48]
Leu503			Buried surface	[37]
Asp504			Buried surface	[37]
Arg505	Glu277/Met314/ Val345/Arg347/ Gln360/Cys364/ Lys414	Glu97/Met131/Val163/ Arg165/ Gln178/Cys182/ Lys230	Hydrogen Bond	[33, 34, 37]
Arg505	Glu277	Glu97	Salt-bridge/Buried surface	[37]
Arg505	Tyr344/Phe363	Tyr162/Phe181	Cation-Pi interaction	[33, 34]

Residues				
Residue FVa	**Residue FXa**	**Chymptrypsin numbering**	**Bindingtype**	**Reference**
Arg506	Arg347/Gln360	Arg165/Gln178	Hydrogen Bond/ Buried surface	[34, 37]
Arg506	Glu310	Glu127	Salt-bridge/Buried surface	[34]
Gly507	Arg347	Arg165		[33]
Arg510	Thr278/Glu310	Thr98/Glu127	Hydrogen Bond/ Buried surface	[33, 34, 37, 48]
Arg510	Glu310	Glu127	Salt-bridge/Buried surface	[33, 34, 37, 48]
Ala511	Leu352	Leu170	Hydrophobic interaction/Buried surface	[37, 38, 47, 48]
Ala511	Leu352/Lys351/ Asn348	Leu170/Lys169/ Asn166	Hydrogen Bond/ Buried surface	[37, 47, 48]
Ala512			Buried surface	[37]
Asp513	Arg306	Arg125b	Hydrogen Bond/ Buried surface	[34, 37, 48]
Asp513	Arg306/Arg347/ Lys351	Arg125b/Arg165/ Lys169	Salt-bridge/Buried surface	[33, 34, 37, 38, 48]
Ile514			Buried surface	[37]
Cys575			Buried surface	[37]
Phe576			Buried surface	[37]
Phe576	Lys414	Lys230	Hydrogen Bond	[37]
Asp577	Arg347/Lys414	Arg165/Lys230	Hydrogen Bond/ Buried surface	[37, 48]
Asp577	Arg347/Lys414/ Lys420	Arg165/Lys230/ Lys236	Salt-bridge/Buried surface	[34, 47, 38, 48]
Asp578	Arg306/Lys351/ Gln360	Arg125b/Lys169/ Gln178	Hydrogen Bond/ Buried surface	[33, 34, 37, 48]
Asp578	Arg306/Arg347/ Lys351/Lys420	Arg125/Arg165/ Lys169/Lys236	Salt-bridge/Buried surface	[33, 34, 37, 38, 48]
Thr579	Asn348/Lys351	Asn166/Lys169	Hydrogen Bond	[37]
Thr579			Buried surface	[37]
Ile604			Buried surface	[37]
Lys607			Buried surface	[37]
Thr624			Buried surface	[37]
Thr626	Asp346	Asp164	Hydrogen Bond/ Buried surface	[37]
Asp628			Buried surface	[37]
Asn629			Buried surface	[37]
Val630			Buried surface	[37]
Arg652				[47]
Lys655	Asp307/Ser311/ Glu440	Asp125c/Ser128/ Glu256	Hydrogen Bond/ Buried surface	[33, 34, 37]
Lys655	Asp307/Glu310/ Glu440	Asp125c/Glu127/ Glu256	Salt-bridge/Buried surface	[33, 34, 37, 38]

Residues				
Residue FVa	Residue FXa	Chymptrypsin numbering	Bindingtype	Reference
Cys656	Lys420	Lys236	Hydrogen Bond/ Buried surface	[34, 37]
Ile657	Ala417	Ala233	Hydrophobic interaction/Buried surface	[37, 38]
Ile657	Arg306	Arg125b	Hydrogen Bond/ Buried surface	[37]
Pro658	Arg273	Arg93	Hydrogen Bond/ Buried surface	[37]
Asp659	Arg306/Lys420	Arg125b/Lys236	Hydrogen Bond/ Buried surface	[37]
Asp659	Arg273/Arg306/ Lys420	Arg93/Arg125b/ Lys236	Salt-bridge/Buried surface	[37, 38]
Asp660	Arg273	Arg93	Hydrogen Bond/ Buried surface	[37]
Asp660	Arg273	Arg93	Salt-bridge/Buried surface	[37]
Asp661	Arg273/Arg424	Arg93/Arg240	Hydrogen Bond/ Buried surface	[37]
Asp661	His271/Arg273/ Arg424	His91/Arg93/Arg240	Salt-bridge/Buried surface	[37, 38]
Asp663	Asn272/Phe274/ Lys276	Asn92/Phe94/Lys96	Hydrogen Bond	[37]
Asp663	Lys276	Lys96	Salt-bridge	[37]
Ser664	Asn272/Arg273	Asn92/Arg93	Hydrogen Bond/ Buried surface	[37]
Tys665	Arg424/Lys427	Arg240/Lys243	Hydrogen Bond/ Buried surface	[37]
Tys665	Arg273	Arg93	Salt-bridge/Buried surface	[37, 38]
Ile667	Val267/Ile269/Thr428/ Pro432	Val87/Ile89/Thr244/ Pro248	Hydrophobic interaction/Buried surface	[37, 38]
Phe668	Arg424	Arg240	Hydrogen Bond/ Buried surface	[37]
Glu669	Arg424/Lys427/ Arg429	Arg240/Lys243/ Arg245	Hydrogen Bond/ Buried surface	[37]
Glu669	Arg243/Arg424/ Lys427/Arg429	Arg64/Arg240/ Lys243/Arg245	Salt-bridge/Buried surface	[37, 38]
Pro670	Val267/Ile269/Thr428/ Pro432	Val87/Ile89/Thr244/ Pro248	Hydrophobic interaction	[38]

Table S1. Factor Xa interacting regions and residues of factor Va A2 domain.

Residue FVa	Residue FXa	Bindingtype	Reference
Asn1547	Asp92/Gln133/Lys204	Hydrogen Bond/Buried surface	[37]
Asn1547	Asp92	Salt-bridge/Buried surface	[37]
Asn1548	Asp92	Hydrogen Bond/Buried surface	[37]
Gly1549	Asp92	Hydrogen Bond/Buried surface	[37]
Arg1551	Leu91/Asp92/Asp95	Hydrogen Bond/Buried surface	[37]
Arg1551	Glu77/Asp95	Salt-bridge/Buried surface	[37]
Arg1552		Buried surface	[37]
Asn1553	Glu82	Hydrogen Bond/Buried surface	[37]
Tyr1555	Gln56/Glu82	Hydrogen Bond/Buried surface	[37]
Leu1596		Buried surface	[37]
Asp1597		Buried surface	[37]
Ser1598	Gln56/Asn57	Hydrogen Bond/Buried surface	[37]
Thr1599		Buried surface	[37]
Lys1602	Glu51/Ser53	Hydrogen Bond/Buried surface	[37]
Lys1602	Glu51	Salt-bridge/Buried surface	[37]
Val1624		Buried surface	[37]
Asp1625	Lys134	Hydrogen Bond/Buried surface	[37]
Asp1625	Lys134	Salt-bridge/Buried surface	[37]
Val1627	Leu88/Leu91	Hydrophobic interaction/ Buried surface	[37, 38]
Gln1629	Phe84	Hydrogen Bond/Buried surface	[37]
Arg1631	Gln56/Asn57/Cys81/ Glu82	Hydrogen Bond/Buried surface	[37]
Ser1648		Buried surface	[37]
Tyr1649		Buried surface	[37]
Glu1650	Leu88/Leu91	Hydrophobic interaction/ Buried surface	[37, 38]
Glu1650	Cys89/Ser90	Hydrogen Bond/Buried surface	[37]
Ser1652	Lys87/Glu102	Hydrogen Bond/Buried surface	[37]
Pro1663		Buried surface	[37]
Trp1665		Buried surface	[37]
Phe1666		Buried surface	[37]
Glu1668		Buried surface	[37]
Ser1677		Buried surface	[37]

Residue FVa	Residue FXa	Bindingtype	Reference
Tyr1678	Asn105	Hydrogen Bond/Buried surface	[37]
Thr1679		Buried surface	[37]
Val1681	Leu88/Leu91	Hydrophobic interaction/ Buried surface	[37, 38]
Trp1682		Buried surface	[37]
His1683		Buried surface	[37, 47]
Thr1685		Buried surface	[37]
Glu1686	Lys134	Salt-bridge/Buried surface	[37]
Arg1687	Asp164	Hydrogen Bond/Buried surface	[37]
Arg1687	Asp164	Salt-bridge/Buried surface	[37]
Lys1725		Buried surface	[37]

Table S2. Factor Xa interacting residues of factor Va A3 domain.

Residue FVa	Residue FII	Chymptrypsin numbering	Bindingtype	Reference
Arg313	Glu514	Glu186d	Salt-bridge	[38]
Arg316	Asp513	Asp168c	Salt-bridge	[38]
Arg317	Glu262		Salt-bridge	[38]
Glu374	Lys511	Lys186	Salt-bridge	[34]
His379	Glu255		Salt-bridge	[34]
Val381	Pro491	Pro166	Hydrophobic interaction	[34]
Lys386	Glu168		Salt-bridge	[34]
Leu503	Leu260		Hydrophobic interaction	[38]
Arg505	Glu489	Glu164	Salt-bridge	[38]
Arg506	Glu255		Salt-bridge	[38]
Leu572	Leu167		Hydrophobic interaction	[34]
Asp628	Arg155		Salt-bridge	[34]
Tys665	Arg443	Arg125b	Salt-bridge	[38]
Val675	Gln571/Ile574	Gln239/Ile242	Hydrophobic interaction	[38]
Ala677	Gln571/Ile574	Gln239/Ile242	Hydrophobic interaction	[38]
Lys680	Glu579	Glu247	Salt-bridge	[38]
Glu686	Lys426	Lys109	Salt-bridge	[38]
Glu690	Lys341	Lys36	Salt-bridge	[38]
Asp695	Arg340	Arg35	Salt-bridge	[38]
Tys698	Lys474	Lys149	Salt-bridge	[38]
Asn700				[60]
Arg701	Glu345	Glu39	Salt-bridge	[38, 60]
Arg709	Glu345	Glu39	Salt-bridge	[38]

Table S3. Prothrombin interacting regions and residues of factor Va A2 domain.

Residue FVa	Residue FII	Bindingtype	Reference
Asn1547	Pro154	Hydrogen Bond	[34]
Asn1548	Thr153	Hydrogen Bond	[34]
Gly1549	Glu85	Hydrogen Bond	[34]
Arg1551	Glu85	Hydrogen Bond	[34]
Tyr1555	Leu88/Ser91	Hydrophobic interaction	[34]
Ile1561	Ile79	Hydrophobic interaction	[38]
Thr1573	Pro94/Pro131	Hydrophobic interaction	[38]
Arg1593	Glu85	Salt-bridge	[38]
Arg1596	Arg90	Hydrogen Bond	[34]
Ser1598	Ser91/Arg92	Hydrogen Bond	[34]
Asp1604	Arg90	Salt-bridge	[34]
Arg1631	Tyr93	Hydrogen Bond	[34]
Arg1631	Tyr93	Cation-Pi interaction	[34]
Pro1639	Met152	Hydrophobic interaction	[38]
Asp1661	Arg155	Salt-bridge	[38]
Ala1671	Met152	Hydrophobic interaction	[38]
Thr1679	Tyr93	Hydrophobic interaction	[34]
His1729	His76	Hydrophobic interaction	[34]
Lys1730	Glu85	Hydrophobic interaction	[34]
Lys1730	Glu85	Salt-bridge	[34]

Table S4. Prothrombin interacting residues of factor Va A3 domain.

Residue FVa	Residue FII	Bindingtype	Reference
Asn1926	Thr35	Hydrogen Bond	[34]
Phe1929	Ser101/Thr102	Buried Surface	[38]
Leu1957	Lys10	Hydrogen Bond	[34]
Lys1958	Gla32	Hydrogen Bond	[34]
Lys1958	Gla29/Gla32	Salt-bridge	[34]
Ile1974	Tyr92	Buried Surface	[38]
Asn1975	Tyr92	Buried Surface	[38]
Leu1984	Gln110	Hydrogen Bond	[34]
Asn1986	Gln110/Glu111	Hydrogen Bond	[34]
Thr2018	Ser33	Hydrogen Bond	[34]
Asn2022	Gla32	Hydrogen Bond	[34]

Table S5. Prothrombin interacting residues of factor Va C1 domain.

Residue FVa	Reference
Lys1954	[70]
His1955	[70]
Tyr1956	[70, 71, 72]
Leu1957	[70, 71, 72]
Arg2023	[70]
Arg2027	[70]

Table S6. Factor Va C1 domain residues involved in anionic membrane binding.

Regions FVa	Reference
Gly2037-Lys2087	[79]
Residue FVa	Reference
Lys2060	[80]
Lys2061	[80]
Trp2063	[71, 72, 80-86]
Trp2064	[71, 72, 80-86]
Trp2068	[81]
Gln2078	[81]
Gly2079	[81]
Asn2082	[81]
Cys2113	[69]
Lys2114	[81]
Leu2116	[81]
Met2120	[81]
Asn2181	[90, 91]
Arg2187	[81]

Table S7. Factor Va C2 domain residues involved in anionic membrane binding.

References

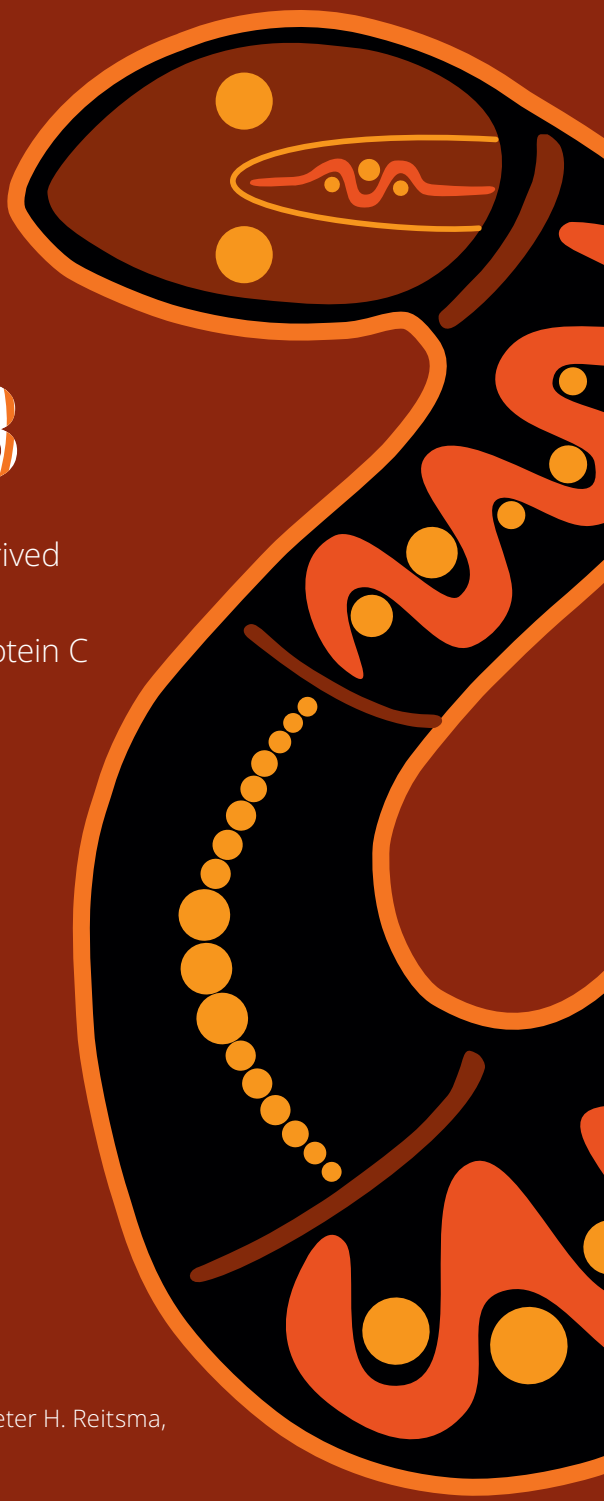
1 Esmon, C. T., Owen, W. G., Duiguid, D. L. & Jackson, C. M. The action of thrombin on blood clotting factor V: conversion of factor V to a prothrombin-binding protein. *Biochim Biophys Acta* **310**, 289-294 (1973).
2 Suzuki, K., Dahlback, B. & Stenflo, J. Thrombin-catalyzed activation of human coagulation factor V. *J Biol Chem* **257**, 6556-6564 (1982).
3 Camire, R. M. & Bos, M. H. The molecular basis of factor V and VIII procofactor activation. *J Thromb Haemost* **7**, 1951-1961, doi:10.1111/j.1538-7836.2009.03622.x (2009).
4 Mann, K. G., Nesheim, M. E., Church, W. R., Haley, P. & Krishnaswamy, S. Surface-dependent reactions of the vitamin K-dependent enzyme complexes. *Blood* **76**, 1-16 (1990).
5 Kalafatis, M. & Mann, K. G. Factor V: Dr. Jeckyll and Mr. Hyde. *Blood* **101**, 20-30 (2003).
6 Nicolaes, G. A. & Dahlback, B. Factor V and thrombotic disease: description of a janus-faced protein. *Arterioscler Thromb Vasc Biol* **22**, 530-538 (2002).
7 Kane, W. H. & Davie, E. W. Cloning of a cDNA coding for human factor V, a blood coagulation factor homologous to factor VIII and ceruloplasmin. *Proc Natl Acad Sci U S A* **83**, 6800-6804 (1986).
8 Jenny, R. J. *et al.* Complete cDNA and derived amino acid sequence of human factor V. *Proc Natl Acad Sci U S A* **84**, 4846-4850 (1987).
9 Bos, M. H. & Camire, R. M. A bipartite autoinhibitory region within the B-domain suppresses function in factor V. *J Biol Chem* **287**, 26342-26351, doi:10.1074/jbc.M112.377168 (2012).
10 Bunce, M. W., Bos, M. H., Krishnaswamy, S. & Camire, R. M. Restoring the procofactor state of factor Va-like variants by complementation with B-domain peptides. *J Biol Chem* **288**, 30151-30160, doi:10.1074/jbc.M113.506840 (2013).
11 Foster, W. B., Nesheim, M. E. & Mann, K. G. The factor Xa-catalyzed activation of factor V. *J Biol Chem* **258**, 13970-13977 (1983).
12 Monkovic, D. D. & Tracy, P. B. Activation of human factor V by factor Xa and thrombin. *Biochemistry* **29**, 1118-1128 (1990).
13 Schuijt, T. J. *et al.* Factor Xa activation of factor V is of paramount importance in initiating the coagulation system: lessons from a tick salivary protein. *Circulation* **128**, 254-266, doi:10.1161/CIRCULATIONAHA.113.003191 (2013).
14 Tans, G. *et al.* Activation of human factor V by meizothrombin. *J Biol Chem* **269**, 15969-15972 (1994).
15 Nesheim, M. E. & Mann, K. G. Thrombin-catalyzed activation of single chain bovine factor V. *J Biol Chem* **254**, 1326-1334 (1979).
16 Dahlback, B. Human coagluation factor V purification and thrombin-catalyzed activation. *J Clin Invest* **66**, 583-591, doi:10.1172/JCI109890 (1980).
17 Rosing, J. *et al.* Effects of protein S and factor Xa on peptide bond cleavages during inactivation of factor Va and factor VaR506Q by activated protein C. *J Biol Chem* **270**, 27852-27858 (1995).
18 Dahlback, B. & Villoutreix, B. O. The anticoagulant protein C pathway. *FEBS Lett* **579**, 3310-3316, doi:10.1016/j.febslet.2005.03.001 (2005).
19 Kalafatis, M., Rand, M. D. & Mann, K. G. The mechanism of inactivation of human factor V and human factor Va by activated protein C. *J Biol Chem* **269**, 31869-31880 (1994).
20 Egan, J. O., Kalafatis, M. & Mann, K. G. The effect of Arg306-->Ala and Arg506-->Gln substitutions in the inactivation of recombinant human factor Va by activated protein C and protein S. *Protein Sci* **6**, 2016-2027, doi:10.1002/pro.5560060922 (1997).
21 Kalafatis, M. & Mann, K. G. Role of the membrane in the inactivation of factor Va by activated protein C. *J Biol Chem* **268**, 27246-27257 (1993).

22 Mann, K. G., Hockin, M. F., Begin, K. J. & Kalafatis, M. Activated protein C cleavage of factor Va leads to dissociation of the A2 domain. *J Biol Chem* **272**, 20678-20683 (1997).
23 Hibbard, L. S. & Mann, K. G. The calcium-binding properties of bovine factor V. *J Biol Chem* **255**, 638-645 (1980).
24 Guinto, E. R. & Esmon, C. T. Formation of a calcium-binding site on bovine activated factor V following recombination of the isolated subunits. *J Biol Chem* **257**, 10038-10043 (1982).
25 Mann, K. G., Lawler, C. M., Vehar, G. A. & Church, W. R. Coagulation Factor V contains copper ion. *J Biol Chem* **259**, 12949-12951 (1984).
26 Song, J., Talbot, K., Hewitt, J., MacGillivray, R. T. & Pryzdial, E. L. Differential contributions of Glu96, Asp102 and Asp111 to coagulation factor V/Va metal ion binding and subunit stability. *Biochem J* **422**, 257-264, doi:10.1042/BJ20090405 (2009).
27 Sorensen, K. W. *et al.* Functional properties of recombinant factor V mutated in a potential calcium-binding site. *Biochemistry* **43**, 5803-5810, doi:10.1021/bi0361362 (2004).
28 Adams, T. E., Hockin, M. F., Mann, K. G. & Everse, S. J. The crystal structure of activated protein C-inactivated bovine factor Va: Implications for cofactor function. *Proc Natl Acad Sci U S A* **101**, 8918-8923, doi:10.1073/pnas.0403072101 (2004).
29 Hansson, K. & Stenflo, J. Post-translational modifications in proteins involved in blood coagulation. *J Thromb Haemost* **3**, 2633-2648, doi:10.1111/j.1538-7836.2005.01478.x (2005).
30 Xue, J., Kalafatis, M. & Mann, K. G. Determination of the disulfide bridges in factor Va light chain. *Biochemistry* **32**, 5917-5923 (1993).
31 Xue, J., Kalafatis, M., Silveira, J. R., Kung, C. & Mann, K. G. Determination of the disulfide bridges in factor Va heavy chain. *Biochemistry* **33**, 13109-13116 (1994).
32 Autin, L., Steen, M., Dahlback, B. & Villoutreix, B. O. Proposed structural models of the prothrombinase (FXa-FVa) complex. *Proteins* **63**, 440-450, doi:10.1002/prot.20848 (2006).
33 Lee, C. J. *et al.* Proposed structural models of human factor Va and prothrombinase. *J Thromb Haemost* **6**, 83-89, doi:10.1111/j.1538-7836.2007.02821.x (2008).
34 Lee, C. J., Wu, S. & Pedersen, L. G. A proposed ternary complex model of prothrombinase with prothrombin: protein-protein docking and molecular dynamics simulations. *J Thromb Haemost* **9**, 2123-2126, doi:10.1111/j.1538-7836.2011.04463.x (2011).
35 Lechtenberg, B. C. *et al.* Crystal structure of the prothrombinase complex from the venom of Pseudonaja textilis. *Blood* **122**, 2777-2783, doi:10.1182/blood-2013-06-511733 (2013).
36 Bos, M. H. *et al.* Venom factor V from the common brown snake escapes hemostatic regulation through procoagulant adaptations. *Blood* **114**, 686-692, doi:10.1182/blood-2009-02-202663 (2009).
37 Pomowski, A., Ustok, F. I. & Huntington, J. A. Homology model of human prothrombinase based on the crystal structure of Pseutarin C. *Biological chemistry* **395**, 1233-1241, doi:10.1515/hsz-2014-0165 (2014).
38 Shim, J. Y., Lee, C. J., Wu, S. & Pedersen, L. G. A model for the unique role of factor Va A2 domain extension in the human ternary thrombin-generating complex. *Biophysical chemistry* **199**, 46-50, doi:10.1016/j.bpc.2015.02.003 (2015).
39 Kojima, Y., Heeb, M. J., Gale, A. J., Hackeng, T. M. & Griffin, J. H. Binding site for blood coagulation factor Xa involving residues 311-325 in factor Va. *J Biol Chem* **273**, 14900-14905 (1998).
40 Kalafatis, M. & Mann, K. G. The role of the membrane in the inactivation of factor va by plasmin. Amino acid region 307-348 of factor V plays a critical role in factor Va cofactor function. *J Biol Chem* **276**, 18614-18623, doi:10.1074/jbc.M007134200 (2001).
41 Kalafatis, M. & Beck, D. O. Identification of a binding site for blood coagulation factor Xa on the heavy chain of factor Va. Amino acid residues 323-331 of factor V represent an interactive site for activated factor X. *Biochemistry* **41**, 12715-12728 (2002).

42 Singh, L. S., Bukys, M. A., Beck, D. O. & Kalafatis, M. Amino acids Glu323, Tyr324, Glu330, and Val331 of factor Va heavy chain are essential for expression of cofactor activity. *J Biol Chem* **278**, 28335-28345, doi:10.1074/jbc.M300233200 (2003).
43 Barhoover, M. A., Orban, T., Beck, D. O., Bukys, M. A. & Kalafatis, M. Contribution of amino acid region 334-335 from factor Va heavy chain to the catalytic efficiency of prothrombinase. *Biochemistry* **47**, 6840-6850, doi:10.1021/bi800057r (2008).
44 Norstrom, E. A., Tran, S., Steen, M. & Dahlback, B. Effects of factor Xa and protein S on the individual activated protein C-mediated cleavages of coagulation factor Va. *J Biol Chem* **281**, 31486-31494, doi:10.1074/jbc.M606441200 (2006).
45 Heeb, M. J., Kojima, Y., Hackeng, T. M. & Griffin, J. H. Binding sites for blood coagulation factor Xa and protein S involving residues 493-506 in factor Va. *Protein Sci* **5**, 1883-1889, doi:10.1002/pro.5560050914 (1996).
46 Gale, A. J., Yegneswaran, S., Xu, X., Pellequer, J. L. & Griffin, J. H. Characterization of a factor Xa binding site on factor Va near the Arg-506 activated protein C cleavage site. *J Biol Chem* **282**, 21848-21855, doi:10.1074/jbc.M702192200 (2007).
47 Steen, M., Villoutreix, B. O., Norstrom, E. A., Yamazaki, T. & Dahlback, B. Defining the factor Xa-binding site on factor Va by site-directed glycosylation. *J Biol Chem* **277**, 50022-50029, doi:10.1074/jbc.M205609200 (2002).
48 Steen, M. *et al.* Mapping of the factor Xa binding site on factor Va by site-directed mutagenesis. *J Biol Chem* **283**, 20805-20812, doi:10.1074/jbc.M802703200 (2008).
49 Bakker, H. M. *et al.* Functional properties of human factor Va lacking the Asp683-Arg709 domain of the heavy chain. *J Biol Chem* **269**, 20662-20667 (1994).
50 Rezaie, A. R. Identification of basic residues in the heparin-binding exosite of factor Xa critical for heparin and factor Va binding. *J Biol Chem* **275**, 3320-3327 (2000).
51 Chattopadhyay, A., James, H. L. & Fair, D. S. Molecular recognition sites on factor Xa which participate in the prothrombinase complex. *J Biol Chem* **267**, 12323-12329 (1992).
52 Kalafatis, M., Xue, J., Lawler, C. M. & Mann, K. G. Contribution of the heavy and light chains of factor Va to the interaction with factor Xa. *Biochemistry* **33**, 6538-6545 (1994).
53 Boskovic, D. S. & Krishnaswamy, S. Exosite binding tethers the macromolecular substrate to the prothrombinase complex and directs cleavage at two spatially distinct sites. *J Biol Chem* **275**, 38561-38570, doi:10.1074/jbc.M006637200 (2000).
54 Krishnaswamy, S. Exosite-driven substrate specificity and function in coagulation. *J Thromb Haemost* **3**, 54-67, doi:10.1111/j.1538-7836.2004.01021.x (2005).
55 Tran, S., Norstrom, E. & Dahlback, B. Effects of prothrombin on the individual activated protein C-mediated cleavages of coagulation factor Va. *J Biol Chem* **283**, 6648-6655, doi:10.1074/jbc.M708036200 (2008).
56 Kalafatis, M., Beck, D. O. & Mann, K. G. Structural requirements for expression of factor Va activity. *J Biol Chem* **278**, 33550-33561, doi:10.1074/jbc.M303153200 (2003).
57 Beck, D. O., Bukys, M. A., Singh, L. S., Szabo, K. A. & Kalafatis, M. The contribution of amino acid region ASP695-TYR698 of factor V to procofactor activation and factor Va function. *J Biol Chem* **279**, 3084-3095, doi:10.1074/jbc.M306850200 (2004).
58 Hirbawi, J., Bukys, M. A., Barhoover, M. A., Erdogan, E. & Kalafatis, M. Role of the acidic hirudin-like COOH-terminal amino acid region of factor Va heavy chain in the enhanced function of prothrombinase. *Biochemistry* **47**, 7963-7974, doi:10.1021/bi800593k (2008).
59 Hirbawi, J., Vaughn, J. L., Bukys, M. A., Vos, H. L. & Kalafatis, M. Contribution of amino acid region 659-663 of Factor Va heavy chain to the activity of factor Xa within prothrombinase. *Biochemistry* **49**, 8520-8534, doi:10.1021/bi101097t (2010).
60 Hirbawi, J. & Kalafatis, M. Spellbinding Effects of the Acidic COOH-Terminus of Factor Va Heavy Chain on Prothrombinase Activity and Function. *ACS omega* **2**, 5529-5537, doi:10.1021/acsomega.7b00769 (2017).

61 Toso, R. & Camire, R. M. Role of Hirudin-like factor Va heavy chain sequences in prothrombinase function. *J Biol Chem* **281**, 8773-8779, doi:10.1074/jbc.M511419200 (2006).
62 Corral-Rodriguez, M. A., Bock, P. E., Hernandez-Carvajal, E., Gutierrez-Gallego, R. & Fuentes-Prior, P. Structural basis of thrombin-mediated factor V activation: the Glu666-Glu672 sequence is critical for processing at the heavy chain-B domain junction. *Blood* **117**, 7164-7173, doi:10.1182/blood-2010-10-315309 (2011).
63 Kotkow, K. J., Deitcher, S. R., Furie, B. & Furie, B. C. The second kringle domain of prothrombin promotes factor Va-mediated prothrombin activation by prothrombinase. *J Biol Chem* **270**, 4551-4557 (1995).
64 Deguchi, H., Takeya, H., Gabazza, E. C., Nishioka, J. & Suzuki, K. Prothrombin kringle 1 domain interacts with factor Va during the assembly of prothrombinase complex. *Biochem J* **321 (Pt 3)**, 729-735 (1997).
65 Huang, M. *et al.* Structural basis of membrane binding by Gla domains of vitamin K-dependent proteins. *Nat Struct Biol* **10**, 751-756, doi:10.1038/nsb971 (2003).
66 Blostein, M. D., Rigby, A. C., Jacobs, M., Furie, B. & Furie, B. C. The Gla domain of human prothrombin has a binding site for factor Va. *J Biol Chem* **275**, 38120-38126, doi:10.1074/jbc.M007174200 (2000).
67 Krishnaswamy, S. & Mann, K. G. The binding of factor Va to phospholipid vesicles. *J Biol Chem* **263**, 5714-5723 (1988).
68 Kalafatis, M., Rand, M. D. & Mann, K. G. Factor Va-membrane interaction is mediated by two regions located on the light chain of the cofactor. *Biochemistry* **33**, 486-493 (1994).
69 Srivastava, A., Quinn-Allen, M. A., Kim, S. W., Kane, W. H. & Lentz, B. R. Soluble phosphatidylserine binds to a single identified site in the C2 domain of human factor Va. *Biochemistry* **40**, 8246-8255 (2001).
70 Saleh, M. *et al.* The factor V C1 domain is involved in membrane binding: identification of functionally important amino acid residues within the C1 domain of factor V using alanine scanning mutagenesis. *Thrombosis and haemostasis* **91**, 16-27, doi:10.1160/TH03-04-0222 (2004).
71 Majumder, R., Quinn-Allen, M. A., Kane, W. H. & Lentz, B. R. A phosphatidylserine binding site in factor Va C1 domain regulates both assembly and activity of the prothrombinase complex. *Blood* **112**, 2795-2802, doi:10.1182/blood-2008-02-138941 (2008).
72 Peng, W., Quinn-Allen, M. A. & Kane, W. H. Mutation of hydrophobic residues in the factor Va C1 and C2 domains blocks membrane-dependent prothrombin activation. *J Thromb Haemost* **3**, 351-354, doi:10.1111/j.1538-7836.2004.01083.x (2005).
73 Majumder, R., Weinreb, G., Zhai, X. & Lentz, B. R. Soluble phosphatidylserine triggers assembly in solution of a prothrombin-activating complex in the absence of a membrane surface. *J Biol Chem* **277**, 29765-29773, doi:10.1074/jbc.M200893200 (2002).
74 Zhai, X., Srivastava, A., Drummond, D. C., Daleke, D. & Lentz, B. R. Phosphatidylserine binding alters the conformation and specifically enhances the cofactor activity of bovine factor Va. *Biochemistry* **41**, 5675-5684 (2002).
75 Qureshi, S. H., Yang, L., Manithody, C. & Rezaie, A. R. Membrane-dependent interaction of factor Xa and prothrombin with factor Va in the prothrombinase complex. *Biochemistry* **48**, 5034-5041, doi:10.1021/bi900240g (2009).
76 Ortel, T. L., Devore-Carter, D., Quinn-Allen, M. & Kane, W. H. Deletion analysis of recombinant human factor V. Evidence for a phosphatidylserine binding site in the second C-type domain. *J Biol Chem* **267**, 4189-4198 (1992).
77 Ortel, T. L., Quinn-Allen, M. A., Charles, L. A., Devore-Carter, D. & Kane, W. H. Characterization of an acquired inhibitor to coagulation factor V. Antibody binding to the second C-type domain of factor V inhibits the binding of factor V to phosphatidylserine and neutralizes procoagulant activity. *J Clin Invest* **90**, 2340-2347, doi:10.1172/JCI116123 (1992).

78 Ortel, T. L. *et al.* Inhibitory anti-factor V antibodies bind to the factor V C2 domain and are associated with hemorrhagic manifestations. *Blood* **91**, 4188-4196 (1998).
79 Ortel, T. L. *et al.* Localization of functionally important epitopes within the second C-type domain of coagulation factor V using recombinant chimeras. *J Biol Chem* **269**, 15898-15905 (1994).
80 Villoutreix, B. O. B., P.; Hofmann, K.; Baumgartner, S.; and Dahlback, B. Molecular Models for the two Discoidin Domains of Human Blood Coagulation Factor V. *Journal of Molecular Modeling* **4**, 8 (1998).
81 Macedo-Ribeiro, S. *et al.* Crystal structures of the membrane-binding C2 domain of human coagulation factor V. *Nature* **402**, 434-439, doi:10.1038/46594 (1999).
82 Nicolaes, G. A., Villoutreix, B. O. & Dahlback, B. Mutations in a potential phospholipid binding loop in the C2 domain of factor V affecting the assembly of the prothrombinase complex. *Blood coagulation & fibrinolysis : an international journal in haemostasis and thrombosis* **11**, 89-100 (2000).
83 Kim, S. W. *et al.* Identification of functionally important amino acid residues within the C2-domain of human factor V using alanine-scanning mutagenesis. *Biochemistry* **39**, 1951-1958 (2000).
84 Peng, W., Quinn-Allen, M. A., Kim, S. W., Alexander, K. A. & Kane, W. H. Trp2063 and Trp2064 in the factor Va C2 domain are required for high-affinity binding to phospholipid membranes but not for assembly of the prothrombinase complex. *Biochemistry* **43**, 4385-4393, doi:10.1021/bi035763o (2004).
85 Majumder, R., Quinn-Allen, M. A., Kane, W. H. & Lentz, B. R. The phosphatidylserine binding site of the factor Va C2 domain accounts for membrane binding but does not contribute to the assembly or activity of a human factor Xa-factor Va complex. *Biochemistry* **44**, 711-718, doi:10.1021/bi047962t (2005).
86 Gilbert, G. E., Novakovic, V. A., Kaufman, R. J., Miao, H. & Pipe, S. W. Conservative mutations in the C2 domains of factor VIII and factor V alter phospholipid binding and cofactor activity. *Blood* **120**, 1923-1932, doi:10.1182/blood-2012-01-408245 (2012).
87 Bevers, E. M., Comfurius, P. & Zwaal, R. F. Changes in membrane phospholipid distribution during platelet activation. *Biochim Biophys Acta* **736**, 57-66 (1983).
88 Heemskerk, J. W., Bevers, E. M. & Lindhout, T. Platelet activation and blood coagulation. *Thrombosis and haemostasis* **88**, 186-193 (2002).
89 Rosing, J., Bakker, H. M., Thomassen, M. C., Hemker, H. C. & Tans, G. Characterization of two forms of human factor Va with different cofactor activities. *J Biol Chem* **268**, 21130-21136 (1993).
90 Kim, S. W. *et al.* Partial glycosylation at asparagine-2181 of the second C-type domain of human factor V modulates assembly of the prothrombinase complex. *Biochemistry* **38**, 11448-11454, doi:10.1021/bi991275y (1999).
91 Nicolaes, G. A., Villoutreix, B. O. & Dahlback, B. Partial glycosylation of Asn2181 in human factor V as a cause of molecular and functional heterogeneity. Modulation of glycosylation efficiency by mutagenesis of the consensus sequence for N-linked glycosylation. *Biochemistry* **38**, 13584-13591 (1999).
92 Bloom, J. W., Nesheim, M. E. & Mann, K. G. Phospholipid-binding properties of bovine factor V and factor Va. *Biochemistry* **18**, 4419-4425 (1979).
93 Du, J., Wichapong, K., Hackeng, K. M. & Nicolaes, G. A. Molecular simulation studies of human coagulation factor VIII C domain-mediated membrane binding. *Thrombosis and haemostasis* **113**, 373-384, doi:10.1160/TH14-02-0180 (2015).



Chapter 3

ptFVa (*Pseudonaja Textilis* Venom-Derived Factor Va) Retains Structural Integrity Following Proteolysis by Activated Protein C

Mark Schreuder, Xiaosong Liu, Ka Lei Cheung, Pieter H. Reitsma, Gerry A.F. Nicolaes, Mettine H.A. Bos

Accepted in Arteriosclerosis, Thrombosis, and Vascular Biology.



Abstract

Objective: The Australian snake venom ptFV (*Pseudonaja textilis* venom-derived factor V) variant retains cofactor function despite APC (activated protein C)-dependent proteolysis. Here, we aimed to unravel the mechanistic principles by determining the role of the absent Arg306 cleavage site that is required for the inactivation of FVa (mammalian factor Va).

Approach and Results: Our findings show that in contrast to human FVa, APC-catalyzed proteolysis of ptFVa at Arg306 and Lys507 does not abrogate ptFVa cofactor function. Remarkably, the structural integrity of APC-proteolyzed ptFVa is maintained indicating that stable non-covalent interactions prevent A2-domain dissociation. Using Molecular Dynamics simulations, we uncovered key regions located in the A1 and A2 domain that may be at the basis of this remarkable characteristic.

Conclusions: Taken together, we report a completely novel role for uniquely adapted regions in ptFVa that prevent A2 domain dissociation. As such, these results challenge our current understanding by which strict regulatory mechanisms control FVa activity.

Introduction

Blood coagulation is a tightly regulated process composed of the sequential and concerted action of several serine proteases and their respective cofactors, together responsible for minimizing blood loss following vascular injury. Central to this process is the activation of coagulation factor V (FV) into the active cofactor Va (FVa)[1-3]. Once FV is partially or fully activated, it functions as cofactor for the serine protease factor Xa (FXa) by formation of the prothrombinase complex on the surface of an anionic membrane in the presence of calcium ions[4,5]. This complex rapidly converts prothrombin to thrombin, a key regulatory enzyme in coagulation. The coagulation system can also be exploited to gain selective advantages. The procoagulant venom of several Australian Elapid snakes contains a powerful enzyme complex that specifically activates prothrombin to disrupt the prey's intrinsic hemostatic balance[6-9]. This prothrombin-activating complex consists of FX- and FV-like proteins[10-13] comprising certain remarkable gain-of-function adaptations that enable this prothrombinase-like complex to initiate coagulation in an uncontrolled manner[14-17]. Rao *et al*[11] and our group[14,18] have demonstrated that venom FV derived from the common brown snake *Pseudonaja textilis* (ptFV), while undergoing selective proteolysis, is functionally resistant to FVa's natural inhibitor activated protein C (APC).

To downregulate the procoagulant response, coagulant FVa is inactivated by APC via proteolysis of the A2 domain residues Arg306, Arg506, and Arg679[19-23]. Cleavage at Arg306 and Arg506 results in A2 domain dissociation and subsequent loss of FXa affinity[24]. While ptFVa is cleaved at a position that is homologous to human Arg506 (Lys507)[14], an Arg306-like cleavage site is absent[11,14]. Furthermore, venom FV comprises a unique disulfide bond that covalently links the A2 and A3 domains[14,16]. Although we have previously reported that this disulfide bond is not responsible for the functional APC resistance[18], whether it might stabilize the A2 domain binding affinity upon introduction of the Arg306 cleavage site remains to be determined.

In the present study, we generated several chimeric ptFV variants with the goal of uncovering the mechanistic principles of its exceptional functional resistance to APC. Our results demonstrate that ptFV has uniquely adapted several structural elements to prevent A2 domain dissociation and ptFVa inactivation. As such, these findings highlight the remarkable evolutionary adaptations that have made ptFVa into an extremely stable procoagulant venom and provide new insights in the structural requirements of APC-induced FVa inactivation.

Materials and Methods

Materials and Reagents: The inhibitor dansylarginine-N-(3-ethyl-1,5-pentanediyl)amide (DAPA) was from Haematologic Technologies (Essex Junction, VT). The peptidyl substrate H-D-Phe-Pip-Arg-pNA (S2238) was obtained from Instrumentation Laboratories (Bedford, MA, USA). All tissue culture reagents were from Life Technologies (Carlsbad, CA, USA). Small unilamellar phospholipid vesicles (PCPS) composed of 75% (wt/wt) hen egg L-phosphatidylcholine (PC) and 25% (wt/wt) porcine brain L-phosphatidylserine (PS) (Avanti Polar Lipids, Alabaster, AL, USA) were prepared and characterized as described previously[25]. FV-depleted human plasma and Neoplastine CI Plus 10 prothrombin time (PT) reagent were obtained from Diagnostica Stago (Paris, France). All functional assays were performed in HEPES buffered saline (HBS: 20 mM HEPES, 0.15 M NaCl, pH 7.5) supplemented with 5 mM $CaCl_2$, 0.1% PEG8000 and filtered over a 0.2 µm filter (assay buffer).

Proteins: The human plasma-derived coagulation factors FXa, prothrombin, α-thrombin, APC, protein S, and plasmin were from Haematologic Technologies (Essex Junction, VT). Restriction endonucleases XcmI and Bsu36I were obtained from New England Biolabs (Ipswich, MA, USA). Recombinant venom-derived *Pseudonaja textilis* FXa (ptFXa) was prepared, purified, and characterized as described[18]. Recombinant constitutively active B-domainless human factor V (FV-810; hFV) and venom-derived ptFV were prepared, purified, and characterized as described previously[14,26]. The molecular weight and the extinction coefficients ($E_{0.1\%,\ 280\ nm}$) of the newly generated hFV-pt306, ptFV-h306, and ptFV-h306 S-S were assumed to be equal to hFV (216,000 kDa; 1.54) and ptFV (163,000 kDa; 1.25), respectively[14,26].

Construction of FV Variants: Constructs encoding for hFV comprising the ptFV Arg306 region (ptFV sequence Gly303-Thr309; Uniprot: Q7SZN0), designated pED-hFV-pt306, and ptFV comprising the human Arg306 region sequence (human full-length FV sequence Pro302-Leu308; Uniprot: P12259), named pED-ptFV-h306 were generated. Subsequently, ptFV's unique disulfide bond (ptFV residues Cys642 and Cys1002[16]; Uniprot: Q7SZN0) was removed by replacing the cysteines for serine residues, thereby creating pED-ptFV-h306 S-S. ptFV-h306 and ptFV-h306 S-S were generated employing mutagenic complementary oligonucleotides as described[14]. The variant hFV-pt306 was generated using a pUC57 plasmid encoding pED-ptFV nucleotides 2124-2144, flanked by pED-hFV nucleotides, which was generated and purchased from Genscript (Piscataway, NJ, USA). The resulting pUC57 plasmid was digested with XcmI and Bsu36I, gel-purified, and subcloned into pED-hFV via digestion with the same enzymes.

Expression and Purification of FV variants: Transfection of the plasmids encoding FV variants into baby hamster kidney cells, the selection of stable clones, and the expression and purification of hFV and ptFV were performed as described previously [14,26]. Briefly, FV proteins were purified employing ion-exchange chromatography on a Q-Sepharose FF (hFV variants) or SP-Sepharose (ptFV variants) column (GE Healthcare) using a NaCl elution gradient in HBS supplemented with 5 mM $CaCl_2$ and 1 mM benzamidine (BZA), pH 7.4. Fractions containing FV activity were pooled and dialyzed against 20 mM HEPES, 5mM $CaCl_2$, pH 7.4 for human FV variants or 20 mM MES, 5 mM $CaCl_2$, pH 6.0 for ptFV variants, loaded on a POROS HQ/20 (hFV variants) or HS/20 column (ptFV variants) (Applied Biosystems) and eluted using a NaCl gradient. Protein purity was assessed by SDS-PAGE analysis using pre-cast 4%–12% gradient gels under nonreducing and reducing conditions (50mM DTT) using the MOPS buffer system (Life technologies; Carlsbad, CA, USA) followed by staining with Coomassie Brilliant Blue R-250. For pretreatment with thrombin, FV variants were incubated for 15 minutes with α-thrombin (molar ratio: hFV 15:1; ptFV 3.75:1) in assay buffer at 37°C, followed by the addition of a 10-fold molar excess of hirudin over thrombin.

Factor Va-dependent Prothrombin Activation: Steady-state initial velocities of macromolecular substrate cleavage were determined discontinuously at 25 °C in assay buffer as described[27,28]. Briefly, unless otherwise stated, progress curves of prothrombin were obtained by incubating PCPS (50 μM), DAPA (10 μM), and prothrombin (1.4 μM) with the various recombinant FV(a) species (0-40 nM), and the reaction was initiated with 0.4 nM of FXa or ptFXa upon which the rate of prothrombin conversion was measured[27].

Activated Protein C-mediated Inactivation of FVa variants: For APC-mediated proteolysis, FVa variants (500 nM) were first incubated at 37 °C with APC (hFVa 10 nM; ptFVa 750 nM) in the presence of PCPS (50 μM). In addition, similar reactions containing ptFVa variants (50 nM) and PCPS (50 μM) were treated with 75 nM APC in the presence of protein S (100nM). Following APC-treatment, aliquots were taken and assayed for cofactor activity. Activity assay mixtures contained prothrombin (1.4 μM), PCPS (50 μM), DAPA (10 μM), APC-proteolyzed hFVa (0.2 nM) or ptFVa variants (0.1 nM), and FXa (2 nM) or ptFXa (1 nM), respectively. Prothrombin activation was determined as described[27]. Identification of the APC cleavage sites by N-terminal sequence analysis was performed at The Protein Facility of the Iowa State University Office of Biotechnology (Ames, IA).

Size-exclusion Chromatography of Activated Protein C-treated FVa Variants: FVa variants (100-500 μg) were subjected to APC treatment (hFVa 154.2 nM; ptFVa 1000 nM) for 15 (hFVa) or 180 min (ptFVa) at 37 °C in the presence of 50 μM PCPS. Reactions were quenched by the addition of 50 μM PPACK and 1 mM BZA. A 10 mm × 300 mm column

containing Superdex 200 Increase (GE Healthcare) was equilibrated in assay buffer supplemented with 50 µM PPACK and 1 mM BZA. The 100-400 µL reaction mixture was then applied to the column and eluted with equilibration buffer at a flow rate of 0.25 mL min^{-1} at room temperature. Fractions (0.25 mL) were collected and analyzed by SDS-PAGE or Western Blot using a polyclonal antibody directed against human FV (Affinity biologicals, Ancaster, Canada) and the monoclonal antibody directed against the Asn307-Arg506 fragment (AHV-5146; Haematologic Technologies, Essex Junction, VT) as described[29].

Molecular Structure Preparation: For molecular dynamics (MD) simulation[30], the 3D structures of hFVa[31] and ptFV (PDB ID: 4BXS) were used to build in missing loops with Loop Modeling suite in YASARA[32]. In addition, to simulate the experimentally used ptFV variant, the original region (303-GNPDTLT-309) was exchanged for the human Arg306 region (302-PKKTRNL-308), and the unique Cys642-Cys1002 disulfide bond was disrupted. To mimic the APC-cleaved protein structure, both human and *P. textilis* FV were separated into two protein fragments, reflecting their state after cleavage by APC at Arg306 and Arg506/Lys507. To expedite simulations, the C1 and C2 domain structures were excluded from simulation for both the human and *P. textilis* FV structures, given that these domains are structurally non-related with the A2 domain.

Molecular Dynamics: Each simulation system was solvated with an explicit TIP3P water model and neutralized by addition of Cl- or Na+ ions. The topology and coordinate files were prepared with the Amber *ff14SB*[33] force field. During MD simulations, two initial energy minimization runs were performed using a steepest descent algorithm of 50,000 steps. Subsequently, each system was gradually heated from 0 K to 300 K within 50 ps. This step was followed by another 50 ps equilibration run with a constant temperature of 300 K. After that, a 100 ns production run was carried out using the SHAKE algorithm[34] to constrain bonds involving hydrogen atoms. The minimization, heating, equilibration, and production runs were all applied using AMBER 16[35].

Binding Free Energy Calculations and Per-residue Free Energy Decomposition Analysis: From the 100 ns production run trajectory, 2000 frames were extracted between t=0-20 ns and t=80-100 ns, to calculate binding free energies. The Molecular Mechanics/Generalized Born Surface Area (MM/GBSA) method[36] was successfully employed using igb = 5 GB model in AMBER, which can be briefly summarized by the following equations:

$$\Delta G_{binding} = G_{complex} - G_{receptor} - G_{ligand} \quad (1)$$

$$\Delta G_{MM/GBSA} = E_{int} + E_{ele} + E_{vdW} + E_{polar} + E_{nonpolar} - T\Delta S \quad (2)$$

The binding free energy was calculated as the differences between free energy of the complex and the sum of the separate receptor and ligand shown in equation (1). The relative free energy DGMM/GBSA was estimated by the sum of every component in equation (2), with E_{int}, E_{ele} and E_{vdW} representing internal, electrostatic and van der Waals interactions; the solvation contribution is shown with E_{polar} and $E_{nonpolar}$. The TDS term represents the contribution of entropy which was not taken into account when calculating relative binding free energies in our study. To determine key residues involved in binding, a per-residue energy contribution was calculated and analyzed based on the same factors used in above calculations.

Statistical Analysis: All statistical analyses were computed using the GraphPad Prizm software. Kinetic data were analyzed by nonlinear regression using a three-parameter logistic function or an one-phase decay function. Statistical significance was accepted for p-value of <0.05. All data are presented as mean ± 1 standard deviation and are the result of at least two to three independent experiments, unless otherwise stated.

Results

Expression and Characterization of FV Variants. Previously we reported that ptFV retains full cofactor activity despite APC-catalyzed proteolysis[11,14]. APC cleaves the ptFV A2 domain at Lys507 and Arg742, homologous to human Arg506 and Arg709, respectively. Intriguingly, sequence analysis revealed the lack of a potential Arg306 cleavage site and a non-conserved sequence relative to mammalian FV consisting of ptFV residues 303-GNPDTLT-309 (**Figure 1A**). The GNPDTLT region is well-conserved in various snakes and reptile species, suggesting that the FV Arg306 cleavage site has been introduced at a later stage in evolution relative to Arg506. As the corresponding region is strictly conserved in mammals, we exchanged the ptFV residues GNPDTLT with the corresponding human Arg306 region (302-PKKTRNL-308) of constitutively active B-domainless hFV (**Figure 1B**) to generate the chimeric variants hFV-pt306 and ptFV-h306 (**Figure 1C**). Since a unique disulfide bond in ptFV covalently links the A2 and A3 domains[16], this structural element could potentially prevent A2 domain dissociation and ptFVa inactivation. To exclude the contribution of this disulfide bond to ptFVa inactivation, we generated an additional variant based on ptFV-h306 in which the cysteines involved were substituted by serines, generating ptFV-h306 S-S (**Figure 1C**). The FV variants were stably expressed in BHK cells and purified to homogeneity by ion-exchange chromatography. Each thrombin-activated FVa variant migrated on SDS-PAGE similar to recombinant wild-type hFVa or ptFVa (**Figure 1D**). In addition, SDS-PAGE analysis confirmed that the unique disulfide bond was preserved in ptFV-h306 but eliminated in ptFV-h306 S-S. Functional assessment of each FV variant

revealed a similar apparent affinity for their respective FXa species (**Table I** in the Data Supplement), indicating that substitution of the Arg306 region does not interfere with cofactor-FXa assembly.

ptFVa Variants Maintain Cofactor Function Upon Proteolysis by APC. We next assessed APC-mediated proteolysis of the ptFVa variants comprising the two major APC cleavage sites that are essential for the inactivation of mammalian FVa[21,24]. Thrombin-activated FVa variants were subjected to APC and the resulting cleavage pattern was analyzed by SDS-PAGE. While in hFVa variants full proteolysis was achieved in 15 min by 10 nM APC, high concentrations of APC (750 nM) were required for significant proteolysis of the ptFVa variants. As previously described[14], ptFVa was cleaved at Lys507 (**Figure IA** in the Data Supplement), which is equivalent to human Arg506. Conversely, we observed additional protein bands consistent with the cleavage of Arg306 in ptFVa-h306 (**Figure 2A**). N-terminal sequencing of the cleavage products confirmed the generation of a ptFVa variant comprising the homologous Arg306 and Arg506 cleavage sites (**Figure II** in the Data Supplement). Removal of the unique disulfide bond in ptFVa-h306 S-S did not affect the cleavage pattern relative to ptFVa-h306 (**Figure IB** in the Data Supplement). Moreover, while hFVa was proteolyzed at Arg306, Arg506, and Arg679 (**Figure IC** in the Data Supplement), an Arg306-like cleavage was absent in hFVa-pt306 (**Figure 2B**), demonstrating that the GNPDTLT region in ptFV is not targeted by APC.

Subsequently, the cofactor activity of the APC-proteolyzed FVa variants was assessed. Whereas hFVa was fully inactivated within 5 minutes, functional analysis employing a purified prothrombinase assay revealed partial inactivation of hFVa-pt306 by APC, in a manner similar to the previously characterized hFVa-Arg306Thr variant[37] (**Figure 2C**). Surprisingly, despite introduction of the Arg306 cleavage site and removal of the unique disulfide bond, both chimeric ptFVa variants maintained full cofactor activity during APC-treatment (**Figure 2C**). In addition, assessment of the ptFVa cofactor activity following an initial APC-treatment in the presence of protein S, a cofactor for APC[38,39], revealed identical results (**Figure 2D**). These findings indicate that the absence of a Arg306-like cleavage site and presence of ptFVa's unique disulfide bond do not contribute to the molecular mechanism that is at the basis of ptFVa's functional APC-resistance.

ptFV Retains Structural Integrity Following APC-mediated Proteolysis. APC-catalyzed proteolysis at the two major FVa cleavage sites Arg306 and Arg506 is known to result in A2 domain dissociation[24]. Since our ptFVa variants maintain full cofactor activity following APC-treatment, we hypothesized that despite selective proteolysis, A2 domain dissociation is prevented. Initial observations employing Native-PAGE analysis suggested

that APC-mediated proteolysis resulted in the fragmentation of hFV, whereas ptFV and ptFV-h306 S-S migrated as single molecules (**Figure SIII** in the Data Supplement). Intriguingly, our results show that non-proteolyzed hFV migrated as multiple species. Although the individual species could not be identified, this observation might be explained by the presence of impurities (~30 and 51 kDa, **Figure 2A**). Alternatively, these results could reflect partial glycosylation at Asn2181, leading to the 71/74 kDa hFVa light chain (Lane 1, **Figure 2A**)[40]. Nevertheless, the observation that APC-proteolyzed hFV migrates markedly different on native-PAGE relative to untreated hFV hints towards the fragmentation of the hFV protein. To explore the structural consequences of proteolysis in more detail we determined the structural integrity of the APC-treated ptFVa variants by size-exclusion chromatography. Following APC treatment, the proteolyzed FVa variants were applied to a 10 x 300 mm Superdex 200 Increase column and fractions were collected and analyzed by SDS-PAGE or Western blotting. In accordance with the native-PAGE, size-exclusion profiles suggested the fragmentation of APC-treated hFVa (**Figure 3A**), whereas a single elution peak was observed for APC-cleaved ptFVa (**Figure 3B**). The elution profile of APC-treated ptFVa-h306 S-S was comparable to that of ptFVa following APC treatment (**Figure 3C**), although an additional elution peak was observed as a result of impurities (**Figure 3F**). As expected from previous observations[24], the two hFVa A2 domain fragments Asn307-Arg506 and Gly507-Arg679 migrated separately from the rest of the molecule (A1-A3-C1-C2 domains) (**Figure 3D**). Conversely, ptFVa eluted as a single complex (**Figure 3E**), corroborating our functional data. Remarkably, despite introduction of the Arg306 region and deletion of the unique disulfide bond, ptFVa-h306 S-S retained structural integrity following proteolysis by APC (**Figure 3F**). The size-exclusion profile of ptFVa-h306 S-S displayed a shoulder in the elution peak which could indicate that the A2 domain has dissociated in a small portion of the total APC-treated FVa pool. As such, these results demonstrate that the dissociation of the ptFVa A2 domain is prevented by non-covalent interactions. Functional analysis of the chimeric FVa variants under conditions of high temperatures (**Figures IVA-B** in the Data Supplement) or high ionic strength (**Figure IVC** in the Data Supplement) did not reveal significant differences relative to wild-type FVa, suggestive of an enhanced A2 domain binding stability. Interestingly, proteolysis by the fibrinolytic serine protease plasmin revealed a striking decrease in ptFVa cofactor activity (**Figure VA** in the Data Supplement). While the loss of cofactor activity was comparable to wild-type FVa, all ptFVa variants retained up to 20% cofactor activity despite that full proteolysis was achieved within 5 minutes (**Figures VB-F** in the Data Supplement). These findings provide additional support for an enhanced structural stability of essential functional regions in ptFVa.

Stable Binding Free Energy for the A1-A2-A3 Domains of APC-proteolyzed ptFVa-h306 S-S during MD Simulations. In order to gain more insight into the structural stability of human and *P. textilis* FV, 100ns MD simulations were performed on hFVa and ptFVa-h306 S-S. The model of ptFVa-h306 S-S was generated from the X-ray structure of ptFV (PDB ID: 4BXS) in which 303-GNPDTLT-309 was substituted for the corresponding human Arg306 region and the Cys642-Cys1002 disulfide bond was disrupted. In addition, the peptide bonds that resemble Arg306 and Arg506/Lys507 cleavage were hydrolyzed in both FVa models to simulate an APC-proteolyzed state, and the C1-C2 domains were excluded from the MD simulations. Calculation of the free energies for the interaction between the A2 and A1-A3 domains revealed that these were comparable for hFVa and ptFVa-h306 S-S during the initial trajectory of the simulation (t=0-20ns), with a binding free energy of -76 ± 25 kcal/mole for hFVa and -76 ± 14 kcal/mole for ptFVa-h306 S-S (**Table 1**). However, in the final part of the MD trajectory (t=80-100ns), the binding free energy was remarkably increased to -39 ± 16 kcal/mole for hFVa, whereas a substantial decrease to -90 ± 14 kcal/mole was observed for ptFVa-h306 S-S. This suggests that over the course of the MD simulation, hFVa lost important interactions that facilitate the binding of the A2 to the A1-A3 domains. To examine these interdomain interactions in more detail, the binding free energies between the A2 and A1 or A2 and A3 domains were individually assessed. Interestingly, a loss of interaction between the A2 and A1 domains in hFVa was observed for the t=80-100ns interval (4 ± 10 kcal/mole, **Table 2**), while the binding free energy characterizing the A2-A3 interaction was nearly identical for both MD trajectories monitored. In contrast, the binding free energy between the A2-A1 or A2-A3 domains in ptFVa-h306 S-S remained unaffected during the simulations, indicative of a stable interaction. As such, these data confirm our *in vitro* studies by indicating that the structural integrity of the A1-A2-A3 domains in *P. textilis* FV is maintained following APC cleavage.

Stable Hydrogen Bond Pairs between the A2 and A1-A3 Domains Preserve A2 Domain Association in *P. textilis* FV. To further uncover the molecular mechanisms that are at the basis of the differential A2-A1 domain interactions observed for hFV and ptFV, the hydrogen bonds that contribute to the overall interdomain binding affinities were assessed. In accordance with the loss of A2-A1 domain interaction, the number of hydrogen bonds between the surfaces of the A2 and A1 domain in hFVa reduced over time during the MD simulations (**Figure 4A**). Representative structural snapshots revealed significant conformational changes in the A2 domain, suggesting that the A1 domain interacting regions are highly flexible following APC-catalyzed proteolysis (**Figures 4B-C**). In contrast, the number of hydrogen bonds formed between the A2 and A3 domains remained in a dynamic equilibrium during the simulation (**Figures 4D-F**), corroborating the stable A2-A3 binding affinity. The hydrogen bond formation

between the A2-A1 and A2-A3 domains in APC-proteolyzed ptFVa-h306 S-S appeared to be balanced and most hydrogen bonds persisted during the simulation (**Figures 4G-L**). These stable interactions might be explained by the conformational constraints of the A2 domain, since only minor structural changes in the binding surfaces were observed between structures at different timepoints. Identification of residues involved in key hydrogen bond interactions during >20% of the MD simulations demonstrated ptFVa-h306 S-S to accommodate a larger fraction of these interactions relative to hFVa (**Figure 5, Table SII** in the Data Supplement). Collectively, these findings indicate that ptFV comprises a high number of A2-A1 interactions that are preserved upon APC cleavage.

A Unique Loop Conformation in the A2 Domain Prevents A2 Domain Dissociation in *P. textilis* FV. Structural comparison of the MD simulations revealed that the A2 domain of hFVa and ptFVa-h306 S-S adopt strikingly different conformations (**Figure 4**). In hFVa, we observed a major conformational change in a surface-exposed A2 domain loop (loop2) that is extended into the solvent and interacts with an A1 domain loop (loop1) via one stable interaction pair (Glu20-Arg439; **Figures 4, VA** in the Data Supplement). While human and *P. textilis* FVa share 55% sequence identity, the positioning of loop1 and loop2 is conserved (**Figure SVI** in the Data Supplement). In addition, sequence analysis showed that loop2 is well-conserved in reptiles, whereas a significantly different sequence is conserved in mammalian FV (**Figure SVII** in the Data Supplement). Interestingly, MD simulations in ptFVa-h306 S-S indicated that loop2 is more compact and does not interact with loop1 (**Figures 4,5B**). Supporting the structural observations, assessment of the solvent accessible surface area (SASA) of individual A domains or A domain complexes over the MD trajectories further revealed that the SASAs of ptFVa-h306 S-S were smaller relative to hFVa (**Figure SVIII** in the Data Supplement). This was found to be the result of a more compact A2 domain, as compared to the A1-A3 domains. To specifically determine the role of loop2 in A2 domain stability, we created an *in silico* chimeric hFVa structure in which the human loop2 was exchanged for the homologous ptFV loop2 region (hFVa-ptloop2), upon which a 100ns MD simulation was performed (**Figure 6A**). As substitution of loop2 destabilized the structure and required several nanoseconds to adopt a stable state, we excluded the initial 20ns from our analysis. Intriguingly, the A2 domain binding free energy in hFVa-ptloop2 was markedly decreased relative to hFVa (hFVa-ptloop2, -64 kcal/mole; hFVa, -39 kcal/mole), although it remained higher compared to ptFVa-h306 S-S (**Table 1**). In similar fashion, exchange of loop2 substantially decreased the average A2 domain SASA (15846.2 ± 0.05 $Å^2$) as compared to hFVa (16689.3 ± 0.04 $Å^2$), but remained larger relative to ptFVa-h306 S-S (14761.8 ± 0.04 $Å^2$), illustrating the compact conformation of the ptFV loop2. Consistent with these findings, the A2-A1 domain hydrogen bonds were stabilized in chimeric

hFVa-ptloop2, while the exchange of loop2 did not affect the interactions between the A2 and A3 domains (**Figures 6B-D**). Nonetheless, we cannot exclude that differences in hydrogen bond pairing between the A2 and A3 domains contribute to the decreased binding free energy for A2 domain binding in hFVa-ptloop2. Collectively, this structural bioinformatics analysis indicates that the compact and inflexible ptFV loop2 stabilizes the surface interactions between the A2 and A1 domains following APC proteolysis and could provide a mechanism that prevents A2 domain dissociation in ptFVa.

Discussion

One of the essential characteristics underlying any hemostatic response is the timely inactivation of proteases and cofactors following proteolytic activation of their respective substrate. The specialized mechanisms of the anticoagulant system thereby prevent uncontrolled blood clotting and life-threatening thrombotic events. Our work, amongst others[11,14,18], highlights the importance of strict regulatory pathways for FV and shows that bypassing these mechanisms can be used as a potent weapon to gain evolutionary advantages.

We previously speculated that absence of the Arg306 cleavage site, required for the inactivation of mammalian FVa, is at the basis of the functional APC-resistance in ptFVa[14,18]. To test this hypothesis, chimeric ptFV variants were generated that lack the unique A2-A3 domain disulfide bond and/or comprise the human Arg306 region. Our functional assessments show that despite Arg306 cleavage and disruption of the unique disulfide bond, ptFVa retains cofactor activity upon APC-catalyzed proteolysis. As such, our findings demonstrate that these elements in ptFV do not play a role in the functional resistance to APC.

Liver-derived ptFV shares 96% sequence identity to its venom paralog[41] and we previously revealed that liver-expressed ptFV shares the procoagulant characteristics of venom-derived ptFV, including the functional resistance to APC[18]. These observations raise fundamental questions on the hemostatic regulatory mechanisms in *P. textilis*. It is currently unknown whether Elapidae express protein C, but if so, it would be of interest to characterize the mechanistic principles that hallmark the anticoagulant response in these snakes. It is also important to note that Arg306 is only conserved in mammals, whereas lower vertebrates do not seem to comprise an homologous Arg306 cleavage site. This indicates that lower vertebrates have a distinct mechanism to inactivate FVa. It has been suggested that reptiles have a primitive intrinsic coagulation pathway and a complete lack of factor XI and factor XII[42-46]. The absence of these factors may favor a more procoagulant system that is required to generate sufficient amounts of

thrombin. Interestingly, our findings revealed that similar to human FVa[47,48], plasmin was able to proteolyze and significantly reduce the cofactor activity of ptFVa, although a 20-fold higher plasmin concentration was required to obtain fully proteolyzed ptFVa. Considering that the plasma concentration of plasminogen is ~2 μM[49], these results could suggest that plasmin plays a physiological role in the regulation of liver-expressed ptFVa. Since the generation of plasmin is taking place at a later stage of hemostasis relative to the activation of protein C, these results may support the hypothesis that liver-expressed ptFV has a more procoagulant role. In contrast, liver- and venom-derived ptFX share ~76% sequence identity[50]. This may indicate that venom-derived ptFX underwent evolutionary adaptations in order to circumvent negative regulatory mechanisms and could potentially suggest that the activity of the liver-expressed ptFVa-ptFXa complex is primarily regulated by antithrombin or tissue factor pathway inhibitor.

Using size-exclusion chromatography, we showed that despite APC-mediated proteolysis A2 domain dissociation in ptFVa is prevented. Remarkably, the A2 domain remained associated following introduction of the Arg306 cleavage site in ptFVa. Attempts to weaken the non-covalent structural integrity of the APC-treated ptFVa variants failed to significantly impact their ability to function as cofactor for ptFXa. These results demonstrate that following selective proteolysis ptFVa maintains structural integrity mediated by strong non-covalent interactions. Strikingly, these findings contradict our current understanding of FVa inactivation[51] and imply the presence of unique structural elements that prevent A2 domain dissociation in ptFVa.

In an attempt to unravel the mechanistic principles of A2 domain association, we identified a potential crucial role for A1-A2 domain interactions. In hFVa, the binding free energy between the A1 and A2 domain increases drastically upon APC-mediated proteolysis. As a consequence, the interaction between the A1 and A2 domain is lost which seemingly triggers the dissociation of the A2 domain. The loss of A1-A2 domain binding affinity coincides with a major conformational change in the hFVa loop2. This highly flexible loop engages in weak interactions with the A1 domain loop1 and facilitates several A1-A2 domain hydrogen bonds. Upon APC-catalyzed proteolysis, the number of hydrogen bonds between the surfaces of the A2 and A1 domains reduces as a result of the conformational changes in the A2 domain. Conversely, the A1-A2 domain binding free energy remains stable following APC-catalyzed cleavage of ptFVa. In contrast to hFVa, the ptFVa loop2 does not interact with loop1 and adopts a rigid conformation that is stabilized by several key hydrogen bonds. Exchange of the ptFV loop2 to hFVa significantly improved the binding affinity between the A2 and A1-A3 domains, providing further support for the central role of loop2 in the A2 domain association. Interestingly, loop2 is located directly distal from the Arg306 cleavage site,

which may suggest that the stable non-covalent interactions are able to compensate for Arg306 cleavage. Additionally, it is possible that ptFXa comprises a structural element that supports the functional APC resistance of ptFVa. Productive interactions between the proteolyzed ptFVa A2 domain and ptFXa could stabilize the conformation of ptFVa in such way that it is able to fulfill its role as cofactor. Moreover, the anionic membrane layer could be another stabilizing factor that allows for cofactor activity following APC-proteolysis. Although the ptFVa-ptFXa complex is able to convert prothrombin in the absence of membranes, it is currently unknown whether functional resistance to APC is maintained when anionic phospholipids are absent. Previous reports proposed that binding of FVa to anionic phospholipids induces conformational changes in the A2 domain that present a FXa interaction site[52,53]. Whether such interactions are required for the procoagulant enhancements in ptFVa remains to be determined.

Overall, characterization of the mechanistic principles and identification of key regions or residues responsible for ptFV's functional resistance to APC could provide unique opportunities for the generation of novel stable FV variants. Our findings might suggest that substitution of human loop2 for the corresponding region in ptFV could create a human FV variant with an improved intrinsic stability resulting from the increased A1-A2 domain binding affinity. Such a FV variant could have an additional advantage over previously reported Arg306Gln/Arg506Gln FV variants, since it will retain procoagulant activity independent of potential APC cleavage. It has been reported that mutation of the three APC cleavage sites in FVa results in FVa inactivation via APC-mediated proteolysis at alternative positions in the A2 domain[29,54]. Moreover, FV has an important role as cofactor for APC in the inactivation of factor VIIIa[55], a crucial reaction to downregulate the procoagulant response[56]. This anticoagulant role is dependent on the cleavage of Arg506 by APC[57,58] and as such this function is absent in Arg506-mutated FV variants.

In conclusion, our findings highlight the exceptional structural features that have converted ptFV into an extremely procoagulant protein. Here we demonstrated that ptFVa maintains functional resistance to APC despite introduction of the Arg306 cleavage site, in sharp contrast to the APC response of mammalian FVa. To do so, ptFV has uniquely adapted non-covalent interactive regions in the A1 and A2 domains that stabilize the A2 domain following proteolysis by APC. Taken together, our findings provide evidence for a unique structural element by which ptFV circumvents the regulatory mechanisms and shed new insights on the mechanistic principles of A2 domain dissociation and FVa inactivation.

Figures

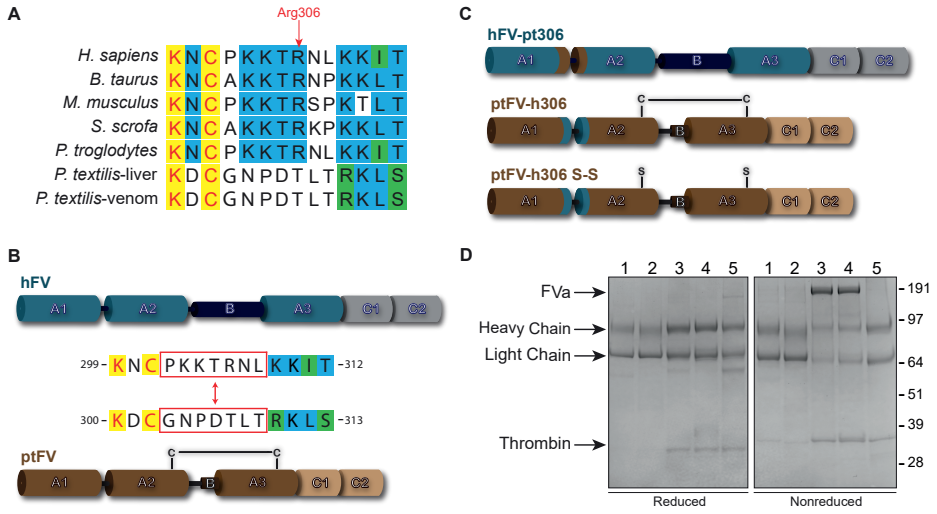


Figure 1. Generation and SDS-PAGE analysis of purified factor Va variants. (A) Sequence alignment of the Arg306 region. Completely conserved residues are highlighted in yellow, partly conserved residues in blue, and residues belonging to the same classification are indicated in green. **(B)** Schematic representation of B domain truncated human FV (hFV) and venom-derived *P. textilis* FV (ptFV). The Arg306 region indicated by the red boxes was exchanged between hFV and ptFV. **(C)** Schematic representation of generated FV variants. Human regions are indicated in blue/grey, ptFV regions are brown/beige. Swapping the Arg306 region generated hFV-pt306 and ptFV-h306. Additional removal of the disulfide bond by replacing the cysteines (Cys642 and Cys1002) for serines in ptFV generated ptFV-h306 S-S. **(D)** SDS-PAGE of purified thrombin-activated FVa variants (2 µg per lane) under reducing (left panel) and non-reducing (right panel) conditions visualized by staining with Coomassie Brilliant Blue R-250. Lane 1, hFVa; lane 2, hFVa-pt306; lane 3, ptFVa; lane 4, ptFVa-h306; lane 5, ptFVa-h306 S-S. Relevant fragments and the apparent molecular weights of the standards are indicated.

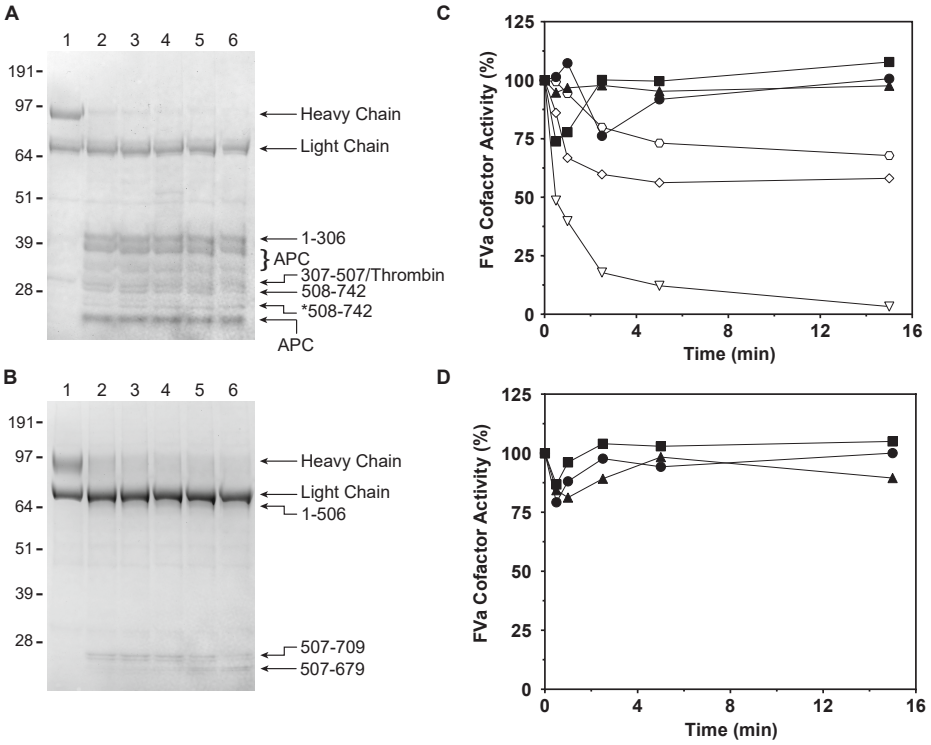


Figure 2. Activated protein C-mediated proteolysis of human and *P. textilis* factor Va variants. (A-B) SDS-PAGE of activated protein C (APC)-treated ptFVa-h306 **(A)** and hFVa-pt306 **(B)** (3 µg per lane) under reducing conditions and visualized by staining with Coomassie Brilliant Blue R-250. Lanes 1-6 represent time samples quenched at 0, 0.5, 1, 2.5, 5, and 15 min. Relevant FVa fragments and the apparent molecular weights of the standards are indicated. We hypothesize that *508-742 is cleaved at a C-terminal position because its N-terminal sequence was determined to be the same as 508-742 (see Supplementary Figure II). **(C-D)** Reaction mixtures containing **(C)** 50 µM PCPS and 500 nM hFVa (open triangles), hFVa-pt306 (open diamonds), or hFVa-Arg306Thr (open hexagons) were incubated with 10 nM APC and similar mixtures containing 500 nM ptFVa (closed circles), ptFVa-h306 (closed squares) or ptFVa-h306 S-S (closed triangles) were incubated with 750 nM APC. In addition, similar reactions containing **(D)** PCPS (50 µM) and ptFVa variants (50 nM) were treated with 75 nM APC in the presence of protein S (100nM). **(C-D)** At selected time intervals, samples were removed for cofactor activity by determining the initial velocity of prothrombin conversion. The data are representative of three independent experiments.

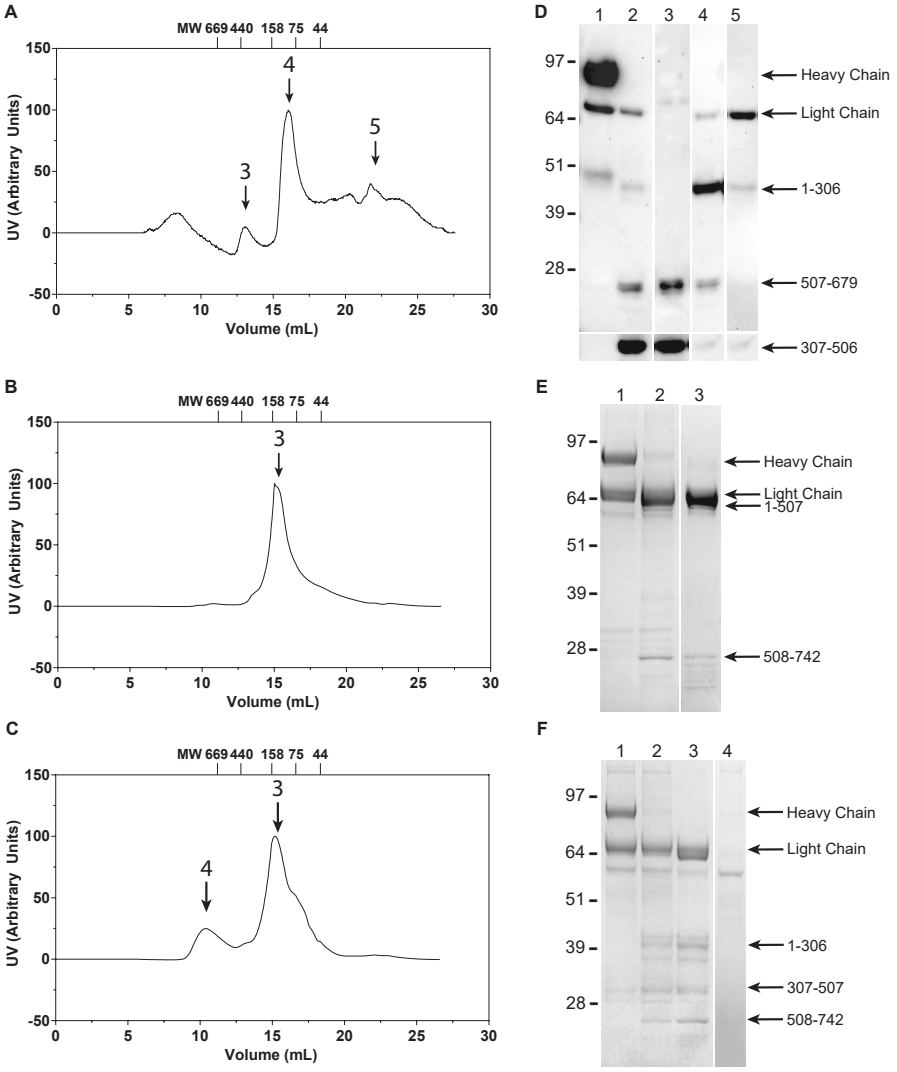


Figure 3. Size-exclusion chromatography of activated protein C-treated FVa variants. (A-C) Size-exclusion elution profiles of APC-treated hFVa **(A)**, ptFVa **(B)**, or ptFVa-h306 S-S **(C)** performed as detailed in 'Materials and Methods'. Arrows and numbers indicate the respective fractions shown in **D-F**. MW, molecular weight. **(D)** Western blot analysis of hFVa under reducing conditions following proteolysis by APC and size-exclusion chromatography elution. Lane 1, thrombin-activated hFVa; lane 2, APC-treated hFVa; lane 3, A2 domain fraction; lane 4, A1-A3-C1-C2 and A2 domain fraction; lane 5, A1-A3-C1-C2 domains fraction. **(E-F)** SDS-PAGE of APC-treated ptFVa **(E)** or ptFVa-h306 S-S **(F)** following size-exclusion chromatography under reducing conditions and visualized by staining with Coomassie Brilliant Blue R-250. Lanes 1, thrombin-activated ptFVa variant; lanes 2, APC-treated ptFVa variant; lanes 3 and 4, elution fractions indicated by the black arrows and numbers in **B-C**. Relevant FVa fragments and the apparent molecular weights of the standards are indicated. The data are representative of two independent experiments. Panels **D-F** are composed of two Western Blots or SDS-PAGE gels, respectively.

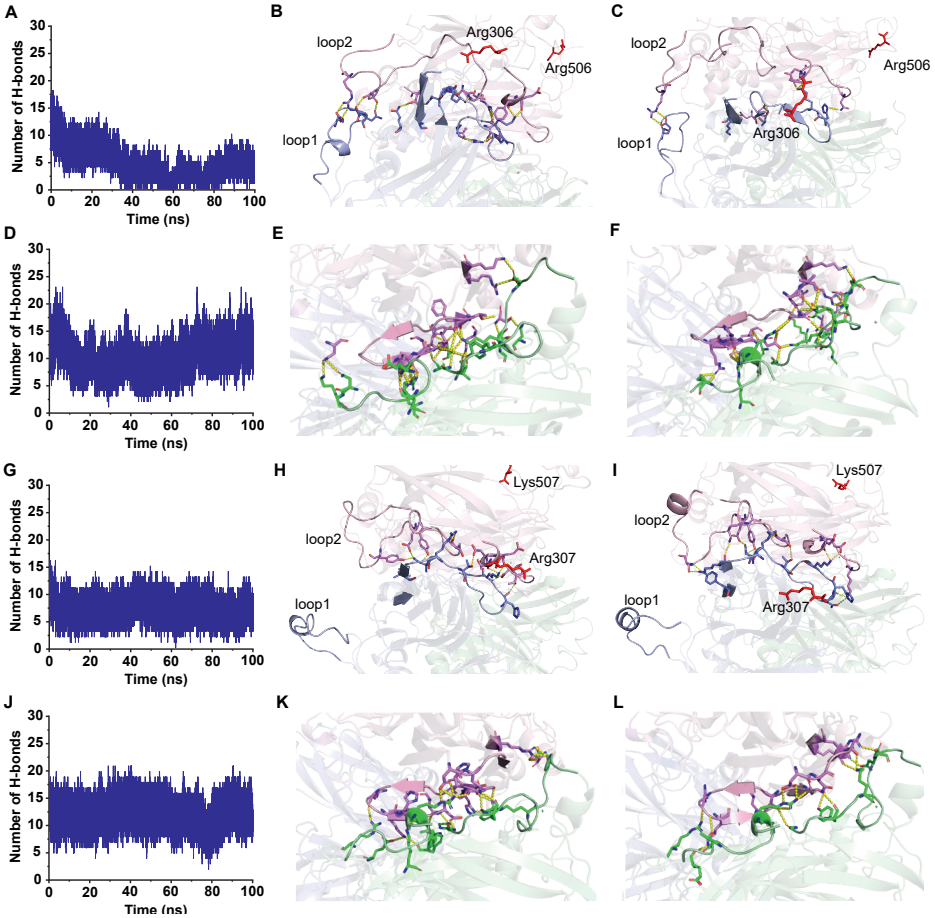


Figure 4. Comparison of interdomain hydrogen bonds between surfaces of the A2 and the A1/A3 domains in human and *P. textilis* FV. The structural conformation and interdomain hydrogen bonds between the surfaces of the A2 and A1 **(B-C, H-I)** or A2 and A3 **(E-F, K-L)** domains are shown at the start (t=0ns) **(B, E, H, K)** and end (t=100ns) **(C, F, I, L)** of the hFVa **(B-C, E-F)** and ptFVa-h306 S-S **(H-I, K-L)** MD simulations. The A1, A2, and A3 domains are indicated in blue, pink, and green, respectively. Residues that engage in hydrogen bond formation and the APC cleavage sites (hFVa, Arg306, Arg506; ptFVa, Arg307, Lys507) are shown in stick configuration, with the latter highlighted in red. Hydrogen bonds are indicated by the yellow dashed lines. The A1 domain loop1 and A2 domain loop2 represent the identified unique loop conformations. **(A, D, G, J)** Interdomain hydrogen bonds between the A2 and A1 **(A, G)** or A2 and A3 **(D, J)** domains were quantified during a 100ns MD simulation of hFVa **(A, D)** and ptFVa-h306 S-S **(G, J)**.

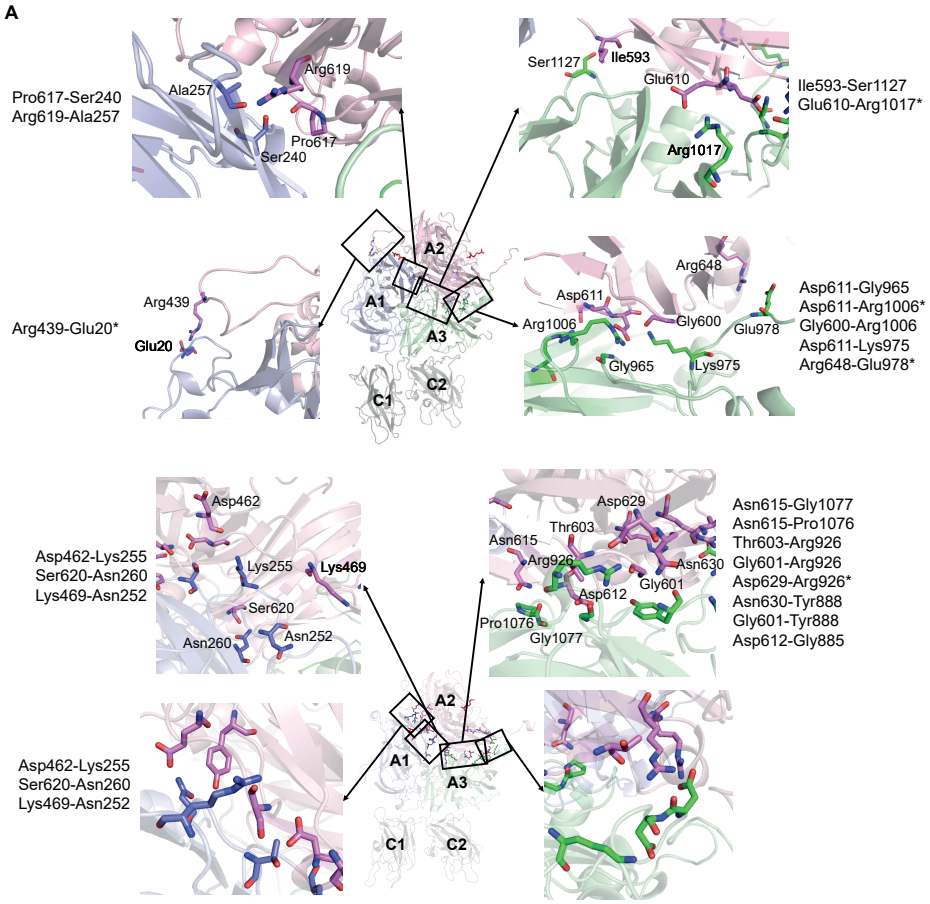


Figure 5. Structural representation of residues involved in key A2-A1 or A2-A3 domain hydrogen bond interaction pairs. (A-B) Residues involved in key hydrogen bond interactions, as defined in 'Materials and Methods', between the A2 domain (pink) and the A1 (blue) or A3 domain (green) in hFVa **(A)** or ptFV **(B)**, and the APC cleavages sites (Arg306, Arg506) are shown in stick configuration, with the latter highlighted in red. The inserts display zoomed-in regions and depict the interaction pairs. The A1, A2, A3, C1, and C2 domains are indicated. * Denotes charged interactions.

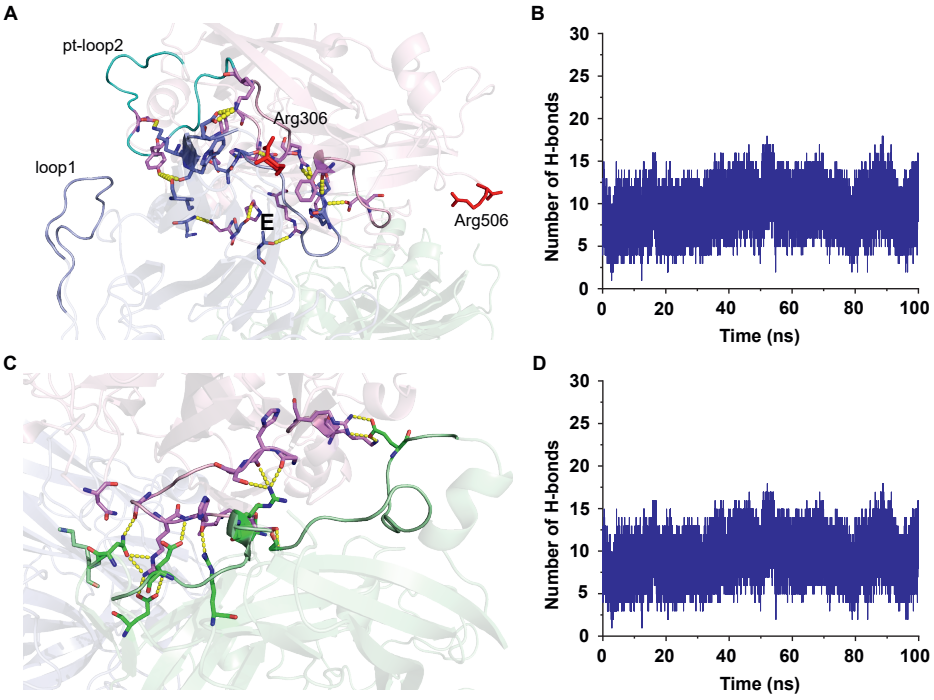


Figure 6. Stable hydrogen bond formation between the A2 and A1 domains upon substitution of human loop2 for the corresponding region in *P. textilis* FV. *In silico* exchange of loop2 in hFVa for the homologous loop2 in ptFV generated a chimeric hFVa variant. **(A, C)** Interdomain hydrogen bonds between the surfaces of the A2 and A1 **(A)** or A2 and A3 **(C)** domains are shown in a representative snapshot of the 100ns MD simulation of chimeric hFVa. The A1, A2, and A3 domains are indicated in blue, pink, and green, respectively. Residues that engage in hydrogen bond formation and the APC cleavage sites (Arg306, Arg506) are shown in stick configuration, with the latter highlighted in red. Hydrogen bonds are indicated by the yellow dashed lines. **(B, D)** Interdomain hydrogen bonds between the A2 and A1 **(B)** or A2 and A3 **(D)** domains were quantified during a 100ns MD simulation of the chimeric hFVa model.

MD trajectory	hFVa (kcal/mole)	ptFVa-h306 S-S (kcal/mole)	hFVa-ptloop2 (kcal/mole)
0-20ns	-75.46 ± 24.99	-75.58 ± 13.68	N.A.
80-100ns	-39.36 ± 15.57	-90.47 ± 13.51	-63.53 ± 15.89

Table 1. The binding free energies of the A2 and A1-A3 domain interaction. Binding free energies were calculated using the MD trajectory from t=0-20ns or t=80-100ns as described in 'Materials and Methods'. N.A., For hFVa-ptloop2 the t=0-20ns trajectory was excluded from the analysis due to the initial destabilization of the structure following loop exchange. Energies are expressed as kcal/mole ± S.D.

MD trajectory	Domain	hFVa (kcal/mole)	ptFVa-h306 S-S (kcal/mole)
0-20ns	A2-A1	-37.20 ± 15.69	-41.37 ± 9.71
	A2-A3	-43.45 ± 13.41	-41.55 ± 9.20
80-100ns	A2-A1	4.37 ± 10.39	-36.44 ± 8.98
	A2-A3	-46.69 ± 10.40	-55.39 ± 10.12

Table 2. Binding free energies for the binding of the A2 domain to the A1 or A3 domain. Binding free energies were calculated using the MD trajectory from t=0-20ns or t=80-100ns as described in 'Materials and Methods'. Energies are expressed as kcal/mole ± S.D.

Supplemental Methods

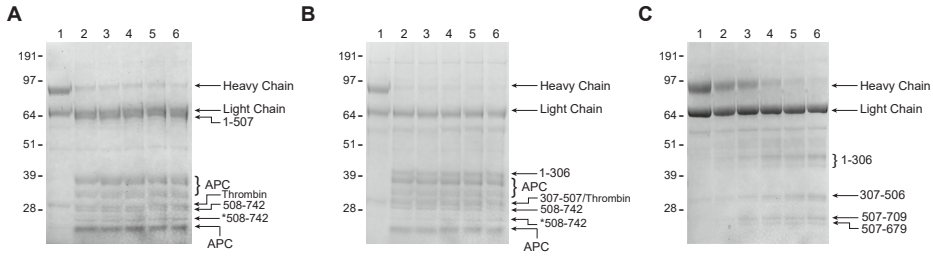
Plasmin-mediated Inactivation of FVa Variants: Plasmin-mediated proteolysis was achieved using FVa variants (500 nM) in the presence of PCPS (50 μM) and addition of plasmin (hFVa 20 nM; ptFVa 400 nM) at 37 °C. Aliquots of the reaction mixtures were withdrawn at the indicated time intervals and analyzed by SDS-PAGE and through assessment of the residual FVa cofactor activity. Activity assay mixtures contained prothrombin (1.4 μM), PCPS (50 μM), DAPA (10 μM), plasmin-proteolyzed hFVa (0.2 nM) or ptFVa variants (0.1 nM), and FXa (2 nM) or ptFXa (1 nM), respectively. Prothrombin activation was determined as described[27].

Thermal Decay of APC-treated FVa Variants: Thrombin-activated ptFV variants (100 nM) were treated with APC (150 nM) in the presence of PCPS (50 μM) for 15 minutes at 37°C and were subsequently incubated in a water bath at 52°C. At indicated timepoints, an aliquot was withdrawn and diluted in assay buffer on ice. Cofactor activity of FVa aliquots were measured using assay mixtures containing prothrombin (1.4 μM), PCPS (50 μM), DAPA (10 μM), APC-proteolyzed ptFVa (0.2 nM) and ptFXa (1 nM). Prothrombin activation was determined as described[27].

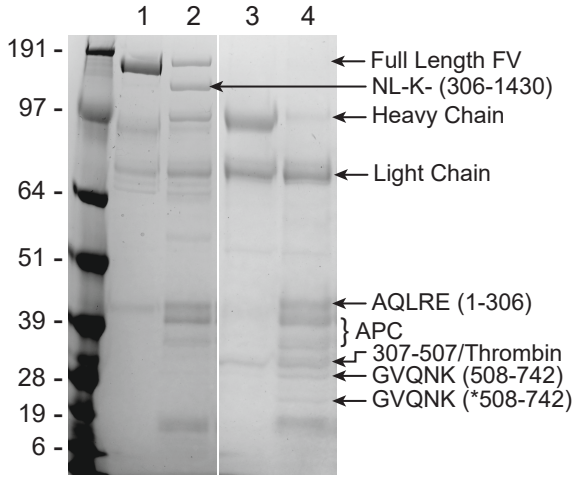
Stability of APC-treated FVa Variants at Increased Ionic Strength: Thrombin-activated ptFVa-h306 S-S (50 nM) was treated with APC (75 nM) for 5 hours at 37°C in the presence of PCPS (50 μM) and increasing concentrations of NaCl (150-2000 mM) in assay buffer Cofactor activity of FVa aliquots were measured using assay mixtures containing prothrombin (1.4 μM), PCPS (50 μM), DAPA (10 μM), APC-proteolyzed ptFVa-h306 S-S (0.1 nM) and ptFXa (1 nM). Prothrombin activation was determined as described[27].

Native PAGE: The structural integrity of FV variants was assessed by Native-PAGE using pre-cast 3-12% Bis-Tris gels (Life technologies; Carlsbad, CA, USA). APC-proteolyzed FV variants were loaded on gels using Native Sample Buffer (Life technologies; Carlsbad, CA, USA) followed by staining with Coomassie Brilliant Blue R-250.

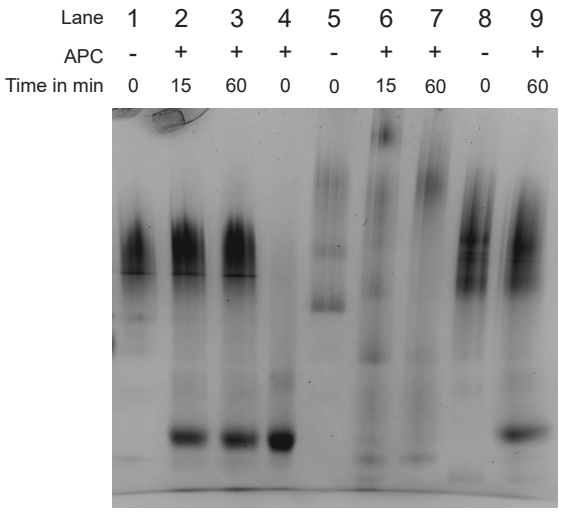
Supplemental Figures



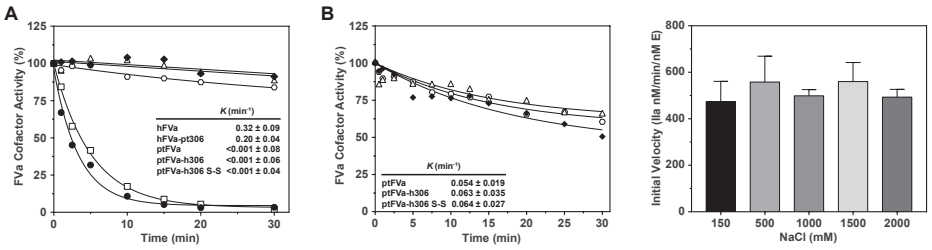
Supplementary figure I. Activated protein C (APC) treatment of human and *P. textilis* factor Va variants. SDS-PAGE of APC-treated ptFVa **(A)**, ptFVa-h306 S-S **(B),** or hFVa **(C)** (3 µg per lane) under reducing conditions and visualized by staining with Coomassie Brilliant Blue R-250. Lanes 1-6 represent time samples quenched at 0, 0.5, 1, 2.5, 5, and 15 min. Relevant fragments including the heavy chain (A1-A2) and light chain (A3-C1-C2) and the apparent molecular weights of the standards are indicated. We hypothesize that *508-742 is cleaved at a C-terminal position because its N-terminal sequence was determined to be the same as 508-742 (see Supplementary Figure 2). The data are representative of two to three independent experiments.



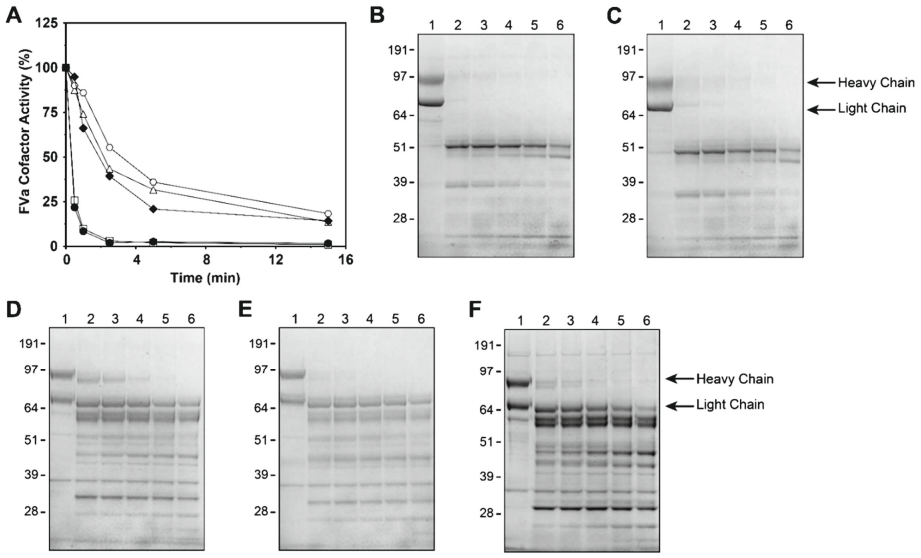
Supplementary figure II. Characterization of APC cleavage sites in ptFV-h306. SDS-PAGE of APC-treated ptFV-h306 and ptFVa-h306 (3 µg per lane) under reducing conditions and visualized by staining with Coomassie Brilliant Blue R-250. Lane 1, ptFV-h306 at t=0; lane 2, ptFV-h306 at t=0.5min; lane 3, ptFVa-h306 at t=0; lane 4, ptFVa-h306 at t=0.5min. N-terminal sequence results of the indicated protein bands and the apparent molecular weights of the standards are shown.



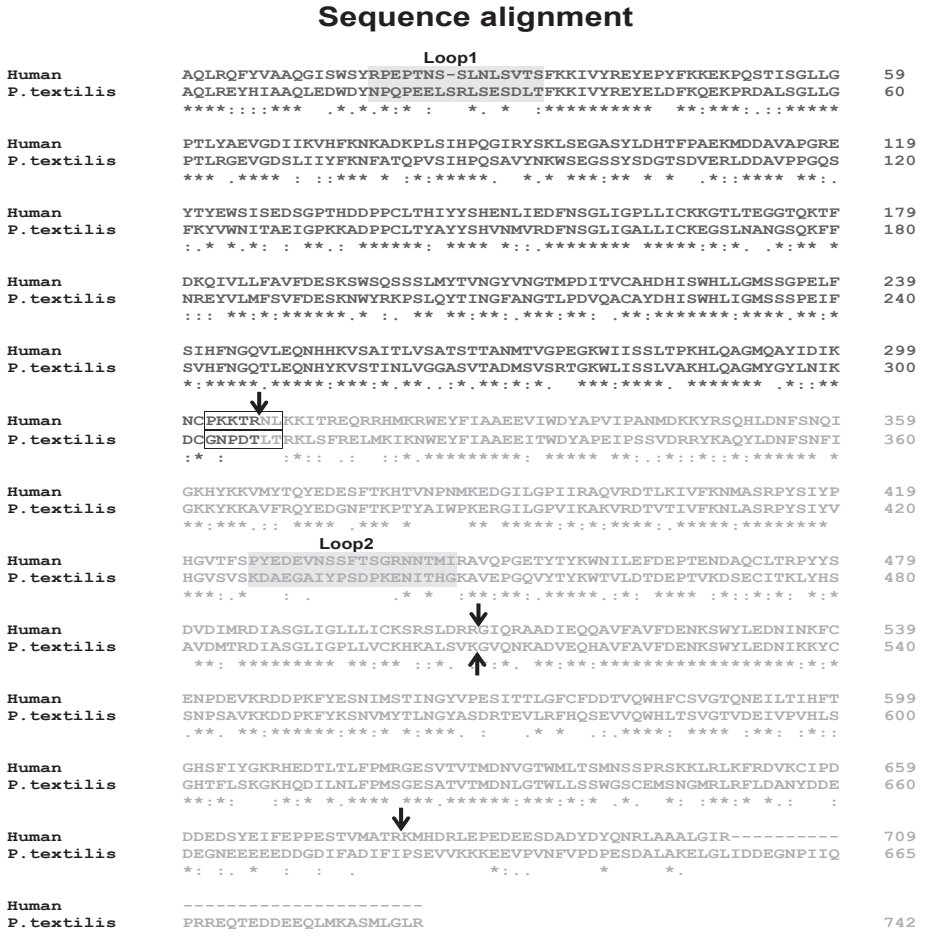
Supplementary figure III. Native-PAGE analysis of APC-proteolyzed human and *P. textilis* factor V variants. Lane 1, ptFV at t=0 min; lane 2, APC-treated ptFV at t=15 min; lane 3, APC-treated ptFV at t=60 min; lane 4, APC; lane 5, hFV at t=0 min; lane 6, APC-treated hFV at t=15 min; lane 7, APC-treated hFV at t=60 min; lane 8, ptFV-h306 S-S at t=0 min; lane 9, APC-treated ptFV-h306 S-S at t=60 min. The data are representative of two independent experiments.



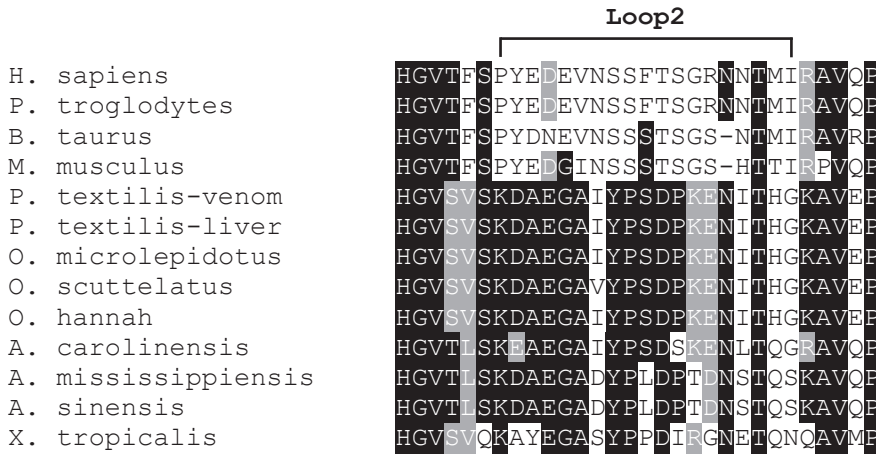
Supplementary figure IV. Factor Va cofactor activity in conditions of increased temperature or high ionic strength. (A) Reaction mixtures containing 20 nM hFVa (closed circles), hFVa-pt306 (open squares), ptFVa (closed diamonds), ptFVa-h306 (open triangles), or ptFVa-h306 S-S (open hexagons) were incubated at 52°C. At selected time intervals, samples were removed and diluted on ice, upon which they were assayed for cofactor activity employing a FV-specific PT-based clotting assay. **(B)** APC-treated ptFVa (closed diamonds), ptFVa-h306 (open triangles), or ptFVa-h306-SS (open hexagons) were incubated at 52°C. At selected time intervals, samples were removed and diluted on ice, upon which they were assayed for cofactor activity by determining the initial velocity of prothrombin conversion as described in 'Materials and Methods'. Cofactor decay rate constants ± 1 S.D. (insets) were determined by fitting the data to a one-phase decay function by non-linear regression. The data are representative of two to three independent experiments. **(C)** ptFVa-h306 S-S (50 nM) was treated with APC (75 nM) at 37°C in the presence of 50 μM PCPS and increasing concentrations of NaCl (150-2000 mM) in assay buffer. After 5 hours of incubation, samples were removed and diluted in assay buffer for cofactor activity assessment by determining the initial velocity of prothrombin conversion. Data represent the mean ± 1 S.D. and are representative of two independent experiments.



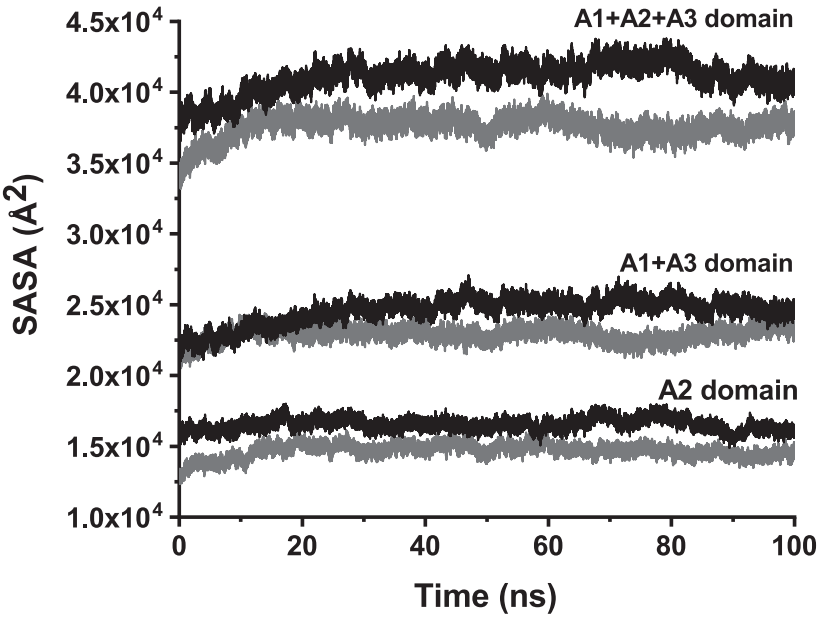
Supplementary figure V. Plasmin treatment of human and *P. textilis* factor Va variants. (A) Reaction mixtures containing 50 µM PCPS and 500 nM hFVa (closed circles) or hFVa-pt306 (open squares) were incubated with 20 nM plasmin, and similar mixtures containing ptFVa (closed diamonds), ptFVa-h306 (open hexagon), or ptFVa-h306 S-S (open triangles) were incubated with 400 nM plasmin. At selected time intervals, samples were taken and assessed for cofactor activity by determining the initial velocity of prothrombin conversion as detailed in 'Materials and Methods'. The data are representative of two to three independent experiments. SDS-PAGE analysis of plasmin-treated hFVa **(B)**, hFVa-pt306 **(C)**, ptFVa **(D)**, ptFVa-h306 **(E)**, or ptFVa-h306 S-S **(F)** (3 µg per lane) under reducing conditions and visualized by staining with Coomassie Brilliant Blue R-250. Lanes 1-6 represent samples quenched at 0, 0.5, 1, 2.5, 5, and 15 min. The FVa heavy (A1-A2 domains) and light (A3-C1-C2 domains) chains and the apparent molecular weights of the standards are indicated. The data are representative of two to three independent experiments.



Supplementary figure VI. Sequence alignment of the human and *P. textilis* A1-A2 domains in FVa. "*" represents identical amino acids, ":" represents very similar amino acids, "." represents somewhat similar amino acids. The A1, A2, and A3 domains are indicated in blue, pink, and green, respectively. The Arg306 region is indicated by the black frame and loop1 and loop2 are highlighted in yellow. Black arrows indicate APC cleavage sites.



Supplementary figure VII. Sequence alignment of the A2 domain loop2 in FV. Alignment of the amino acid sequences comprising the FV A2 domain loop2 (Clustal Omega Module; EMBL-EBI, UK). Residues identical to the consensus are shown in black; residues similar to the column consensus are shown in grey. The amino acids corresponding to the A2 domain loop2 are indicated.



Supplementary figure VIII. Solvent accessible surface areas (SASA) in human and *P. textilis* FV. The SASA of the A2 domain, the A1 and A3 domain complex, and the A1, A2, and A3 domain complex were calculated as described in 'Materials and Methods'. The black and red lines represent human and *P. textilis* FV, respectively.

	hFV	hFV-pt306	ptFV	ptFV-h306	ptFV-h306 S-S
$K_{d,\ app}$ (nM)	0.71 ± 0.20	0.97 ± 0.20	0.83 ± 0.18	0.48 ± 0.16	0.97 ± 0.29

Supplementary table I. Apparent binding affinity for the cofactor. The apparent binding affinity of hFXa or ptFXa for their respective cofactor species was obtained as described in 'Materials and Methods'. The mean values ± S.D. are representative of two to three independent experiments.

Binding surfaces	hFVa	ptFVa-h306 S-S	hFVa-ptloop2
A2-A1	Arg439-Glu20* Pro617-Ser240 Arg619-Ala257	Lys469-Asn252 Glu430-Asn245 Tyr419-Asn245 Asp464-Thr248 Asp462-Lys255 Ser620-Asn260 Ser424-Arg275	Arg475-Lys254 Gly421-Gly245 Tyr418-Asn244 Asp469-Lys254* Asp480-Asn244 Tyr433-Trp278 Phe462-Lys254 Asp480-Ser281 Pro617-Ser240 Asn591-Lys286 Glu621-His253 Arg619-Thr259
A2-A3	Ile593-Ser1127 Asp611-Gly965 Arg648-Glu978* Asp611-Arg1006* Glu610-Arg1017* Gly600-Arg1006 Asp611-Lys975*	Gly601-Arg926 Asn630-Tyr888 Asp629-Arg926* Asp612-Gly885 Thr603-Arg926 Asn615-Gly1077 Asn615-Pro1076 Arg649-Asp898* Arg651-Asp898* Gly601-Tyr888 Thr633-Lys890 Arg651-Asp899*	Ile593-Ser1127 Asp611-Arg1006* Asp611-Gly965 Glu610-Arg1017* Asn467-Asn1145 Arg608-Glu1143* His609-Glu1010 Arg648-Glu978*

* Denotes the charged interactions

Supplementary table II. Key hydrogen bond interaction pairs between the A2 domain and the A1 or A3 domain. Hydrogen bond pairs were identified as described in 'Materials and Methods'.

References

1 Owren, P. A. Parahaemophilia; haemorrhagic diathesis due to absence of a previously unknown clotting factor. *Lancet* **1**, 446-448 (1947).
2 Camire, R. M. & Bos, M. H. The molecular basis of factor V and VIII procofactor activation. *J Thromb Haemost* **7**, 1951-1961, doi:10.1111/j.1538-7836.2009.03622.x (2009).
3 Bos, M. H. & Camire, R. M. A bipartite autoinhibitory region within the B-domain suppresses function in factor V. *J Biol Chem* **287**, 26342-26351, doi:10.1074/jbc.M112.377168 (2012).
4 Schreuder, M., Reitsma, P. H. & Bos, M. H. A. Blood coagulation factor Va's key interactive residues and regions for prothrombinase assembly and prothrombin binding. *J Thromb Haemost* **17**, 1229-1239, doi:10.1111/jth.14487 (2019).
5 Mann, K. G., Nesheim, M. E., Church, W. R., Haley, P. & Krishnaswamy, S. Surface-dependent reactions of the vitamin K-dependent enzyme complexes. *Blood* **76**, 1-16 (1990).
6 Broad, A. J., Sutherland, S. K. & Coulter, A. R. The lethality in mice of dangerous Australian and other snake venom. *Toxicon* **17**, 661-664, doi:10.1016/0041-0101(79)90245-9 (1979).
7 Masci, P. P., Whitaker, A. N. & de Jersey, J. Purification and characterization of a prothrombin activator from the venom of the Australian brown snake, Pseudonaja textilis textilis. *Biochem Int* **17**, 825-835 (1988).
8 Speijer, H., Govers-Riemslag, J. W., Zwaal, R. F. & Rosing, J. Prothrombin activation by an activator from the venom of Oxyuranus scutellatus (Taipan snake). *J Biol Chem* **261**, 13258-13267 (1986).
9 Walker, F. J., Owen, W. G. & Esmon, C. T. Characterization of the prothrombin activator from the venom of Oxyuranus scutellatus scutellatus (taipan venom). *Biochemistry* **19**, 1020-1023, doi:10.1021/bi00546a029 (1980).
10 St Pierre, L. *et al.* Comparative analysis of prothrombin activators from the venom of Australian elapids. *Mol Biol Evol* **22**, 1853-1864, doi:10.1093/molbev/msi181 (2005).
11 Rao, V. S., Swarup, S. & Kini, R. M. The nonenzymatic subunit of pseutarin C, a prothrombin activator from eastern brown snake (Pseudonaja textilis) venom, shows structural similarity to mammalian coagulation factor V. *Blood* **102**, 1347-1354, doi:10.1182/blood-2002-12-3839 (2003).
12 Rao, V. S., Swarup, S. & Manjunatha Kini, R. The catalytic subunit of pseutarin C, a group C prothrombin activator from the venom of Pseudonaja textilis, is structurally similar to mammalian blood coagulation factor Xa. *Thrombosis and haemostasis* **92**, 509-521, doi:10.1160/TH04-03-0144 (2004).
13 Rao, V. S. & Kini, R. M. Pseutarin C, a prothrombin activator from Pseudonaja textilis venom: its structural and functional similarity to mammalian coagulation factor Xa-Va complex. *Thrombosis and haemostasis* **88**, 611-619 (2002).
14 Bos, M. H. *et al.* Venom factor V from the common brown snake escapes hemostatic regulation through procoagulant adaptations. *Blood* **114**, 686-692, doi:10.1182/blood-2009-02-202663 (2009).
15 Bos, M. H. & Camire, R. M. Procoagulant adaptation of a blood coagulation prothrombinase-like enzyme complex in australian elapid venom. *Toxins (Basel)* **2**, 1554-1567, doi:10.3390/toxins2061554 (2010).
16 Lechtenberg, B. C. *et al.* Crystal structure of the prothrombinase complex from the venom of Pseudonaja textilis. *Blood* **122**, 2777-2783, doi:10.1182/blood-2013-06-511733 (2013).
17 Schreuder, M. *et al.* Evolutionary Adaptations in Pseudonaja Textilis Venom Factor X Induce Zymogen Activity and Resistance to the Intrinsic Tenase Complex. *Thrombosis and haemostasis* **120**, 1512-1523, doi:10.1055/s-0040-1715441 (2020).

18 Verhoef, D. *et al.* Functional implications of the unique disulfide bond in venom factor V from the Australian common brown snake Pseudonaja textilis. *Toxin Reviews* **33**, 37-41, doi:10.3109/15569543.2013.844712 (2014).
19 Egan, J. O., Kalafatis, M. & Mann, K. G. The effect of Arg306-->Ala and Arg506-->Gln substitutions in the inactivation of recombinant human factor Va by activated protein C and protein S. *Protein Sci* **6**, 2016-2027, doi:10.1002/pro.5560060922 (1997).
20 Dahlback, B. & Villoutreix, B. O. The anticoagulant protein C pathway. *FEBS Lett* **579**, 3310-3316, doi:10.1016/j.febslet.2005.03.001 (2005).
21 Kalafatis, M., Rand, M. D. & Mann, K. G. The mechanism of inactivation of human factor V and human factor Va by activated protein C. *J Biol Chem* **269**, 31869-31880 (1994).
22 Kalafatis, M. & Mann, K. G. Role of the membrane in the inactivation of factor Va by activated protein C. *J Biol Chem* **268**, 27246-27257 (1993).
23 Nicolaes, G. A. *et al.* Peptide bond cleavages and loss of functional activity during inactivation of factor Va and factor VaR506Q by activated protein C. *J Biol Chem* **270**, 21158-21166, doi:10.1074/jbc.270.36.21158 (1995).
24 Mann, K. G., Hockin, M. F., Begin, K. J. & Kalafatis, M. Activated protein C cleavage of factor Va leads to dissociation of the A2 domain. *J Biol Chem* **272**, 20678-20683 (1997).
25 Higgins, D. L. & Mann, K. G. The interaction of bovine factor V and factor V-derived peptides with phospholipid vesicles. *J Biol Chem* **258**, 6503-6508 (1983).
26 Toso, R. & Camire, R. M. Removal of B-domain sequences from factor V rather than specific proteolysis underlies the mechanism by which cofactor function is realized. *J Biol Chem* **279**, 21643-21650, doi:10.1074/jbc.M402107200 (2004).
27 Krishnaswamy, S. & Walker, R. K. Contribution of the prothrombin fragment 2 domain to the function of factor Va in the prothrombinase complex. *Biochemistry* **36**, 3319-3330, doi:10.1021/bi9623993 (1997).
28 Verhoef, D. *et al.* Engineered factor Xa variants retain procoagulant activity independent of direct factor Xa inhibitors. *Nat Commun* **8**, 528, doi:10.1038/s41467-017-00647-9 (2017).
29 van der Neut Kolfschoten, M. *et al.* Factor Va is inactivated by activated protein C in the absence of cleavage sites at Arg-306, Arg-506, and Arg-679. *J Biol Chem* **279**, 6567-6575, doi:10.1074/jbc.M308574200 (2004).
30 Rapaport, D. C. The Art of Molecular Dynamics Simulation. *J. Chem. Educ.* **76**, 171 (1999).
31 Shim, J. Y., Lee, C. J., Wu, S. & Pedersen, L. G. A model for the unique role of factor Va A2 domain extension in the human ternary thrombin-generating complex. *Biophysical chemistry* **199**, 46-50, doi:10.1016/j.bpc.2015.02.003 (2015).
32 Krieger, E. & Vriend, G. YASARA View - molecular graphics for all devices - from smartphones to workstations. *Bioinformatics* **30**, 2981-2982, doi:10.1093/bioinformatics/btu426 (2014).
33 Maier, J. A. *et al.* ff14SB: Improving the Accuracy of Protein Side Chain and Backbone Parameters from ff99SB. *J Chem Theory Comput* **11**, 3696-3713, doi:10.1021/acs.jctc.5b00255 (2015).
34 Ryckaert, J., Ciccotti, G. & Berendsen, H. J. C. Numerical integration of the cartesian equations of motion of a system with constraints: molecular dynamics of n-alkanes. *J. Chem. Theory Comput.* **23**, 327–341 (1977).
35 Case, D. A. *et al.* AMBER 2016. *University of California, San Francisco* (2016).
36 Genheden, S. & Ryde, U. The MM/PBSA and MM/GBSA methods to estimate ligand-binding affinities. *Expert Opin Drug Discov* **10**, 449-461, doi:10.1517/17460441.2015.1032936 (2015).
37 Norstrom, E., Thorelli, E. & Dahlback, B. Functional characterization of recombinant FV Hong Kong and FV Cambridge. *Blood* **100**, 524-530, doi:10.1182/blood-2002-02-0343 (2002).
38 Rosing, J. *et al.* Effects of protein S and factor Xa on peptide bond cleavages during inactivation of factor Va and factor VaR506Q by activated protein C. *J Biol Chem* **270**, 27852-27858 (1995).

39 Walker, F. J. Regulation of activated protein C by a new protein. A possible function for bovine protein S. *J Biol Chem* **255**, 5521-5524 (1980).
40 Nicolaes, G. A., Villoutreix, B. O. & Dahlback, B. Partial glycosylation of Asn2181 in human factor V as a cause of molecular and functional heterogeneity. Modulation of glycosylation efficiency by mutagenesis of the consensus sequence for N-linked glycosylation. *Biochemistry* **38**, 13584-13591, doi:10.1021/bi991165r (1999).
41 Minh Le, T. N., Reza, M. A., Swarup, S. & Kini, R. M. Gene duplication of coagulation factor V and origin of venom prothrombin activator in Pseudonaja textilis snake. *Thrombosis and haemostasis* **93**, 420-429, doi:10.1160/TH04-11-0707 (2005).
42 Jiang, Y. & Doolittle, R. F. The evolution of vertebrate blood coagulation as viewed from a comparison of puffer fish and sea squirt genomes. *Proc Natl Acad Sci U S A* **100**, 7527-7532, doi:10.1073/pnas.0932632100 (2003).
43 Ponczek, M. B., Gailani, D. & Doolittle, R. F. Evolution of the contact phase of vertebrate blood coagulation. *J Thromb Haemost* **6**, 1876-1883, doi:10.1111/j.1538-7836.2008.03143.x (2008).
44 Doolittle, R. F. & Feng, D. F. Reconstructing the evolution of vertebrate blood coagulation from a consideration of the amino acid sequences of clotting proteins. *Cold Spring Harb Symp Quant Biol* **52**, 869-874 (1987).
45 Davidson, C. J., Tuddenham, E. G. & McVey, J. H. 450 million years of hemostasis. *J Thromb Haemost* **1**, 1487-1494 (2003).
46 Joseph, J. S., Chung, M. C., Mirtschin, P. J. & Kini, R. M. Effect of snake venom procoagulants on snake plasma: implications for the coagulation cascade of snakes. *Toxicon* **40**, 175-183 (2002).
47 Omar, M. N. & Mann, K. G. Inactivation of factor Va by plasmin. *J Biol Chem* **262**, 9750-9755 (1987).
48 Kalafatis, M. & Mann, K. G. The role of the membrane in the inactivation of factor va by plasmin. Amino acid region 307-348 of factor V plays a critical role in factor Va cofactor function. *J Biol Chem* **276**, 18614-18623, doi:10.1074/jbc.M007134200 (2001).
49 Cederholm-Williams, S. A. Concentration of plasminogen and antiplasmin in plasma and serum. *J Clin Pathol* **34**, 979-981, doi:10.1136/jcp.34.9.979 (1981).
50 Reza, M. A., Minh Le, T. N., Swarup, S. & Manjunatha Kini, R. Molecular evolution caught in action: gene duplication and evolution of molecular isoforms of prothrombin activators in Pseudonaja textilis (brown snake). *J Thromb Haemost* **4**, 1346-1353, doi:10.1111/j.1538-7836.2006.01969.x (2006).
51 Kalafatis, M. & Mann, K. G. Factor V: Dr. Jeckyll and Mr. Hyde. *Blood* **101**, 20-30 (2003).
52 Majumder, R., Quinn-Allen, M. A., Kane, W. H. & Lentz, B. R. A phosphatidylserine binding site in factor Va C1 domain regulates both assembly and activity of the prothrombinase complex. *Blood* **112**, 2795-2802, doi:10.1182/blood-2008-02-138941 (2008).
53 Qureshi, S. H., Yang, L., Manithody, C. & Rezaie, A. R. Membrane-dependent interaction of factor Xa and prothrombin with factor Va in the prothrombinase complex. *Biochemistry* **48**, 5034-5041, doi:10.1021/bi900240g (2009).
54 Dirven, R. J., Vos, H. L. & Bertina, R. M. The R306G and R506Q mutations in coagulation Factor V reveals additional cleavage sites for Activated Protein C in the R313-R321 region and at R505. *Thromb Res* **125**, 444-450, doi:10.1016/j.thromres.2009.12.005 (2010).
55 Shen, L. & Dahlback, B. Factor V and protein S as synergistic cofactors to activated protein C in degradation of factor VIIIa. *J Biol Chem* **269**, 18735-18738 (1994).
56 Wilhelm, A. R. *et al.* Activated Protein C has a Regulatory Role in Factor VIII Function. *Blood* **137**, 2532-2543, doi:10.1182/blood.2020007562 (2021).
57 Thorelli, E., Kaufman, R. J. & Dahlback, B. Cleavage of factor V at Arg 506 by activated protein C and the expression of anticoagulant activity of factor V. *Blood* **93**, 2552-2558 (1999).
58 Castoldi, E. *et al.* Impaired APC cofactor activity of factor V plays a major role in the APC resistance associated with the factor V Leiden (R506Q) and R2 (H1299R) mutations. *Blood* **103**, 4173-4179, doi:10.1182/blood-2003-10-3578 (2004).



Chapter 4

Pseudonaja textilis Venom Factor Va Circumvents Natural Regulatory Mechanisms via a Unique A2 domain Region

Mark Schreuder, Ka Lei Cheung, Lynn Kruijsdijk, Pieter H. Reitsma, Mettine H.A. Bos

Manuscript in Preparation



Abstract

The coagulation factor V (FV) variant derived from the venom of the Australian snake Pseudonaja textilis (ptFV) has several unique procoagulant adaptations that circumvent the normal regulatory mechanisms in order to initiate coagulation in an uncontrolled manner. Interestingly, ptFV comprises a significantly extended A2 domain C-terminus (A2T), a region of which the role in human FV biology is poorly understood. In this study, we generated several chimeric FV variants to explore the functional relevance of this extended structural region. Surprisingly, our findings demonstrate that ptFV's enhanced procoagulant function is mediated by the A2T. Using this structural element, ptFV bypasses the need for membrane binding by facilitating productive interactions with P. textilis venom FXa and prothrombin in solution. Moreover, via a peptide-based approach we have established that the N-terminal region in the ptFV A2T plays a key role in the lipid-independent activity. Remarkably, substitution of the human A2T for the corresponding region in ptFV enabled human FVa to function in the absence of membranes, in a similar fashion to ptFVa. In addition, the ptFV A2T region was found to be of paramount importance for the functional activated protein C-resistance. Unlike in mammalian FVa, a ptFVa variant comprising the human FV A2T retained structural integrity despite loss of cofactor function. Taken together, the ptFV A2T represents an exceptional structural element responsible for the enhanced procoagulant functions that are at the basis of the snake venom's extreme toxicity.

Introduction

The coagulation cascade is composed of serine proteases and cofactors that act in a concerted manner to minimize blood loss following vascular injury. The regulatory mechanisms that strictly confine the activity of these coagulation proteins are of critical importance to maintain hemostasis. Intriguingly, the venom of various snake species comprises uniquely modified proteins that specifically act on coagulation pathways, aiming to disrupt the host's hemostatic system and incapacitate prey animals[1-4]. In humans, snake envenoming can lead to venom-induced consumptive coagulopathy (VICC), the most commonly observed clinical phenotype following envenomation in Australia[5]. VICC is characterized by uncontrolled activation of the coagulation system resulting in the consumption of fibrinogen, factors V and VIII, elevated D-dimer levels, and an international normalized ratio >3[6-8]. As a consequence, patients are at significantly increased risk for spontaneous and life-threatening hemorrhages[9].

Previously we, amongst others, reported that the FV(a)- and FX(a)-like proteins found in the venom of the Australian snake *Pseudonaja textilis* (ptFV[10,11] and ptFX[12,13], respectively) comprise several remarkable procoagulant adaptations that could be at the basis of the venom's potent toxicity[10,14,15]. ptFXa exhibits a reduced sensitivity towards antithrombin[16], in part due to extension of the 99-loop located directly adjacent to the active site[16,17]. Recently, we showed that the shortened ptFX activation peptide allows the zymogen form of ptFX to interact with the cofactor FVa and proteolytically convert prothrombin[18]. With respect to ptFV, it lacks the basic and acidic B-domain regions that keep FV in a procofactor state[19,20], thereby generating a constitutively active cofactor[14]. Moreover, ptFV has circumvented several negative regulatory pathways by bypassing the need for membrane binding and maintaining cofactor activity following activated protein C (APC)-dependent proteolysis[10,14]. For the latter we recently demonstrated that the ptFVa A2 domain loop2 facilitates stable A1-A2 domain interactions which likely prevent A2 domain dissociation following APC-proteolysis[21]. Despite this, the full molecular mechanism underpinning the procoagulant gain-of-functions of ptFV remains largely unexplained, suggesting that ptFV has developed other unique structural features to escape normal hemostatic regulation.

The characteristic acidic region hallmarking the A2 domain C-terminus (A2T) is significantly extended in ptFV relative to other FV species[10,11]. Although the functional role of the human FV A2T is poorly understood, previous reports have implicated the A2T in the formation of the prothrombinase complex and engagement of prothrombin[22-27]. In line with this, Shim *et al.* reported a complete 3D-model for the human prothrombinase–prothrombin complex, which revealed an extensive interaction

between the FVa A2T, the protease FXa, and substrate prothrombin[28]. Here we show that the ptFV A2T is responsible for the remarkable procoagulant enhancements of ptFV by facilitating productive interactions with ptFXa and prothrombin in the absence of membranes and following APC-proteolysis of the cofactor. As such, we have identified a unique structural element that gives ptFV the ability to promote uncontrolled blood clotting. These findings highlight the exceptional mechanism by which ptFV has been converted into a potent procoagulant weapon.

Materials and Methods

Construction and purification of FV variants: The construction, expression, and purification of FV variants are described in the Supplementary Information.

Macromolecular substrate activation: Steady-state initial velocities of macromolecular substrate cleavage were determined discontinuously at 25°C in assay buffer as described[17,29]. Briefly, progress curves of prothrombin were obtained by incubating PCPS (50 μM), DAPA (10 μM), and prothrombin (1.4 μM) with the recombinant FVa species (20 nM), and the reaction was initiated with 0.1–1 nM of hFXa or ptFXa upon which the rate of prothrombin conversion was measured[29].

APC-induced inactivation of FVa variants: FVa variants (500 nM) were incubated at 37°C with APC (10 nM for human FVa (hFVa); 750 nM for ptFVa) in the presence of PCPS (50 μM). Aliquots of the reaction mixtures were withdrawn at the indicated time intervals and analyzed by SDS-PAGE and via residual FVa cofactor activity assessment. FVa cofactor activity assay mixtures contained prothrombin (1.4 μM), PCPS (50 μM), DAPA (10 μM), hFVa (0.2 nM) or ptFVa (0.1 nM) variants and hFXa (2 nM) or ptFXa (1 nM), respectively. Prothrombin activation was determined as described under "Macromolecular substrate activation".

Peptide inhibition of prothrombinase-mediated prothrombin conversion: The inhibition of prothrombinase activity was measured continuously at 25°C in assay buffer. Assay mixtures containing prothrombin (1.4 μM), DAPA (10 μM), S2238 (100 μM), hFVa-ptA2T or ptFVa (5 pM), and peptides at indicated concentrations were incubated for 5 min at 25°C, and reactions were initiated with 1 nM ptFXa. The conversion of S2238 (100 μM) was followed for 60 min upon which the prothrombin conversion rate was measured[29].

Size-exclusion chromatography of APC-treated FVa variants: ptFVa-hA2T (500 μg) was subjected to APC (1 mM) treatment for 180 min at 37°C in the presence of

50 μM PCPS. Reactions were quenched by the addition of 50 μM PPACK and 1 mM benzamidine (BZA). A 10 mm × 300 mm column containing Superdex 200 Increase (Cytiva, Marlborough MA, USA) was equilibrated in assay buffer supplemented with 50 μM PPACK and 1 mM BZA. The 400 μL reaction mixture was applied to the column and eluted with equilibration buffer at a flow rate of 0.25 mL/min at room temperature. Fractions (0.25 mL) were collected and analyzed by SDS-PAGE.

Statistical analysis: All in vitro data are presented as mean ± 1 standard deviation and are the result of at least two to three independent experiments, unless otherwise stated.

Results

Generation of FV variants. The FVa A2T consists of an extended series of negatively charged amino acids with a currently unknown tertiary structure and poorly understood function. Sequence analysis revealed that ptFV comprises a significantly extended A2T (extended by 31 residues) compared to human FV (hFV) or other FV species, including that of several reptiles **(Fig. S1A)**. To examine the functional relevance of this extended region we created chimeric FV variants by exchanging the A2T between hFV and ptFV, resulting in hFV-ptA2T and ptFV-hA2T, respectively (**Figs. 1A**, **S1B**). The FV variants were stably expressed in BHK cells and purified to homogeneity by ion-exchange chromatography. Thrombin-activated FVa variants were subjected to SDS-PAGE under reducing **(Fig. 1B)** and non-reducing **(Fig. S2)** conditions. Each variant migrated on SDS-PAGE with the expected mobility; ptFV migrates as a single molecule under non-reducing conditions due to disulfide linkage of the A2-A3 domains[14,16].

Contribution of the ptFV A2T to prothrombinase assembly and prothrombin conversion. Previous studies have implicated the A2T as a FXa and/or prothrombin binding region[22-27], yet contradictory findings have been reported[30,31]. To assess the function of the extended ptFV A2T, we determined the kinetics for prothrombinase assembly by titration of the cofactor in the presence of hFXa/ptFXa and saturating amounts of anionic phospholipids. Similar to previously reported values[17,19,32,33], the apparent binding affinity of hFVa for hFXa was ~1.6 nM, **(Figure 2A; Table 1)**. hFVa-ptA2T displayed a near identical affinity for hFXa (~1.7 nM), indicating that the ptFV A2T does not significantly contribute to assembly of the human prothrombinase complex. Although the apparent affinity of the ptFVa variants for ptFXa was lower relative to those of the human system and to previously reported values[14,34], no differences were observed between ptFVa and ptFVa-hA2T **(Figure 2A; Table 1)**. Steady-state kinetic constants for prothrombin conversion revealed that in the presence of FXa the chimeric

FVa variants engaged prothrombin in a manner similar to the respective wild-type FVa species **(Figure 2B; Table 1)**. Conversely, the catalytic rates of prothrombin activation appeared modestly affected following exchange of the A2T between hFVa and ptFVa **(Figure 2B; Table 1)**. Nevertheless, the kinetic parameters were comparable to those earlier reported[14,17,31,34,35]. These findings may indicate that the ptFV A2T interacts with prothrombin in a different manner which could affect the orientation of the prothrombin activation sites towards FXa and as such the rate of catalysis.

The ptFV A2T facilitates macromolecular substrate conversion in the absence of anionic phospholipids. One of the procoagulant characteristics of ptFV is its unique ability to function in the absence of anionic membranes[14]. We next aimed to assess whether A2T plays a role in this gain-of-function feature. While the initial velocity of prothrombin activation was comparable between ptFVa and ptFVa-hA2T in the presence of anionic membranes, the velocity of prothrombin conversion by the ptFVa/ptFXa complex was 3.5-fold reduced in reaction mixtures lacking phospholipids **(Figure 3A)**. In contrast, the activity of the human FVa/FXa complex was virtually abolished in the absence of anionic membranes **(Figure 3B)**, consistent with previous findings[14]. Strikingly, upon exchange of the A2T, ptFVa-hA2T completely lost its ability to function in solution **(Figure 3A)**, indicating that the A2T is at the basis of ptFV's lipid-independent cofactor function. Following functional assessment of hFVa-ptA2T prothrombin conversion rates similar to hFVa were obtained in the presence or absence of anionic membranes when assayed with hFXa **(Figure 3B)**. However, as ptFX(a) comprises unique modifications that could contribute to the lipid-independent prothrombin conversion as well, the cofactor function of the human FVa variants was also assessed using ptFXa as protease. In the presence of ptFXa and phospholipids, hFVa-ptA2T exhibited a similar initial velocity of prothrombin conversion compared to hFVa **(Figure 3B)**. Remarkably, when anionic membranes were absent, the hFVa-ptA2T/ptFXa complex displayed a 24-fold increased rate of prothrombin conversion relative to hFVa/ptFXa **(Figure 3B)**, which was similar to that observed for the ptFVa/ptFXa complex **(Figure 3A)**. Comparable results were obtained using the chimeric variant hFVa-ptA2T-Y656C **(Figure S3A)** that comprises the complete ptFV A2T in which the highly conserved human Cys575-Cys656 disulfide bond is reintroduced **(Figs. 1A, S1B)**.

Importantly, these results could be explained by the contamination of phospholipids during purification, as described previously[36]. To remove putative lipid contaminants, FVa variants were treated with phospholipase C in the presence of phospholipids. Incubation with phospholipase C nearly abolished cofactor activity of hFVa and ptFVa-hA2T likely due phospholipid cleavage **(Figure S3B).** In contrast, the rate of prothrombin activation was markedly higher for the cofactors hFVa-ptA2T and ptFVa,

suggesting that the ptFV A2T is responsible for this unique lipid-independent activity. Further assessment of the lipid-independent prothrombin conversion as a function of the phospholipid concentration (0.05-100 μM) in the presence of ptFXa revealed similar initial rates of prothrombin conversion for hFVa and hFVa-ptA2T **(Figure 3C)**. However, phospholipid concentrations <0.05 μM had no appreciable effect on the rate of prothrombin activation with hFVa-ptA2T as cofactor, whereas the generation of thrombin was virtually undetected using hFVa **(Figure 3C)**. These results show that the lipid-independent effects exerted by the A2T become apparent in conditions with low phospholipid concentrations (<0.05 μM).

The ability of prothrombin to bind anionic membranes and thereby promote assembly of the prothrombinase-prothrombin complex might interfere with the interpretation of our results. To overcome this we determined the kinetics of prethrombin-1 conversion, which is a prothrombin derivative that lacks the kringle-1 and membrane binding Gla domains and does not interact with a lipid surface. Strikingly, using ptFXa as protease hFVa-ptA2T was able to activate prethrombin-1 both in the presence of anionic membranes and in solution phase with equivalent kinetic parameters, similar to ptFV **(Figure 3D, Table 1)**[14]. Conversely, prethrombin-1 conversion was absent in reaction mixtures with hFVa or ptFVa-hA2T as cofactor for ptFXa on membranes. Analysis of cleavage products of prothrombin and prethrombin-1 conversion by ptFV-ptFXa demonstrated that, similar to human prothrombinase, prothrombin conversion on anionic membranes proceeds through initial cleavage at Arg320, thereby forming the intermediate meizothrombin, and subsequent proteolysis at Arg271 resulting in the formation of thrombin and fragment 1.2 typical to the meizothrombin pathway **(Figure S4A)**[37]. Interestingly, we and others observed that in the absence of phospholipids ptFV-ptFXa proteolysis of prothrombin follows the opposite order of cleavage, generating the intermediates prethrombin-2 and fragment 1.2 via the prethrombin-2 pathway **(Figure S4B)**[16], similar to membrane-bound hFXa in the absence of cofactor[37]. In sharp contrast, prethrombin-1 proteolysis by ptFV-ptFXa proceeded via the prethrombin-2 pathway in the presence and absence of membranes **(Figure S4C,D)**. These observations indicate an important role for the substrate-membrane interaction in directing the order of substrate cleavage, consistent with findings by others[38]. Control experiments in the absence of $CaCl_2$ and with EDTA added to abolish any potential lipid binding as a consequence of residual lipid present in the protein preparations revealed significant prethrombin-1 conversion (**Table S1**).

Inhibition of the lipid-independent cofactor activity of ptFV-hA2T by peptide A2T fragments. To gain more insight into the mechanistic principles by which the ptFV A2T bypasses the need for membrane binding, we assessed the ability of three peptides

representing segments of the ptFV A2T (**Figure 4A**) to inhibit the lipid-independent activity of the hFVa-ptA2T/ptFXa complex in a continuous assay. Interestingly, in the absence of membranes addition of increasing concentrations of peptide 1 markedly reduced prothrombin activation **(Figure 4B)**. Conversely, peptide 2 exhibited a modest inhibitory effect **(Figure 4C),** whereas addition of up to 350 μM of peptide 3 had practically no impact on the lipid-independent prothrombin conversion **(Figure 4D)**. Comparable results were obtained using the ptFVa/ptFXa enzyme complex **(Figure S5)**. These data suggest that the Asp653-Ser681 sequence covered by peptide 1 and part of the Glu682-Leu709 sequence in peptide 2 could play a crucial role in the lipid-independent cofactor activity of ptFV.

The ptFV A2T plays a major role in the functional resistance to APC. In a recent study, we demonstrated that APC-mediated proteolysis of ptFVa at the essential cleavage sites equivalent to Arg306 and Arg506 had no appreciable effect on the cofactor activity[21], indicating that ptFV comprises unique structural elements that prevent inactivation. To further identify these, we assessed the functional consequences of APC-catalyzed proteolysis following A2T exchange between hFVa and ptFVa. SDS-PAGE analysis of APC-treated FVa variants revealed that ptFVa-hA2T was cleaved at the introduced human Arg679 cleavage site, whereas this cleavage was absent in ptFVa and hFVa-ptA2T **(Figure S6A-D)**. Evaluating the cofactor activity in a purified component assay showed that APC-proteolyzed ptFVa retained full cofactor activity upon a two hour incubation with APC **(Figure 4A)**, despite being fully proteolyzed **(Figure 5A)**. Intriguingly, a significant loss of cofactor activity was observed using APC-treated ptFVa-hA2T as cofactor **(Figure 4A)**. In case of the latter, the newly introduced human Arg679 cleavage site may be responsible for the loss of cofactor ptFVa-hA2T activity. To assess this, a chimeric ptFV variant comprising the Arg679Glu substitution was generated and analyzed (ptFVa-hA2T-R679Q, **Figure S1B**). Whereas ptFVa-hA2T displayed a ~75% loss of cofactor activity following APC-proteolysis, only a ~35% loss of activity was observed for APC-catalyzed ptFVa-hA2T-R679Q **(Figure 4A,S6E)**. Collectively, these findings suggest that the C-terminal region of ptFV A2T (Pro680-Arg740) plays an important role in the functional APC resistance.

Functional analysis of human FVa variants using hFXa revealed that hFVa-ptA2T was inactivated upon APC-mediated proteolysis in identical fashion to hFVa **(Figure 4B)**. We hypothesized that despite comprising the ptFV A2T, the APC-mediated inactivation resulted from proteolysis at the two major human APC cleavage sites in FVa, Arg306 and Arg506, whereas ptFVa is only targeted at the homologous Arg506 site[14]. To test this, the human Arg306 region in hFV-ptA2T was substituted for the corresponding ptFV region[21], generating hFV-ptA2T-pt306. Functional assessment revealed that hFVa-

ptA2T-pt306 retained ~50% cofactor activity following cleavage by APC **(Figure 4B)**, similar to previously reported FVa variants comprising an Arg306 mutation[39]. When APC-proteolyzed human FVa variants were assayed with ptFXa, the inactivation of hFVa-ptA2T was found to be slower relative to assessments in the presence of hFXa, indicating that ptFXa is able to support the cofactor function of APC-cleaved cofactor **(Figure 4B)**. Remarkably, APC-proteolyzed hFVa-ptA2T-pt306 maintained full cofactor activity in the presence of ptFXa **(Figure 4B,S6F)**. Furthermore, we generated a ptFVa molecule in which the human Arg306 region was introduced and ptFVa's unique disulfide bond connecting the A2-A3 domains was eliminated[21] (ptFVa-hA2T-h306-SS). Following a two hour incubation with APC, ptFVa-hA2T-h306-SS retained a similar activity (~15%) relative to ptFVa-hA2T **(Figure 4A,S6G)**, highlighting the extraordinary stability of ptFVa. As such, our findings demonstrate that the ptFV A2T and absence of the Arg306 cleavage site are of substantial importance for the functional APC-resistance of ptFV.

ptFVa-hA2T maintains structural integrity despite loss of cofactor function. Recently we demonstrated that ptFVa comprises stable non-covalent A2-A1 interactions that prevent A2 domain dissociation following APC-mediated proteolysis[21]. We next examined whether the loss of ptFVa-hA2T activity correlates with A2 domain dissociation. Following size-exclusion chromatography of APC-treated ptFVa-hA2T, elution fractions were analyzed by SDS-PAGE. In contrast to hFVa, APC-proteolyzed ptFVa-hA2T displayed a similar elution profile **(Figure 5A)** as proteolyzed ptFVa[21]. Furthermore, SDS-PAGE analysis revealed that ptFVa-hA2T eluted as a single complex, demonstrating that ptFVa-hA2T maintained structural integrity **(Figure 5B)**. These data therefore indicate that the loss of ptFVa-hA2T activity following APC-proteolysis is the result of a reduced affinity for ptFXa and/or prothrombin rather than A2 domain dissociation, corroborating our previous findings that non-covalent A2-A1 domain interactions in ptFVa are responsible for its unique structural integrity[21].

Discussion

The requirement for a negatively-charged phospholipid layer in support of enzymatic reactions is one of the hallmarks of coagulation and confines the procoagulant response to the site of injury while dramatically enhancing the enzyme assembly process[40,41]. Remarkably, ptFV has bypassed the need for membrane binding by forming a high affinity complex with ptFXa in solution[14]. This unique feature could potentially allow the systemic disruption of hemostasis upon envenomation. Our findings show that the ptFV A2T is responsible for this exceptional characteristic. This study thereby provides novel insights in the mechanistic role of the FVa A2T in the binding and conversion of prothrombin.

Previous studies into the functional role of the human FV A2T have reported contradictory results[22-26,31,33]. Here, we made use of a uniquely modified natural FV variant comprising an extended A2T. Functional characterization of chimeric FVa variants following A2T exchange between human and *P. textilis* FV revealed modest differences in the maximal prothrombin conversion rates at saturating conditions of membranes. The slightly reduced prothrombin activation rate in FVa variants comprising the ptFV A2T might reflect the use of human prothrombin and could indicate that the ptFV A2T interacts with prothrombin in a somewhat different and less efficient manner relative to the hFV A2T. These results are in accordance with previous reports suggesting that the A2T plays a role in the positioning of the prothrombin activation sites towards the catalytic triad of FXa[26,33,42]. In sharp contrast to the human system, we observed that the ptFV A2T facilitates prothrombin conversion in the absence of a lipid membrane layer. These findings suggest that the FV A2T plays an important role in the interaction with FXa and prothrombin at physiological phosphatidylserine concentrations (<5%) or in conditions with limiting FXa/membranes[43,44].

Exchange of the A2T resulted in a unique gain-of-function in human FVa by enabling hFVa-ptA2T to bypass the need for membrane binding. Using peptide inhibition studies we identified a potential role for the N-terminal region of the ptFV A2T by facilitating prothrombin activation when anionic membranes are not available. Interestingly, the lipid-independent activity of hFVa-ptA2T was only observed when the cofactor activity was assayed using the protease ptFXa, indicating that the venom-derived FXa comprises an essential element that contributes to the formation of a prothrombinase-like complex in the absence of membranes. Supporting our peptide-based approach, the X-ray structure of Pseutarin C revealed that the N-terminal part of the acidic ptFVa A2T interacts with ptFXa via the highly basic heparin binding site[16], providing evidence that this ptFXa region comprises an essential element that allows for the

formation of a high affinity ptFVa/ptFXa complex in solution. However, global structural comparison of the Pseutarin C structure with the human ternary model did not reveal major conformational alterations in the FXa A2T binding site that could readily explain the different effects between ptFXa and hFXa[16,28] **(Figure S7)**. Future studies focusing on *in silico* analysis of the molecular interactions may provide enhanced insight. In an attempt to identify the responsible structural element, we examined a potential role for the extended 99-loop of ptFXa by experimental assessment of several previously reported FXa variants[17]. However, these variants were unable to support thrombin generation in the absence of anionic membranes (data not shown), excluding a role for this insertion. An alternative explanation might be a structural modification in the Gla domain, which could allosterically influence the conformation of FVa binding sites[42].

Previous work suggests that the increased FVa/FXa affinity upon binding to negatively charged membranes is the result of conformational constraints that increase the chance of productive interactions[41]. Moreover, interaction with anionic membranes was speculated to induce structural rearrangements in the lipid-binding C domains of FVa, resulting in allosteric changes within the FXa binding regions of the A2 domain[42,45]. The latter is supported by two C2 domain crystal structures revealing an 'open' and 'closed' conformation of the phospholipid protruding spikes[46]. In contrast, our data suggest that such structural rearrangements are not essential for prothrombinase assembly since the human variant hFVa-ptA2T was able to engage ptFXa with high affinity in the absence of membranes. Although it is possible that ptFVa or hFVa-ptA2T binding to ptFXa mimics the conformational changes of membrane-bound hFVa, no structural data is available to support this notion.

Our findings further show that introduction of the human A2T in ptFVa results in a reduced cofactor activity upon APC-mediated proteolysis, demonstrating that the ptFV A2T significantly contributes to its functional APC-resistance. Interestingly, substitution of the human Arg679 APC cleavage site in ptFVa-hA2T, thereby rendering it resistant to APC proteolysis, partly rescued the loss of cofactor activity. Considering that the A2T is a long and highly flexible region, it is unlikely that proteolysis at Arg679 destabilizes any region outside of the A2T itself. As such, these results might indicate that the C-terminal part of the ptFV A2T plays a substantial role in the APC-resistance. Based on the available data we hypothesize that the ptFV A2T allows the formation of productive interactions with ptFXa and/or prothrombin. However, these interactions only become functionally relevant in unfavorable conditions, with the cofactor being proteolyzed or in the absence of membranes. This is supported by our observation that the loss of cofactor activity upon APC-mediated proteolysis was not a consequence of A2 domain dissociation. Moreover, no difference in APC inactivation was observed for ptFVa-hA2T

and a variant in which the human APC cleavage region Arg306 was introduced and the disulfide bond connecting the ptFV A2-A3 domains eliminated (ptFVa-hA2T-h306-SS). Collectively, this indicates that ptFVa comprises mechanisms to support ptFXa affinity that are distinct from the essential requirements of mammalian FVa inactivation.

We previously demonstrated that ptFV comprises a rigid A2 domain loop that forms stable interactions with the A1 domain following APC-mediated proteolysis[21]. These interactions might be responsible for preventing A2 domain dissociation and could explain the residual and stable cofactor activity (~15%) of ptFVa-hA2T and ptFVa-hA2T-h306-SS following cleavage by APC. In similar fashion, we recently observed that proteolysis by plasmin significantly reduced the cofactor activity of ptFVa to a residual ~20% cofactor activity[21]. Taken together, our body of work indicates that the ptFV A2T plays an elementary role in the functional resistance to APC, whereas the residual cofactor activity of APC-proteolyzed ptFVa-hA2T or plasmin-proteolyzed ptFVa is a result of the regions that stabilize A2 domain binding.

Translation of the procoagulant enhancements of ptFV to hFV might provide unique opportunities for the generation of novel procoagulant and more stable FV products as potential therapeutic agents for bleeding disorders. Previous reports have demonstrated the efficacy of engineered FVa variants with improved stability in bleeding disorders such as hemophilia[47-50]. Furthermore, the peptide-mediated inhibition of the ptFVa/ptFXa complex suggests that targeting the A2T could be a viable strategy to generate the first specific antidote for envenomation by brown snakes and likely other Elapids[51]. The uncontrolled activation and consumption of the coagulation system that hallmarks VICC[8] follows from the procoagulant action of the FV(a)- and FX(a)-like proteins in brown snake and other snake venoms. A strategy that specifically aims to inhibit these procoagulant effects could therefore significantly improve the efficacy of antidote therapy.

In conclusion, we have identified a unique structural element responsible for the remarkable procoagulant enhancements that have transformed ptFV into a potent hemostatic toxin. Furthermore, by creating a human chimeric variant comprising the ptFV A2T, we have for the first time generated a human FVa molecule that has circumvented the need for membrane binding, one of the hallmarks of coagulation. As such, the ptFV A2T represents the exceptional modifications that are generated by evolutionary pressure to provide selective advantage.

Acknowledgements

This work was financially supported by the Bayer Hemophilia Awards Program (Special Project Award) and Landsteiner Foundation for Blood Transfusion (LSBR, grant. no. 1451). The funding agencies had no role in the preparation, review, or approval of the manuscript.

Figures

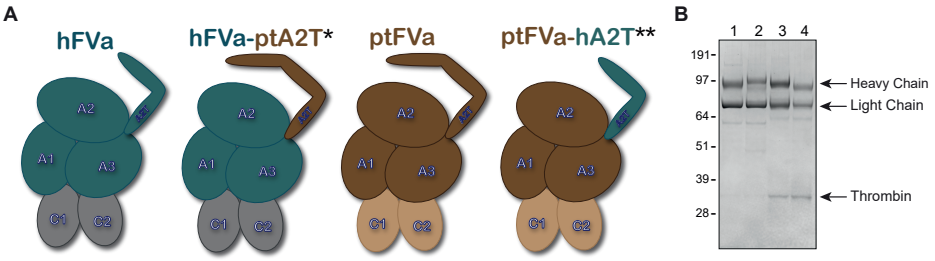


Figure 1. Generation of chimeric FVa variants. (A) Schematic representation of human FVa (hFVa, blue) and venom-derived *P. textilis* FVa (ptFVa, brown). The A2 domain C-terminus (A2T) was swapped between hFV and ptFV, generating hFVa-ptA2T and ptFVa-hA2T. * The human FV A2T region Glu662-Arg709 was replaced for the corresponding ptFV A2T region Gly663-Arg742 since exchange of the complete A2T resulted in a dysfunctional hFV protein due to disruption of the highly conserved C575-C656 disulfide bond. In addition, a hFVa-ptA2T variant in which the complete A2T was exchanged and C656 was reintroduced was generated (hFVa-ptA2T-Y656C). ** ptFVa-hA2T comprises the complete human A2T. Additional Arg680Gln substitution generated ptFVa-hA2T-R679Q. The specific A2T sequences of the FV variants are displayed in **Fig. S1B**. **(B)** SDS-PAGE analysis of purified thrombin-activated FVa variants (2 µg per lane) under reducing conditions and visualized by staining with Coomassie Brilliant Blue R-250. Lane 1, hFVa; lane 2, hFVa-ptA2T; lane 3, ptFVa; lane 4, ptFVa-hA2T. The apparent molecular weights of the standards are indicated on the left. Relevant FVa fragments are indicated on the right.

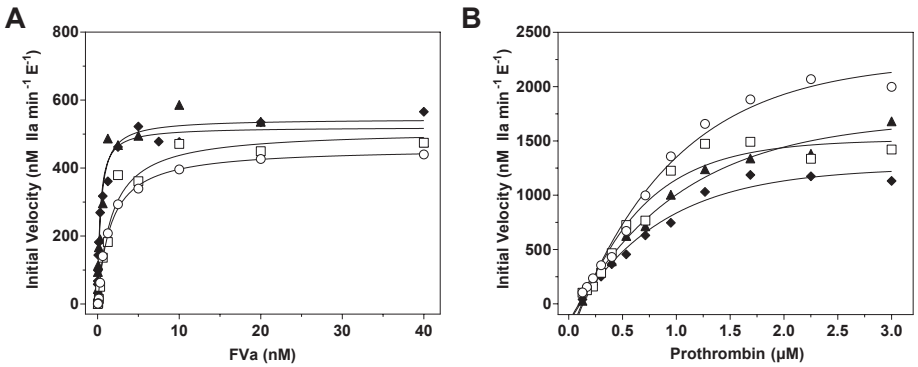


Figure 2. Steady-state kinetics for prothrombinase assembly and prothrombin conversion. **(A)** Reaction mixtures containing 1.4 μM prothrombin, 50 μM PCPS, 10 μM DAPA, and increasing concentrations (0-40 nM) of FVa variant were incubated for 5 min at 25°C. The reaction was initiated with 0.4 nM hFXa (for hFVa and hFVa-ptA2T) or 0.2 nM ptFXa (for ptFVa and ptFVa-hA2T), and thrombin formation was monitored during 3 min as described under "Materials and Methods". **(B)** Reaction mixtures containing 0-3 μM prothrombin, 50 μM PCPS, 10 μM DAPA, and 20 nM FVa variant were incubated for 5 min at 25°C. The reaction was initiated with 0.1 nM hFXa (for hFVa and hFVa-ptA2T) or ptFXa (for ptFVa and ptFVa-hA2T), and thrombin formation was monitored during 3 min as described under "Materials and Methods". The FVa variants are hFVa (open circles), hFVa-ptA2T (open squares), ptFVa (closed diamonds), or ptFVa-hA2T (closed triangles). Kinetic parameters of prothrombin conversion were determined by fitting the data to a Michaelis-Menten function by non-linear regression (Table 1). The data are representative of two to three independent experiments.

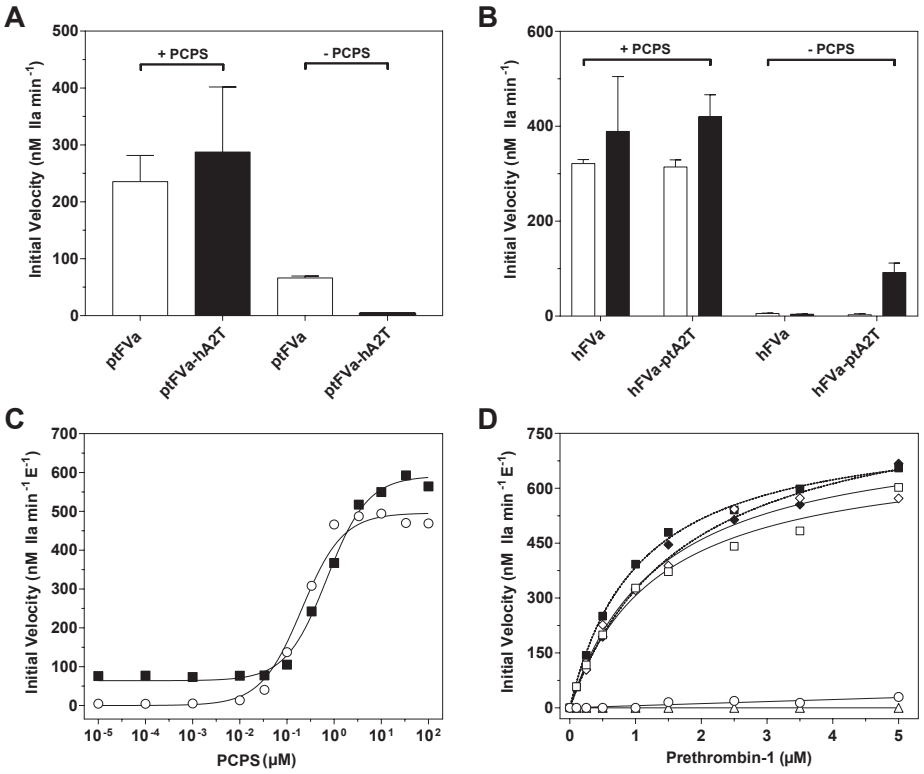


Figure 3. The *P. textilis* factor V A2 domain C-terminus confers lipid-independent prothrombin activation. **(A-B)** Reaction mixtures containing 1.4 μM prothrombin, 10 μM DAPA, and **(A)** 1 nM ptFVa or ptFVa-hA2T, or **(B)** 1 nM hFVa or hFVa-ptA2T were incubated for 5 min at 25°C in the presence or absence of 50 μM PCPS, as indicated. The reaction was initiated with **(A)** 10 nM ptFXa, or **(B)** by 10 nM hFXa (white bars) or ptFXa (black bars) and thrombin generation was monitored during 1.5-5 min as described under "Materials and Methods". **(C)** Initial velocity of thrombin generation determined in reaction mixtures containing 1.4 μM prothrombin, 10 μM DAPA, 1 nM hFVa (open circles) or hFVa-ptA2T (closed squares), 10 nM ptFXa and increasing concentrations of PCPS (0.00001-100 μM). **(D)** Initial velocity of thrombin generation determined in reaction mixtures containing 10 μM DAPA, 1 nM hFVa (circles), hFVa-ptA2T (squares), ptFVa (diamonds), or ptFVa-hA2T (triangles), 10 nM ptFXa, and increasing concentrations of prethrombin-1 in the presence (open symbols) or absence of PCPS (closed symbols; dotted lines). Bars depict mean ± 1 standard deviation. The lines were drawn following nonlinear regression analysis. The data are representative of two to three independent experiments.

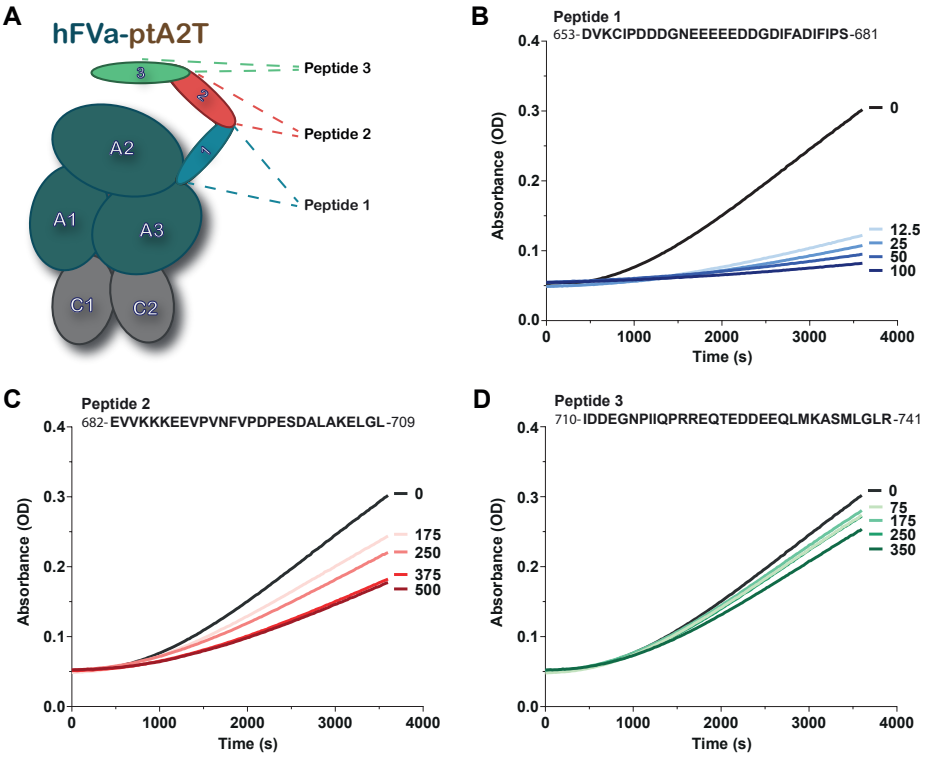


Figure 4. Peptide-mediated inhibition of the lipid-independent prothrombin conversion by the hFVa-ptA2T/ptFXa complex. (A) Schematic representation of ptFVa and the three peptides that represent a specific region of the ptFV A2T. The three A2T regions were selected based on their assumed interactions in the FVa-FXa-prothrombin complex[16]; specifically: peptide 1 may bind FXa/prothrombin, peptide 2 may interact with prothrombin, and peptide 3 appears as an extended region. **(B-D)** Reaction mixtures comprised 1.4 µM prothrombin, 10 µM DAPA, 100 µM S2238, 5 pM hFVa-ptA2T, and indicated concentrations (µM) of either peptide 1 **(E)**, peptide 2 **(F)**, or peptide 3 **(G)**, and prothrombin conversion was initiated by the addition of 10 nM ptFXa. Thrombin formation was continuously monitored during 60 min at 25°C as described under "Materials and Methods", and the absorbance (optical density, OD) at 405 nm representing S2238 hydrolysis was plotted over time. The data are representative of three independent experiments.

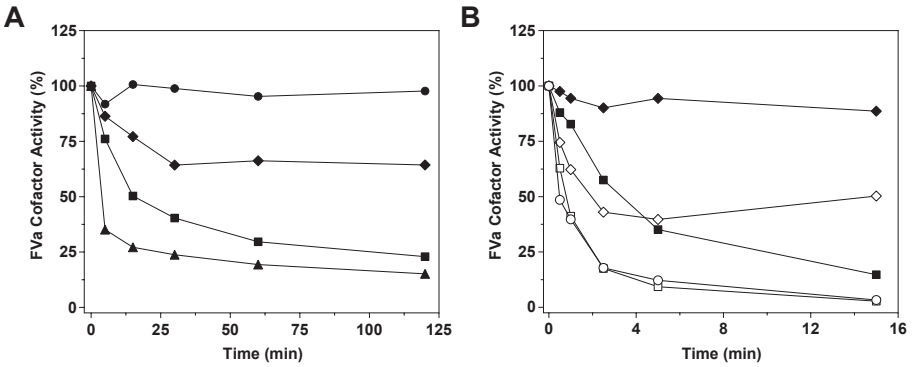


Figure 5. Functional resistance to activated protein C in factor Va variants comprising the *P. textilis* factor V A2 domain C-terminus. (A) Reaction mixtures containing 50 μM PCPS and 500 nM ptFVa (circles), ptFVa-hA2T (squares) ptFVa-hA2T-R679Q (diamonds) or ptFVa-hA2T-h306-SS (triangles) were incubated with 750 nM APC and **(B)** similar mixtures containing hFVa (circles), hFVa-ptA2T (squares) or hFVa-ptA2T-pt306 (diamonds) were incubated with 10 nM APC at 37°C. At selected time intervals, samples were removed for cofactor activity by determination of the initial velocity of prothrombin conversion, initiated by either hFXa (open symbols) or ptFXa (closed symbols). The data are representative of two to three independent experiments.

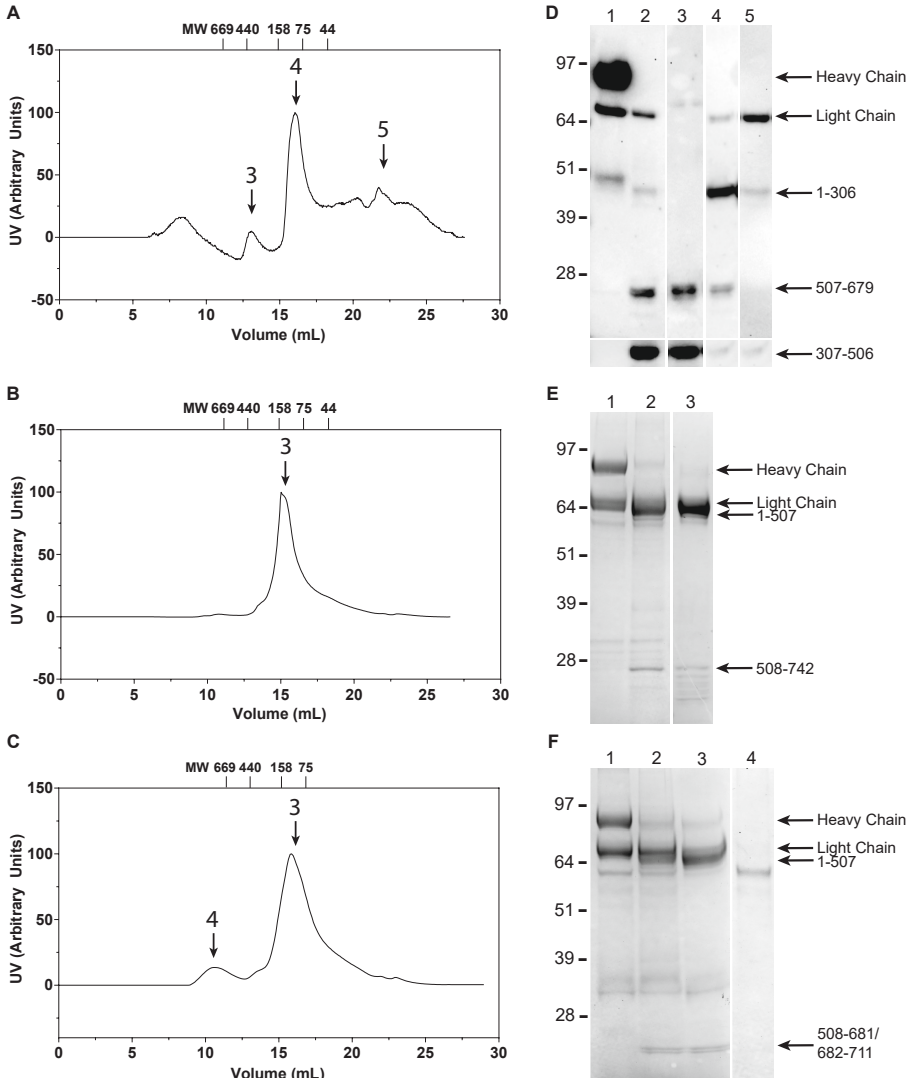


Figure 6. Structural integrity of activated protein C-treated FVa following exchange of the A2T. (A-C) Size-exclusion elution profile of APC-treated hFVa **(A)**, ptFVa **(B)**, or ptFVa-hA2T **(C)** performed as detailed in 'Materials and Methods'. Arrows and numbers indicate the respective fractions shown in **D-F** (**A-B**, data from reference[21]). **(D)** Western blot analysis of hFVa under reducing conditions following proteolysis by APC and size-exclusion chromatography elution. Lane 1, thrombin-activated hFVa; lane 2, APC-treated hFVa; lane 3, A2 domain fraction; lane 4, A1-A3-C1-C2 and A2 domain fraction; lane 5, A1-A3-C1-C2 domains fraction. **(E-F)** SDS-PAGE of APC-treated ptFVa **(E)** or ptFVa-hA2T **(F)** following size-exclusion chromatography under reducing conditions and visualized by staining with Coomassie Brilliant Blue R-250 (**E-F**, data from reference[21]). Lanes 1, thrombin-activated ptFVa variant; lanes 2, APC-treated ptFVa variant; lanes 3 and 4, elution fractions indicated by the black arrows and numbers in **B-C**. The apparent molecular weights of the standards are indicated on the left. Relevant FVa fragments are indicated on the right. Panel **D** and **F** are composed of two Western Blots or SDS-PAGE gels, respectively.

	FXa*	Prothrombinase* - prothrombin		Prothrombinase* – prethrombin-1		FVa/FXa* – prethrombin-1	
	$K_{d,\,app}$ (nM)	K_m (μM)	k_{cat} (min^{-1})	K_m (μM)	k_{cat} (min^{-1})	K_m (μM)	k_{cat} (min^{-1})
hFVa	1.58 ± 0.28[a]	0.47 ± 0.32	2385 ± 541	N.A.	N.A.	N.D.	N.D.
hFVa-ptA2T	1.69 ± 0.69[a]	0.48 ± 0.21	1406 ± 229	1.03 ± 0.53	591 ± 102	1.18 ± 0.17	829 ± 43
ptFVa	0.27 ± 0.08[b]	0.68 ± 0.15	1325 ± 112	1.46 ± 0.76	796 ± 153	1.68 ± 0.66	818 ± 131
ptFVa-hA2T	0.46 ± 0.17[b]	0.71 ± 0.22	1947 ± 426	N.A.	N.A.	N.D.	N.D.

Table 1. Kinetic constants for macromolecular substrate cleavage. The kinetic constants were obtained as described in 'Materials and Methods' in the presence (prothrombinase) or absence (FVa/FXa) of PCPS. Fitted values ± 1 standard deviation of the induced fit are representative of two to three independent experiments. N.D., not determined. N.A., for this experiment, rates were too low to accurately assess kinetic parameters. * The kinetic parameters for hFVa or hFVa-ptA2T were determined using hFXa and for ptFVa or ptFVa-hA2T using ptFXa, respectively.

Supplemental Methods

Materials and Reagents: The inhibitor dansylarginine-N-(3-ethyl-1,5-pentanediyl)amide (DAPA) was from Haematologic Technologies (Essex Junction, VT). The peptidyl substrate H-D-Phe-Pip-Arg-pNA (S2238) was obtained from Instrumentation Laboratories (Bedford, MA, USA). All tissue culture reagents were from Life Technologies (Carlsbad, CA, USA). Small unilamellar phospholipid vesicles (PCPS) composed of 75% (wt/wt) hen egg L-phosphatidylcholine (PC) and 25% (wt/wt) porcine brain L-phosphatidylserine (PS) (Avanti Polar Lipids, Alabaster, AL, USA) were prepared and characterized as described previously[52]. All functional assays were performed in HEPES-buffered saline (HBS: 20 mM HEPES, 0.15 M NaCl, pH 7.5) supplemented with 5 mM $CaCl_2$, 0.1% PEG8000 and filtered over a 0.2 µm filter (assay buffer).

Proteins: The human plasma-derived coagulation factors, prothrombin, α-thrombin, and activated protein C were from Haematologic Technologies (Essex Junction, VT). Restriction endonucleases BbvCI and Bsu36I were obtained from New England Biolabs (Ipswich, MA, USA), while AbsI was purchased from SibEnzyme (Novosibirsk, Russia). Hirudin and phospholipase C were from Sigma-Aldrich (St Louis, MO, USA). Recombinant human (hFXa) and venom-derived *Pseudonaja textilis* FXa (ptFXa) were prepared, purified, and characterized as described[17,53]. Recombinant constitutively active B-domainless human factor V (FV-810; hFV) and venom-derived *P. texilis* FV (ptFV), were prepared, purified, and characterized as described previously[14,34]. The peptides DVKCIPDDDGNEEEEEDDGDIFADIFIPS (designated peptide 1), EVVKKKEEVPVNFVPDPESDALAKELGL (designated peptide 2) and IDDEGNPIIQPRREQTEDDEEQLMKASMLGLR (designated peptide 3) were generated and purchased from Genscript (Piscataway, NJ, USA) and dissolved in ultrapure water or Dulbecco's Phosphate Buffered Saline (Life Technologies, Carlsbad, CA, USA) at 5-10 mg mL^{-1}.

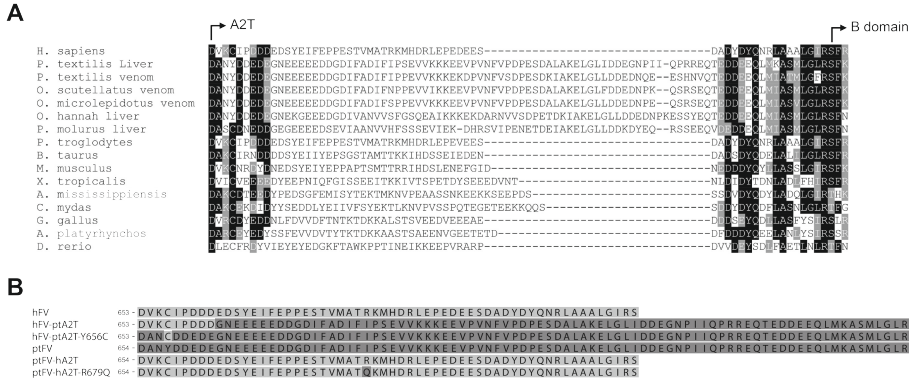
Construction of FV Variants: Initially, we generated constructs encoding for hFV (pED-hFV-810) comprising the venom-derived *P. textilis* A2T, designated pED-hFV-ptA2T$^{(1)}$ (ptFV sequence Gly693-Arg772; Uniprot: Q7SZN0 replacing hFV sequence Glu690-Arg737; Uniprot: P12259), and pED-hFV-ptA2T$^{(2)}$ (ptFV sequence Asp684-Arg772; Uniprot: Q7SZN0 replacing hFV sequence Asp681-Arg737; Uniprot: P12259). Furthermore, we generated ptFV constructs (pED-ptFV) comprising the human A2T sequence named pED-ptFV-hA2T$^{(1)}$ (hFV sequence Ser692-Arg737; Uniprot: P12259, replacing Gly693-Arg772; Uniprot: Q7SZN0) and pED-ptFV-hA2T$^{(2)}$ (hFV sequence Asp681-Arg737; Uniprot: P12259, replacing Asp684-Arg772; Uniprot: Q7SZN0). The constructs were generated by restriction enzyme digestion (hFV-ptA2T, BbvCI and AbsI;

ptFV-hA2T, BbvCI and Bsu36I) of pUC57 plasmids encoding the specifically designed FV A2T region flanked by pED-hFV-810 or pED-ptFV nucleotides, which were generated and purchased from Genscript (Piscataway, NJ, USA). The digested product was gel-purified and subcloned in pED vectors using identical restriction enzymes. Upon transfection, the variants hFV-ptA2T$^{(2)}$ and ptFV-hA2T$^{(1)}$ were not secreted or did not display FV activity. We were able to rescue expression of hFV-ptA2T$^{(2)}$ by Tyr656Cys (Tyr707; Uniprot: Q7SZN0) substitution, designated as pED-hFV-ptA2T-Y656C, since in hFV this cysteine forms a highly conserved disulfide bond with Cys575 (Cys603; Uniprot: P12259). pED-hFV-ptA2T-Y656C was generated from pED-ptFV-hA2T$^{(2)}$ by employing mutagenic complementary oligonucleotides (primers, tgatgatgaagatgagggaaatg and caattggcatccctgaatttcag) using the Q5® Site-Directed Mutagenesis Kit (New England Biolabs, Ipswich, MA, USA) according to manufacturer's protocol. The constructs pED-hFV-ptA2T$^{(1)}$ and pED-ptFV-hA2T$^{(2)}$ were subsequently used for the generation of pED-hFV-ptA2T-pt306 and pED-ptFV-hA2T-h306-SS by substitution of the Arg306 region (human full-length FV sequence Pro302-Leu308; Uniprot: P12259. ptFV sequence Gly303-Thr309; Uniprot: Q7SZN0) and deletion of ptFV's unique disulfide bond (ptFV residues Cys642 and Cys1002[16]; Uniprot: Q7SZN0). The variant pED-hFV-ptA2T-pt306 was generated using a pUC57 plasmid encoding pED-ptFV nucleotides 2124-2144, flanked by pED-hFV nucleotides, which was generated and purchased from Genscript (Piscataway, NJ, USA). The resulting pUC57 plasmid was digested with XcmI and Bsu36I, gel-purified, and subcloned into pED-hFV-ptA2T via digestion with the same enzymes. For pED-ptFV-hA2T-h306-SS, first pED-ptFV-hA2T-h306 was generated by employing mutagenic complementary oligonucleotides (primers, caggaatcttagaaagttatcctttagagaac and gttttctttggacagtctttgatatttagataacc) as described[21]. Subsequently, the residues encoding ptFV's unique disulfide bond were substituted (primers Cys642Ser, tgagatgagcaatggcatgagattg and gaggagccccatgatgacagaag; primers Cys1002Ser, gaagagaaacttataggagtccaatc and agaagtgcttttgtcagattttgg) to generate pED-ptFV-hA2T-h306-SS using the Q5® Site-Directed Mutagenesis Kit (New England Biolabs, Ipswich, MA, USA) according to manufacturer's protocol. Additionally, we used pED-ptFV-hA2T$^{(2)}$ to generate the construct pED-ptFV-hA2T-R679Q comprising a Arg679Gln substitution (Arg707; Uniprot: P12259). (primers, caggaatcttagaaagttatcctttagagaac and gttttctttggacagtctttgatatttagataacc) employing the Q5® Site-Directed Mutagenesis Kit.

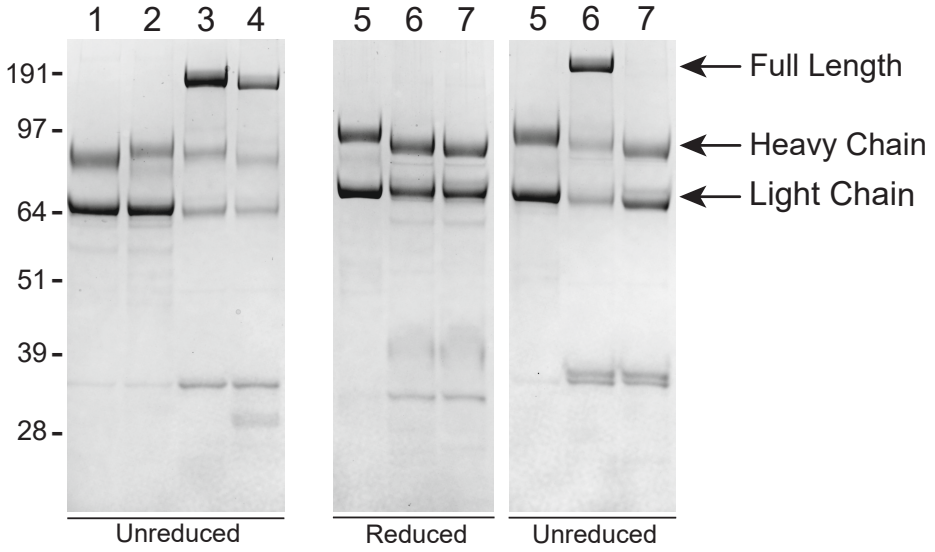
Expression and purification of FV variants: Transfection of the plasmids encoding FV constructs into baby hamster kidney cells, the selection of stable clones, and the expression and purification of hFV and ptFV were performed as described previously[14,34]. Briefly, FV proteins were purified employing ion-exchange chromatography on a Q-Sepharose FF column (GE Healthcare) using a NaCl elution gradient in HBS supplemented with 5 mM $CaCl_2$ and 1 mM BZA, pH 7.4. Fractions containing FV activity

were pooled and dialyzed versus 20 mM HEPES, 5mM $CaCl_2$, pH 7.4 for human FV variants and 20 mM MES, 5 mM $CaCl_2$, pH 6.0 for ptFV variants, loaded on a POROS HQ/20 (hFV) or HS/20 column (ptFV) (Applied Biosystems) and eluted using a NaCl gradient. Protein purity was assessed by SDS-PAGE using pre-cast 4%–12% gradient gels under nonreducing and reducing conditions (50mM DTT) using the MOPS buffer system (Life technologies; Carlsbad, CA, USA) followed by staining with Coomassie Brilliant Blue R-250. For pretreatment with thrombin, FV variants were incubated for 15 minutes with α-thrombin (molar ratio 15:1 for hFV or 3.75:1 for ptFV) in assay buffer at 37°C, followed by the addition of a 10-fold molar excess of hirudin. Following transfection and purification, the protein variants generated by pED-hFV-ptA2T[(1)] and pED-ptFV-hA2T[(2)] were designated as hFV-ptA2T and ptFV-hA2T, respectively. The molecular weight of the newly generated variants was assumed as follows, hFV-ptA2T, hFV-ptA2T-Y656C, and hFV-ptA2T-pt306: 220,000 kDa; ptFV-hA2T, ptFV-hA2T-R679Q, and ptFV-hA2T-h306-SS: 159,000 kDa[14,34]. The extinction coefficients (E0.1%, 280 nm) of the FV variants were assumed to be equal to hFV (1.54) and ptFV (1.25), respectively[14,34].

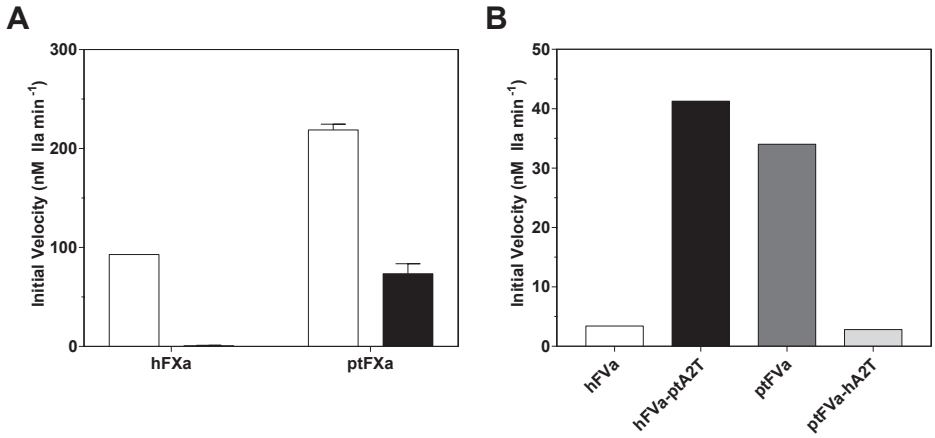
Supplemental Figures



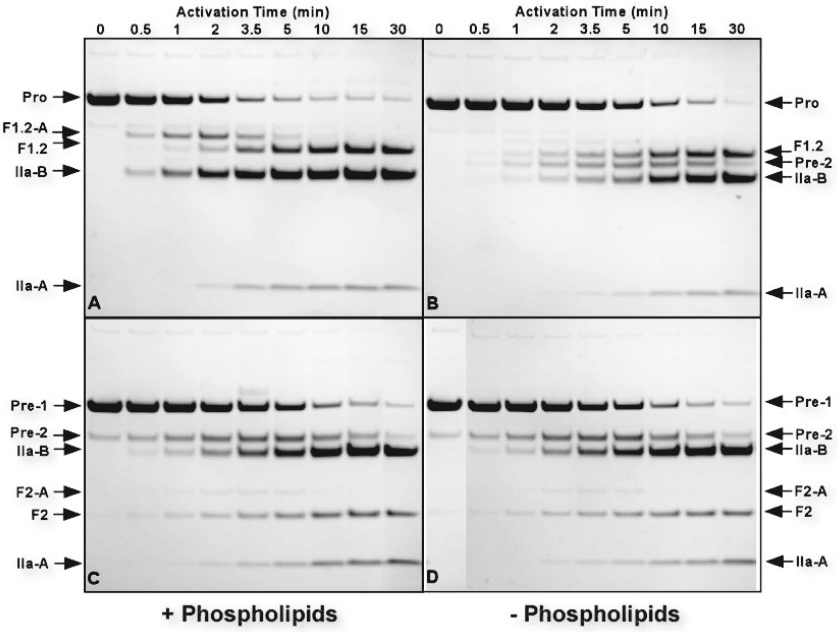
Supplementary figure 1. (A) Alignment of the amino acid sequences comprising the FV A2 domain C-terminus (A2T) (Clustal Omega Module; EMBL-EBI, UK). Residues identical to the column consensus are shown in black; residues similar to the column consensus are shown in grey. The start of A2T and the B domain are indicated. **(B)** Sequence alignment defining the A2T of the generated recombinant FV variants. Human A2T residues are shown in blue, ptFV A2T residues are shown in brown.



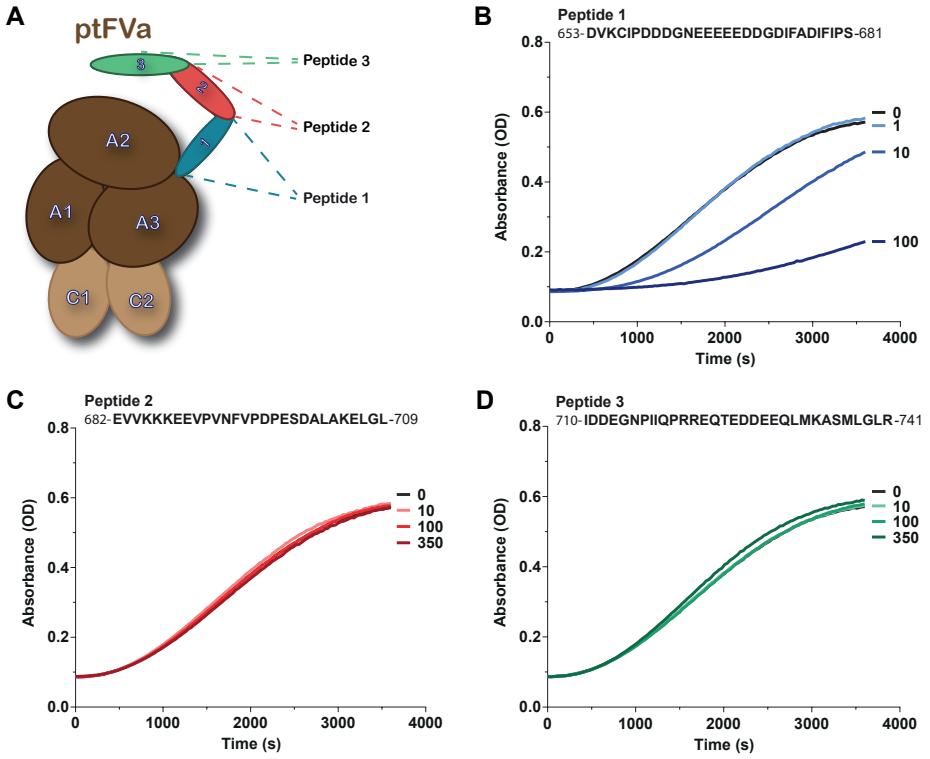
Supplementary figure 2. SDS-PAGE of FVa variants. SDS-PAGE analysis of purified thrombin-activated FVa variants (2 µg per lane) under reducing and non-reducing conditions, visualized by staining with Coomassie Brilliant Blue R-250. Lane 1, hFVa; lane 2, hFVa-ptA2T; lane 3, ptFVa; lane 4, ptFVa-hA2T; lanes 5, hFVa-ptA2T-pt306; lanes 6, ptFVa-hA2T-h306; lanes 7, ptFVa-hA2T-h306-SS. The apparent molecular weights of the standards are indicated on the left. Relevant FVa fragments are indicated on the right.



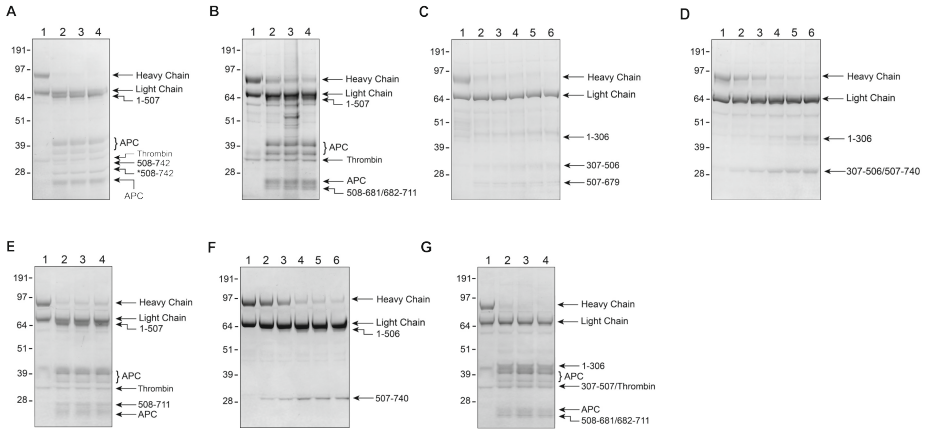
Supplementary Figure 3. Lipid-independent prothrombin conversion. (A) The initial velocity of thrombin generation was determined in the presence of 1.4 μM prothrombin, 10 μM DAPA, 1 nM hFVa-ptA2T-Y656C and 10 nM hFXa or ptFXa in the presence (open bars) or absence (closed bars) of PCPS (50 μM). **(B)** Mixtures containing 12.5 nM FVa variant and 125 μM PCPS were incubated with phospholipase C (25 U/mL) for 10 min at 37°C. Samples were removed for cofactor activity by determination of the initial velocity of thrombin generation in reaction mixtures containing 1.4 μM prothrombin, 10 μM DAPA, 10 nM ptFXa, 1 nM phospholipase C-treated hFVa, hFVa-ptA2T, ptFVa or ptFVa-hA2T. Bars depict mean ± 1 standard deviation for one to three independent experiments.



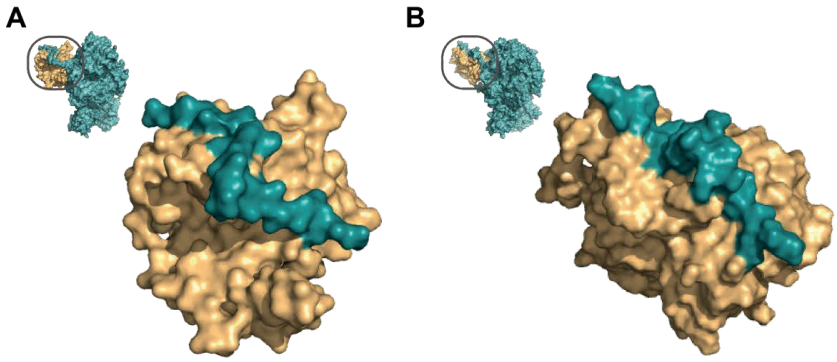
Supplementary Figure 4. Macromolecular substrate cleavage by ptFV-ptFXa. At the indicated time points samples were taken from reaction mixtures containing 5.4 mM prothrombin (panels A,B) or prethrombin-1 (panels C,D), 1 nM ptFXa, and 30 nM ptFV with (panels A,C) or without (panels B,D) 30 mM PCPS present. Samples were quenched, subjected to SDS-PAGE under reducing conditions, and visualized by staining with Coomassie Brilliant Blue R-250. Identities of the relevant species are indicated next to the gels, and time point 0 in panel D is taken from panel C. The proteins used in this assay were gifted by Dr. Camire (Children's Hospital of Philadelphia, Philadelphia, United States).



Supplementary figure 5. Peptide-mediated inhibition of the lipid-independent prothrombin conversion by the ptFVa/ptFXa complex. (A) Schematic representation of ptFVa and the three peptides that represent a specific region of the ptFV A2T. The three A2T regions were selected based on their hypothesized interaction in the FVa-FXa-prothrombin complex. **(B-D)** Inhibition of ptFVa/ptFXa activity using peptides comprising parts of the ptFV A2T in a continuous assay. Reaction mixtures containing 1.4 μM prothrombin, 10 μM DAPA, 100 μM S2238, 5 pM ptFVa and indicated concentrations of either peptide 1 **(B)**, peptide 2 **(C)**, or peptide 3 **(D)** were initiated by 10 nM ptFXa. Thrombin formation was continuously monitored during 1.5-5 min as described under "Materials and Methods". The data are representative of two independent experiments.



Supplementary figure 6. Activated protein C treatment of human and *P. textilis* factor Va variants. SDS-PAGE of APC-treated **(A)** ptFVa, **(B)** ptFVa-hA2T, **(C)** hFVa, **(D)** hFVa-ptA2T, **(E)** ptFVa-hA2T-R679Q, **(F)** hFVa-ptA2T-pt306, and **(G)** ptFVa-hA2T-h306-SS (3 µg per lane) under reducing conditions and visualized by staining with Coomassie Brilliant Blue R-250. **(A, B, E, G)** Lanes 1-4 represent time samples quenched at 0, 30, 60, and 120 min. **(C, D, F)** Lanes 1-6 represent time samples quenched at 0, 0.5, 1, 2.5, 5, and 15 min. The apparent molecular weights of the standards are indicated on the left. Relevant FVa fragments are indicated on the right. We hypothesize that *508-742 is cleaved at a C-terminal position because its N-terminal sequence was determined to be the same as 508-742[21].



Supplementary figure 7. Interface between the factor Va A2 domain C-terminus and factor Xa. (A) A zoomed-in region of the Pseutarin C crystal structure[16] or **(B)** the human ternary model by Shim *et al.* is shown[28]; the insert outlines the specific region depicted. The FVa A2T is shown in teal, the serine protease domain of FXa is depicted in yellow. The additional FVa regions, the FXa light chain, and prothrombin have been removed for clarity.

	K_m μM	K_{cat} min^{-1}
+ PCPS	1.1 ± 0.1	1610 ± 28
- PCPS	1.1 ± 0.1	1570 ± 38
- $CaCl_2$	1.9 ± 0.2	530 ± 12
+ EDTA	2.6 ± 0.5	350 ± 21

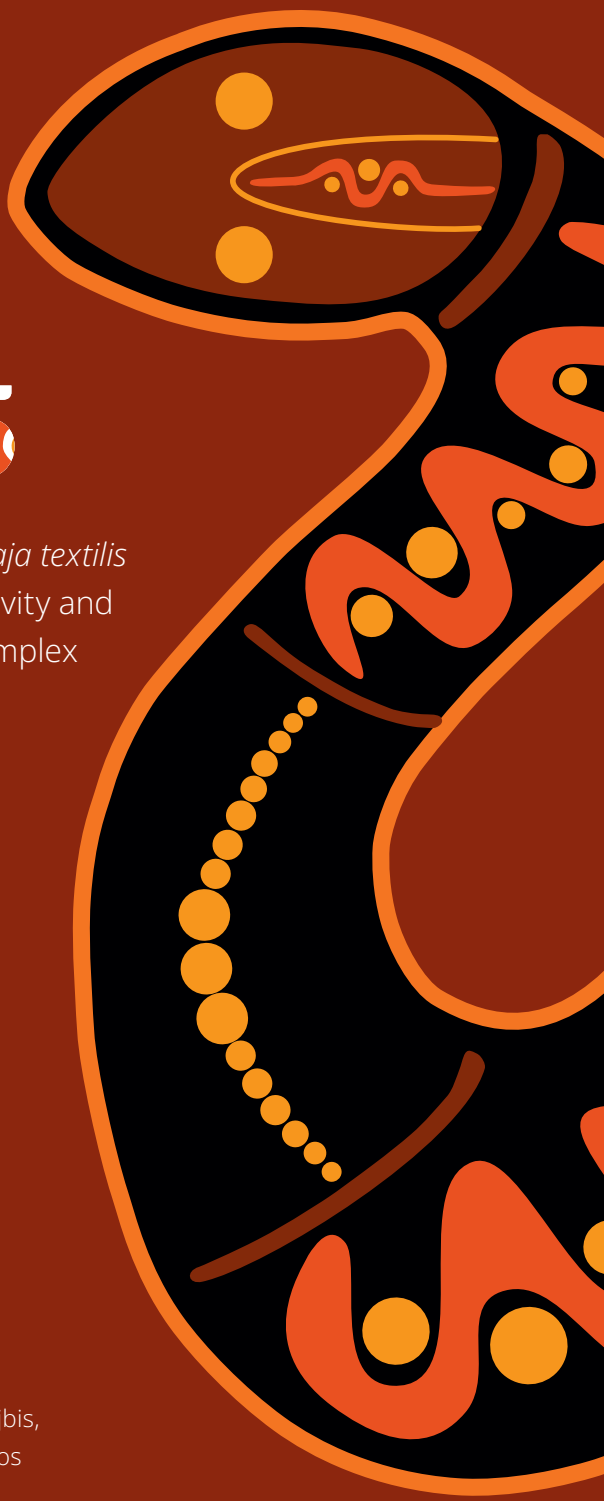
Supplementary Table 1. Kinetic constants for prethrombin-1 cleavage. The initial velocity of thrombin generation was determined at increasing concentrations of prethrombin-1 with 0.1 nM ptFXa and 20 nM ptFV. Substrate cleavage was assayed in the presence (+ PCPS) or absence (- PCPS) of 50 μM phospholipid vesicles; under the latter conditions, 5 mM CaCl2 was omitted from the reaction mixture (- CaCl2), or, additionally, 50 mM EDTA (+ EDTA) was added. Data sets were analyzed, and the fitted constants are shown. The data are representative of two similar experiments. The proteins used in this assay were gifted by Dr. Camire (Children's Hospital of Philadelphia, Philadelphia, United States).

References

1 Fry, B. G. Structure-function properties of venom components from Australian elapids. *Toxicon* **37**, 11-32, doi:10.1016/s0041-0101(98)00125-1 (1999).
2 Tans, G. & Rosing, J. Snake venom activators of factor X: an overview. *Haemostasis* **31**, 225-233, doi:10.1159/000048067 (2001).
3 Rao, V. S. & Kini, R. M. Pseutarin C, a prothrombin activator from Pseudonaja textilis venom: its structural and functional similarity to mammalian coagulation factor Xa-Va complex. *Thrombosis and haemostasis* **88**, 611-619 (2002).
4 Kini, R. M. The intriguing world of prothrombin activators from snake venom. *Toxicon* **45**, 1133-1145, doi:10.1016/j.toxicon.2005.02.019 (2005).
5 Berling, I. & Isbister, G. K. Hematologic effects and complications of snake envenoming. *Transfus Med Rev* **29**, 82-89, doi:10.1016/j.tmrv.2014.09.005 (2015).
6 Masci, P. P., Rowe, E. A., Whitaker, A. N. & de Jersey, J. Fibrinolysis as a feature of disseminated intravascular coagulation (DIC) after Pseudonaja textilis textilis envenomation. *Thromb Res* **59**, 859-870, doi:10.1016/0049-3848(90)90399-w (1990).
7 Isbister, G. K. Procoagulant snake toxins: laboratory studies, diagnosis, and understanding snakebite coagulopathy. *Semin Thromb Hemost* **35**, 93-103, doi:10.1055/s-0029-1214152 (2009).
8 Isbister, G. K. *et al.* Factor deficiencies in venom-induced consumption coagulopathy resulting from Australian elapid envenomation: Australian Snakebite Project (ASP-10). *J Thromb Haemost* **8**, 2504-2513, doi:10.1111/j.1538-7836.2010.04050.x (2010).
9 Johnston, C. I. *et al.* The Australian Snakebite Project, 2005-2015 (ASP-20). *Med J Aust* **207**, 119-125, doi:10.5694/mja17.00094 (2017).
10 Rao, V. S., Swarup, S. & Kini, R. M. The nonenzymatic subunit of pseutarin C, a prothrombin activator from eastern brown snake (Pseudonaja textilis) venom, shows structural similarity to mammalian coagulation factor V. *Blood* **102**, 1347-1354, doi:10.1182/blood-2002-12-3839 (2003).
11 Minh Le, T. N., Reza, M. A., Swarup, S. & Kini, R. M. Gene duplication of coagulation factor V and origin of venom prothrombin activator in Pseudonaja textilis snake. *Thrombosis and haemostasis* **93**, 420-429, doi:10.1160/TH04-11-0707 (2005).
12 Rao, V. S., Swarup, S. & Manjunatha Kini, R. The catalytic subunit of pseutarin C, a group C prothrombin activator from the venom of Pseudonaja textilis, is structurally similar to mammalian blood coagulation factor Xa. *Thrombosis and haemostasis* **92**, 509-521, doi:10.1160/TH04-03-0144 (2004).
13 Reza, M. A., Minh Le, T. N., Swarup, S. & Manjunatha Kini, R. Molecular evolution caught in action: gene duplication and evolution of molecular isoforms of prothrombin activators in Pseudonaja textilis (brown snake). *J Thromb Haemost* **4**, 1346-1353, doi:10.1111/j.1538-7836.2006.01969.x (2006).
14 Bos, M. H. *et al.* Venom factor V from the common brown snake escapes hemostatic regulation through procoagulant adaptations. *Blood* **114**, 686-692, doi:10.1182/blood-2009-02-202663 (2009).
15 Bos, M. H. & Camire, R. M. Procoagulant adaptation of a blood coagulation prothrombinase-like enzyme complex in australian elapid venom. *Toxins (Basel)* **2**, 1554-1567, doi:10.3390/toxins2061554 (2010).
16 Lechtenberg, B. C. *et al.* Crystal structure of the prothrombinase complex from the venom of Pseudonaja textilis. *Blood* **122**, 2777-2783, doi:10.1182/blood-2013-06-511733 (2013).
17 Verhoef, D. *et al.* Engineered factor Xa variants retain procoagulant activity independent of direct factor Xa inhibitors. *Nat Commun* **8**, 528, doi:10.1038/s41467-017-00647-9 (2017).

18 Schreuder, M. *et al.* Evolutionary adaptations in Pseudonaja textilis venom factor X induce zymogen activity and resistance to the intrinsic tenase complex. *Accepted in Thrombosis and Haemostasis* (2020).
19 Bos, M. H. & Camire, R. M. A bipartite autoinhibitory region within the B-domain suppresses function in factor V. *J Biol Chem* **287**, 26342-26351, doi:10.1074/jbc.M112.377168 (2012).
20 Bunce, M. W., Bos, M. H., Krishnaswamy, S. & Camire, R. M. Restoring the procofactor state of factor Va-like variants by complementation with B-domain peptides. *J Biol Chem* **288**, 30151-30160, doi:10.1074/jbc.M113.506840 (2013).
21 Schreuder, M., Verhoef, D., Cheung, K. L., Reitsma, P. H. & Bos, M. H. A. *Pseudonaja textilis* Factor Va Retains Structural Integrity and Cofactor Function. *Research and Practice in Thrombosis and Haemostasis* **3**, PB0626 (2019).
22 Bakker, H. M. *et al.* Functional properties of human factor Va lacking the Asp683-Arg709 domain of the heavy chain. *J Biol Chem* **269**, 20662-20667 (1994).
23 Kalafatis, M., Beck, D. O. & Mann, K. G. Structural requirements for expression of factor Va activity. *J Biol Chem* **278**, 33550-33561, doi:10.1074/jbc.M303153200 (2003).
24 Beck, D. O., Bukys, M. A., Singh, L. S., Szabo, K. A. & Kalafatis, M. The contribution of amino acid region ASP695-TYR698 of factor V to procofactor activation and factor Va function. *J Biol Chem* **279**, 3084-3095, doi:10.1074/jbc.M306850200 (2004).
25 Bukys, M. A., Kim, P. Y., Nesheim, M. E. & Kalafatis, M. A control switch for prothrombinase: characterization of a hirudin-like pentapeptide from the COOH terminus of factor Va heavy chain that regulates the rate and pathway for prothrombin activation. *J Biol Chem* **281**, 39194-39204, doi:10.1074/jbc.M604482200 (2006).
26 Hirbawi, J., Bukys, M. A., Barhoover, M. A., Erdogan, E. & Kalafatis, M. Role of the acidic hirudin-like COOH-terminal amino acid region of factor Va heavy chain in the enhanced function of prothrombinase. *Biochemistry* **47**, 7963-7974, doi:10.1021/bi800593k (2008).
27 Schreuder, M., Reitsma, P. H. & Bos, M. H. A. Blood coagulation factor Va's key interactive residues and regions for prothrombinase assembly and prothrombin binding. *J Thromb Haemost* **17**, 1229-1239, doi:10.1111/jth.14487 (2019).
28 Shim, J. Y., Lee, C. J., Wu, S. & Pedersen, L. G. A model for the unique role of factor Va A2 domain extension in the human ternary thrombin-generating complex. *Biophysical chemistry* **199**, 46-50, doi:10.1016/j.bpc.2015.02.003 (2015).
29 Higgins, D. L. & Mann, K. G. The interaction of bovine factor V and factor V-derived peptides with phospholipid vesicles. *J Biol Chem* **258**, 6503-6508 (1983).
30 Camire, R. M. Prothrombinase assembly and S1 site occupation restore the catalytic activity of FXa impaired by mutation at the sodium-binding site. *J Biol Chem* **277**, 37863-37870, doi:10.1074/jbc.M203692200 (2002).
31 Toso, R. & Camire, R. M. Removal of B-domain sequences from factor V rather than specific proteolysis underlies the mechanism by which cofactor function is realized. *J Biol Chem* **279**, 21643-21650, doi:10.1074/jbc.M402107200 (2004).
32 Krishnaswamy, S. & Walker, R. K. Contribution of the prothrombin fragment 2 domain to the function of factor Va in the prothrombinase complex. *Biochemistry* **36**, 3319-3330, doi:10.1021/bi9623993 (1997).
33 Kalafatis, M. & Mann, K. G. The role of the membrane in the inactivation of factor va by plasmin. Amino acid region 307-348 of factor V plays a critical role in factor Va cofactor function. *J Biol Chem* **276**, 18614-18623, doi:10.1074/jbc.M007134200 (2001).
34 Toso, R. & Camire, R. M. Role of Hirudin-like factor Va heavy chain sequences in prothrombinase function. *J Biol Chem* **281**, 8773-8779, doi:10.1074/jbc.M511419200 (2006).
35 Mann, K. G., Nesheim, M. E., Hibbard, L. S. & Tracy, P. B. The role of factor V in the assembly of the prothrombinase complex. *Ann N Y Acad Sci* **370**, 378-388, doi:10.1111/j.1749-6632.1981.tb29750.x (1981).

36 Hirbawi, J., Vaughn, J. L., Bukys, M. A., Vos, H. L. & Kalafatis, M. Contribution of amino acid region 659-663 of Factor Va heavy chain to the activity of factor Xa within prothrombinase. *Biochemistry* **49**, 8520-8534, doi:10.1021/bi101097t (2010).
37 Toso, R., Zhu, H. & Camire, R. M. The conformational switch from the factor X zymogen to protease state mediates exosite expression and prothrombinase assembly. *J Biol Chem* **283**, 18627-18635, doi:10.1074/jbc.M802205200 (2008).
38 Gilbert, G. E., Novakovic, V. A., Kaufman, R. J., Miao, H. & Pipe, S. W. Conservative mutations in the C2 domains of factor VIII and factor V alter phospholipid binding and cofactor activity. *Blood* **120**, 1923-1932, doi:10.1182/blood-2012-01-408245 (2012).
39 Krishnaswamy, S. Exosite-driven substrate specificity and function in coagulation. *J Thromb Haemost* **3**, 54-67, doi:10.1111/j.1538-7836.2004.01021.x (2005).
40 Bradford, H. N., Orcutt, S. J. & Krishnaswamy, S. Membrane binding by prothrombin mediates its constrained presentation to prothrombinase for cleavage. *J Biol Chem* **288**, 27789-27800, doi:10.1074/jbc.M113.502005 (2013).
41 Norstrom, E., Thorelli, E. & Dahlback, B. Functional characterization of recombinant FV Hong Kong and FV Cambridge. *Blood* **100**, 524-530, doi:10.1182/blood-2002-02-0343 (2002).
42 Krishnaswamy, S., Jones, K. C. & Mann, K. G. Prothrombinase complex assembly. Kinetic mechanism of enzyme assembly on phospholipid vesicles. *J Biol Chem* **263**, 3823-3834 (1988).
43 Mann, K. G., Nesheim, M. E., Church, W. R., Haley, P. & Krishnaswamy, S. Surface-dependent reactions of the vitamin K-dependent enzyme complexes. *Blood* **76**, 1-16 (1990).
44 Qureshi, S. H., Yang, L., Manithody, C. & Rezaie, A. R. Membrane-dependent interaction of factor Xa and prothrombin with factor Va in the prothrombinase complex. *Biochemistry* **48**, 5034-5041, doi:10.1021/bi900240g (2009).
45 Bevers, E. M., Comfurius, P. & Zwaal, R. F. Changes in membrane phospholipid distribution during platelet activation. *Biochim Biophys Acta* **736**, 57-66 (1983).
46 Heemskerk, J. W., Bevers, E. M. & Lindhout, T. Platelet activation and blood coagulation. *Thrombosis and haemostasis* **88**, 186-193 (2002).
47 Majumder, R., Quinn-Allen, M. A., Kane, W. H. & Lentz, B. R. A phosphatidylserine binding site in factor Va C1 domain regulates both assembly and activity of the prothrombinase complex. *Blood* **112**, 2795-2802, doi:10.1182/blood-2008-02-138941 (2008).
48 Macedo-Ribeiro, S. *et al.* Crystal structures of the membrane-binding C2 domain of human coagulation factor V. *Nature* **402**, 434-439, doi:10.1038/46594 (1999).
49 Schlachterman, A. *et al.* Factor V Leiden improves in vivo hemostasis in murine hemophilia models. *J Thromb Haemost* **3**, 2730-2737, doi:10.1111/j.1538-7836.2005.01639.x (2005).
50 von Drygalski, A. *et al.* Improved hemostasis in hemophilia mice by means of an engineered factor Va mutant. *J Thromb Haemost* **12**, 363-372, doi:10.1111/jth.12489 (2014).
51 van 't Veer, C. *et al.* An in vitro analysis of the combination of hemophilia A and factor V(LEIDEN). *Blood* **90**, 3067-3072 (1997).
52 Bos, M. H., Meijerman, D. W., van der Zwaan, C. & Mertens, K. Does activated protein C-resistant factor V contribute to thrombin generation in hemophilic plasma? *J Thromb Haemost* **3**, 522-530, doi:10.1111/j.1538-7836.2005.01181.x (2005).
53 Zdenek, C. N. *et al.* Coagulotoxic effects by brown snake (Pseudonaja) and taipan (Oxyuranus) venoms, and the efficacy of a new antivenom. *Toxicol In Vitro* **58**, 97-109, doi:10.1016/j.tiv.2019.03.031 (2019).



Chapter 5

Evolutionary Adaptations in *Pseudonaja textilis* Venom Factor X induce Zymogen Activity and Resistance to the Intrinsic Tenase Complex

Mark Schreuder, Geraldine Poenou, Viola J.F. Strijbis, Ka Lei Cheung, Pieter H. Reitsma, Mettine H.A. Bos

Thrombosis and Haemostasis. 2020 120(11):1512-1523



Abstract

The venom of the Australian snake *Pseudonaja textilis* comprises powerful prothrombin activators consisting of factor X (v-ptFX)- and factor V-like proteins. While all vertebrate liver-expressed factor X (FX) homologs, including that of *Pseudonaja textilis*, comprise an activation peptide of ~45-65 residues, the activation peptide of v-ptFX is significantly shortened to 27 residues. In this study, we demonstrate that exchanging the human FX activation peptide for the snake venom ortholog impedes proteolytic cleavage by the intrinsic factor VIIIa-factor IXa tenase complex. Furthermore, our findings indicate that the human FX activation peptide comprises an essential binding site for the intrinsic tenase complex. Conversely, incorporation of factor X into the extrinsic tissue factor-factor VIIa tenase complex is completely dependent on exosite-mediated interactions. Remarkably, the shortened activation peptide allows for factor V-dependent prothrombin conversion while in zymogen-state. This indicates that the active site of FX molecules comprising the v-ptFX activation peptide partially matures upon assembly into a premature prothrombinase complex. Taken together, the shortened activation peptide is one of the remarkable characteristics of v-ptFX that has been modified from its original, thereby transforming FX into a powerful procoagulant protein. Moreover, these results shed new light on the structural requirements for serine protease activation and indicate that catalytic activity can be obtained without formation of the characteristic Ile^{16}-Asp^{194} salt bridge via modification of the activation peptide.

Introduction

Coagulation factor X (FX) is a vitamin K-dependent protein that circulates as an inactive zymogen precursor and is composed of a heavy and light chain that are covalently linked via a disulfide bond. The N-terminal light chain comprises a γ-carboxyglutamic acid-containing domain that is responsible for anionic phospholipid binding and two epidermal growth factor-like domains that have been implicated in macromolecular interactions[1]. The C-terminal heavy chain consists of an activation peptide and the serine protease domain that comprises the active site, which is hallmarked by the catalytic triad residues His[95], Asp[102], and Ser[195] (chymotrypsinogen numbering).

Transition from the zymogen to the protease state requires conformational changes in the FX serine protease domain resulting in a functional realignment of the active site and exosite regions[2]. This essential step is tightly regulated by intrinsic (tissue factor (TF) and factor VIIa (FVIIa)) or extrinsic (factors VIIIa (FVIIIa) and IXa (FIXa)) tenase complex-mediated proteolysis of the highly conserved Arg[15]-Ile[16] scissile bond, resulting in liberation of the 52-residue activation peptide. The activation peptide is considered to be important for the specificity of the tenase complexes towards FX, with glycosylation of the human FX activation peptide contributing to the cofactor-dependent substrate recognition[3,4]. The newly formed N-terminus (Ile[16]) engages in a salt bridge with active site residue Asp[194] that induces conformational changes leading to maturation of the serine protease domain[5,6]. The mature protease FXa is capable of interacting with the activated cofactor Va (FVa) in the presence of an anionic phospholipid membrane and calcium ions, thereby forming the prothrombinase complex that rapidly converts prothrombin to thrombin.

Interestingly, the venom of some Australian Elapid snakes comprises powerful prothrombin-activating enzyme complexes consisting of FXa- and FVa-like proteins that are specifically expressed in the venom gland[7,8]. Due to selective pressure these venom proteins have been evolutionary adapted to disrupt the hemostatic balance in prey animals, resulting in incapacitation of the prey[8]. The catalytic subunit (v-ptFX) shares ~42% sequence homology with mammalian FX and comprises several unique features[9-11], including a 13-residue insertion directly N-terminal from Tyr[99] that results in an extended 99-loop. Recently, we have reported that insertion of this region into human FX (generating 'FX-A'[12]) not only impairs inhibition by antithrombin and tissue factor pathway inhibitor, but also induces insensitivity towards the direct FXa inhibitors that are now widely used as oral anticoagulants[12]. Another striking difference between v-ptFX and mammalian blood coagulation FX is the length of the activation peptide[9]. Intriguingly, while all vertebrate liver-expressed FX homologs, including that of *P.*

textilis[13], comprise an activation peptide of at least 40 residues, the activation peptide of v-ptFX is only 27 residues long.

In the present study we generated and characterized chimeric FX variants in which the activation peptide was exchanged between human FX (hFX) and v-ptFX to examine the functional role of the shortened activation peptide of v-ptFX. Our results demonstrate that this unique structural element encompasses some remarkable characteristics that significantly impact the procoagulant activity of v-ptFX. These findings thereby highlight the ability of selective pressure to develop unique biologic properties and further show how evolutionary adaptations can improve our understanding of protein biology.

Materials and Methods

Materials: Apixaban was from Alsachim (Illkirch, France). The inhibitor dansylarginine-N-(3-ethyl-1,5-pentanediyl)amide (DAPA) and corn trypsin inhibitor (CTI) were from Haematologic Technologies (Essex Junction, VT). 4-amidinophenylmethanesulfonyl fluoride hydrochloride (APMSF) was from Sigma. The peptidyl substrate methoxycarb onylcyclohexylglycylglycyl-Arg-pNA (SpecXa) was from Sekisui Diagnostics (Stamford, CT, USA); the peptidyl substrates N-α-benzyloxycarbonyl-D-Arg-Gly-Arg-pNA (S2765) and H-D-Phe-Pip-Arg-pNA (S2238) were from Instrumentation Laboratories (Bedford, MA, USA). All tissue culture reagents were from Life Technologies (Carlsbad, CA, USA). Calibrator and fluorescent substrate (FluCa) were from Thrombinoscope (Maastricht, the Netherlands). Small unilamellar phospholipid vesicles (PCPS) composed of 75% (wt/wt) hen egg L-phosphatidylcholine (PC) and 25% (wt/wt) porcine brain L-phosphatidylserine (PS) (Avanti Polar Lipids, Alabaster, AL, USA) were prepared and characterized as described previously[14]. FX-depleted human plasma, Neoplastine CI Plus 10 prothrombin time (PT) reagent, TriniCLOT automated activated partial thromboplastin time (aPTT) reagent, and substrate buffer (FluCa) were from Diagnostica Stago (Paris, France). Normal pooled plasma (NPP) was from Sanquin (Amsterdam, the Netherlands). All functional assays were performed in HEPES-buffered saline (HBS: 20 mM HEPES, 0.15 M NaCl, pH 7.5) supplemented with 5 mM $CaCl_2$, 0.1% PEG8000 and filtered over an 0.2 µm filter (assay buffer).

Proteins: The proteins hFX-R15Q and hFXa-S195A were gifted by Dr. Camire (Children's Hospital of Philadelphia, Philadelphia, United States). Tissue factor pathway inhibitor (TFPI) was a gift from Dr. van 't Veer (Amsterdam University Medical Centers, Amsterdam, The Netherlands). The human plasma-derived coagulation proteins FVIIa, FIXa, factor XIa (FXIa), prothrombin, α-thrombin, antithrombin, and RVV-X were from Haematologic Technologies (Essex Junction, VT, USA). NovoEight was from Novo Nordisk

(Plainsboro, NJ, USA). Human tissue factor (TF, Innovin) was from Siemens (Newark, NY, USA), and recombinant hirudin was from Hyphen Biomed (Neuville-sur-Oise, France). Recombinant wild-type human factor X (hFX) and venom-derived *Pseudonaja textilis* FX and FXa (v-ptFX and v-ptFXa) were prepared, purified, and characterized as described[15]. Recombinant constitutively active B-domainless human factor V (FV-810; hFV) and venom-derived *P. texilis* FV (v-ptFV) were prepared, purified, and characterized as described[12,16]. The extinction coefficients ($E_{0.1\%,\ 280\ nm}$) of the newly generated hFX-ptAP and ptFX-hAP variants were assumed to be similar to hFX and v-ptFX (1.16)[16,17]. The molecular weights of the various proteins used were taken as follows: hFX 58.0 kDa; hFX-ptAP 55.0 kDa; v-ptFX 55.0 kDa; ptFX-hAP 58 kDa.

Construction and Purification of FX Variants: Plasmid constructs encoding the chimeric FX variants were prepared from the pCMV4 vector carrying wild-type hFX or v-ptFX. Inserts encoding for the human or *P. textilis* FX activation peptide were synthesized and subcloned into the pCMV4 FX vectors using either BstBI and KasI (hFX-ptAP) or BstEII and BstBI (ptFX-hAP) by Genscript (Piscataway, NJ, USA). Transfection of the plasmids encoding the FX constructs into HEK293 cells, stable clone selection, and the expression and purification of the FX variants were performed as described previously[12]. Briefly, FX proteins were purified employing ion-exchange chromatography on a Q-Sepharose FF column (GE Healthcare) using a NaCl elution gradient in TRIS-buffer, pH 7.4. Fractions containing FX activity were pooled and dialyzed versus 20 mM TRIS, 1 mM EDTA, pH 7.0 for 3 hours at 4ºC, followed by a two-step dialysis (3 hours and subsequently overnight) versus a 40 mM sodium phosphate buffer, pH 6.8 at 4ºC. The dialysate was loaded on a CHT Ceramic Hydroxy Apatite column type I column (Bio-Rad, Hercules, CA, USA) and eluted using a sodium phosphate gradient. Protein purity was assessed by SDS-PAGE analysis using pre-cast 4–12% gradient gels under non-reducing and reducing conditions (50 mM DTT) using the MES buffer system (Life technologies; Carlsbad, CA, USA) followed by staining with Coomassie Brilliant Blue R-250 (CBB).

FX Activation by FVIIa-TF or FIXa-FVIIIa: The rate of FX (9.1 – 2500 nM) activation by the FVIIa-TF complex (FVIIa 0.5 nM; TF 100 nM) was determined in the presence of PCPS (50 µM) in assay buffer at 25 °C. At selected time points, aliquots were taken and quenched in HBS supplemented with 50 mM EDTA. The amidolytic activity of each sample was determined by SpecXa conversion (250 µM), measuring the absorbance at 405 nm and the initial rates of chromogenic substrate hydrolysis were converted to nanomolar of product by reference to a FXa standard curve. The apparent K_m and k_{cat} values for substrate activation were calculated from Michaelis-Menten equations. For FX activation by the FIXa-FVIIIa complex a similar approach was used. FVIII (NovoEight, 40 nM) was activated by thrombin (100 nM) for 30 sec at 25 °C and the reaction was

stopped by the addition of a 10-fold molar excess of hirudin. Immediately thereafter (within 30 sec), the intrinsic tenase complex was assembled by the addition of activated FVIIIa (5 nM) to FIXa (0.5 nM) and PCPS (20 μM), and the reactions were initiated by the addition of increasing concentrations of zymogen FX (9.1 – 2500 nM) variants. At selected time points, aliquots were taken and quenched, and the amidolytic activity of each sample was determined by SpecXa conversion as described above. The rate of hFX (50 nM) activation by the intrinsic tenase complex (FIXa, 0.5 nM; FVIIIa, 5 nM; PCPS, 50 μM) was also assessed in the presence of hFX-ptAP or hFX-R15Q (9.1 – 2500 nM), upon which the inhibitory constant (K_i) was determined for inhibition of hFX activation by hFX-ptAP or hFX-R15Q by fitting the data sets to a four-parameter logistic function.

Clotting-based FX Activation Assays. The specific extrinsic clotting activity was determined using a modified FX-specific PT-based assay. Purified FX samples were serially diluted in assay buffer with 0.1% BSA. FX-depleted plasma (45 μl) was mixed with 5 μl sample, followed by a 60 s incubation period at 37 °C. Coagulation was initiated by the addition of 50 μl PT reagent, and the time to fibrin clot formation was monitored using a Start4 coagulation instrument (Diagnostica Stago). The specific intrinsic clotting activity was determined using a modified FX-specific aPTT-based assay. FX samples were serially diluted in assay buffer with 0.1% BSA. FX-depleted plasma (45 μl) was mixed with sample (5 μl) and aPTT reagent (50 μl), followed by an 180 s incubation period at 37 °C. Coagulation was initiated by the addition of 50 μl of 25 mM $CaCl_2$, upon which the time to fibrin clot formation was monitored. Reference curves consisted of serial dilutions of NPP.

Calibrated Automated Thrombography. Thrombin generation was adapted from protocols earlier described[18]. Thrombin generation curves were obtained by supplementing FX-depleted plasma with TF (0.5 or 6 pM) or FXIa (0.25 nM), CTI (70 μg/mL), PCPS (20 μM), and 10 μg/mL FX variant. Thrombin formation was initiated by adding substrate buffer (FluCa) to the plasma. The final reaction volume was 120 μl, of which 80 μl was plasma. Thrombin formation was determined every 15s for 60min and corrected for the calibrator using Thrombinoscope software.

Prothrombin Activation: Factor X variants (1 μM) and plasma-derived prothrombin (5.6-20 μM) were pre-treated with APMSF (100 μM) and incubated for 60 min at 37 °C in order to allow for the decomposition of unbound inhibitor, thereby preventing interference in the assay[19]. Steady-state initial velocities of macromolecular substrate cleavage were determined discontinuously at 25 °C in assay buffer as described[12]. Briefly, unless otherwise stated, progress curves of prothrombin were obtained by incubating PCPS (50 μM), DAPA (10 μM), prothrombin (1.4 μM) and FV810 or v-ptFV

(300 nM), and the reaction was initiated with 250 nM of FX, upon which the rate of prothrombin conversion was measured[12].

Assessment of FXa Active Site Maturation: The human FX variants were activated with RVV-X (0.78 µg/mL) for 60 min at 37 °C. Following activation, the kinetics of peptidyl substrate hydrolysis (SpecXa and S2765) by FXa (7.5 nM) were measured in assay buffer upon initiation by the addition of chromogenic substrate (10–800 µM). The rate of inactivation of FXa by antithrombin or apixaban was measured under similar conditions: RVV-X activated FXa variants were incubated at room temperature with apixaban (0.001-100 nM) or antithrombin (0-400 nM) for 10 or 60 min, respectively. Residual FXa activity was assessed by monitoring SpecXa (250 µM) conversion.

Competitive Inhibition of FXa by hFX-ptAP or FXa-S195A: The rate of prothrombinase-assembled FXa inhibition using apixaban, antithrombin, or tissue factor pathway inhibitor (TFPI) was determined in the absence or presence of hFX-ptAP or FXa-S195A, assuming competitive inhibition by FXa and hFX-ptAP/FXa-S195A would occur if the inhibitors are able to bind hFX-ptAP/FXa-S195A. Reaction mixtures (100 µL) in assay buffer contained FXa (1 nM), PCPS (50 µM), FV810 (60 nM) in the absence or presence of hFX-ptAP or FXa-S195A (50 nM). The inhibitors apixaban (0.001-100 nM), antithrombin (0-400 nM), or TFPI (0-10 nM) were added and incubated at room temperature for 10 or 60 min for apixaban/TFPI or antithrombin, respectively. The reaction was initiated with S2765 (100 µM) and the inhibitory constant (K_i) or the half maximal inhibitory concentration (IC_{50}) values were determined by exponential decay function or a four-parameter logistic function, respectively.

Data Analysis: All data are presented as mean ± 1 standard deviation and are the result of at least two to three experiments.

Results

Construction and Expression of FX Variants. Although the activation peptide of FX is poorly conserved throughout vertebrate evolution, the number of amino acids has remained relatively constant (~45-65 residues; **Figure S1**). Sequence alignments have revealed that *P. textilis* liver-expressed FX comprises an activation peptide of similar length (56 residues; **Figure 1A**)[13]. Strikingly, the v-ptFX activation peptide is considerable shorter and consists of 27 residues[10,11]. As the functional relevance of the shortened activation peptide is unclear, we aimed to examine the role of this structural element by generating two chimeric FX variants. The activation peptide of hFX was exchanged for the corresponding region of v-ptFX and vice versa, thereby creating hFX-ptAP and ptFX-

hAP, respectively **(Figure 1B)**. Each variant migrated on SDS-PAGE with the expected mobility **(Figure 1C)**. The appearance of the venom FX light chain as a doublet likely results of heterogeneous O-glycosylation[17].

Factor X Activation by the Intrinsic and Extrinsic Tenase Complexes. As tenase-mediated proteolysis of the activation peptide induces the zymogen to protease transition, FX activation by either the intrinsic FVIIIa-FIXa or extrinsic TF-FVIIa tenase complex was functionally assessed. The kinetic parameters for TF-FVIIa-mediated activation of the chimeric variant hFX-ptAP (K_m 332 ± 54 nM, k_{cat} 40 ± 2 s^{-1}) were identical to those of hFX (K_m 349 ± 66 nM, k_{cat} 37 ± 3 s^{-1}) **(Figure 2A)**. This demonstrates that introduction of the *P. textilis* venom-derived activation peptide into hFX did not alter the interaction with or cleavage by the extrinsic tenase complex. Furthermore, assessment of the FX activation mediated by the FX activating protease from Russell's viper venom (RVV-X) revealed that RVV-X activated hFX-ptAP in a similar manner to hFX **(Figure S2A)**.

Conversely, activation of hFX by the intrinsic FVIIIa-FIXa tenase complex was not detectable following introduction of the venom-derived activation peptide **(Figure 2B)**. Moreover, using similar conditions no FXa formation could be detected following incubation of the venom FX derivatives v-ptFX or ptFX-hAP with the human intrinsic or extrinsic tenase complexes (data not shown). Further assessment of the human FX variants demonstrated a nine-fold reduction in the specific intrinsic clotting activity of hFX-ptAP, while its specific extrinsic clotting activity was unperturbed **(Figure 2C)**. Additional support for a severe defect in the FVIIIa-FIXa-dependent activation of hFX-ptAP came from thrombin generation analyses in FX-depleted plasma supplemented with plasma concentrations of FX (10 mg/mL) triggered by FXIa **(Figure 2D)** or by a low amount of TF (0.5 pM) **(Figure S2B)**. In case of the latter, not only FX but also FIX is activated in the so-called Josso-loop[20,21]. These experiments demonstrated an abrogated hFX-ptAP-dependent thrombin generation when coagulation was triggered by FXIa **(Figure 2D)**. Furthermore, the thrombin generation was considerably reduced using hFX-ptAP relative to hFX in the presence of a low amount of TF **(Figure S2B)**. . In contrast, a similar amount of thrombin was generated with hFX or hFX-ptAP following a high TF-trigger (6 pM) that incorporates a larger contribution of FX in the extrinsic pathway **(Figure 2E)**.

We made use of a functional competitive assay to examine whether incorporation of the v-ptFX activation peptide reduces binding to the intrinsic tenase complex or induces loss of Arg^{15}-Ile^{16} cleavage site recognition. Our data show that titration of hFX-ptAP into the FVIIIa-FIXa-dependent activation of hFX inhibited the formation of hFXa (K_i 1257 ± 208 nM) **(Figure 2F)**. However, hFX-ptAP proved to be a significantly weaker

competitor relative to hFX-R15Q (K_i 105 ± 44 nM), which is a non-activatable FX molecule due to a substitution at the Arg[15] cleavage site in which the human activation peptide is preserved. These results suggest that the activation peptide of hFX comprises an essential binding site for the intrinsic tenase complex, while the extrinsic tenase complex may require various distinct binding regions for substrate recognition[22-25].

Prothrombin Conversion by Zymogen FX Variants. *P. textilis* isoform FX, which is thought to be an evolutionary intermediate between liver and venom FX[13], comprises an activation peptide of identical length and over 90% sequence identity relative to v-ptFX (**Figure S1**). Previously, isoform FX was reported to display zymogen activity towards the macromolecular substrate prothrombin in conjunction with its cofactor v-ptFV[26]. To assess whether the shortened *P. textilis* FX activation peptide may contribute to zymogen activity, the zymogen variants were analyzed for their prothrombin conversion activity in a purified component assay using high concentrations of FX and cofactor (FV-810 for human variants and v-ptFV for ptFX variants). Prior to this, all zymogens including prothrombin were separately incubated with 100 μM APMSF to irreversibly inhibit any active protease, as an up to 0.18 nM FXa activity was observed in the FX protein preparations **(Table S1)**. Control experiments revealed no loss of FX clotting activity as a result of the prolonged incubations with APMSF (**Figure S3**). In the presence of cofactor and anionic membranes hFX was able to convert considerable amounts of prothrombin over prolonged incubation periods **(Figure 3A)**, corroborating previous findings[27]. Remarkably, the zymogen FX variants carrying the *P. textilis* activation peptide demonstrated a striking increase in prothrombin conversion relative to hFX, which is reduced following insertion of the human activation peptide **(Figure 3A)**. Kinetic assessments of prothrombin conversion revealed that the FX molecules comprising the snake venom activation peptide exhibited an up to 20-fold enhanced prothrombin activation rate relative to those zymogens carrying the human activation peptide **(Figure 3B)**. Despite this, the overall catalytic rates of prothrombin conversion were approximately five orders of magnitude lower than those observed for prothrombinase-assembled FXa (**Table 1**), which is consistent with previous findings[28]. In contrast, macromolecular substrate binding was practically unaffected following exchange of the activation peptides **(Table 1)**. Moreover, the K_m values obtained indicate that in the presence of cofactor-membranes all zymogen variants were able to engage with prothrombin in a manner similar to FXa[12,17]. Whereas the kinetics of cofactor binding could not be accurately determined for hFX **(Figure 3C)**, the apparent affinity of hFX-ptAP, v-ptFX, and ptFX-hAP for their respective cofactor was ~50-90-fold reduced relative to previously reported values for hFXa or ptFXa **(Figure 3C,D, Table 1)**[16,17,29-31]. We further observed that the FX zymogen activity was fully dependent on the presence of the cofactor, as no prothrombin conversion could be detected for zymogen FX-lipids

(data not shown). This is consistent with the fact that the FVa-prothrombin interaction facilitates efficient proteolytic conversion to thrombin[32].

To better understand the observed zymogen activity, we next examined the putative contribution of auto-activation or thrombin-mediated activation of zymogen FX. Prolonged incubations of zymogen FX in the presence of cofactor-lipids did not effectuate enzymatic activity towards the peptidyl substrate SpecXa (<0.04% mol/mol FXa) **(Table S1)**, suggestive of incomplete maturation of the active site. In addition, no thrombin-mediated proteolysis of the FX heavy chain was observed following SDS-PAGE analysis **(Figure S4A,B)**. These results indicate that the *P. textilis* venom-derived activation peptide promotes FX zymogen activity towards the macromolecular substrate in the presence of cofactor only. The cofactor is essential in driving this zymogen-dependent prothrombin conversion, as it mediates productive substrate interactions in the FX serine protease domain resulting in the catalytic conversion of prothrombin.

Competitive Active Site Binding in Zymogen FX. Given that our data suggest that the FX zymogen active site is available for macromolecular substrate engagement and catalysis, we next questioned whether prothrombinase-assembled zymogen FX could be targeted by several active site inhibitors. Since prothrombinase-assembled hFX-ptAP was incapable of SpecXa hydrolysis both in the absence and presence of cofactor-lipids **(Table S1)**, we made use of a functional competitive approach and first assessed antithrombin inhibition of purified hFXa in the presence of FV-810 and PCPS. While addition of a 50-fold molar excess of the catalytically inactive FXa variant hFXa-S195A impaired the inhibition of hFXa by antithrombin, no competitive effect was observed upon the addition of hFX-ptAP **(Figure 4A; Table 2)**, indicating that antithrombin is unable to bind to prothrombinase-assembled hFX-ptAP. Similar results were obtained for the inhibition of hFXa by apixaban and TFPI **(Figure 4B-C; Table 2)**. This indicates that whereas the activation peptide of v-ptFX allows for a cofactor-mediated productive prothrombin interaction, it is incompatible with specifc engagement of the active site only. This would provide further support for incomplete maturation of the active site in the FX variants comprising the *P. textilis* activation peptide.

Assessment of Active Site Maturation in FXa Variants. In order to assess whether the activation peptide induces changes in the active site pocket that may further explain the observed zymogen activity, we assessed the active site maturation of FX variants in their protease state (FXa) using several active site probes. In these assays, we focused on the human FXa variants, as ptFXa is highly insensitive to the direct FXa inhibitor apixaban and the macromolecular inhibitor antithrombin[12,26]. Following RVV-X activation, the hydrolysis rates of SpecXa and S2765 were examined for hFXa and hFXa-ptAP, revealing similar kinetics for both substrates **(Table 3)**. Furthermore, titration of the small active

site inhibitor apixaban showed identical IC_{50} values for both protease variants **(Table 3)**. In addition, exchange of the activation peptide did not affect inhibition by antithrombin **(Table 3)**. Together, these results show that following proteolytic removal of the v-ptFX activation peptide, the conformation of the FXa active site is identical to wild-type FXa.

Discussion

In the current study the functionality of the short activation peptide of venom-derived *P. textilis* FX, v-ptFX, was assessed. Steady state kinetic assessment of intrinsic tenase-mediated FX activation revealed that substitution of the human activation peptide for that of v-ptFX severely impaired intrinsic FX activation, which was hallmarked by a reduction in: i) the k_{cat}, ii) the FX-specific aPTT clotting activity, and iii) thrombin generation following a FXIa or low TF trigger **(Figure 2)**. This indicates that the *P. textilis* venom-derived FX activation peptide infers resistance to the human intrinsic tenase complex. Previously, similarly reduced catalytic efficiencies of the intrinsic tenase complex were observed by others who made use of human FX derivatives that lacked most of the activation peptide, but retained the P_1-P_3 residues Leu^{13}-Arg^{154}[4,33]. Employing bovine or human protein components, the absence of the FX activation peptide residues P_4-P_{52} was demonstrated to result in a lower catalytic rate or K_m, respectively[4,33], pointing to an essential role in substrate recognition and catalysis for this region of the human FX activation peptide. While the naturally occurring venom activation peptide assessed in the current study is substantially longer and comprises 27 amino acids, our findings indicate that it does not play a role in substrate recognition and catalysis by the human FVIIIa-FIXa complex. This is because we not only observed a severely reduced catalytic rate of hFX-ptAP activation **(Figure 2B)**, but also revealed that hFX-ptAP is a poor competitive inhibitor of hFX activation by the intrinsic tenase complex **(Figure 2F)**. Despite this, hFX-ptAP did demonstrate some competition for the intrinsic tenase-mediated hFX activation. This may suggest that FX comprises additional binding sites for intrinsic tenase that are situated outside of the activation peptide, supporting mutagenesis studies which have identified multiple interactive regions in FX[23,34-36].

In sharp contrast, steady state kinetic analyses of FX activation by the extrinsic tenase complex yielded comparable kinetic parameters for hFX and hFX-ptAP, indicating that TF-FVIIa binding and cleavage site recognition are not affected upon introduction of the v-ptFX activation peptide **(Figures 1A,S1)**. These findings make clear that the human FX activation peptide is not primarily responsible for substrate binding and catalysis, which is supported by earlier studies demonstrating a relatively modest change in kinetic parameters of extrinsic tenase-dependent activation following truncation of the

activation peptide in human FX[4,37]. As such, these results provide further support for the hypothesis that the substrate-specificity of the extrinsic tenase complex is entirely regulated by distinct regions in the FX heavy and light chains[22-25]. These data are also consistent with observations in other coagulation protease complexes, indicating that proper presentation and activation of the macromolecular substrates are critically dependent on binding of exosite regions[38,39].

Other structural elements that play a role in FX activation are the carbohydrate chains that are present in the FX activation peptide, with the human FX activation peptide comprising two O-linked and two N-linked glycosylation sites[40]. Inhibition studies using the isolated human activation peptide revealed that it interacts with FIXa in a carbohydrate-dependent manner[41]. Furthermore, non-specific glycosidase or sialic-acid-binding lectin treatments were shown to inhibit FX activation by both the extrinsic and intrinsic tenase complexes[42,43]. To specifically explore the contribution of the individual carbohydrates to FX activation, a mutagenesis-based approach was used by Yang *et al.* demonstrating that elimination of the glycosylation sites did not significantly alter the catalytic efficiency of extrinsic tenase[4]. In contrast, removal of the O-linked glycans from the FX activation peptide resulted in a reduced catalytic efficiency of the intrinsic tenase complex[4]. More specifically, the O-glycan at Thr^{17} was shown to contribute to intrinsic tenase recognition and binding, while the O-linked carbohydrate at position Thr^{29} was found to play a role in the stabilization of the FX transition-state intermediate. This indicates that both O-linked carbohydrates make productive interactions with the intrinsic tenase complex. While no experimental data is available on the glycosylation status of the venom FX activation peptide, artificial neural networks predict one N-linked (QNA) and one O-linked carbohydrate (ATL) **(Figure 1A)**[40,44]. Whether an O-linked carbohydrate is available for productive intrinsic tenase interactions in FX variants comprising the v-ptAP activation peptide remains to be determined.

Using supraphysiological protein concentrations and extended incubation times, all zymogen FX variants demonstrated prothrombin conversion activity in a cofactor-dependent manner **(Figure 3)**, albeit at an approximate 10,000-fold lower catalytic rate relative to the FXa protease state **(Table 1)**. To ensure that the observed activity was not due to the presence of traces of FXa protease in the protein preparations, the FX variants were preincubated before each assessment with the short-lived non-reversible serine protease inhibitor APMSF. Moreover, the FX zymogen activity was not attributable to cofactor-lipid-mediated auto-activation **(Table S1)** nor to thrombin-mediated FX proteolysis **(Figures S4,S5)**. In line with our results, zymogen activity of FX has previously been observed for both human FX and the *P. textilis* isoform FX-ptFV

Pseutarin C-isoform complex[26,27]. Here we show that the shortened activation peptide of v-ptFX is at the basis of this remarkable characteristic, with the zymogen activity being completely dependent on the presence of the cofactor as no prothrombin conversion could be detected for any of the zymogen FX-lipids without the cofactor present. However, no apparent binding affinity defining the FV-810-zymogen hFX interaction could be determined, suggesting that the $K_{d,app}$ may be in the ~300-500 nM range or higher **(Figure 3C, Table 1)**, consistent with data obtained in earlier binding studies[2]. In contrast, all other zymogen FX variants displayed an apparent binding affinity for their respective cofactor that is ~50-90-fold lower in comparison with the human and venom *P. textilis* FXa protease states **(Figure 3C, Table 1)**[16,17,29-31]. Strikingly, our FX-cofactor complexes bind prothrombin with a similar affinity relative to previously reported values for prothrombinase-assembled FXa[2,12,45,46], suggesting that the prothrombin-interactive sites are available in zymogen FX. From this we conclude that the proteolytic activation of FX and subsequent FVa binding might induce structural rearrangements that allow for the maturation of the active site only and enable catalytic activity towards its natural macromolecular substrate, rather than formation of binding sites for substrate recognition. This is consistent with previous observations revealing that FXa binds with a similar affinity to prothrombin in the presence or absence of FVa[45]. Based on our data we propose that the shortened venom FX activation peptide allows for cofactor binding and formation of a premature prothrombinase complex complex at FX-FVa concentrations that exceed those in plasma but are likely compatible with those found in venom[1,8]. Perhaps the absence of the acidic/hydrophobic region found in the human activation peptide and/or modified N- or O-linked carbohydrates in the v-ptFX activation peptide might allow for these premature but productive FX-FVa interactions.

The observed zymogen activity may provide v-ptFX with a unique procoagulant gain-of-function that could significantly contribute to its toxic effects once injected into the bloodstream of the prey. However, it is yet to be unequivocally determined whether venom FX is injected in a zymogen or protease form. Protein sequencing of FX peptides derived from the venom of two individual *P. textilis* snakes has failed to identify the activation peptide[9,11], suggesting that ptFX exists in a protease state in venom. Similar results have been obtained for homologous venom FX species that require cofactor Va from the host to function and comprise a similarly short activation peptide (*Tropidechus carinatus* and *Hoplocephalus stephensi*; **Figure S1**)[47,48]. Information on whether the venom glands express proteases that are specialized in the proteolytic removal of the FX activation peptide is lacking thus far. Preservation of the activation peptide may be of relevance for the circulatory survival of venom FX. This because the half-life of human FX is mediated by the two N-linked glycans within the activation peptide, as these protect the protein from clearance[49]. To what extend a similar mechanism

would provide a selective advantage to a venom that is considered to act in a matter of seconds is unclear.

Interestingly, hFX-ptAP displays remarkable similarities to a previously published 'zymogen form' of FXa[2]. In this variant, Ile[16] is substituted for a leucine (FXa-I16L), thereby inducing an equilibrium between a partially and fully matured serine protease that results in a 5- to 15-fold reduced catalytic activity that is fully cofactor-dependent[50]. Furthermore, this variant displayed a longer half-life due to a diminished reactivity with antithrombin and TFPI. Zymogen activity has also been reported for trypsinogen, prothrombin, prethrombin-2, and plasminogen, which is induced via the so-called 'molecular sexuality' mechanism[51-54]. Peptides sequentially similar to the Ile16 N-terminus are able to engage the zymogen's preformed Ile16 cleft[51]. In addition, bacterial proteins such as streptokinase, staphylocoagulase, and von Willebrand factor-binding protein comprise an Ile16 N-terminus-like region that is inserted into the zymogen's activation pocket following interaction with the zymogen[52-54]. Upon insertion of such N-terminal-like sequences/peptides, the exogenous Ile1 forms a salt bridge with zymogen Asp194. This triggers the zymogen activation, resulting in a conformational change and maturation of the substrate recognition site and oxyanion hole[53]. Interestingly, other mechanisms may also lead to zymogen activity. For instance, the zymogen tissue type plasminogen activator comprises intrinsic protease activity due to the formation of an intrinsic Lys156-Asp194 salt bridge that promotes an active trypsin-like conformation[55]. Moreover, recent reports have shown that factor XII and prekallikrein are proteolytically active in zymogen form[56,57]. Although their activity is several orders of magnitude weaker than that of the activated proteases, these findings may indicate a role in the onset of contact activation in intrinsic coagulation. In a similar manner, v-ptFX may initially generate small amounts of thrombin to activate the feedback mechanisms of the coagulation cascade. The subsequent excessive generation of thrombin could lead to venom-induced consumptive coagulopathy (VICC), which is characterized by a (complete) consumption of fibrinogen and factors V and VIII, elevated D- dimer levels, and an international normalized ratio >3[58,59]. VICC is the most commonly observed clinical envenoming phenotype in humans following a snakebite by the brown snake *P. textilis*[60].In order to further study the active site maturation in hFX-ptAP, we explored its accessibility for several active site inhibitors using a cofactor-dependent competition assay. None of the ligands were able to engage the active site pocket of hFX-ptAP **(Table 2)**. Future studies are therefore required to fully elucidate this remarkable property, which will likely advance our understanding of serine protease biology.

To conclude, we observed that a shortened activation peptide derived from *P. textilis* venom FX infers resistance to intrinsic tenase, thereby confirming that the hFX activation peptide contains a crucial binding site for the intrinsic tenase complex. In addition, v-ptFX has acquired a unique procoagulant gain-of-function as this short activation peptide allows for the formation of productive cofactor interactions and subsequent catalytic activity towards the macromolecular substrate prothrombin while in the zymogen state. As such, these results shed new light on the structural requirements for serine protease activation. Consequently, these data suggest that the characteristic Ile^{16}-Asp^{194} salt bridge is not an essential requirement for serine protease maturation and activity of FX.

Acknowledgements

We gratefully acknowledge Dr. Rodney Camire (Division of Hematology, Department of Pediatrics, Perelman School of Medicine, University of Pennsylvania, USA) for generously providing hFX-R15Q and hFXa-S195A and Dr. Kees van 't Veer for providing TFPI. This work was financially supported by the Bayer Hemophilia Awards Program (Special Project Award) and Landsteiner Foundation for Blood Transfusion (LSBR, grant. no. 1451). The funding agencies had no role in the preparation, review, or approval of the manuscript.

Figures

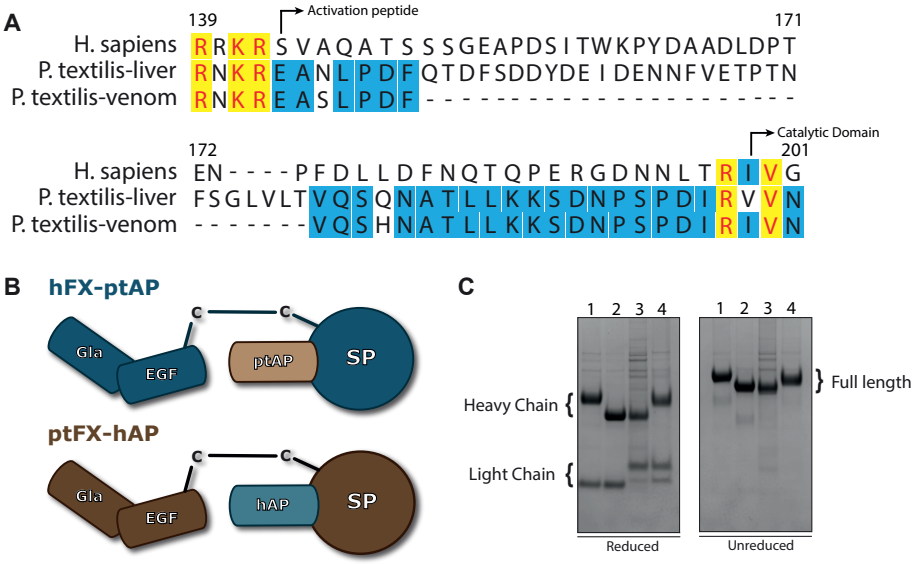


Figure 1. Chimeric factor X variants. (A) Sequence alignment of the activation peptide of human FX (H. sapiens), *P. textilis* liver-expressed FX (P. textilis-liver), and *P. textilis* venom-expressed FX (P. textilis-venom). Residues fully conserved between all three FX species are indicated in yellow; amino acids partially conserved between all of the FX derivatives are indicated in blue. The start of the activation peptide and serine protease domain are indicated; amino acid numbering is according to mature human FX. **(B)** Schematic representation of the chimeric FX variants. The activation peptide was swapped between human FX (blue) and venom-expressed *P. textilis* FX (brown), thereby generating variants hFX-ptAP and ptFX-hAP, respectively. **(C)** SDS-PAGE analysis of purified chimeric FX variants (2 µg/lane) under reducing and non-reducing conditions and visualized by staining with CBB. Lane 1, human FX; lane 2, hFX-ptAP; lane 3, v-ptFX; lane 4, ptFX-hAP. Relevant FX fragments (heavy chain, light chain, or full-length FX) and the apparent molecular weights of the standards are indicated.

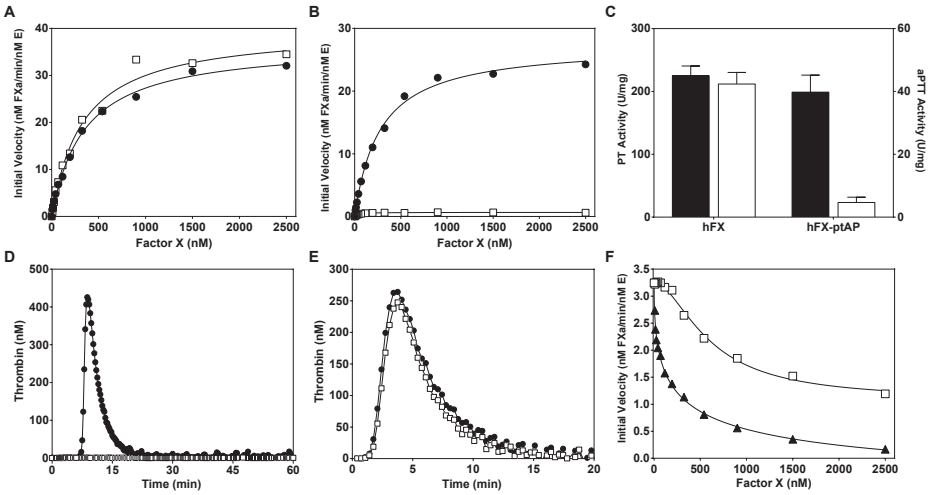


Figure 2. Extrinsic or intrinsic tenase-mediated activation of human factor X variants. The initial velocity of FXa generation was assessed at increasing concentrations of recombinant human FX (hFX) (●) or hFX-ptAP (□) in the presence of 50 μM PCPS and **(A)** TF (100 nM) and FVIIa (0.5 nM) or **(B)** FVIIIa (5 nM) and FIXa (0.5 nM). The lines were drawn by fitting the data to the Michaelis-Menten equation using non-linear regression, and the K_m and k_{cat} ± 1 standard deviation of the induced fit were obtained. TF-FVIIa: hFX, K_m 349 ± 143 nM, k_{cat} 37 ± 5 s^{-1}; hFX-ptAP, K_m 332 ± 116 nM, k_{cat} 40 ± 5 s^{-1}. FVIIIa-FIXa: hFX, K_m 275 ± 104 nM, k_{cat} 28 ± 3 s^{-1}. Rates of hFX-ptAP conversion were very low precluding an accurate assessment of kinetic contants. **(C)** The specific extrinsic (PT Activity; black bars) or intrinsic (aPTT Activity, open bars) clotting activity of FX-deficient plasma supplemented with 1-10 μg/mL hFX or hFX-ptAP was determined as described in 'Materials and Methods'. **(D-E)** Thrombin generation was measured for 60 min at 37 °C in FX-deficient plasma supplemented with 10 μg/ml hFX (●) or hFX-ptAP (□) in the presence of 0.25 nM FXIa **(D)** or 6 pM TF **(E)** and 20 μM PCPS. Thrombin generation was initiated with $CaCl_2$ and a thrombin fluorogenic substrate as detailed in 'Materials and Methods'. **(F)** The initial velocity of hFX (50 nM) conversion was determined in the presence of FVIIIa (5 nM), FIXa (0.5 nM), 50 μM PCPS, and increasing concentrations of hFX-ptAP (□) or hFX-R15Q (▲). The lines were drawn by fitting the data to a four-parameter logistic function, and the K_i ± 1 standard deviation of the induced fit were obtained. K_i: hFX-ptAP 1257 ± 208 nM; hFX-R15Q 105 ± 44 nM. Data are representative of two to three independent experiments.

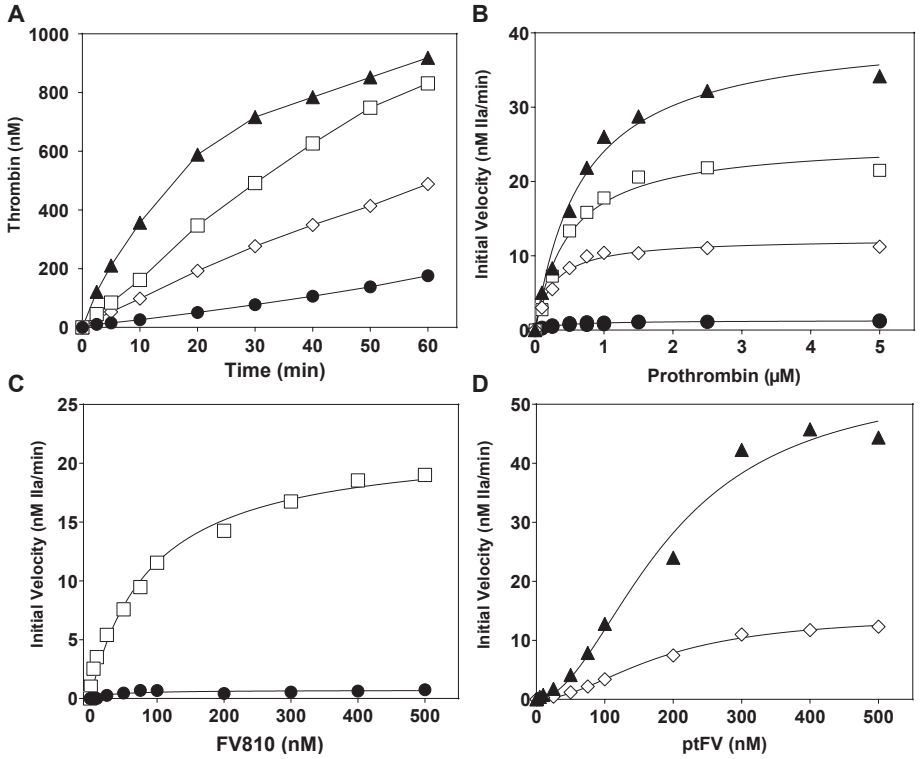


Figure 3. The *P. textilis a*ctivation peptide confers cofactor-dependent zymogen activity. (A) Reaction mixtures containing 1.4 μM prothrombin, 50 μM PCPS, 10 μM DAPA, and 300 nM cofactor (FV-810 for human FX variants or v-ptFV for ptFX variants) were incubated for 5 min at 25 °C. The reaction was initiated with 250 nM FX variant, and thrombin generation was monitored during 60 minutes as described under "Materials and Methods". SDS-PAGE analysis of the prothrombin conversion by hFX-ptAP and FV-810 under these conditions is shown in **Figure S3**. **(B-D)** The initial velocity of thrombin formation was determined at increasing concentrations of prothrombin **(B),** FV-810 **(C)** or v-ptFV **(D)** in the presence of 50 μM PCPS and 10 μM DAPA following initiation by 250 nM FX variant, and thrombin generation was monitored during 25 minutes as described under "Materials and Methods". Prothrombin titrations were performed in the presence of 300 nM cofactor, and FV-810 or v-ptFV titrations were performed with 1.4 μM prothrombin. The symbols represent the following: ● hFX, □ hFX-ptAP, ▲ v-ptFX, ◇ ptFX-hAP. The lines were drawn after analysis of all datasets to a rectangular hyperbola, and the fitted kinetic constants can be found in Table 1. The data are representative of two to three independent experiments.

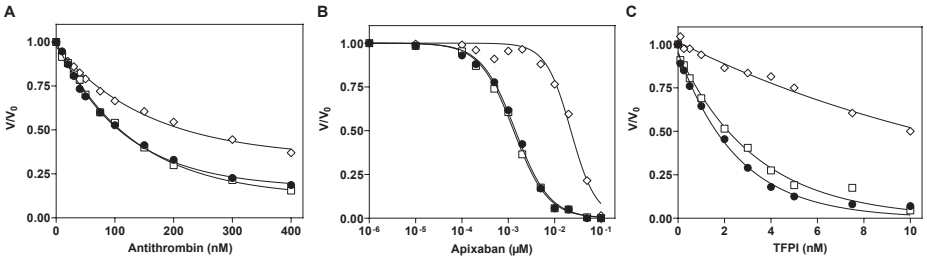


Figure 4. Targeted inhibition of prothrombinase-assembled zymogen factor X. The initial velocity of peptidyl substrate hydrolysis (100 μM S-2765) catalyzed by prothrombinase (1 nM FXa; 60 nM FV-810; 50 μM PCPS) in the absence (●) or presence of 50 nM hFX-ptAP (□) or hFXa-S195A (◇) was determined at increasing concentrations of the inhibitors **(A)** antithrombin, **(B)** apixaban, or **(C)** tissue factor pathway inhibitor (TFPI). The data were normalized to the ratio of the velocity at a given concentration (V) over the initial starting velocity (V_0). Data are representative of two to three independent experiments.

	Prothrombin Km (μM)	Prothrombin kcat (min-1)	Cofactor* Kd, app (nM)
hFX	0.36 ± 0.06	N.A.[a]	N.A.[b]
hFX-ptAP	0.49 ± 0.08	0.10 ± 0.003	90 ± 12
v-ptFX	0.69 ± 0.09	0.16 ± 0.007	193 ± 31
ptFX-hAP	0.26 ± 0.04	0.05 ± 0.001	180 ± 12
hFXa	0.51 ± 0.10	933 ± 51	N.A.

Table 1. Kinetic constants for macromolecular substrate conversion by zymogen FX variants. The kinetic constants were obtained as described in 'Materials and Methods'. Fitted values ± 1 standard deviation of the induced fit are representative of two to three independent measurements. N.A., [a]The k_{cat} value is difficult to estimate because the $K_{d,app}$ between hFX and FV-810 could not be determined. Thus, the total enzyme concentration in this experiment is not known with certainty; the Vmax was 1.3 ± 0.1 nM min^{-1}. [b]For this experiment, rates were very low precluding an accurate assessment of apparent binding affinity. *The Va-like cofactor employed was FV-810 for the hFX variants and v-ptFV for the (v-)ptFX variants.

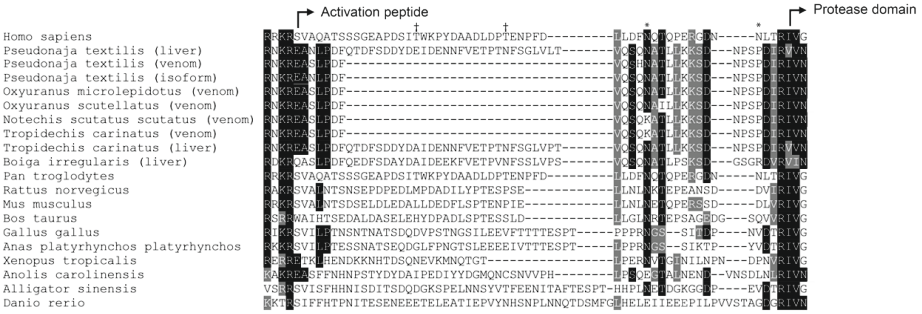
Competitor	Antithrombin K_i (nM)	Apixaban IC_{50} (nM)	TFPI K_i (nM)
No competitor	127 ± 14	1.4 ± 0.2	1.4 ± 0.2
hFX-ptAP	122 ± 8	1.3 ± 0.1	2.3 ± 0.3
hFXa-S195A	260 ± 32	22.4 ± 3.0	10.4 ± 1.5

Table 2. Kinetic parameters for the inhibition of prothrombinase-assembled factor Xa. The kinetic parameters of inhibition were obtained as described in 'Materials and Methods'. Mean values are given ± 1 standard deviation of two to three independent experiments.

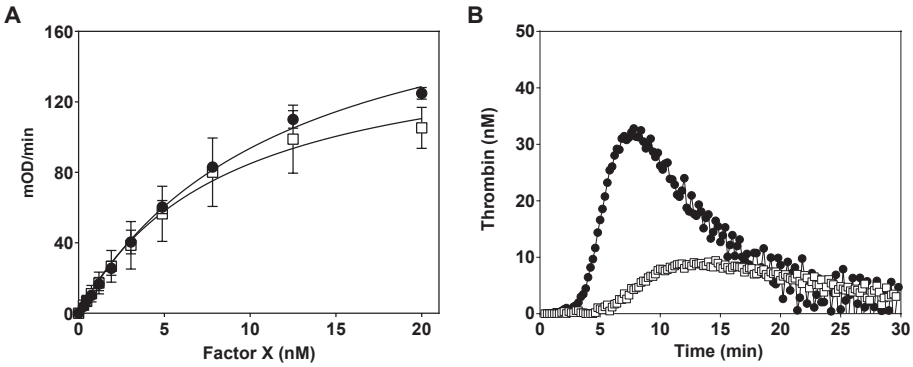
	SpecXa K_m (μM)	SpecXa k_{cat} (min^{-1})	S2765 K_m (μM)	S2765 k_{cat} (min^{-1})	Apixaban IC_{50} (nM)	Antithrombin K_i (nM)
hFXa	92 ± 4	85 ± 1	65 ± 5	80 ± 2	1.5 ± 0.2	80 ± 6
hFXa-ptAP	87 ± 5	73 ± 1	57 ± 5	70 ± 2	1.6 ± 0.2	71 ± 4

Table 3. Assessment of active site maturation. Factor X variants were activated by RVV-X and active site formation was assessed as described in 'Materials and Methods'. Mean values are given ± 1 standard deviation of two to three independent experiments.

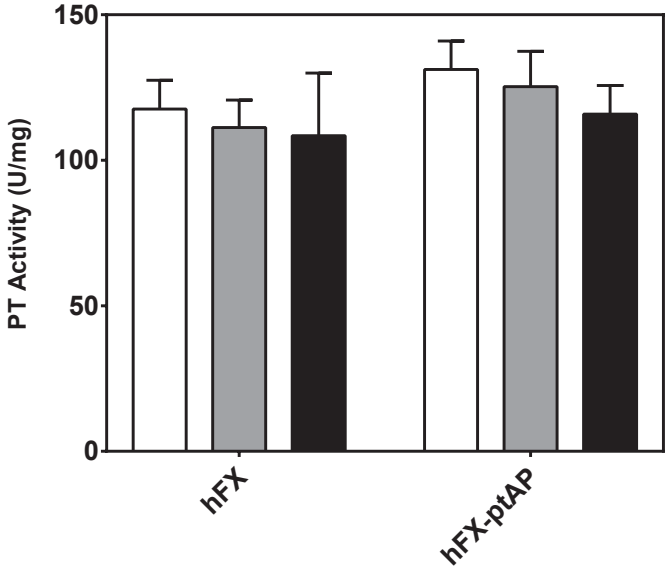
Supplemental Figures



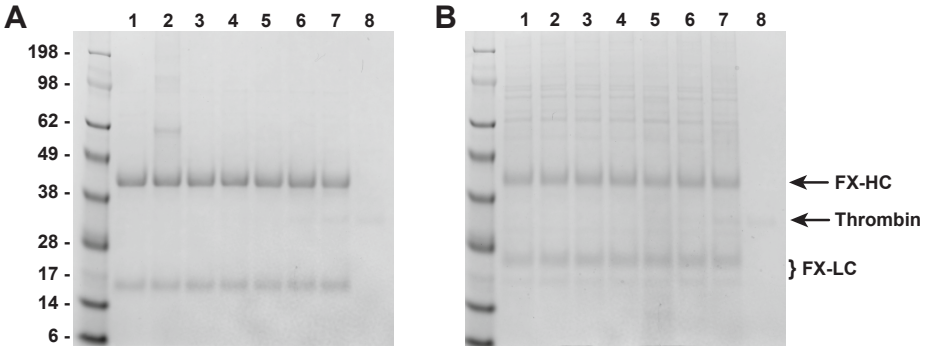
Supplementary figure 1. Alignment of the amino acid sequences comprising the FX activation peptide (Clustal Omega Module; EMBL-EBI, UK). Residues identical to the column consensus are shown in black; residues similar to the column consensus are shown in grey. The start of activation peptide and serine protease domain (Ile16) are indicated. The three-amino acid peptide Arg-Lys-Arg immediately N-terminal to the start of the activation peptide is excised during intracellular processing. The N-linked glycosylation sites Asn181 and Asn191 in human FX are indicated by * and the O-linked glycosylation sites by †(1).



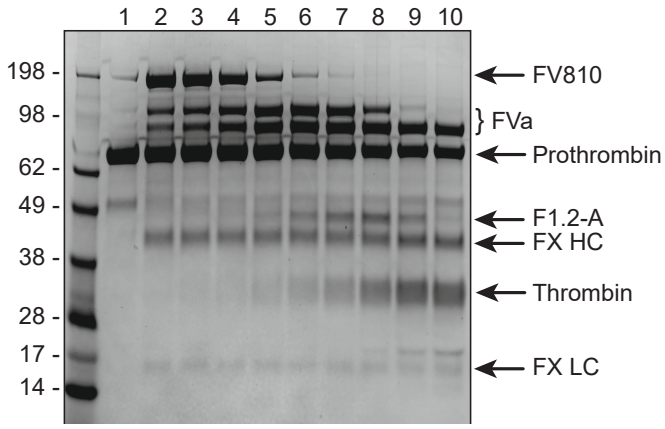
Supplementary figure 2. Activation of human factor X variants by RVV-X or a low TF trigger. **(A)** The initial velocity of peptidyl substrate hydrolysis (250 µM SpecXa) was determined at increasing concentrations of hFX (●) or hFX-ptAP (□) in the presence of RVV-X (10 pM). **(B)** Thrombin generation was measured for 60 min at 37 °C in FX-deficient plasma supplemented with 10 µg/ml hFX (●) or hFX-ptAP (□) in the presence of 0.5 pM TF and 20 µM PCPS. Thrombin generation was initiated with $CaCl_2$ and a thrombin fluorogenic substrate as detailed in 'Materials and Methods'.



Supplementary figure 3. Stability of factor X during APMSF treatment. The specific extrinsic clotting activity (PT Activity) was determined using a modified FX-specific PT-based assay. hFX or hFX-ptAP (1 μM) were kept on ice (white bars) or were incubated in the absence (grey bars) or presence (black bars) of APMSF (100 μM) for 60 min at 37 ˚C. FX variants (1 μg/mL) were added to FX-deficient plasma and the extrinsic clotting activity was determined as described in 'Materials and Methods'.



Supplementary figure 4. Thrombin-mediated cleavage of factor X. The recombinant factor X (FX) variants (2500 nM) hFX-ptAP **(A)** or v-ptFX **(B)** were incubated with PCPS (50 μM) and increasing concentrations of thrombin (1-100 nM) in assay buffer for 30 minutes at 37°C. Samples (3 μg per lane) were subjected to SDS-PAGE under reducing conditions using the MES buffer system and visualized by staining with CBB. Lane 1: FX variant; lanes 2-7: FX variant incubated with 1, 5, 10, 20, 50, or 100 nM thrombin; lane 8: 100 nM thrombin in the absence of FX. Relevant protein bands are indicated; FX-HC, FX heavy chain; FX-LC, factor X light chain. The apparent molecular weights of the standards (kDa) are indicated. The data are representative of two independent experiments.



Supplementary figure 5. Prothrombin cleavage by hFX-ptAP. Plasma-derived protrombin (1.4 µM) was incubated with 250 nM hFX-ptAP in the presence of FV-810 (300 nM) and PCPS (50 µM) in assay buffer for 1–60 minutes at 25°C. Samples (3 µg per lane) were subjected to SDS-PAGE under reducing conditions using the MES buffer system and visualized by staining with CBB. Lane 1: prothrombin; lanes 2-10: prothrombin incubated for 1, 2.5, 5, 10, 15, 20, 30, 45 or 60 minutes. Relevant protein bands are indicated. F1.2-A, fragment 1.2 (thrombin A chain); FX-HC, factor X heavy chain; FX-LC, factor X light chain. The apparent molecular weights of the standards (kDa) are indicated. The data represents one experiment. The amount of thrombin formed over time is shown in **Figure 3A**.

	Zymogen FX (mOD/min)	Zymogen FX + APMSF (mOD/min)	Zymogen-assembled prothrombinase + APMSF (mOD/min)	FX auto-activation + APMSF (mOD/min)
hFX	0.05 ± 0.00	0.02 ± 0.01	N.D.	N.D.
hFX-ptAP	3.31 ± 0.06	0.03 ± 0.02	0.19 ± 0.07	0.06 ± 0.02
v-ptFX	0.04 ± 0.01	0.08 ± 0.08	N.D.	0.13 ± 0.01
ptFX-hAP	0.05 ± 0.01	0.00 ± 0.00	N.D.	N.D.
hFXa (0.1 nM)	2.0 ± 0.0	N.D.	N.D.	N.D.
hFXa (1 nM)	18.5 ± 0.1	0.06 ± 0.00	N.D.	N.D.

Supplementary table 1. Chromogenic activity of recombinant FX variants. The initial velocity of peptidyl substrate hydrolysis (250 µM SpecXa) catalyzed by recombinant zymogen FX variants (250 nM) was determined using non-treated (Zymogen FX) or pre-treatment (Zymogen FX + APMSF) of zymogen FX variants with 100 µM APMSF as described in "Materials and Methods". The amidolytic activity of hFX-ptAP was also determined in the presence of FV-810 (250 nM), PCPS (50 µM) and SpecXa (250 µM) (zymogen-assembled prothrombinase + APMSF). FX auto-activation was assessed by incubation of APMSF-treated FX (250 nM) with 250 nM cofactor (FV-810 for hFX-ptAP or v-ptFV for v-ptFX) and PCPS (50 µM) at 25 °C for 60 minutes followed by the assessment of FXa activity using peptidyl substrate hydrolysis (250 µM SpecXa). Mean values are given ± 1 standard deviation of two independent experiments. N.D. indicates not determined.

References

1 Bos, M. H. A., Van 't Veer, C. & Reitsma, P. H. Molecular biology and biochemistry of the coagulation factors and pathways of hemostasis. *Williams Hematology* **9th edn.**, 1915–1948 (2016).
2 Toso, R., Zhu, H. & Camire, R. M. The conformational switch from the factor X zymogen to protease state mediates exosite expression and prothrombinase assembly. *J Biol Chem* **283**, 18627-18635, doi:10.1074/jbc.M802205200 (2008).
3 Rudolph, A. E., Mullane, M. P., Porche-Sorbet, R., Daust, H. A. & Miletich, J. P. The role of the factor X activation peptide: a deletion mutagenesis approach. *Thrombosis and haemostasis* **88**, 756-762 (2002).
4 Yang, L., Manithody, C. & Rezaie, A. R. Functional role of O-linked and N-linked glycosylation sites present on the activation peptide of factor X. *J Thromb Haemost* **7**, 1696-1702, doi:10.1111/j.1538-7836.2009.03578.x (2009).
5 Huber, R. & Bode, W. Structural Basis of the Activation and Action of Trypsin. *Accounts of Chemical Research* **11**, 114-122 (1978).
6 Hedstrom, L. Serine protease mechanism and specificity. *Chem Rev* **102**, 4501-4524 (2002).
7 Rao, V. S. & Kini, R. M. Pseutarin C, a prothrombin activator from Pseudonaja textilis venom: its structural and functional similarity to mammalian coagulation factor Xa-Va complex. *Thrombosis and haemostasis* **88**, 611-619 (2002).
8 Bos, M. H. & Camire, R. M. Procoagulant adaptation of a blood coagulation prothrombinase-like enzyme complex in australian elapid venom. *Toxins (Basel)* **2**, 1554-1567, doi:10.3390/toxins2061554 (2010).
9 Rao, V. S., Swarup, S. & Manjunatha Kini, R. The catalytic subunit of pseutarin C, a group C prothrombin activator from the venom of Pseudonaja textilis, is structurally similar to mammalian blood coagulation factor Xa. *Thrombosis and haemostasis* **92**, 509-521, doi:10.1160/TH04-03-0144 (2004).
10 Filippovich, I. *et al.* Cloning and functional expression of venom prothrombin activator protease from Pseudonaja textilis with whole blood procoagulant activity. *Br J Haematol* **131**, 237-246, doi:10.1111/j.1365-2141.2005.05744.x (2005).
11 St Pierre, L. *et al.* Comparative analysis of prothrombin activators from the venom of Australian elapids. *Mol Biol Evol* **22**, 1853-1864, doi:10.1093/molbev/msi181 (2005).
12 Verhoef, D. *et al.* Engineered factor Xa variants retain procoagulant activity independent of direct factor Xa inhibitors. *Nat Commun* **8**, 528, doi:10.1038/s41467-017-00647-9 (2017).
13 Reza, M. A., Minh Le, T. N., Swarup, S. & Manjunatha Kini, R. Molecular evolution caught in action: gene duplication and evolution of molecular isoforms of prothrombin activators in Pseudonaja textilis (brown snake). *J Thromb Haemost* **4**, 1346-1353, doi:10.1111/j.1538-7836.2006.01969.x (2006).
14 Higgins, D. L. & Mann, K. G. The interaction of bovine factor V and factor V-derived peptides with phospholipid vesicles. *J Biol Chem* **258**, 6503-6508 (1983).
15 Larson, P. J. *et al.* Structure/function analyses of recombinant variants of human factor Xa: factor Xa incorporation into prothrombinase on the thrombin-activated platelet surface is not mimicked by synthetic phospholipid vesicles. *Biochemistry* **37**, 5029-5038, doi:10.1021/bi972428p (1998).
16 Toso, R. & Camire, R. M. Removal of B-domain sequences from factor V rather than specific proteolysis underlies the mechanism by which cofactor function is realized. *J Biol Chem* **279**, 21643-21650, doi:10.1074/jbc.M402107200 (2004).

17 Bos, M. H. *et al.* Venom factor V from the common brown snake escapes hemostatic regulation through procoagulant adaptations. *Blood* **114**, 686-692, doi:10.1182/blood-2009-02-202663 (2009).
18 Hemker, H. C. *et al.* Calibrated automated thrombin generation measurement in clotting plasma. *Pathophysiol Haemost Thromb* **33**, 4-15, doi:10.1159/000071636 (2003).
19 Muczynski, V. *et al.* A Thrombin-Activatable Factor X Variant Corrects Hemostasis in a Mouse Model for Hemophilia A. *Thrombosis and haemostasis* **119**, 1981-1993, doi:10.1055/s-0039-1697662 (2019).
20 Lu, G., Broze, G. J., Jr. & Krishnaswamy, S. Formation of factors IXa and Xa by the extrinsic pathway: differential regulation by tissue factor pathway inhibitor and antithrombin III. *J Biol Chem* **279**, 17241-17249, doi:10.1074/jbc.M312827200 (2004).
21 Zur, M. & Nemerson, Y. Kinetics of factor IX activation via the extrinsic pathway. Dependence of Km on tissue factor. *J Biol Chem* **255**, 5703-5707 (1980).
22 Thiec, F., Cherel, G. & Christophe, O. D. Role of the Gla and first epidermal growth factor-like domains of factor X in the prothrombinase and tissue factor-factor VIIa complexes. *J Biol Chem* **278**, 10393-10399, doi:10.1074/jbc.M212144200 (2003).
23 Chattopadhyay, A. & Fair, D. S. Molecular recognition in the activation of human blood coagulation factor X. *J Biol Chem* **264**, 11035-11043 (1989).
24 Pinotti, M. *et al.* Reduced activation of the Gla19Ala FX variant via the extrinsic coagulation pathway results in symptomatic CRMred FX deficiency. *Thrombosis and haemostasis* **88**, 236-241 (2002).
25 Baugh, R. J., Dickinson, C. D., Ruf, W. & Krishnaswamy, S. Exosite interactions determine the affinity of factor X for the extrinsic Xase complex. *J Biol Chem* **275**, 28826-28833, doi:10.1074/jbc.M005266200 (2000).
26 Lechtenberg, B. C. *et al.* Crystal structure of the prothrombinase complex from the venom of Pseudonaja textilis. *Blood* **122**, 2777-2783, doi:10.1182/blood-2013-06-511733 (2013).
27 Estry, D. W. & Tishkoff, G. H. Apparent intrinsic prothrombinase activity of human Factor X zymogen: identification with Factor VIII inhibitor bypassing activity (FEIBA). *Thromb Res* **36**, 549-562, doi:10.1016/0049-3848(84)90194-4 (1984).
28 Mann, K. G., Nesheim, M. E., Church, W. R., Haley, P. & Krishnaswamy, S. Surface-dependent reactions of the vitamin K-dependent enzyme complexes. *Blood* **76**, 1-16 (1990).
29 Mann, K. G., Nesheim, M. E., Hibbard, L. S. & Tracy, P. B. The role of factor V in the assembly of the prothrombinase complex. *Ann N Y Acad Sci* **370**, 378-388, doi:10.1111/j.1749-6632.1981.tb29750.x (1981).
30 Hirbawi, J., Vaughn, J. L., Bukys, M. A., Vos, H. L. & Kalafatis, M. Contribution of amino acid region 659-663 of Factor Va heavy chain to the activity of factor Xa within prothrombinase. *Biochemistry* **49**, 8520-8534, doi:10.1021/bi101097t (2010).
31 Bos, M. H. & Camire, R. M. A bipartite autoinhibitory region within the B-domain suppresses function in factor V. *J Biol Chem* **287**, 26342-26351, doi:10.1074/jbc.M112.377168 (2012).
32 Schreuder, M., Reitsma, P. H. & Bos, M. H. A. Blood coagulation factor Va's key interactive residues and regions for prothrombinase assembly and prothrombin binding. *J Thromb Haemost* **17**, 1229-1239, doi:10.1111/jth.14487 (2019).
33 Duffy, E. J. & Lollar, P. Intrinsic pathway activation of factor X and its activation peptide-deficient derivative, factor Xdes-143-191. *J Biol Chem* **267**, 7821-7827 (1992).
34 Chen, L., Manithody, C., Yang, L. & Rezaie, A. R. Zymogenic and enzymatic properties of the 70-80 loop mutants of factor X/Xa. *Protein Sci* **13**, 431-442, doi:10.1110/ps.03406904 (2004).
35 Baroni, M. *et al.* Asymmetric processing of mutant factor X Arg386Cys reveals differences between intrinsic and extrinsic pathway activation. *Biochim Biophys Acta* **1854**, 1351-1356, doi:10.1016/j.bbapap.2015.05.012 (2015).

36 Vanden Hoek, A. L. *et al.* Coagulation factor X Arg386 specifically affects activation by the intrinsic pathway: a novel patient mutation. *J Thromb Haemost* **10**, 2613-2615, doi:10.1111/jth.12021 (2012).
37 Baugh, R. J. & Krishnaswamy, S. Role of the activation peptide domain in human factor X activation by the extrinsic Xase complex. *J Biol Chem* **271**, 16126-16134, doi:10.1074/jbc.271.27.16126 (1996).
38 Kumar, A. & Fair, D. S. Specific molecular interaction sites on factor VII involved in factor X activation. *Eur J Biochem* **217**, 509-518 (1993).
39 Krishnaswamy, S. Exosite-driven substrate specificity and function in coagulation. *J Thromb Haemost* **3**, 54-67, doi:10.1111/j.1538-7836.2004.01021.x (2005).
40 Gupta, R., Jung, E. & Brunak, S. Prediction of N-glycosylation Sites in Human Proteins. **Available online:** http://www.cbs.dtu.dk/services/NetNGlyc/ **(accessed on April 2018).** (2004).
41 Iino, M. *et al.* The role of human factor X activation peptide in activation of factor X by factor IXa. *J Biochem* **116**, 335-340, doi:10.1093/oxfordjournals.jbchem.a124528 (1994).
42 Inoue, K. & Morita, T. Identification of O-linked oligosaccharide chains in the activation peptides of blood coagulation factor X. The role of the carbohydrate moieties in the activation of factor X. *Eur J Biochem* **218**, 153-163 (1993).
43 Sinha, U. & Wolf, D. L. Carbohydrate residues modulate the activation of coagulation factor X. *J Biol Chem* **268**, 3048-3051 (1993).
44 Steentoft, C. *et al.* Precision mapping of the human O-GalNAc glycoproteome through SimpleCell technology. *EMBO J* **32**, 1478-1488, doi:10.1038/emboj.2013.79 (2013).
45 Pozzi, N., Chen, Z., Pelc, L. A., Shropshire, D. B. & Di Cera, E. The linker connecting the two kringles plays a key role in prothrombin activation. *Proc Natl Acad Sci U S A* **111**, 7630-7635, doi:10.1073/pnas.1403779111 (2014).
46 Ahnstrom, J., Gierula, M., Temenu, J., Laffan, M. A. & Lane, D. A. Partial rescue of naturally occurring active site factor X variants through decreased inhibition by tissue factor pathway inhibitor and antithrombin. *J Thromb Haemost* **18**, 136-150, doi:10.1111/jth.14627 (2020).
47 Joseph, J. S., Chung, M. C., Jeyaseelan, K. & Kini, R. M. Amino acid sequence of trocarin, a prothrombin activator from Tropidechis carinatus venom: its structural similarity to coagulation factor Xa. *Blood* **94**, 621-631 (1999).
48 Rao, V. S., Joseph, J. S. & Kini, R. M. Group D prothrombin activators from snake venom are structural homologues of mammalian blood coagulation factor Xa. *Biochem J* **369**, 635-642, doi:10.1042/BJ20020889 (2003).
49 Gueguen, P., Cherel, G., Badirou, I., Denis, C. V. & Christophe, O. D. Two residues in the activation peptide domain contribute to the half-life of factor X in vivo. *J Thromb Haemost* **8**, 1651-1653, doi:10.1111/j.1538-7836.2010.03905.x (2010).
50 Bunce, M. W., Toso, R. & Camire, R. M. Zymogen-like factor Xa variants restore thrombin generation and effectively bypass the intrinsic pathway in vitro. *Blood* **117**, 290-298, doi:10.1182/blood-2010-08-300756 (2011).
51 Bode, W. & Huber, R. Induction of the bovine trypsinogen-trypsin transition by peptides sequentially similar to the N-terminus of trypsin. *FEBS Lett* **68**, 231-236, doi:10.1016/0014-5793(76)80443-7 (1976).
52 Boxrud, P. D., Verhamme, I. M., Fay, W. P. & Bock, P. E. Streptokinase triggers conformational activation of plasminogen through specific interactions of the amino-terminal sequence and stabilizes the active zymogen conformation. *J Biol Chem* **276**, 26084-26089, doi:10.1074/jbc.M101966200 (2001).
53 Friedrich, R. *et al.* Staphylocoagulase is a prototype for the mechanism of cofactor-induced zymogen activation. *Nature* **425**, 535-539, doi:10.1038/nature01962 (2003).

54 Kroh, H. K., Panizzi, P. & Bock, P. E. Von Willebrand factor-binding protein is a hysteretic conformational activator of prothrombin. *Proc Natl Acad Sci U S A* **106**, 7786-7791, doi:10.1073/pnas.0811750106 (2009).
55 Renatus, M. *et al.* Lysine 156 promotes the anomalous proenzyme activity of tPA: X-ray crystal structure of single-chain human tPA. *EMBO J* **16**, 4797-4805, doi:10.1093/emboj/16.16.4797 (1997).
56 Ivanov, I. *et al.* Proteolytic properties of single-chain factor XII: a mechanism for triggering contact activation. *Blood* **129**, 1527-1537, doi:10.1182/blood-2016-10-744110 (2017).
57 Ivanov, I. *et al.* Protease activity in single-chain prekallikrein. *Blood* **135**, 558-567, doi:10.1182/blood.2019002224 (2020).
58 Isbister, G. K. Procoagulant snake toxins: laboratory studies, diagnosis, and understanding snakebite coagulopathy. *Semin Thromb Hemost* **35**, 93-103, doi:10.1055/s-0029-1214152 (2009).
59 Masci, P. P., Rowe, E. A., Whitaker, A. N. & de Jersey, J. Fibrinolysis as a feature of disseminated intravascular coagulation (DIC) after Pseudonaja textilis textilis envenomation. *Thromb Res* **59**, 859-870, doi:10.1016/0049-3848(90)90399-w (1990).
60 Johnston, C. I. *et al.* The Australian Snakebite Project, 2005-2015 (ASP-20). *Med J Aust* **207**, 119-125, doi:10.5694/mja17.00094 (2017).

Supplemental References

1. Hansson K, Stenflo J. Post-translational modifications in proteins involved in blood coagulation. Journal of thrombosis and haemostasis : JTH 2005; 3(12): 2633-48.



Chapter 6

Reversal Agents for the Direct Factor Xa Inhibitors: Biochemical Mechanisms of Current and Newly Emerging Therapies

Mark Schreuder, Pieter H. Reitsma, Mettine H.A. Bos

Seminars in Thrombosis and Hemostasis. 2020 46(8):986-998



Abstract

The direct oral anticoagulants targeting coagulation factor Xa or thrombin are widely used as alternatives to vitamin K antagonists in the management of venous thromboembolism and nonvalvular atrial fibrillation. In case of bleeding or emergency surgery, reversal agents are helpful to counteract the anticoagulant therapy and restore hemostasis. While idarucizumab has been established as antidote for the direct thrombin inhibitor dabigatran, reversal strategies for the direct factor Xa inhibitors have been a focal point in clinical care over the past years. In the absence of specific reversal agents, the off-label use of (activated) prothrombin complex concentrate and recombinant factor VIIa has been suggested as effective treatment options during inhibitor-induced bleeding complications. Meanwhile, several specific reversal agents have been developed. In this review, an overview of the current state of non-specific and specific reversal agents for the direct factor Xa inhibitors is provided, focusing on the biochemistry and mechanism of action and the preclinical assessment of newly emerging therapies.

Introduction

The direct oral anticoagulants (DOAC) are a class of synthetic anticoagulant drugs that consist of a direct thrombin inhibitor (dabigatran) and several direct factor Xa (FXa) inhibitors (apixaban, rivaroxaban, edoxaban, and betrixaban). These drugs are characterized by a superior pharmacodynamic profile relative to the classic oral anticoagulant vitamin K antagonists, and their use is therefore considered as the preferred anticoagulant therapy[1]. The DOACs are prescribed for the prevention of venous thrombosis following surgery or during atrial fibrillation, and for the treatment of venous thromboembolism[2]. Unfortunately, as with all anticoagulant treatment options, bleeding complications associated with DOAC use remain the main concern in clinical practice. Therefore, rapid reversal of the anticoagulant DOAC activity may be required in case of life-threatening hemorrhage, major trauma, emergency surgery or DOAC overdose. DOAC reversal can be achieved by the use of non-specific or specific reversal agents. In the absence of specific reversal agents, non-specific plasma protein concentrates and recombinant factor VIIa have been suggested to overcome the anticoagulant effects of the DOACs. Specific reversal of the thrombin-targeting DOAC dabigatran is effectively achieved by administration of the US Food and Drug Administration (FDA)- and European Medicines Agency (EMA)-approved monoclonal antibody fragment idarucizumab[3]. More recently, andexanet alfa, a specific antidote for the FXa-targeting DOACs was approved for the treatment of uncontrollable bleeds. In addition, several specific antidotes for the FXa-targeting DOACs are currently in preclinical development, which include the synthetic small molecule ciraparantag, a modified FXa-α2 macroglubulin complex and several prohemostatic factor X (FX)-based reversal agents. Since the direct FXa inhibitors apixaban and rivaroxaban are increasingly prescribed rather than the direct thrombin inhibitor dabigatran[4], the importance of an effective reversal agent for the direct FXa inhibitors is substantial. In this review, we will highlight the reversal of the FXa-targeting DOACs by specific and non-specific reversal agents, with a main focus on the biochemical mechanisms of the newly emerging reversal therapies that are in preclinical development.

Mechanistic Principles of the Direct Factor Xa Inhibitors

The FXa-targeting DOACs are small synthetic molecules with overall similar chemical structures that have identical mechanisms of action. Their anticoagulant effect stems from the fact that these inhibitors interact with the active site pocket of FXa, thereby effectively blocking the natural substrate prothrombin from accessing the active site **(Figure 1)** and preventing thrombin formation. The characteristic L-shape of these small molecule inhibitors mediates the high affinity interaction with the FXa active

site, resulting in a potent subnanomolar FXa inhibitory activity (K_i of 0.08-0.56 nM)[5-7]. Although the overall composition of the active site of serine proteases is generally conserved[8], the direct FXa inhibitors have an over 10,000-fold greater selectivity for FXa compared to other human serine proteases[9]. Binding to FXa is reversible and regulated via the S1 and S4 active site subpockets[5,6]. The *p*-methoxyphenyl P_1 moiety of apixaban and the chlorothiophene moiety of rivaroxaban are inserted deep into the S1 specificity pocket. Although the P_1 moiety of apixaban does not appear to directly interact with FXa, the choline substituent of rivaroxaban interacts with the aromatic ring of Tyr228 (chymotrypsinogen numbering) that is located at the bottom of the S1 subpocket and provides a high affinity interaction[5,6]. Apixaban interacts with the Gln192 backbone via its pyrazole N-2 and via a carboxyl interaction with Gly216[6]. Rivaroxaban forms two hydrogen bonds with Gly219 that serve an important role by directing its substituents into the S1 and S4 subpockets[5]. The S4 subsite of FXa is a narrow hydrophobic pocket defined by the aromatic rings of residues Tyr99, Phe174, and Trp215[10]. In this binding pocket, the P_4 ring of apixaban and the morpholinone ring of rivaroxaban are sandwiched between the residues Tyr99 and Phe174, thereby providing important binding stability and enabling high affinity binding[5,6]. While structural information on the interaction of the direct FXa inhibitors edoxaban or betrixaban with the FXa active site is lacking, these are considered to also engage the FXa S1 and S4 subsites[11].

The pharmacokinetic and pharmacodynamic profiles of the direct FXa inhibitors have several key advantages over that of the vitamin K antagonists. Their rapid onset makes them ideal for clinical use as no bridging therapies are needed and they sustain their anticoagulant effect up to 24 hours, with a half-life of 6-14 hours[12,13]. Unlike the vitamin K antagonists, the direct FXa inhibitors are characterized by linear and predictable pharmacodynamics, no known interactions with food components, and limited drug-drug interactions[14]. It is for these reasons that patients treated with a DOAC do not require routine monitoring.

Reversal of the Direct factor Xa Inhibitors

Bleeding complications remain a major concern of anticoagulant therapy. Compared to the conventional vitamin K antagonists, the direct FXa inhibitors are associated with comparable or slightly lower risks of major bleeding, stroke, and fatality. Still, major bleeding is observed in 1-5% of the patients receiving DOACs[15-17]. Since millions of people worldwide require anticoagulant treatment and this is projected to increase significantly in the coming decades, bleeding complications will remain a major healthcare burden[18,19]. In order to treat these DOAC-associated bleeding complications, the off-label use of several non-specific reversal agents used in hemophilia-associated and vitamin K antagonist-induced bleedings have been suggested as potential candidates for

reversal therapy, although supporting evidence is lacking or incomplete. In addition to these non-specific treatment options, the specific antidote for the direct FXa inhibitors andexanet alfa has recently been approved by the FDA and EMA and could significantly improve the management of major bleeding events[20,21]. Furthermore, various specific reversal agents with different modes of action are currently in preclinical development. In the following sections we will discuss the efficacy of the non-specific and specific reversal strategies and focus on their molecular details and mechanisms of action.

Non-Specific Reversal Strategies

Prothrombin Complex Concentrate

Prothrombin complex concentrates (PCC) are derived from human plasma and contain vitamin K-dependent coagulation factors which are partly purified via ion-exchange chromatography[22,23]. Strong ion exchangers produce 4-factor concentrates (4F-PCC), consisting of factor VII, factor IX, factor X, and prothrombin, while weak ion exchangers produce 3-factor concentrates (3F-PCC) that do not contain factor VII. Most PCC products have been supplemented with heparin to prevent factor activation[24] and may contain various concentrations of the vitamin K-dependent anticoagulants protein C and protein S. PCCs are used for the reversal of vitamin K antagonists by replenishing the lowered and defective circulating vitamin K-dependent factors if patients present with an urgent need to restore hemostasis[25]. In contrast, the direct FXa inhibitors do not affect the level or posttranslational modification of coagulation factors, thereby obviating the necessity for factor supplementation and replacement. PCC-mediated reversal of FXa inhibition has been studied in several animal models and in small-sized human studies. In rabbit models of apixaban or rivaroxaban-induced bleeding, 4F-PCC partially improved laboratory parameters but was not able to reduce blood loss[26,27]. In contrast, 4F-PCC significantly shortened the bleeding time of rivaroxaban-induced bleeding in a rat model and could reduce the prothrombin time (PT) in rivaroxaban-treated baboon plasma[28]. 4F-PCC was also able to dose-dependently reverse hematoma expansion in a murine intracerebral hemorrhage model following pretreatment with rivaroxaban[29]. In humans, the efficacy of PCC has mostly been assessed in healthy non-bleeding volunteers using surrogate laboratory tests. Similar to the animal models, these studies have led to variable reports on the efficacy of direct FXa reversal by PCC. While both 3F- and 4F-PCC administration was demonstrated to restore some parameters of coagulation (PT and endogenous thrombin potential (ETP) in thrombin generation [TG]) in rivaroxaban treated healthy individuals, other parameters such as the activated partial thromboplastin time (aPTT), anti-FXa activity, and the TG lag time were unaffected[30-33]. Similar results were obtained following 3F- and 4F-PCC administration to apixaban- or edoxaban-dosed healthy individuals[34-37]. A more

clinically relevant study in which bleeding following a punch biopsy in edoxaban-treated healthy individuals was assessed revealed that 4F-PCC reversed edoxaban's effect on the duration of bleeding and on the ETP, while the PT and total blood loss could only be partially restored[38]. It is important to consider that restoration of laboratory parameters has to be interpreted with caution as these do not accurately represent the clinical setting. To overcome this, the efficacy of PCC has been evaluated in the management of major bleeding events in patients using the direct FXa inhibitors. In clinical studies, 4F-PCC proved to be effective in 65-75% of the major bleeding events in patients treated with apixaban or rivaroxaban[39-42]. Collectively, the available clinical data indicates that both 3F- and 4F-PCC may provide an effective reversal agent for the majority of patients presenting with major bleeding events associated with direct FXa inhibitor therapy. However, larger studies would be required to evaluate the true potential of this non-specific reversal strategy in a real world patient population. When specific reversal agents are unavailable or unattainable, PCC is considered as the most effective reversal agent and has therefore been included as the first treatment of choice in life-threatening bleeding events[43].

Activated Prothrombin Complex Concentrate

Activated prothrombin complex concentrate (aPCC), or factor eight inhibitor bypassing activity (FEIBA), is a PCC product that contains small amounts of factor VIII and the activated factors factor VIIa, factor IXa, factor Xa, and thrombin. This product was originally used as bypassing agent for the treatment of bleeding complications in hemophilia patients with inhibitors[44-46]. Given that aPCC elevates the circulating levels of several coagulation factors thereby stimulating coagulation, it has the potential to be a reversal agent in DOAC-induced bleeding. Perzborn *et al.* reported that aPCC significantly reduced the bleeding time and partially restored the PT in rivaroxaban-induced bleeding in rat and baboon models[28]. Similarly, aPCC was found to dose-dependently reduce the bleeding time in edoxaban-treated rats[47]. Furthermore, *in vitro* and *ex vivo* studies have shown significant but variable improvements of surrogate endpoints, including the PT, aPTT, anti-Xa activity, and several TG parameters[30,48-51]. The administration of aPCC as reversal agent for the direct FXa inhibitors has also been evaluated in a few patient studies. In two small-scale studies, aPCC-mediated reversal of apixaban and rivaroxaban was associated with a reduction in intracranial hemorrhage (ICH) expansion[52,53]. In two larger studies, administration of aPCC led to an overall stable hemorrhage progression and a 14-29% mortality rate[54,55]. Collectively, aPCC is associated with reversal of direct FXa inhibitors in major bleeding events. Therefore, the off-label use of aPCC has been included in the guidelines for the management of uncontrolled bleeding in patients on DOACs[43]. However, as more (pre)clinical data

has become available pointing to a beneficial effect of PCCs in this setting, these are currently preferred over aPCC as non-specific reversal agent.

Recombinant Activated Factor VII

Recombinant human activated factor VII (rFVIIa), or NovoSeven (eptacog alfa), was initially developed for the treatment of hemophilia in patients presenting with inhibitors[56,57]. However, its off-label use has increased significantly for uncontrolled bleeding following trauma and surgery[58] and rFVIIa has been suggested as treatment option in DOAC-related bleeding. Evaluation of the efficacy of rFVIIa in animal models and healthy volunteers has shown variable results. In edoxaban-treated rats, rFVIIa dose-dependently reduced the bleeding time and restored the PT[47]. Comparable results were obtained for rivaroxaban reversal employing rat and baboon models[28]. Conversely, rFVIIa did not affect the PT or blood loss in an apixaban- and rivaroxaban-induced bleeding model in rabbits, while the aPTT and several rotational thrombelastography (ROTEM) parameters were at least partially restored[26,27]. These inconsistent and thus far unexplained effects reflect *in vitro* reversal studies, displaying mostly marginal effects of rFVIIa on the restoration of laboratory parameters[30,48,50,51,59] Thus far no reports on the efficacy of rFVIIa in major bleeding events that are associated with DOAC therapy are available. Therefore, the benefit of rFVIIa therapy in a non-hemophilia setting remains uncertain and as such, clinical guidelines state that rFVIIa might be considered for the reversal of the direct FXa inhibitors on an individual basis[60].

Mechanistic Principles of the Non-Specific Reversal Agents

Although the exact mechanism by which the non-specific reversal agents PCC, aPCC, and rFVIIa bypass the anticoagulant effect of the DOACs is currently not fully understood, it is generally acknowledged to result from an increase in factor concentrations that promote thrombin generation **(Figure 2)**. The latter is also at the basis of their factor VIII-bypassing activity that supports their use in hemophilia treatment. The plasma concentrates contain a variety of procoagulant clotting factors, with coagulation factors X and prothrombin being considered the main procoagulant components[61]. Turecek *et al.* revealed that aPCC was unable to generate thrombin in factor V (FV)-deficient plasma, indicating that prothrombinase activity is essential[62]. Furthermore, a highly purified complex of FXa and prothrombin was able to shorten the prolonged aPTT in hemophilia A plasma, in a similar manner as aPCC. The fact that both factors are essential was illustrated by TG assessment in which FXa addition induced a slight improvement in thrombin formation, while subsequent prothrombin supplementation dramatically increased the amount of thrombin formed[62,63]. Consequently, administration of FXa and prothrombin in equivalent amounts as obtained following aPCC administration normalized blood loss in a rabbit hemophilia model[62,63]. These results show that the administration of FXa and

its substrate prothrombin is sufficient to initiate blood coagulation. As FXa is capable of directly activating FV[64], a positive feedback loop is generated via assembly of the prothrombinase complex and conversion of prothrombin to thrombin[65]. Additionally, the thrombin formed will initiate the intrinsic pathway by activation of factors VIII and XI, thereby further propagating FXa and thrombin generation. While the latter mechanism describes the mode of action of aPCC, PCC is considered to mainly function by elevating the circulating levels of several coagulation factor substrates. In general, increasing the substrate concentration for the appropriate enzymes will enhance the catalytic turnover if the substrate concentration is limited. As such, PCC likely achieves its procoagulant effect by supplementation of the factors IX (substrate of factors VIIa and XIa) and X (substrate of factors VIIa and IXa) following PCC administration.

While the above mentioned mode of action predicts a procoagulant response under conditions where bypassing of FVIII is required, the question remains how this mechanism explains effectiveness in the presence of DOACs, given that the latter will target the newly formed FXa or thrombin. A possible explanation can be found in the reversible binding nature of these inhibitors. The direct inhibitors interact with the active site pocket of their respective targets and as a result they compete with the natural and irreversible inhibitor antithrombin that engages the FXa and thrombin active site through the S1 subsite[66,67]. In the absence of the DOACs, antithrombin rapidly inhibits free FXa or thrombin. However, Thalji *et al.* described that with the direct FXa inhibitor rivaroxaban present, the majority of FXa reversibly interacts with rivaroxaban rather than forming the slower but irreversible FXa-antithrombin complex[68]. As such, an equilibrium is formed between the FXa-antithrombin and the FXa-rivaroxaban complexes, in addition to the generation of a pool of free and uninhibited FXa. As the free FXa reaches steady-state, a persistent amount of free FXa is established under these conditions. While in most scenario's this pool of free FXa is likely functionally irrelevant, the enhanced factor levels and the subsequent increase in FXa formed ensuing supplementation with the non-specific reversal agents could significantly elevate the steady-state levels of free FXa. Thalji and colleagues suggest that these elevated levels of free FXa restore hemostasis in the presence of rivaroxaban[68].

These mechanistic principles might also provide an explanation for the reduced effectiveness of rFVIIa in DOAC-reversal. In hemophila, rFVIIa stimulates blood clot formation by FXa generation via tissue factor localized at the site of injury as well as on the surface of platelets independent of tissue factor[69]. While PCC and aPCC promote the generation of multiple active serine proteases, rFVIIa focuses largely on the formation of FXa. The rate of FXa and subsequent thrombin generation could therefore be lower and prove insufficient in the presence of the DOACs.

Specific Reversal Strategies

Andexanet Alfa

The specific antidote andexanet alfa (andexanet) is a universal reversal agent for the direct FXa inhibitors and is currently the only FDA- and EMA-approved treatment option for major bleeding events induced by these anticoagulants **(Figure 3)**. Andexanet is a recombinant modified human FXa variant that is expressed in its mature FXa form due to the replacement of the activation peptide by a double Arg-Lys-Arg linker (RKRRKR), which is intracellularly and proteolytically removed by proprotein convertases[21]. Furthermore, andexanet lacks the membrane-binding γ-carboxyglutamic acid (GLA) domain of native FXa which prevents its assembly into the prothrombinase complex. Additionally, andexanet is enzymatically inactive due to replacement of the catalytic triad residue serine 195 by alanine[21]. Despite this active site substitution, andexanet displays a similar apparent binding affinity for the direct FXa inhibitors compared to wild-type (wt-)FXa[21]. Consequently, andexanet will compete with endogenous FXa for the direct inhibitor binding and as such, when administrated in molar excess, will effectively bind and clear the circulation of inhibitors, thereby restoring thrombin generation via liberated endogenous FXa **(Figure 3)**. This mechanism has been proven effective against all currently approved direct FXa inhibitors, since andexanet dose-dependently reversed the anti-FXa activity in both purified and plasma systems[21,70]. Andexanet was also able to restore hemostasis in an inhibitor-infused rat model and was shown to reduce blood loss following liver laceration in a rabbit bleeding model[21,70,71]. Reversal of the direct FXa inhibitors was not associated with major adverse effects in monkeys, as no histopathological evidence of andexanet-related thrombosis was observed[71]. Based on these data, a randomized placebo-controlled study was performed in healthy volunteers treated with apixaban (ANNEXA-A) or rivaroxaban (ANNEXA-R)[72]. Within minutes after a bolus injection or bolus injection followed by a 1-2 hour infusion of andexanet, the anti-FXa activity was reversed by more than 90% and the ETP was restored in both apixaban- or rivaroxaban-treated volunteers. These parameters returned gradually to placebo levels within 1-2 hours as andexanet was eliminated from the circulation. Moreover, in a safety and dose-escalation study in healthy individuals, andexanet was well tolerated and thrombotic events were not observed, despite the detection of increased levels of D-dimer and prothrombin fragment 1.2[73].

The ANNEXA-4 study was designed to examine the use of andexanet in patients with potential life-threatening bleeding[20]. Recently, the study was completed and included 352 patients with major bleeding complications. While in 92% of the patients treatment with andexanet resulted in excellent or good efficacy as determined by anti-FXa activity, this primary outcome did not correlate with the overall hemostatic efficacy

(good efficacy occurring in 82% of the evaluated patients). Additionally, thrombotic events occurred in 10% of the patients within 30 days following andexanet treatment, which was relatively higher than idarucizumab-mediated reversal of dabigatran (4.8%)[3] and other anticoagulant reversal studies (3.9-7%)[25,74]. A possible explanation for the relative high percentage of thrombosis might be the interaction of andexanet with the natural anticoagulant tissue factor pathway inhibitor (TFPI). Ersayin *et al.* showed that andexanet demonstrates high affinity binding to TFPI, similar to GLA-domainless FXa[75]. The TFPI-neutralizing capacity of andexanet was further underscored by the observation that addition of supratherapeutic levels of andexanet to hemophilic or normal pooled plasma (in the absence of a FXa inhibitor) resulted a dose-dependent increase in the thrombin peak height in a TFPI-sensitive TG assay[75-77]. Importantly, a major limitation of the ANNEXA-4 study is the absence of a randomized comparison with PCC, the standard treatment option in the absence of a specific reversal agent. Interestingly, such a randomized comparison with PCC is also lacking for idaruzicumab. A randomized controlled trial evaluating andexanet with a PCC-control group is underway (NCT03661528).

Specific Reversal Strategies in Clinical Development

Ciraparantag

Ciraparantag (Aripazine, PER 977) is a synthetic small molecule that consists of two L-arginine units connected with a piperazine containing linker chain, which is considered a universal anticoagulant antidote capable of reversing the effects of low-molecular weight heparins and the direct thrombin and FXa inhibitors[78-80] **(Figure 4A)**. Data on this antidote is scarce and mainly derived from abstracts. As such, the mechanistic principles remain largely unknown. Yet, it has been stated that ciraparantag binds directly to the DOACs and heparins via non-covalent hydrogen bonding based on *in silico* modeling and dynamic light scattering data, while binding to any human coagulation factor or albumin was not observed[81]. Therefore, the mode of action of ciraparantag appears relatively similar to that of andexanet: interaction with and removal of the inhibitors from their intended target in order to generate free endogenous FXa. In line with this, ciraparantag was observed to completely reverse the anti-FXa activity in apixaban- and rivaroxaban-spiked human plasma[82]. Additionally, *in vivo* assessments employing rat tail transection and rat and rabbit liver laceration models revealed that ciraparantag significantly decreased apixaban-, rivaroxaban-, and edoxaban-induced bleeding[81-84]. Moreover, ciraparantag was well tolerated in rats and dogs up to doses of 20 mg/kg per day, and no toxicity was observed[85]. Data from a first-in-human study in 80 edoxaban-treated healthy volunteers who received an intravenous injection of 100 mg or 300 mg ciraparantag demonstrated a shortening of the whole blood clotting

time to within 10% of baseline levels and restoration of the fibrin clot diameter[78,86]. In addition, ciraparantag did not induce serious adverse effects or an increase in the procoagulant markers D-dimer or prothrombin fragment 1.2, nor were alterations in TFPI levels observed.

One of the main concerns when addressing the therapeutic potential of ciraparantag is the fact that no data concerning the direct binding of ciraparantag to the DOACs have been published thus far. This complicates our understanding of the mechanisms that are at the basis of the apparent selectivity of ciraparantag for heparins and DOACs and that prevent its interaction with other proteins and molecules. These concerns are also highlighted by studies in which ciraparantag was shown to be incapable of restoring the anti-FXa activity of either apixaban, rivaroxaban, or edoxaban in plasma or a purified system[87,88]. Furthermore, ciraparantag was found to be unable to restore the augmented clotting time induced by rivaroxaban and edoxaban, but could normalize the clot structure and fibrin fiber diameter[87]. More importantly, using isothermal titration calorimetry, direct binding of ciraparantag to either edoxaban or rivaroxaban could not be established[87]. In contrast, a direct interaction with factor IXa, but not FIX, was observed[87], corroborating earlier reports on ciraparantag-dependent stimulation of the FIXa-dependent activation of FX[88]. These results may suggest a role in FX activation for ciraparantag, as opposed to direct binding and interfering with anticoagulant molecules. It is essential that its exact mechanistic principles will be elucidated and potential off-target effects are fully characterized in order for ciraparantag to be used in clinical practice.

Specific Reversal Strategies in Preclinical Development

GLA-domainless Factor Xa in Complex with α2-macroglobulin

Similar to andexanet, Jourdi *et al.* have generated a specific antidote for the direct FXa inhibitors based on GLA-domainless FXa[89]. As andexanet might interact with several pro- and anticoagulant macromolecules such as factor Va (FVa), prothrombin, antithrombin, and most importantly TFPI[21,75,76,90], Jourdi *et al.* hypothesized that a complex between GLA-domainless FXa and α2-macroglobulin (GDFXa-α2M) would prevent these macromolecular interactions while retaining its ability to sequester the direct FXa inhibitors **(Figure 4B)**. Alpha2-macroglobulin (α2M) is a molecular trap inhibitor that targets a broad spectrum of proteases in the circulation without directly blocking the protease active site[91,92]. The inhibitor is composed of four identical subunits, each including a bait region targeted by the protease, although only two proteases are able to interact with the tetramer. Upon interaction and cleavage by the protease, α2M undergoes an irreversible conformational change which traps the

protein within a cage-like structure[91,92]. By making use of GLA-domainless FXa that retains its native active site, as opposed to catalytically inactive andexanet due to the Ser195Ala substitution, incubation with α2M results in cleavage of the α2M bait region, generating the irreversible GDFXa-α2M complex. Evaluation of the constants of apixaban and rivaroxaban inhibition revealed somewhat lower binding affinities for interaction with the GDFXa-α2M complex[89,93], although still in the low nanomolar range (1-2.5 nM) similar to wild-type FXa. Furthermore, GDFXa-α2M could fully reverse the effects of supraphysiological levels of rivaroxaban and apixaban in human plasma and restored blood loss and bleeding time in a rivaroxaban-treated mouse model following lateral tail vein transection[89]. Importantly, the GDFXa-α2M complex did not have any detectable effect on a clot waveform assay and was found to be resistant to heparin-catalyzed antithrombin and TFPI, indicating that the trapped FXa does not interact with any of the naturally occurring anticoagulation proteins. This was corroborated by the observation that the D-dimer and thrombin-antithrombin (TAT) complex levels in mice following GDFXa-α2M administration were comparable to vehicle-treated controls. Surprisingly, GDFXa-α2M also partially neutralized the anticoagulant effect of dabigatran[89]. Although the mechanism that lies at the basis of this observation has not been defined thus far, it could involve a non-specific dabigatran binding site in α2M. Together, the GDFXa-α2M complex provides an alternative for andexanet and could potentially be a safer option as it does not interact with relevant macromolecular molecules, i.e. prothrombin, antithrombin, and TFPI. However, since α2M is a large 720 kDa protein, large-scale recombinant production may prove difficult, requiring purification from human plasma.

Zymogen-like Factor Xa (FXa-Ile16Leu)

Besides specific bait antidotes that bind and sequester the direct FXa inhibitors, several prohemostatic bypassing agents have been developed that are able to enhance thrombin generation in the presence of the FXa-targeting inhibitors. One such reversal agent is a FXa variant comprising an Ile16Leu substitution (chymotrypsin numbering)[68,94] **(Figure 5A)**. Upon activation via proteolytic cleavage at the highly conserved Arg15-Ile16 site, serine proteases are converted to their protease state by insertion of the newly formed N-terminus in the active site, thereby forging an internal salt bridge of Ile16 with Asp194. This transition induces maturation of the serine protease domain, specifically following conformational rearrangement of the S1 specificity pocket and oxyanion hole[95]. Disrupting the zymogen to protease transition through modification of the N-terminus (Ile16Leu) induces a zymogen-like conformation in which the active site of FXa retains a partially immature state[94]. As a result, FXa-Ile16Leu displays an impaired chromogenic substrate conversion and is less sensitive to small molecule inhibitors. Although FXa-Ile16Leu also demonstrated weaker FVa binding and prothrombin

activation, saturating concentrations of the cofactor and anionic membranes partly restored thrombin conversion, suggesting that FVa acts as a stabilizing factor in the zymogen to protease transition of this variant. Further assessments revealed a 20- to 40-fold reduced sensitivity for the natural inhibitors antithrombin and TFPI, while, in contrast, prothrombinase-assembled FXa-Ile16Leu was similarly inhibited by antithrombin compared to wt-FXa[96]. Due to the reduced sensitivity, the FXa-Ile16Leu half-life was extended to ~40 min in plasma and approximately 5 min in mice relative to wt-FXa (half-life of ~1 min and <20 sec, respectively)[96-98]. These data indicate that FXa-Ile16Leu is protected from being targeted by natural anticoagulants in the circulation but still retains the ability to catalyze thrombin formation upon binding to FVa on an anionic membrane layer. As such, FXa-Ile16Leu was examined for its bypassing potential in various clinical bleeding settings and was found to be effective in hemophilia (in the presence and absence of inhibitors) and capable of reversing the effects of warfarin[96-99]. Moreover, it was hypothesized that the properties of FXa-Ile16Leu might enable this variant to bypass the direct oral anticoagulants. *In vitro* evaluation by TG and ROTEM assays demonstrated that FXa-Ile16Leu dose-dependently reversed the anti-FXa effects of rivaroxaban-spiked plasma and whole blood[68]. These results could be translated to murine *in vivo* models as mouse FXa-Ile16Leu completely restored hemostasis in several thrombosis and bleeding models in the presence of rivaroxaban[68]. Infusion of this FXa variant in mice did increase the circulating TAT levels, but only in the absence of rivaroxaban, while D-dimer levels remained unaltered[68]. The possible mechanism by which FXa-Ile16Leu reverses the effect of the direct FXa inhibitors might be similar to that of previously mentioned bypassing agents. In the presence of rivaroxaban, antithrombin and rivaroxaban are competing for FXa binding. As a consequence, an equilibrium is formed, characterized by a steady-state pool of free FXa[68]. Computional simulations revealed that the free FXa-Ile16Leu steady-state levels were substantially higher compared to those of wt-FXa. However, the net effect on thrombin generation was identical to wt-FXa due to the reduced catalytic activity of FXa-Ile16Leu. This suggests that besides FXa-Ile16Leu, wt-FXa could also be able to reverse the direct FXa inhibitor-induced anticoagulant state. Yet, FXa-Ile16Leu is dependent on the binding of FVa in order to rescue its catalytic activity, which could be beneficial in terms of safety and prothrombotic risks. As such, administration of FXa-Ile16Leu would only result in local clot formation at the sites of injury. Collectively, these studies highlight the potential efficacy of FXa-Ile16Leu as a rescue agent in a variety of bleeding disorders, including direct FXa inhibitor-induced bleeding complications. This prohemostatic agent therefore provides a rapid-onset alternative for the bait antidotes, thereby requiring significantly lower amounts of the reversal agent to control bleeding.

The clinical development of FXa-Ile16Leu is currently ongoing. Assessment of the pharmacokinetics and pharmacodynamics in rats and monkeys displayed a half-life of 2-3 min[100]. Furthermore, FXa-Ile16Leu administration resulted in a dose-dependent shortening of the aPTT in non-human primates, but simultaneously led to increased TAT levels. A first-in-human dose escalation study in 49 healthy volunteers revealed that FXa-Ile16Leu was well tolerated with no observed toxicity or serious adverse events[101]. The pharmacodynamics displayed shortening of the aPTT and TG lag time, as well as an increase in TG peak height, D-dimer, TAT, and prothrombin fragments 1.2 with all parameters returning to baseline within 24 hours. Finally, a clinical trial evaluating the safety and tolerability of FXa-Ile16Leu in subjects with spontaneous ICH is underway (NCT02687191). Whether this reversal agent will be further tested in the setting of the direct FXa inhibitors is unknown.

The 99-loop Factor X Variant (FX-C)

The 99-loop FX variant, also known as FX-C, is a chimeric FX protein comprising a structural modification derived from the so-called isoform FX variant that is expressed in the venom and liver of the eastern common brown snake (*Pseudonaja textilis)*[102] **(Figure 5B)**. Characterization of the isoform and venom FXa proteases revealed a high resistance for the direct FXa inhibitors rivaroxaban and apixaban. Sequence analysis showed that these FXa variants comprise an extended 99-loop (His91-Asp102) located N-terminal to the S4 subsite. Since the S4 pocket was demonstrated to be a primary binding site for the FXa inhbitors and stabilizes their positioning in the active site[5,6,102], this non-conserved structural element was hypothesized to be responsible for the observed resistance towards the direct FXa inhibitors. In order to further investigate the reduced sensitivity, the 99-loop extension of isoform FX was recombinantly inserted into human FX, thereby generating FX(a)-C. Insertion of this structural element significantly reduced the FXa sensitivity for apixaban and edoxaban (up to 700-fold), although this came at the cost of a 3-fold lower catalytic efficiency towards the natural substrate prothrombin[102]. To examine whether the reduced inhibitor sensitivity of FXa-C was sufficient to restore the thrombin formation, TG assays were employed in apixaban- and edoxaban-spiked plasma. These experiments revealed that the addition of zymogen FX-C resulted in a dose-dependent increase in thrombin generation. Moreover complete TG normalization was observed with the addition of 20-40 µg/mL of the FX-C variant. Interestingly, molecular dynamics simulations revealed that the extended 99-loop in FXa-C adopts a helical conformation which displays substantial mobility. This structural mobility results in the rapid displacement of the apixaban molecule, indicative of steric hindrance leading to impaired inhibitor binding. As such, significant levels of free FXa-C are formed that, despite its reduced prothrombin conversion rate, are able to restore thrombin

generation parameters to near-normal conditions, indicative of a restored hemostasis. The inhibitor-resistant variant FX-C is currently in preclinical and clinical development.

Phe174-substituted FX Variants

Arising from the FX-C study, a Phe174-substituted FXa variant displayed potential as bypassing agent for the direct FXa inhibitors **(Figure 5C)**. Molecular dynamics simulations of the human FXa-apixaban complex demonstrated a tight inhibitor interaction with the FXa S4 subsite pocket[102]. In this pocket, the P_4 moiety of apixaban is sandwiched between the aromatic side-chains of S4 subsite residues Tyr99 and Phe174. Replacing the S4 subsite residues Tyr99 and/or Phe174 with alanine disrupted apixaban binding, resulting in a markedly decreased FXa sensitivity for the inhibitor. While the Tyr99Ala substitution was accompanied by an almost complete diminished FXa activity, substitution of Phe174 retained the intrinsic clotting potential. As such, human FX variants were generated comprising an alanine (FX-F174A) or serine (FX-F174S) substitution at position 174[103] **(Figure 5C)**. These variants displayed a 10-fold reduced sensitivity towards apixaban and a 4-7-fold reduced sensitivity for inhibition by rivaroxaban and edoxaban. Similar effects were demonstrated in human plasma spiked with the direct FXa inhibitors, revealing a 6-17-fold loss of inhibitor sensitivity. Furthermore, addition of 30-45 µg/mL of these variants completely rescued the thrombin peak height in the presence of 1 µM apixaban and rivaroxaban, while an 80% improvement was found in identical conditions with edoxaban. Although further research is needed to fully elucidate the effects of the Phe174-substituted FX variants, these agents might prove to be a potential treatment option.

Concluding Remarks

Bleeding complications associated with DOAC-use remain a major concern, creating a critical need for rapid-onset reversal agents. Although a specific antidote is available for the direct thrombin inhibitor in idarucizumab, counteracting the effect of the direct FXa inhibitors has been a point of focus over the last years. In the absence of specific antidotes for the direct FXa inhibitors, off-label use of prohemostatic agents has been recommended as standard of care. In the meantime, considerable efforts have been made by researchers to fill the unmet need for a specific reversal agent, leading to the recent FDA and EMA approval of andexanet alfa. Furthermore, several specific reversal agents are currently in (pre)clinical development. Since the potential interaction of andexanet with TFPI might raise some concerns, other specific reversal agents that are currently in various stages of (pre)clinical development may prove to be alternative options for reversal. For instance, the Gla-domainless FXa-α2-macroglobulin complex did not display interactions with endogenous inhibitors.

Another potential option is ciraparantag, a small synthetic molecule that reportedly binds and sequesters the FXa-targeting inhibitors, although its mode of action seems unresolved at this point. Interestingly, several prohemostatic bypassing agents have been developed, including FXa-Ile16Leu, FX(a)-C, and the Phe174-substituted variants FX-F174A and FX-F174S. Their key advantage resides in the limited amount of protein that is needed to correct inhibitor-induced bleeding, in contrast to the stoichiometric bait antidotes. Concomitantly, these prohemostatic bypassing agents may increase the risk for thrombotic complications, and as such more caution might be required in clinical practice. Additionally, the protein modifications in the FX(a) variants may induce an antibody response, limiting the efficacy of repeated use. Further characterization of these specific agents is therefore imperative, but a future with specific, safe, and effective reversal agents for the direct FXa inhibitors seems imminent.

Acknowledgements

We thank Dr. F.A. Klok for critical evaluation of this manuscript and M. Zuurmond for generating the images. Our work in this area has been financially supported by the Bayer Hemophilia Awards Program (Special Project Award) and Landsteiner Foundation for Blood Transfusion (LSBR, grant. no. 1451). The funding agencies had no role in the preparation, review, or approval of the manuscript.

Figures

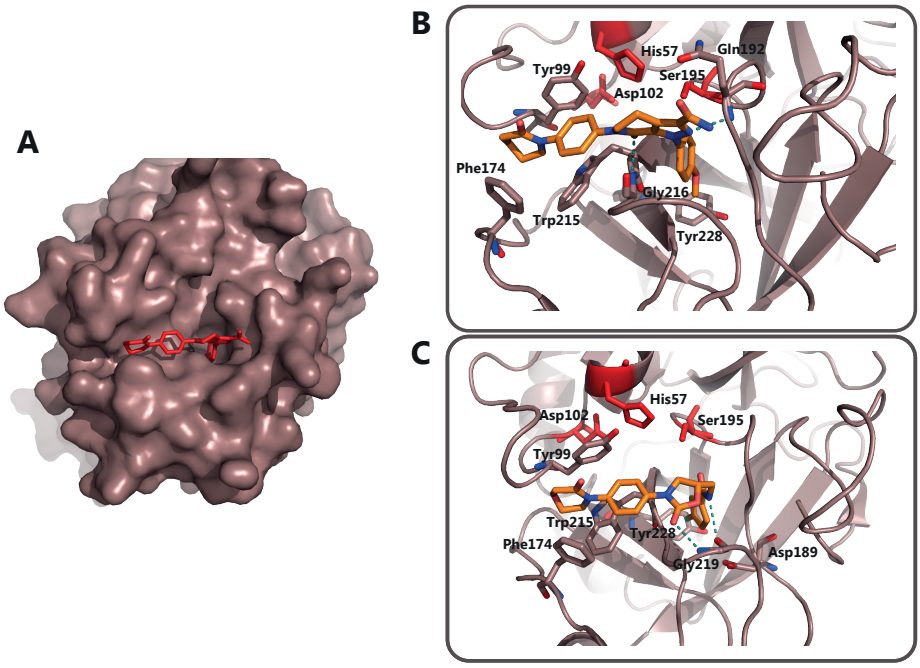


Figure 1. Binding mode of the direct factor Xa inhibitors. (A) Surface representation of the FXa X-ray structure in complex with the direct FXa inhibitor apixaban shown in red. **(B-C)** Close up view of apixaban **(B)** and rivaroxban **(C)** binding to FXa. Apixaban and rivaroxban are depicted in orange, with the oxygen atoms indicated in red and nitrogen atoms in blue. Essential amino acids in FXa are shown in stick configuration in which the catalytic triad residues His57, Asp102, and Ser195 are colored in red. All FXa residues are indicated in chymotrypsinogen numbering. Hydrogen bond interactions are shown in teal dashed lines.

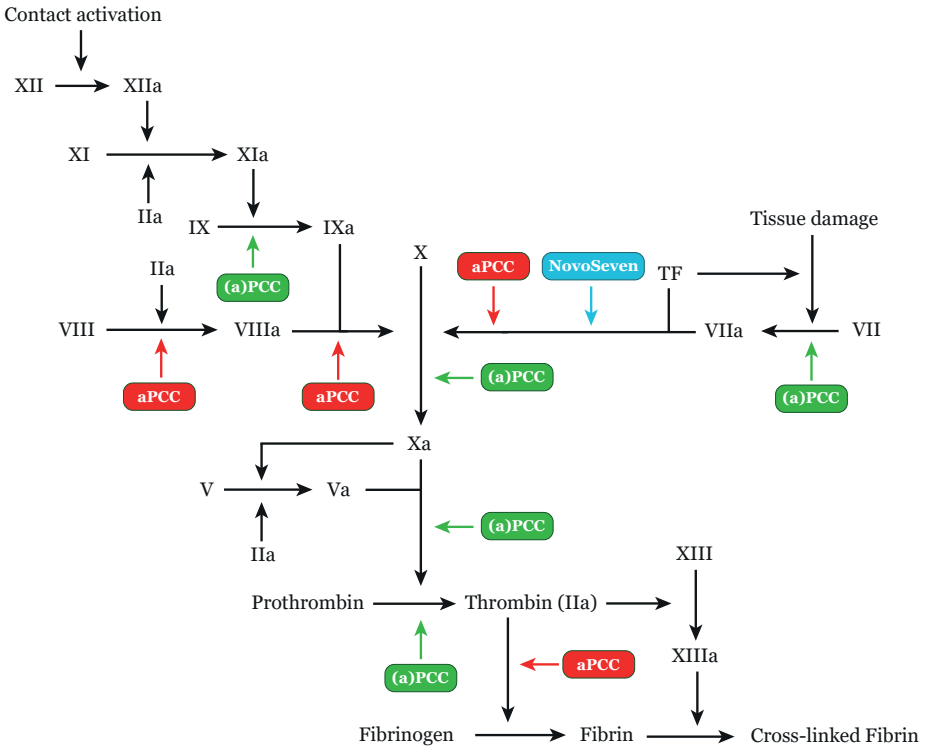


Figure 2. Schematic representation of the procoagulant actions exerted by non-specific reversal agents. The non-specific reversal agents promote various procoagulant reactions of the coagulation cascade in order to drive thrombin generation in the presence of the direct factor Xa inhibitors. The overlapping actions of the activated and non-activated prothrombin complex concentrates ((a)PCC) are indicated in green arrows. The distinct effects of aPCC are shown in red, and that of recombinant activated factor VIIa (rFVIIa) is shown in blue. TF indicates tissue factor.

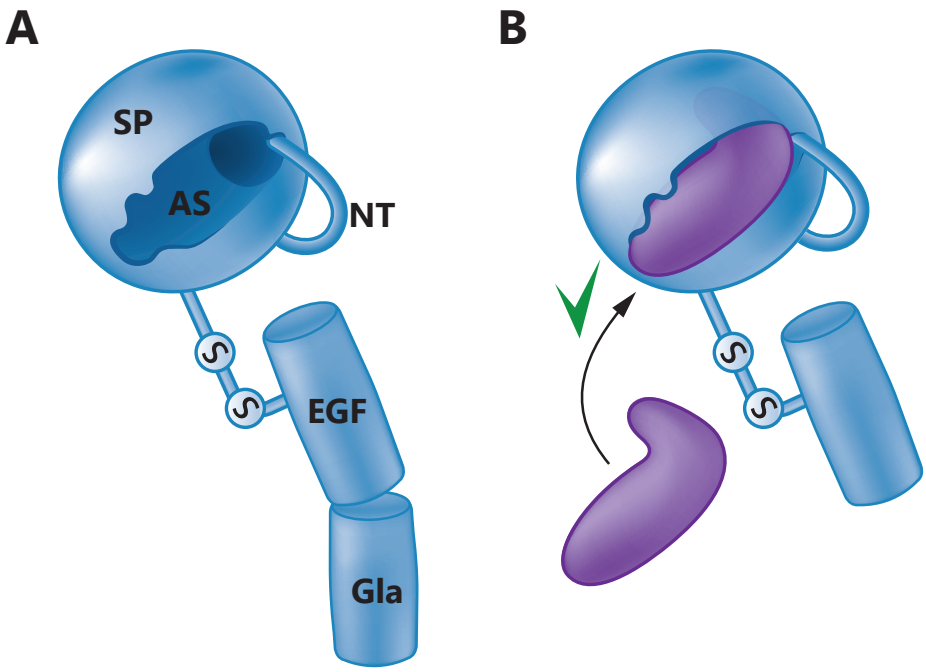


Figure 3. Schematic representation of human factor Xa and the reversal agent andexanet alfa. (A) The light chain of factor Xa (FXa) consisting of the γ-carboxyglutamic acid domain (GLA), the endothelial growth factor 1 and 2 domains (EGF), and the heavy chain comprising the serine protease domain (SP) and active site pocket (AS) are shown, linked by a disulfide bond (S-S). The heavy chain N-terminus (NT), formed upon proteolytic activation of factor X, is shown as an insertion into the active site pocket, representing the salt bridge between Ile16 and Asp194. **(B)** Schematic respresentation of andexanet alfa. Despite being enzymatically inactive due to a Ser195Ala substitution, andexanet alfa encompasses a high binding affinity for the direct FXa inhibitors, which are shown in purple. Removal of the Gla domain prevents incorporation of andexanet alfa into the prothrombinase complex.

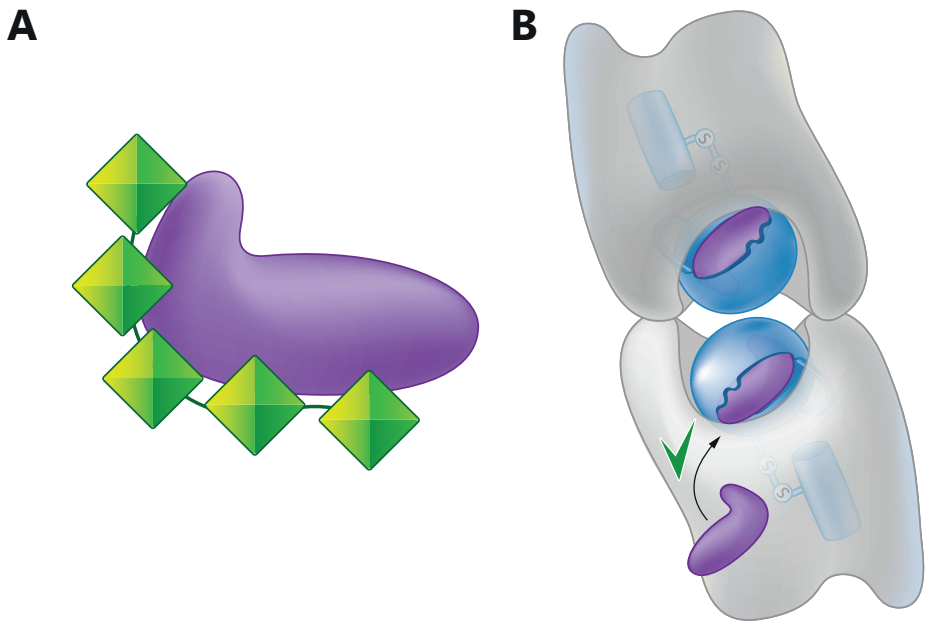


Figure 4. Schematic representation of the universal reversal agent ciraparantag and the GLA-domainless factor Xa in complex with α2-macroglobulin. (A) Ciraparantag (the green squares represent two L-arginine units at each end that are connected via a linker consisting of three units of which a piperazine comprises the middle unit) reportedly binds directly to the direct factor Xa inhibitors (shown in purple) via hydrogen-bonding, thereby sequestering the inhibitors from the circulation. **(B)** α2-macroglobulin consists of four identical subunits that allow for the interaction with two factor Xa (FXa) proteases. Despite being trapped, GLA-domainless FXa retains its ability to bind the direct FXa inhibitors (shown in purple), thereby clearing the inhibitors from the circulation. Complex formation with α2-macroglobulin further prevents macromolecular interactions with FXa.

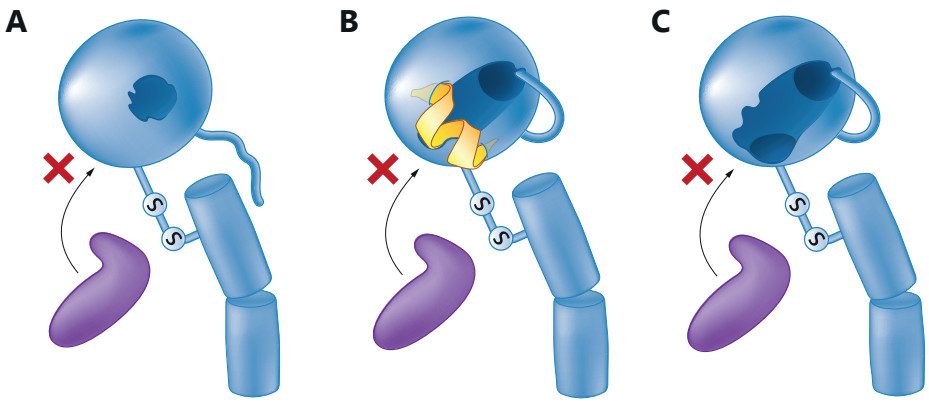


Figure 5. Schematic representation of the prohemostatic reversal agents in preclinical development. (A) Substitution of Ile16 for leucine (shown in red) disrupts the insertion of the newly formed N-terminus upon factor X activation, thereby destabilizing the formation of the characteristic internal salt bridge with Asp194. As a consequence, the active site of FXa-Ile16Leu is partly matured (indicated as a smaller active site), thereby inducing a zymogen-like state. This zymogen-like state prevents the inhibition of FXa-Ile16leu by the direct FXa inhibitors (shown in purple). Binding to factor Va rescues the maturation of the serine protease domain. **(B)** Factor Xa-C (FXa-C) is resistant to the direct factor Xa inhibitors (shown in purple) due to an insertion within the active site 99-loop. This structural element (highlighted in yellow) sterically hinders the binding of the direct FXa inhibitors to the active site. **(C)** The prohemostatic factor Xa (FXa) comprises an alanine or serine substitution of the phenylalanine 174 (shown in red). Altough the direct FXa inhibitors (shown in purple) are able to engage the active site, substitution of the phenylalanine 174 destabilizes inhibitor binding, resulting in a loss of affinity.

References

1 Cuker, A. & Siegal, D. Monitoring and reversal of direct oral anticoagulants. *Hematology Am Soc Hematol Educ Program* **2015**, 117-124, doi:10.1182/asheducation-2015.1.117 (2015).
2 Barnes, G. D., Lucas, E., Alexander, G. C. & Goldberger, Z. D. National Trends in Ambulatory Oral Anticoagulant Use. *Am J Med* **128**, 1300-1305 e1302, doi:10.1016/j.amjmed.2015.05.044 (2015).
3 Pollack, C. V., Jr. *et al.* Idarucizumab for Dabigatran Reversal - Full Cohort Analysis. *N Engl J Med* **377**, 431-441, doi:10.1056/NEJMoa1707278 (2017).
4 Loo, S. Y., Dell'Aniello, S., Huiart, L. & Renoux, C. Trends in the prescription of novel oral anticoagulants in UK primary care. *Br J Clin Pharmacol* **83**, 2096-2106, doi:10.1111/bcp.13299 (2017).
5 Roehrig, S. *et al.* Discovery of the novel antithrombotic agent 5-chloro-N-({(5S)-2-oxo-3-[4-(3-oxomorpholin-4-yl)phenyl]-1,3-oxazolidin-5-yl}methyl)thiophene- 2-carboxamide (BAY 59-7939): an oral, direct factor Xa inhibitor. *J Med Chem* **48**, 5900-5908, doi:10.1021/jm050101d (2005).
6 Pinto, D. J. *et al.* Discovery of 1-(4-methoxyphenyl)-7-oxo-6-(4-(2-oxopiperidin-1-yl)phenyl)-4,5,6,7-tetrahydro-1H -pyrazolo[3,4-c]pyridine-3-carboxamide (apixaban, BMS-562247), a highly potent, selective, efficacious, and orally bioavailable inhibitor of blood coagulation factor Xa. *J Med Chem* **50**, 5339-5356, doi:10.1021/jm070245n (2007).
7 Furugohri, T. *et al.* DU-176b, a potent and orally active factor Xa inhibitor: in vitro and in vivo pharmacological profiles. *J Thromb Haemost* **6**, 1542-1549, doi:10.1111/j.1538-7836.2008.03064.x (2008).
8 Hedstrom, L. Serine protease mechanism and specificity. *Chem Rev* **102**, 4501-4524 (2002).
9 Wong, P. C., Pinto, D. J. & Zhang, D. Preclinical discovery of apixaban, a direct and orally bioavailable factor Xa inhibitor. *J Thromb Thrombolysis* **31**, 478-492, doi:10.1007/s11239-011-0551-3 (2011).
10 Padmanabhan, K. *et al.* Structure of human des(1-45) factor Xa at 2.2 A resolution. *J Mol Biol* **232**, 947-966, doi:10.1006/jmbi.1993.1441 (1993).
11 Zhang, P. *et al.* Discovery of betrixaban (PRT054021), N-(5-chloropyridin-2-yl)-2-(4-(N,N-dimethylcarbamimidoyl)benzamido)-5-methoxybenz amide, a highly potent, selective, and orally efficacious factor Xa inhibitor. *Bioorg Med Chem Lett* **19**, 2179-2185, doi:10.1016/j.bmcl.2009.02.111 (2009).
12 Samama, M. M. The mechanism of action of rivaroxaban--an oral, direct Factor Xa inhibitor--compared with other anticoagulants. *Thromb Res* **127**, 497-504, doi:10.1016/j.thromres.2010.09.008 (2011).
13 Masotti, L. & Campanini, M. Pharmacology of new oral anticoagulants: mechanism of action, pharmacokinetics, pharmacodynamics. *Italian Journal of Medicine* **7**, 1-7 (2013).
14 Gomez-Outes, A., Suarez-Gea, M. L., Lecumberri, R., Terleira-Fernandez, A. I. & Vargas-Castrillon, E. Direct-acting oral anticoagulants: pharmacology, indications, management, and future perspectives. *Eur J Haematol* **95**, 389-404, doi:10.1111/ejh.12610 (2015).
15 Connolly, S. J. *et al.* Dabigatran versus warfarin in patients with atrial fibrillation. *N Engl J Med* **361**, 1139-1151, doi:10.1056/NEJMoa0905561 (2009).
16 Patel, M. R. *et al.* Rivaroxaban versus warfarin in nonvalvular atrial fibrillation. *N Engl J Med* **365**, 883-891, doi:10.1056/NEJMoa1009638 (2011).
17 Agnelli, G. *et al.* Oral apixaban for the treatment of acute venous thromboembolism. *N Engl J Med* **369**, 799-808, doi:10.1056/NEJMoa1302507 (2013).

18 Deitelzweig, S. B., Johnson, B. H., Lin, J. & Schulman, K. L. Prevalence of clinical venous thromboembolism in the USA: current trends and future projections. *Am J Hematol* **86**, 217-220, doi:10.1002/ajh.21917 (2011).
19 Chugh, S. S. *et al.* Worldwide epidemiology of atrial fibrillation: a Global Burden of Disease 2010 Study. *Circulation* **129**, 837-847, doi:10.1161/CIRCULATIONAHA.113.005119 (2014).
20 Connolly, S. J. *et al.* Full Study Report of Andexanet Alfa for Bleeding Associated with Factor Xa Inhibitors. *N Engl J Med* **380**, 1326-1335, doi:10.1056/NEJMoa1814051 (2019).
21 Lu, G. *et al.* A specific antidote for reversal of anticoagulation by direct and indirect inhibitors of coagulation factor Xa. *Nat Med* **19**, 446-451, doi:10.1038/nm.3102 (2013).
22 Hellstern, P. Production and composition of prothrombin complex concentrates: correlation between composition and therapeutic efficiency. *Thromb Res* **95**, S7-12, doi:10.1016/s0049-3848(99)00078-x (1999).
23 Franchini, M. & Lippi, G. Prothrombin complex concentrates: an update. *Blood Transfus* **8**, 149-154, doi:10.2450/2010.0149-09 (2010).
24 Cada, D. J., Levien, T. L. & Baker, D. E. Prothrombin complex concentrate. *Hosp Pharm* **48**, 951-957, doi:10.1310/hpj4811-951 (2013).
25 Sarode, R. *et al.* Efficacy and safety of a 4-factor prothrombin complex concentrate in patients on vitamin K antagonists presenting with major bleeding: a randomized, plasma-controlled, phase IIIb study. *Circulation* **128**, 1234-1243, doi:10.1161/CIRCULATIONAHA.113.002283 (2013).
26 Godier, A. *et al.* Evaluation of prothrombin complex concentrate and recombinant activated factor VII to reverse rivaroxaban in a rabbit model. *Anesthesiology* **116**, 94-102, doi:10.1097/ALN.0b013e318238c036 (2012).
27 Martin, A. C. *et al.* Evaluation of recombinant activated factor VII, prothrombin complex concentrate, and fibrinogen concentrate to reverse apixaban in a rabbit model of bleeding and thrombosis. *Int J Cardiol* **168**, 4228-4233, doi:10.1016/j.ijcard.2013.07.152 (2013).
28 Perzborn, E. *et al.* Reversal of rivaroxaban anticoagulation by haemostatic agents in rats and primates. *Thrombosis and haemostasis* **110**, 162-172, doi:10.1160/TH12-12-0907 (2013).
29 Zhou, W. *et al.* Hemostatic therapy in experimental intracerebral hemorrhage associated with rivaroxaban. *Stroke* **44**, 771-778, doi:10.1161/STROKEAHA.112.675231 (2013).
30 Herrmann, R. *et al.* Thrombin generation using the calibrated automated thrombinoscope to assess reversibility of dabigatran and rivaroxaban. *Thrombosis and haemostasis* **111**, 989-995, doi:10.1160/TH13-07-0607 (2014).
31 Levi, M. *et al.* Comparison of three-factor and four-factor prothrombin complex concentrates regarding reversal of the anticoagulant effects of rivaroxaban in healthy volunteers. *J Thromb Haemost* **12**, 1428-1436, doi:10.1111/jth.12599 (2014).
32 Eerenberg, E. S. *et al.* Reversal of rivaroxaban and dabigatran by prothrombin complex concentrate: a randomized, placebo-controlled, crossover study in healthy subjects. *Circulation* **124**, 1573-1579, doi:10.1161/CIRCULATIONAHA.111.029017 (2011).
33 Barco, S. *et al.* In vivo reversal of the anticoagulant effect of rivaroxaban with four-factor prothrombin complex concentrate. *Br J Haematol* **172**, 255-261, doi:10.1111/bjh.13821 (2016).
34 Song, Y. *et al.* Reversal of apixaban anticoagulation by four-factor prothrombin complex concentrates in healthy subjects: a randomized three-period crossover study. *J Thromb Haemost* **15**, 2125-2137, doi:10.1111/jth.13815 (2017).
35 Brown, K. S. *et al.* The impact of a three-factor prothrombin complex concentrate on the anticoagulatory effects of the factor Xa inhibitor edoxaban. *Thromb Res* **136**, 825-831, doi:10.1016/j.thromres.2015.07.012 (2015).
36 Nagalla, S. *et al.* Reversibility of Apixaban Anticoagulation with a Four-Factor Prothrombin Complex Concentrate in Healthy Volunteers. *Clin Transl Sci* **9**, 176-180, doi:10.1111/cts.12398 (2016).

37 Cheung, Y. W. *et al.* In vivo increase in thrombin generation by four-factor prothrombin complex concentrate in apixaban-treated healthy volunteers. *J Thromb Haemost* **13**, 1799-1805, doi:10.1111/jth.13115 (2015).
38 Zahir, H. *et al.* Edoxaban effects on bleeding following punch biopsy and reversal by a 4-factor prothrombin complex concentrate. *Circulation* **131**, 82-90, doi:10.1161/CIRCULATIONAHA.114.013445 (2015).
39 Schulman, S. *et al.* Prothrombin Complex Concentrate for Major Bleeding on Factor Xa Inhibitors: A Prospective Cohort Study. *Thrombosis and haemostasis* **118**, 842-851, doi:10.1055/s-0038-1636541 (2018).
40 Majeed, A. *et al.* Management of rivaroxaban- or apixaban-associated major bleeding with prothrombin complex concentrates: a cohort study. *Blood* **130**, 1706-1712, doi:10.1182/blood-2017-05-782060 (2017).
41 Arachchillage, D. R. J. *et al.* Efficacy and safety of prothrombin complex concentrate in patients treated with rivaroxaban or apixaban compared to warfarin presenting with major bleeding. *Br J Haematol* **184**, 808-816, doi:10.1111/bjh.15705 (2019).
42 Gerner, S. T. *et al.* Association of prothrombin complex concentrate administration and hematoma enlargement in non-vitamin K antagonist oral anticoagulant-related intracerebral hemorrhage. *Ann Neurol* **83**, 186-196, doi:10.1002/ana.25134 (2018).
43 Tomaselli, G. F. *et al.* 2017 ACC Expert Consensus Decision Pathway on Management of Bleeding in Patients on Oral Anticoagulants: A Report of the American College of Cardiology Task Force on Expert Consensus Decision Pathways. *J Am Coll Cardiol* **70**, 3042-3067, doi:10.1016/j.jacc.2017.09.1085 (2017).
44 Sjamsoedin, L. J. *et al.* The effect of activated prothrombin-complex concentrate (FEIBA) on joint and muscle bleeding in patients with hemophilia A and antibodies to factor VIII. A double-blind clinical trial. *N Engl J Med* **305**, 717-721, doi:10.1056/NEJM198109243051301 (1981).
45 Hilgartner, M. W. & Knatterud, G. L. The use of factor eight inhibitor by-passing activity (FEIBA immuno) product for treatment of bleeding episodes in hemophiliacs with inhibitors. *Blood* **61**, 36-40 (1983).
46 Hilgartner, M., Aledort, L., Andes, A. & Gill, J. Efficacy and safety of vapor-heated anti-inhibitor coagulant complex in hemophilia patients. FEIBA Study Group. *Transfusion* **30**, 626-630, doi:10.1046/j.1537-2995.1990.30790385521.x (1990).
47 Fukuda, T., Honda, Y., Kamisato, C., Morishima, Y. & Shibano, T. Reversal of anticoagulant effects of edoxaban, an oral, direct factor Xa inhibitor, with haemostatic agents. *Thrombosis and haemostasis* **107**, 253-259, doi:10.1160/TH11-09-0668 (2012).
48 Halim, A. B., Samama, M. M. & Mendell, J. Ex vivo reversal of the anticoagulant effects of edoxaban. *Thromb Res* **134**, 909-913, doi:10.1016/j.thromres.2014.07.036 (2014).
49 Schultz, N. H. *et al.* The reversal effect of prothrombin complex concentrate (PCC), activated PCC and recombinant activated factor VII against anticoagulation of Xa inhibitor. *Thromb J* **15**, 6, doi:10.1186/s12959-017-0129-1 (2017).
50 Perzborn, E., Heitmeier, S., Laux, V. & Buchmuller, A. Reversal of rivaroxaban-induced anticoagulation with prothrombin complex concentrate, activated prothrombin complex concentrate and recombinant activated factor VII in vitro. *Thromb Res* **133**, 671-681, doi:10.1016/j.thromres.2014.01.017 (2014).
51 Marlu, R. *et al.* Effect of non-specific reversal agents on anticoagulant activity of dabigatran and rivaroxaban: a randomised crossover ex vivo study in healthy volunteers. *Thrombosis and haemostasis* **108**, 217-224, doi:10.1160/TH12-03-0179 (2012).
52 Mao, G., King, L., Young, S. & Kaplan, R. Factor Eight Inhibitor Bypassing Agent (FEIBA) for Reversal of Target-Specific Oral Anticoagulants in Life-Threatening Intracranial Bleeding. *J Emerg Med* **52**, 731-737, doi:10.1016/j.jemermed.2016.11.011 (2017).

53 Dibu, J. R., Weimer, J. M., Ahrens, C., Manno, E. & Frontera, J. A. The Role of FEIBA in Reversing Novel Oral Anticoagulants in Intracerebral Hemorrhage. *Neurocrit Care* **24**, 413-419, doi:10.1007/s12028-015-0213-y (2016).
54 Dager, W. E., Roberts, A. J. & Nishijima, D. K. Effect of low and moderate dose FEIBA to reverse major bleeding in patients on direct oral anticoagulants. *Thromb Res* **173**, 71-76, doi:10.1016/j.thromres.2018.11.009 (2019).
55 Engelbart, J. M. *et al.* Safety and effectiveness of Factor Eight Inhibitor Bypassing Activity for direct oral anticoagulant-related hemorrhage reversal. *Am J Emerg Med* **37**, 214-219, doi:10.1016/j.ajem.2018.05.023 (2019).
56 Lentz, S. R. *et al.* Recombinant factor VIIa analog in the management of hemophilia with inhibitors: results from a multicenter, randomized, controlled trial of vatreptacog alfa. *J Thromb Haemost* **12**, 1244-1253, doi:10.1111/jth.12634 (2014).
57 Lusher, J. M. *et al.* A randomized, double-blind comparison of two dosage levels of recombinant factor VIIa in the treatment of joint, muscle and mucocutaneous haemorrhages in persons with haemophilia A and B, with and without inhibitors. rFVIIa Study Group. *Haemophilia* **4**, 790-798 (1998).
58 Goodnough, L. T. & Levy, J. H. The Judicious Use of Recombinant Factor VIIa. *Semin Thromb Hemost* **42**, 125-132, doi:10.1055/s-0035-1569068 (2016).
59 Schmidt, K. *et al.* Reversal of apixaban induced alterations in haemostasis by different coagulation factor concentrates in patients after hip or knee replacement surgery. *Blood Transfus* **17**, 157-162, doi:10.2450/2018.0028-18 (2019).
60 Hemphill, J. C., 3rd *et al.* Guidelines for the Management of Spontaneous Intracerebral Hemorrhage: A Guideline for Healthcare Professionals From the American Heart Association/American Stroke Association. *Stroke* **46**, 2032-2060, doi:10.1161/STR.0000000000000069 (2015).
61 Turecek, P. L., Varadi, K., Gritsch, H. & Schwarz, H. P. FEIBA: mode of action. *Haemophilia* **10 Suppl 2**, 3-9, doi:10.1111/j.1365-2516.2004.00934.x (2004).
62 Turecek, P. L. *et al.* Factor Xa and prothrombin: mechanism of action of FEIBA. *Vox Sang* **77 Suppl 1**, 72-79, doi:10.1159/000056722 (1999).
63 Himmelspach, M. *et al.* A fully recombinant partial prothrombin complex effectively bypasses fVIII in vitro and in vivo. *Thrombosis and haemostasis* **88**, 1003-1011 (2002).
64 Schuijt, T. J. *et al.* Factor Xa activation of factor V is of paramount importance in initiating the coagulation system: lessons from a tick salivary protein. *Circulation* **128**, 254-266, doi:10.1161/CIRCULATIONAHA.113.003191 (2013).
65 Schreuder, M., Reitsma, P. H. & Bos, M. H. A. Blood coagulation factor Va's key interactive residues and regions for prothrombinase assembly and prothrombin binding. *J Thromb Haemost* **17**, 1229-1239, doi:10.1111/jth.14487 (2019).
66 Johnson, D. J., Li, W., Adams, T. E. & Huntington, J. A. Antithrombin-S195A factor Xa-heparin structure reveals the allosteric mechanism of antithrombin activation. *EMBO J* **25**, 2029-2037, doi:10.1038/sj.emboj.7601089 (2006).
67 Li, W., Johnson, D. J., Esmon, C. T. & Huntington, J. A. Structure of the antithrombin-thrombin-heparin ternary complex reveals the antithrombotic mechanism of heparin. *Nat Struct Mol Biol* **11**, 857-862, doi:10.1038/nsmb811 (2004).
68 Thalji, N. K. *et al.* A rapid pro-hemostatic approach to overcome direct oral anticoagulants. *Nat Med* **22**, 924-932, doi:10.1038/nm.4149 (2016).
69 Monroe, D. M., Hoffman, M., Oliver, J. A. & Roberts, H. R. Platelet activity of high-dose factor VIIa is independent of tissue factor. *Br J Haematol* **99**, 542-547, doi:10.1046/j.1365-2141.1997.4463256.x (1997).

70 Lu, G. *et al.* Andexanet alfa effectively reverses edoxaban anticoagulation effects and associated bleeding in a rabbit acute hemorrhage model. *PLoS One* **13**, e0195122, doi:10.1371/journal.pone.0195122 (2018).
71 Lu, G. *et al.* Preclinical safety and efficacy of andexanet alfa in animal models. *J Thromb Haemost* **15**, 1747-1756, doi:10.1111/jth.13768 (2017).
72 Siegal, D. M. *et al.* Andexanet Alfa for the Reversal of Factor Xa Inhibitor Activity. *N Engl J Med* **373**, 2413-2424, doi:10.1056/NEJMoa1510991 (2015).
73 Siegal, D. *et al.* Safety, pharmacokinetics, and reversal of apixaban anticoagulation with andexanet alfa. *Blood Adv* **1**, 1827-1838, doi:10.1182/bloodadvances.2017007112 (2017).
74 Goldstein, J. N. *et al.* Four-factor prothrombin complex concentrate versus plasma for rapid vitamin K antagonist reversal in patients needing urgent surgical or invasive interventions: a phase 3b, open-label, non-inferiority, randomised trial. *Lancet* **385**, 2077-2087, doi:10.1016/S0140-6736(14)61685-8 (2015).
75 Ersayin, A. *et al.* Catalytically inactive Gla-domainless factor Xa binds to TFPI and restores ex vivo coagulation in hemophilia plasma. *Haematologica* **102**, e483-e485, doi:10.3324/haematol.2017.174037 (2017).
76 Marlu, R. & Polack, B. Gla-domainless factor Xa: molecular bait to bypass a blocked tenase complex. *Haematologica* **97**, 1165-1172, doi:10.3324/haematol.2011.055699 (2012).
77 Lu, G., Lin, J. P., Curnutte, J. T. & Conley, P. B. Abstract: Effect of Andexanet-TFPI Interaction on in Vitro Thrombin Formation and Coagulation Markers in the TF-Pathway. *Blood* **130**, 629 (2017).
78 Ansell, J. E. *et al.* Single-dose ciraparantag safely and completely reverses anticoagulant effects of edoxaban. *Thrombosis and haemostasis* **117**, 238-245, doi:10.1160/TH16-03-0224 (2017).
79 Weitz, J. I. & Eikelboom, J. W. Ciraparantag for enoxaparin reversal: Adding to the evidence. *Thromb Res* **146**, 106-107, doi:10.1016/j.thromres.2016.08.013 (2016).
80 Ansell, J. E. *et al.* Ciraparantag safely and completely reverses the anticoagulant effects of low molecular weight heparin. *Thromb Res* **146**, 113-118, doi:10.1016/j.thromres.2016.07.008 (2016).
81 Laulicht, B. E. *et al.* Abstract: Antidote for new oral anticoagulants: mechanism of action and binding specificity of PER977. *Journal of Thrombosis and Haemostasis* **11** (2013).
82 Laulicht, B. E. *et al.* Abstract 11395: Small Molecule Antidote for Anticoagulants. *Circulation* **126** (2018).
83 Bakhru, S. H. *et al.* Abstract 19361: Reversal of Anticoagulant-induced Bleeding in External and Internal Bleeding Models by PER977, a Small Molecule Anticoagulant Antidote. *Circulation* **130** (2018).
84 Hollenbach, S. J. *et al.* Abstract 14657: Andexanet-alfa and PER977 (Arapazine) Correct Blood Loss in a Rabbit Liver Laceration Model - Only Andexanet Reverses Markers of fXa-mediated Anticoagulation. *Circulation* **130** (2018).
85 Sullivan, D. W., Jr., Gad, S. C., Laulicht, B., Bakhru, S. & Steiner, S. Nonclinical Safety Assessment of PER977: A Small Molecule Reversal Agent for New Oral Anticoagulants and Heparins. *Int J Toxicol* **34**, 308-317, doi:10.1177/1091581815590667 (2015).
86 Ansell, J. E. *et al.* Use of PER977 to reverse the anticoagulant effect of edoxaban. *N Engl J Med* **371**, 2141-2142, doi:10.1056/NEJMc1411800 (2014).
87 Kalathottukaren, M. T. *et al.* Comparison of reversal activity and mechanism of action of UHRA, andexanet, and PER977 on heparin and oral FXa inhibitors. *Blood Adv* **2**, 2104-2114, doi:10.1182/bloodadvances.2016003616 (2018).
88 Lu, G. *et al.* Abstract 18218: In Vitro Characterization of Andexanet Alfa (PRT064445), a Specific fXa Inhibitor Antidote versus Aripazine (PER977), a Non-specific Reversal Agent. *Circulation* **130** (2018).

89 Jourdi, G. *et al.* FXa-alpha2-Macroglobulin Complex Neutralizes Direct Oral Anticoagulants Targeting FXa In Vitro and In Vivo. *Thrombosis and haemostasis* **118**, 1535-1544, doi:10.1055/s-0038-1667014 (2018).
90 Lu, G., Lin, J. P., Curnutte, J. T. & Conley, P. B. Abstract: Effect of Andexanet-TFPI Interaction on in Vitro Thrombin Formation and Coagulation Markers in the TF-Pathway. *Blood* **130** (2017).
91 Qazi, U., Kolodziej, S. J., Gettins, P. G. & Stoops, J. K. The structure of the C949S mutant human alpha(2)-macroglobulin demonstrates the critical role of the internal thiol esters in its proteinase-entrapping structural transformation. *J Struct Biol* **131**, 19-26, doi:10.1006/jsbi.2000.4269 (2000).
92 Rehman, A. A., Ahsan, H. & Khan, F. H. alpha-2-Macroglobulin: a physiological guardian. *J Cell Physiol* **228**, 1665-1675, doi:10.1002/jcp.24266 (2013).
93 Jourdi, G. *et al.* Association rate constants rationalise the pharmacodynamics of apixaban and rivaroxaban. *Thrombosis and haemostasis* **114**, 78-86, doi:10.1160/TH14-10-0877 (2015).
94 Toso, R., Zhu, H. & Camire, R. M. The conformational switch from the factor X zymogen to protease state mediates exosite expression and prothrombinase assembly. *J Biol Chem* **283**, 18627-18635, doi:10.1074/jbc.M802205200 (2008).
95 Huber, R. & Bode, W. Structural Basis of the Activation and Action of Trypsin. *Accounts of Chemical Research* **11**, 114-122 (1978).
96 Bunce, M. W., Toso, R. & Camire, R. M. Zymogen-like factor Xa variants restore thrombin generation and effectively bypass the intrinsic pathway in vitro. *Blood* **117**, 290-298, doi:10.1182/blood-2010-08-300756 (2011).
97 Ivanciu, L. & Camire, R. M. Hemostatic agents of broad applicability produced by selective tuning of factor Xa zymogenicity. *Blood* **126**, 94-102, doi:10.1182/blood-2015-03-634329 (2015).
98 Ivanciu, L. *et al.* A zymogen-like factor Xa variant corrects the coagulation defect in hemophilia. *Nat Biotechnol* **29**, 1028-1033, doi:10.1038/nbt.1995 (2011).
99 Greene, L. A., Thalji, N. K., Raffini, L. J. & Camire, R. M. Abstract: Zymogen-like FXa Variant As a Short-Acting Warfarin Reversal Agent: Pre-Clinical Evaluation and Mechanism of Action. *Blood* **124** (2014).
100 Parng, C. *et al.* Preclinical Pharmacokinetics, Pharmacodynamics, Tissue Distribution, and Interspecies Scaling of Recombinant Human Coagulation Factor Xa(I16L). *J Pharm Sci* **106**, 2136-2143, doi:10.1016/j.xphs.2017.03.035 (2017).
101 Parsons-Rich, D. *et al.* Phase 1 dose-escalating study to evaluate the safety, pharmacokinetics, and pharmacodynamics of a recombinant factor Xa variant (FXa(I16L)). *J Thromb Haemost* **15**, 931-937, doi:10.1111/jth.13673 (2017).
102 Verhoef, D. *et al.* Engineered factor Xa variants retain procoagulant activity independent of direct factor Xa inhibitors. *Nat Commun* **8**, 528, doi:10.1038/s41467-017-00647-9 (2017).
103 Schreuder, M. *et al.* Abstract: Phe174-Mutated Human Factor X As Bypassing Agent to the Direct FXa Inhibitors. *Blood* **130** (2017).



Chapter 7

F174-Substituted Human Factor X as Bypassing Agent for Direct Factor Xa Inhibitors

Mark Schreuder, Georges Jourdi, Koen M. Visscher, Ka Lei Cheung, Geraldine Poenou, Daniel Verhoef, Stella Thomassen, Laura F.H. Janssen, Alain Stepanian, Tilman M. Hackeng, Pascale Gaussem, Pieter H. Reitsma, Daan P. Geerke, Virginie Siguret, Mettine H.A. Bos

Manuscript in Preparation



Abstract

Direct factor Xa inhibiting oral anticoagulants are widely used as alternatives to conventional vitamin K antagonists in the management of venous thromboembolism and nonvalvular atrial fibrillation. Unfortunately, bleeding-related adverse effects remain a major safety concern in clinical practice. In case of bleeding or emergency surgery, rapid-onset reversal agents may be required to counteract the anticoagulant activity and restore normal hemostasis. Here we show the ability of F174-substituted human factor X variants to rapidly restore thrombin generation in the presence of direct factor Xa inhibitors (apixaban, rivaroxaban, edoxaban). Their ability to bypass the anticoagulant effects relies on a decreased sensitivity for the direct factor Xa inhibitors due to a disrupted factor Xa-inhibitor binding stability. Furthermore, modification of F174 resulted in a partial loss of inhibition by tissue factor pathway inhibitor, adding to the procoagulant effect of F174-substituted factor X. Consequently, our F174-substituted factor X variant effectively counteracted the anticoagulant effects of apixaban and rivaxoraban in plasma of atrial fibrillation and venous thromboembolism patients. As such, these variants have the potential to serve as a rescue reversal strategy to overcome the effect of direct factor Xa inhibitors in case of life-threatening bleeding events or emergency surgical interventions.

Introduction

Thromboembolic events contribute significantly to morbidity with a global incidence rate of 2.000 cases per 100.000 and have been estimated to account for 1 in 4 deaths, representing the leading cause of mortality worldwide[1]. Individuals with a heightened tendency to form thrombi are at increased risk for ischemic heart disease and stroke, deep-vein thrombosis, pulmonary embolism, and other cardiovascular disorders. The direct oral anticoagulants (DOACs) targeting the key proteases factor Xa (FXa)[2-5] or thrombin[6] are widely used in the management and prevention of thrombotic events[7]. However, major bleeding complications are observed in 1-5% of the patients receiving DOACs[8-10]. Considering that these anticoagulants are prescribed to millions of people worldwide, anticoagulant-associated bleeding will remain a prominent clinical concern[11,12]. Life-threatening or uncontrollable bleeding requires the use of agents that enable rapid reversal of the anticoagulant activity[13,14]. With the direct FXa inhibitors representing the vast majority of DOAC prescription[15,16], access to an effective reversal agent for the direct FXa inhibitors is of critical importance. Currently, andexanet alfa (andexanet)[17], is the only US Food and Drug Administration and European Medicines Agency approved specific reversal agent for the direct FXa inhibitors. While clinical guidelines state that andexanet can be useful for the reversal of rivaroxaban and apixaban, the drug is not readily available at many centers and patient selection is critical[18-21]. In the absence of a specific reversal agent, the guidelines instead recommend administration of 4-factor prothrombin complex concentrate (PCC; 50U/kg) or activated PCC (50U/kg)[18-20].

The development of agents specific for FXa inhibitor reversal is mostly based on recombinant modification of FXa and its inactive zymogen FX[22]. Zymogen FX is composed of a heavy and light chain that are covalently linked via a disulfide bond. The N-terminal light chain consists of a gamma-carboxyglutamic acid (Gla) domain and two epidermal growth factor-like domains that are responsible for anionic phospholipid-binding and have been implicated in macromolecular interactions, respectively[23]. The C-terminal heavy chain comprises an activation peptide that is proteolytically removed upon activation and the serine protease domain that includes the active site, hallmarked by the catalytic triad residues His95, Asp102, and Ser195 (chymotrypsinogen numbering). FX is converted into FXa upon proteolytic activation by the extrinsic factor VIIa (FVIIa) and tissue factor (TF) complex or the intrinsic factor IXa (FIXa) and factor VIIIa (FVIIIa) complex. The newly-formed FXa assembles with its cofactor factor Va (FVa) into the prothrombinase complex that is responsible for the conversion of prothrombin to the active protease thrombin. The spatiotemporal assembly of this complex occurs exclusively on the surface of anionic membranes in the presence of calcium ions.

Downregulation of FXa activity proceeds via inactivation by the endogenous Kunitz-type inhibitor tissue factor pathway inhibitor (TFPI) and serpin antithrombin (AT).

At present, bioengineering of FXa has generated several FXa-based reversal agents that function either by sequestering or bypassing the direct FXa inhibitors. The currently approved antidote andexanet is a catalytically inactive Gla-domainless FXa that functions as a decoy by stoichiometric binding of the inhibitors in order to restore endogenous thrombin generation[24]. Yet, the active site and exosites remain available for potential interactions with pro- and anticoagulant proteins[25-28]. To prevent such macromolecular interactions, Jourdi *et al.* generated a Gla-domainless FXa sequestered by α_2-macroglobulin (GDFXa-α_2M), which retains its affinity for the direct FXa inhibitors[29]. Alternatively, several prohemostatic bypassing agents have been proposed such as a zymogen-like FXa variant (FXa-I16L) exhibiting impaired binding of FXa inhibitors[30,31]. In addition, we recently reported a FX variant comprising an extended 99-loop (FX-C) that sterically prevents interactions with the direct FXa inhibitors[32]. Herein, we showed that the S4 subsite region in the FXa active site, formed by residues Y99, F174, and W215, stabilizes the binding of the FXa inhibitor apixaban. We further demonstrated that disruption of the S4 subsite through alanine-substitution of Y99 and/or F174 resulted in a moderate loss of apixaban sensitivity[32].

In this study, we explored the ability of F174-substituted FX variants to support thrombin generation in the presence of the direct FXa inhibitors. Our data demonstrate that these FX variants exhibit a reduced sensitivity for the natural inhibitor TFPI and for the direct FXa inhibitors due to the destabilization of inhibitor binding. Furthermore, our FX variants were able to restore thrombin generation in plasma derived from atrial fibrillation and venous thrombosis patients treated with apixaban or rivaroxaban. As such, these FX variants have the potential to serve as an alternative therapeutic option to counteract bleeding induced by direct FXa inhibitors.

Material and Methods

Materials: Apixaban (Adooq Bioscience, Irvine, CA, USA) was dissolved to 5 mg/mL in vehicle (10% EtOH, 10% glycerol, 10% PEG400, 3.5% dextrose (v/v)). Rivaroxaban and edoxaban (10 mM in dimethyl sulfoxide (DMSO) were from Hölzel Diagnostika (Cologne, Germany). The peptidyl substrate methoxycarbonylcyclohexylglycylglycyl-Arg-pNA (SpecXa) was from Sekisui Diagnostics (Stamford, CT, USA), and N-α-benzyloxycarbonyl-D-Arg-Gly-Arg-pNA (S2765) and H-D-Phe-Pip-Arg-pNA (S2238) were from Instrumentation Laboratories (Bedford, MA, USA). All tissue culture reagents were from Life Technologies (Carlsbad, CA, USA). Calibrator and fluorescent substrate

(FluCa) were from Thrombinoscope (Maastricht, the Netherlands). FX-depleted human plasma, prothrombin time (PT) reagent (Neoplastine CI Plus), and activated partial thromboplastin time (aPTT) reagent (Triniclot) were from Stago (Asnière-Sur-Seine, France). Normal pooled plasma (NPP) was from Sanquin (Amsterdam, the Netherlands). Unfractionated heparin (UFH) was from LEO Pharma (Ballerup, Denmark). Small unilamellar phospholipid vesicles (PCPS) composed of 75% (wt/wt) hen egg L-phosphatidylcholine (PC) and 25% (wt/wt) porcine brain L-phosphatidylserine (PS) (Avanti Polar Lipids, Alabaster, AL, USA) were prepared and characterized as described[33]. All functional assays were performed in HEPES-buffered saline (HBS: 20 mM HEPES, 0.15 M NaCl, pH 7.5) supplemented with 5 mM $CaCl_2$, 0.1% PEG8000 filtered over an 0.2 µm filter (assay buffer).

Patient Plasma: Blood samples from 89 patients (male/female, 56/44%; mean age, 62 ± 8 years) treated with direct FXa inhibitors were collected from Cochin and Lariboisière University Hospitals (Assistance Publique – Hôpitaux de Paris (AP-HP), Paris, France). Forty-seven patients were treated for non-valvular atrial fibrillation (AF) (23 with apixaban; 24 with rivaroxaban) and 54 for venous thromboembolic (VTE) disease (27 with apixaban; 27 with rivaroxaban). Patients gave their written informed consent, and the investigation was conducted according to the Declaration of Helsinki. Blood was collected in 0.109 M buffered trisodium citrate (9:1 v/v) (Greiner Bio One, Courtaboeuf, France), and platelet-poor plasma (PPP) was prepared following two sequential centrifugation steps at 2500 g for 15 min at room temperature and stored at −80°C. Plasma was briefly thawed at 37°C immediately prior to analysis; all assays were performed in a blinded manner and according to the manufacturers' instructions. Plasma concentrations of direct FXa inhibitors were assessed using a specific anti-Xa assay (STA Liquid Anti-Xa, Stago) on STAR analysers using dedicated calibrators and controls with a lower limit of quantification of 18 ng/mL. Fibrinogen levels were measured by Clauss method (Dade Thrombin, Siemens, Munich, Germany). Prothrombin time results were expressed as international normalized ratio (INR).

Proteins: Human plasma-derived factor V (FV), FVIIa, FIXa, prothrombin, α-thrombin, AT, and the inhibitor dansylarginine-N-(3-ethyl-1,5-pentanediyl)amide (DAPA), RVV-X activator, and corn trypsin inhibitor (CTI) were from Haematologic Technologies (Essex Junction, VT). TFPI) was a generous gift from dr. Cornelis van 't Veer (Amsterdam UMC, The Netherlands). Inhibitory antibodies against the TFPI Kunitz 1 domain, the TFPI Kunitz 2 domain or a mix of anti-Kunitz 1 domain, anti-Kunitz domain 2, and anti-TFPI C-terminus were obtained from Sanquin (Amsterdam, the Netherlands). Human TF (Innovin) was obtained from Siemens (Newark, NY, USA), recombinant factor VIII (FVIII, NovoEight) was from NovoNordisk (Plainsboro, NJ, USA). Recombinant constitutively

active B-domainless human factor V (FV-810; hFV)[34] was large-scale expressed in BHK cells and conditioned media was collected and purified as described[32].

Construction and Purification of Factor X Variants: DNA constructs encoding FX variants comprising the Phe174Ala (FX-F174A), or Phe174Ser (FX-F174S) were prepared from the pCMV4 vector carrying wild-type (wt) human FX[35] by site-directed mutagenesis using the Q5-mutagenesis kit (New England Biolabs; Ipswich, MA, USA). Transfection of the plasmids encoding the FX constructs into HEK293 cells, the selection of stable clones, and the expression and purification of the FX variants were performed as described previously[32]. Partially purified FXa variants were obtained by expanding the stable cell line into three 175 cm^2 cell flasks and conditioning for 24 h in FX-specific expression media. Conditioned media was collected for three consecutive days, centrifuged at 4000 g, filtered over an 0.45 µm polyethersulfone membrane, and supplemented with 1mM benzamidine prior to storage at −20 °C. Following thawing of the conditioned media, the media was ultrafiltrated employing Amicon Ultra-15 centrifugal filter units with 30 kDa molecular weight cutoff to ~2 mL in HBS, 50% (v/v) glycerol, and stored at −20 °C.

Purification of Factor Xa: Purified recombinant FX (r-FX) was activated with RVV-X (1.15 µg/mL FX), applied to a benzamidine sepharose 6B column (GE Healthcare) equilibrated in HBS and eluted using HBS supplemented with 4 mM benzamidine. Fractions were analyzed for FXa activity employing peptidyl substrate hydrolysis (SpecXa). Fractions containing FXa activity were pooled and precipitated using ammonium sulphate (Sigma Aldrich, St Louis, Mo, USA). Precipitate was dissolved to ~3 mg/mL in HBS containing 50% (v/v) glycerol and stored at −20°C. Purified products were visualized by SDS-PAGE employing Coomassie Brilliant Blue staining.

Specific Factor X Activity: The specific extrinsic clotting activity was determined using a modified FX-specific PT-based assay. FX-depleted plasma (45 µL) was mixed with 5 µL FX sample, followed by a 60 s incubation period at 37°C. Coagulation was initiated with the addition of 50 µL PT reagent, and the coagulation time was monitored using a Start4 coagulation instrument (Stago). The specific intrinsic clotting activity was determined using a modified FX-specific aPTT-based assay. FX-depleted plasma (45 µL) was mixed with FX sample (5 µL) and aPTT reagent (50 µL), followed by an 180 s incubation period at 37°C. Coagulation was initiated with the addition of 50 µL of 25 mM CaCl2, upon which the coagulation time was monitored. Reference curves consisted of serial dilutions of NPP. Clotting times were converted to U/mg via the reference curves, assuming 1U FX equals 9 µg/mL.

Macromolecular Substrate Activation: Steady-state initial velocities of macromolecular substrate cleavage were determined discontinuously at 25°C in assay buffer as described[36,37]. Briefly, progress curves of prothrombin activation were obtained by incubating PCPS (50 μM), DAPA (10 μM), and prothrombin (1.4 μM) with recombinant FV-810 (20 nM), and the reaction was initiated with 0.1–0.4 nM of r-FXa, FXa-F174A or FXa-F174S upon which the rate of prothrombin conversion was measured. The kinetic parameters and equilibrium binding constants for prothrombin and cofactor Va (FV-810) were determined using increasing concentration of respective proteins[36]. Prothrombin conversion was assayed in the absence or presence of the direct FXa inhibitors apixaban, rivaroxaban or edoxaban (1 pM–100 μM) in order to determine IC_{50} concentrations for each prothrombinase-assembled FXa variant.

Inhibition by TFPI was assessed using 0-10 nM TFPI incubated with PCPS (50 μM), DAPA (10 μM), prothrombin (1.4 μM) and FV-810 (2 nM). Reactions were initiated with 0.05 nM FXa and at selected time points (5-60 min), aliquots were taken and quenched in HBS supplemented with 50 mM EDTA (EDTA-buffer). The rate of prothrombin conversion was measured as described above and corrected for substrate consumption according to a previously established model system[38]. Inhibitory constant values were determined using normalized thrombin values at 30 min and subsequent analysis by linear regression.

The rate of FX (9.1–2,500nM) activation by the TF-FVIIa complex (TF, 0.1 nM; FVIIa, 0.5 nM) was determined in the presence of PCPS (50 μM) in assay buffer at 25°C. At selected time points (0.5-4 min), aliquots were taken and quenched in EDTA-buffer. The amidolytic activity of each sample was determined by SpecXa conversion (250 μM) and the initial rates of chromogenic substrate hydrolysis were converted to nanomolar of product by reference to a standard curve. The apparent K_M and k_{cat} values for substrate activation were calculated from the Michaelis-Menten equation. For FX activation by the FVIIIa-FIXa complex (FVIIIa 5 nM; FIXa 0.5 nM; PCPS 50 μM) a similar approach was used. FVIII (NovoEight; 40nM) was activated by thrombin (100 nM) for 30 s at 25°C and the reaction was stopped by the addition of a 10-fold molar excess of hirudin. FXa formation was assessed as described above.

Chromogenic Substrate Hydrolysis. The kinetics of peptidyl substrate hydrolysis were measured in assay buffer using increasing concentrations of SpecXa (10–600 μM) or S2765 (1.2–1200 μM) and initiated with 5 nM of the FXa variants. Chromogenic conversion was assayed in the absence or presence of the direct FXa inhibitors apixaban, rivaroxaban or edoxaban (0.0001–100 μM; SpecXa 250 μM) in order to determine IC_{50} concentrations for each free FXa variant.

Inhibition of Factor Xa by Antithrombin. The rate of inactivation of FXa by AT was measured in assay buffer under pseudo-first-order rate conditions at ambient temperatures. Uncatalyzed reactions were prepared in assay buffer containing 0.1–0.8 µM AT and 7.5 nM FXa. At 0–110 min residual enzyme activity was determined with the addition of 250 µM SpecXa. Catalyzed reactions were prepared in assay buffer containing 0.5–6 mIE/mL UFH, 0.5 µM AT, initiated with 5nM FXa. At 0.5–10 min residual enzyme activity was determined with the addition of 250 µM SpecXa. The rate of AT inhibition was determined by fitting the obtained values to an exponential decay function (*k*1) and subsequent analysis by linear regression (*k*2) using GraphPad Prism software suite.

Calibrated Automated Thrombography. Thrombin generation curves were obtained by supplementing NPP with TF (2 or 6 pM), CTI (70 µg/mL), PCPS (20 µM), and 15–45 µg/mL FX variant in the absence or presence of the direct FXa inhibitors apixaban, rivaroxaban or edoxaban. Thrombin formation was initiated by addition of substrate buffer (FluCa) to the plasma. The final reaction volume was 120 µL, of which 80 µL was plasma. Thrombin formation was determined every 15 s for 30–60 min and corrected for the calibrator using Thrombinoscope software. The lag time, mean endogenous thrombin potential (ETP), thrombin peak height, and velocity index were calculated from at least three individual experiments.

Molecular Dynamics Simulations. Molecular Dynamics (MD) simulations of FXa-F174A and FXa-F174S in complex with apixaban were performed using GROMACS version 5.1.4[39], starting from the crystal structure with PDB ID 2P16[5] in which F174 was mutated *in silico* into alanine or serine, respectively. Starting from these structures, energy minimization and four independent MD simulations were performed per system (starting from different randomly assigned atomic velocities), using identical set-up and settings as previously described for FXa simulations[32]. Each production MD run as used for further analysis was 500 ns long, and root-mean-square deviations (RMSDs) during simulation of apixaban atomic positions were calculated after conformational fitting on the MD starting structure with respect to backbone atoms of the protein. Averaging over 10 ns intervals generated block-averaged time series for the analyzed data, and subsequently standard deviations were computed.

Statistical Analysis: All statistical analyses were computed using the GraphPad Prizm software. Kinetic data were analyzed by nonlinear regression using a three-parameter logistic function. Coefficients of determination (R^2) were given by linear regression. Parameters of calibrated automated thrombography in patient plasma and in the absence versus presence of TFPI-inhibiting antibodies were compared by one-way

ANOVA. Statistical significance was accepted for p-value of <0.05. All data are presented as mean ± 1 standard deviation and are the result of at least two-three experiments, unless stated otherwise.

Results

Characterization of F174-substituted Factor X Variants. Previously we reported that partially purified F174A-substituted FXa demonstrates a moderate loss of sensitivity for the direct FXa inhibitor apixaban (9-fold enhanced IC_{50}) while retaining procoagulant activity[32]. In addition to an alanine replacement, the S4 subsite Phe174 was also substituted by a similarly hydrophobic Ile residue and a hydrophilic Ser, thereby generating FX-F174I and FX-F174S, respectively. Following stable FX expression in HEK293 cells, initial analysis of partially purified FXa variants revealed a reduced apixaban inhibition (10-16-fold enhanced IC_{50}) (**Figure S1**), consistent with earlier observations[32]. Given that all F174-substituted variants displayed similar IC_{50} values for apixaban inhibition, we next subjected the FX variants with the most significant change in the S4 subsite (FX-F174A and FX-F174S) to further characterization following purification. SDS-PAGE analysis showed each FX(a) variant to migrate similar to recombinant wild-type FXa (r-FXa) **(Figures 1A,B; S2)**. Analysis of PT- or APTT-based fibrin clot formation initiated by the extrinsic **(Figure 1C)** or intrinsic coagulation pathway **(Figure 1D)** revealed FX-specific clotting activities similar to that of r-FX**,** indicating that substitution of F174 by either alanine or serine does not affect FXa procoagulant function.

F174 Substitution in Factor X Reduces the Sensitivity for the Direct Factor Xa Inhibitors. In concordance with a reduced apixaban inhibition in partially purified FXa variants **(Figure S1)**, assessing the inhibitory constant of the direct FXa inhibitors in a purified system demonstrated a ~2-5-fold reduced sensitivity for purified free FXa-F174 variants relative to r-FXa. Assembly of FXa-F174 variants into prothrombinase resulted in a 5-10-fold decreased sensitivity for inhibition by either apixaban, rivaroxaban or edoxaban compared to r-FXa **(Table 1)**. These results confirm our initial observations and suggest that F174-substituted FXa variants might support thrombin generation in the presence of the direct FXa inhibitors.

To determine the capacity of the purified F174-substituted FX variants to overcome inhibition by the direct FXa inhibitors, their thrombin-forming potential was assessed using a high TF-trigger (6 pM) resulting in direct FX activation by TF-FVIIa. Following supplementation of NPP with r-FX at three-fold the FX plasma concentration (30 µg/mL), apixaban dose-dependently decreased thrombin peak with half-maximum inhibition

at 0.1μM **(Figure 2A; Table S1).** The latter was markedly higher than the values of free FXa inhibition in a purified system **(Table 2)**[5], which may be due to the plasma setting and supraphysiologic amounts of FX in this system. Conversely, supplementation with FX-F174A or FX-F174S resulted in a 15-35-fold reduction in apixaban sensitivity relative to r-FX **(Figure 2A; Table S1)**. In a similar fashion, addition of F174-substituted FX variants demonstrated a 10-15-fold reduced sensitivity to inhibition by rivaroxaban or edoxaban compared with r-FX **(Figure 2B,C; Table S1)**. Next, the ability of the FX variants to support thrombin generation was explored under conditions when FX activation is mainly driven by FIXa[40,41], via the so-called Josso loop using a low amount of TF (2 pM). Similar to previous observations, supplementation with either FX-F174A or FX-F174S demonstrated a 10-40-fold reduced sensitivity for apixaban, rivaroxaban, or edoxaban relative to r-FX **(Figure S3; Table S1)**.

S4 Subsite Displacement of Apixaban in Complex with F174-substituted Factor Xa. To gain insight into the molecular mechanism underpinning the reduced sensitivity of the F174-substituted FXa variants for the FXa inhibitors, we performed MD simulations of the FXa variants in complex with apixaban. The F174A and F174S substitutions were modelled into apixaban-bound FXa (PDB ID 2P16)[5], and four 500 ns MD simulations of each FXa–apixaban complex were independently performed. Each simulation was initiated from an identical conformation but with different atomic starting velocities. As we previously described[32], MD simulations with wild-type FXa produced little if any shifts in apixaban positioning, which is indicative of a high binding stability of apixaban in the FXa active site **(Figure 3A)**. In contrast, substantial movement of the apixaban molecule was observed in the MD trajectories of at least two out of the four simulations of the FXa-F174A and FXa-F174S apixaban complexes **(Figure 3B,C)**. This was reflected by root-mean-square deviation (RMSD) values of >0.1 nm, as well as by displacement of apixaban from either the S4 subsite alone or in combination with displacement from the S1 subsite. As such, these findings indicate an enhanced mobility of apixaban in the FXa active site and a loss of apixaban binding stability following F174-substitution.

Reduced TFPI Inhibition of F174-substituted Factor Xa Augments the Direct Factor Xa Inhibitor Bypassing Effect. We next assessed the kinetic parameters of the FXa-F174 variants to examine the effects of F174 substitution on the FXa active site. Evaluation of the ability of the FXa variants to hydrolyze the FXa-specific chromogenic substrates SpecXa and S2765 revealed no differences in k_{cat} relative to r-FXa **(Table 2)**. Conversely, the binding affinities of both substrates were significantly altered in the FXa-F174 variants **(Table 2)**, indicative of a modified substrate binding cleft. This would imply that either the chromogenic substrates engage the FXa S4 subsite[42] or that F174 substitution induces conformational changes in the substrate binding

region. Importantly, the kinetic parameters of prothrombin conversion by the FXa-F174 variants, as well as the apparent binding affinity for the FVa-like cofactor FV-810, were similar to those of r-FXa **(Table 2)**. This demonstrates that F174 modification does not significantly impact the assembly of the prothrombinase complex or the catalytic efficiency of FXa's natural substrate prothrombin.

To examine the effects of F174 substitution on FXa inhibition, we assessed the second-order rate constants of the natural active site inhibitor AT. Inhibition of FXa-F174 variants proceeded at an identical rate relative to r-FXa in the absence or presence of UFH **(Table 1**), consistent with previous reports[32,43,44]. These observations might reflect the interaction of AT with the FXa S1 subsite rather than the S4 subsite, as shown by X-ray structures[45,46]. On the other hand, assessment of prothrombinase-assembled FXa inhibition by the natural active site inhibitor TFPI revealed that FXa-F174A and FXa-F174S displayed a 1.3- and 4.5-fold reduced TFPI sensitivity relative to r-FXa, respectively **(Figure 4, Table 1)**. To gain more insight in the TFPI resistance, we next explored the thrombin-forming potential of FX-F174 variants using calibrated automated thrombography in plasma supplemented with antibodies that specifically block the function of individual TFPI domains. In the absence of TFPI antibodies, FX-F174 variants displayed a two-fold increased thrombin peak height relative to r-FX **(Figure S4)**. In contrast, similar thrombin peak heights were observed in the presence of TFPI-inhibiting antibodies **(Figure S4)**. This indicates that the initial increased thrombin-forming potential of FX-F174 variants is induced by a partial loss of inhibition by TFPI. As such, these results suggest an additional mode of action by which the F174-substituted FX variants bypass the direct FXa inhibitors.

F174-substituted Factor X Variants Bypass the Direct FXa Inhibitors and Restore Thrombin Generation. The reduced sensitivity for the direct FXa inhibitors and TFPI **(Table 1, S1)** might enable FX-F174 variants to reverse the anticoagulant effect of the direct FXa inhibitors. We therefore studied the ability of our FX-F174 variants to overcome therapeutic peak inhibitor levels[47-49] using calibrated automated thrombography in response to a high TF-trigger (6 pM). Following supplementation of NPP with apixaban, rivaroxaban, or edoxaban (1 μM), r-FX (60 μg/mL) only minimally improved the thrombin generation (up to 20% of NPP peak height; **Figure 5A**). In contrast, supplementation with 30 μg/mL FX-F174A or FX-F174S fully restored the thrombin generation in the presence of apixaban, whereas 15 μg/mL improved the thrombin peak height to 75% of NPP **(Figure 5B)**. Similarly, the anticoagulant activity of rivaroxaban was completely reversed by the FX-F174 variants **(Figure 5C)** and improved up to 60-75% of NPP in edoxaban-spiked plasma **(Figure 5D)**. This is consistent with the initially observed ~11-fold increase in IC_{50} for edoxaban compared to the 15-35-fold increase for apixaban or

rivaroxaban **(Table S1)**. Of note, supplementation with the FX-F174 variants prolonged both the lag time and time to peak by 1.3-2-fold in the presence but not in the absence of an inhibitor **(Figure S5)**. However, this delay in thrombin generation was not induced by a diminished FX activation considering the steady-state kinetics for activation by the intrinsic or extrinsic tenase complexes were unperturbed **(Table S2)**. Furthermore, no delay in the activation of FV was observed since FXa-F174A activated FV in an identical manner to r-FXa **(Figure S6)**. In addition, assessment of the thrombin-forming potential under conditions of a limited TF-trigger (2 pM) revealed that the anticoagulant activity of the direct FXa inhibitors was largely reversed via supplementation of 15-30 µg/mL FX-F174A or FX-F174S **(Figure S7)**. Consistent with previous results in the presence of a high TF-trigger, the FX-F174 variants maintained an increased lag time relative to NPP in the absence of an inhibitor.

F174-substituted Factor X Reverses the Anticoagulant Activity of Apixaban and Rivaroxaban in Atrial Fibrillation and Venous Thromboembolism Patient Plasma. Since both FX-F174 variants behaved in a similar fashion, we selected FX-F174A for assessment in patient plasma. The ability of FX-F174A to bypass the direct FXa inhibitors was validated in plasma derived from AF and VTE patients who were treated with apixaban or rivaroxaban **(Table S3)** using calibrated automated thrombography in response to a high TF-trigger (6 pM). Assessment of the thrombin-forming potential demonstrated that supplementation of patient plasma with FX-F174A increased the thrombin peak height in all individual patient samples **(Figure 6A,B)**. In AF patient plasma, the thrombin peak height was increased to near-NPP conditions (290-330 nM). In addition to the thrombin peak height, AF and VTE patient plasma displayed a significant prolonged lag time relative to NPP **(Figure 6C)**. Supplementation with FX-F174A markedly shortened the lag time in all individual patients samples **(Figures 6C,D)**. Additional assessment revealed that FX-F174A reversed the anticoagulant effect on the thrombin generation velocity in similar fashion as the thrombin peak height and lag time **(Figures S8A,B)**. In contrast, the ETP in AF and VTE patient plasma was only modestly reduced in the absence of FX-F174A relative to NPP **(Figures S8C,D)** as a result of the inhibitor-induced extension of the thrombin generation curves over time. Still, FX-F174A significantly elevated the ETP in all patient groups. As such, these results demonstrate that F174-substituted FX variants have the ability to reverse the anticoagulant activity of the direct FXa inhibitors in patient plasma.

Discussion

In this study, we present FX variants that could act as prohemostatic bypassing agents by initiating coagulation in the presence of direct FXa inhibitors. We showed that a FX variant comprising a single substitution in the S4 subsite effectively counteracted the anticoagulant effects of apixaban or rivaroxaban in plasma from AF and VTE patients. While FX-F174A is inhibited by rivaroxaban and apixaban to some extent (**Figure S9**), FX-F174A is nonetheless capable of promoting thrombin formation in the presence of therapeutic concentrations of FXa inhibitor. Unfortunately, we were unable to obtain plasma samples from the same individual patients before treatment initiation. As thrombin generation profiles of individual plasmas can vary substantially, such samples would provide valuable information on the level of anticoagulant reversal in these patients [50]. Nevertheless, our FX variant successfully restored the thrombin-forming potential within the therapeutically useful inhibitor range (>100 nM), at which patients are likely at an increased risk for bleeding[49].

In the presence of therapeutic peak inhibitor levels we were able to restore thrombin generation using 15-45 µg/mL of our F174-substituted FX variants. The increased amounts of FX-F174 variant that are required to bypass the direct FXa inhibitors relative to the FX plasma concentration[51] could reflect the competition for activation by the intrinsic and extrinsic tenase complexes with endogenous FX. Furthermore, FX-F174 variants displayed a 1.3-2-fold increase in lag time compared to r-FX. However, the kinetic constants for the activation of FX by the intrinsic or extrinsic tenase complexes were unperturbed. Moreover, a delay in the FXa-mediated activation of FV is known to specifically prolong the thrombin generation lag time[52], yet the activation of FV was identical between FXa-F174A and r-FXa. An alternative explanation might be a delay in FV activation in the presence of the direct FXa inhibitors. The small amounts of FXa that are being generated during the initial phase of coagulation are likely targeted by direct FXa inhibitors. Minor differences in the affinity of these inhibitors for FXa might therefore induce the observed inhibitor-dependent prolongation in lag time.

Interestingly, we observed a reduced sensitivity of FXa-F174 variants for the natural inhibitor TFPI. Previous studies have shown that the inhibition or sequestration of TFPI could restore hemostasis in hemophilic plasma and patients[25,26,53-55], thus providing evidence for an additional mode of action by which our FX-F174 variants are able to bypass direct FXa inhibitors. Despite the three-fold reduction in TFPI sensitivity of FXa-F174S relative to FXa-F174A **(Figures 4,S4, Table 2)**, their minor functional differences might be explained by the relatively low plasma concentration of free TFPIα (~0.3nM)[56,57]. The partial resistance for TFPI might also explain the augmented IC_{50} values of FX-F174

variants for the direct FXa inhibitors observed in plasma relative to the inhibition of free or prothrombinase-assembled FXa. Collectively, our findings reveal that FX-F174 variants bypass direct FXa inhibitors via an unique mechanism compared to previously described reversal agents and indicate that modulation of FXa inhibition by TFPI might be a viable strategy to overcome the anticoagulant effects of direct FXa inhibitors.

To get further insights into the mechanistic principles of our FX-F174 variants, we examined the impaired FXa-apixaban interaction using MD simulations. Although the active site of FXa is able to accommodate the inhibitor, the increased mobility of apixaban following F174 substitution indicates a loss of binding stability. Previous studies suggested an important role for the S4 subsite in the stabilization of apixaban binding[5,32]. In line with our MD simulations the S4 subsite is confirmed to be less compact due to the substitution of the large aromatic phenylalanine by the relatively small alanine or serine **(Figure S10)**, resulting in decreased binding stability. Interestingly, Qu *et al.* recently performed similar MD simulations (with lengths of 200-500 ns) using a modelled FXa-F174A variant based on the FXa-rivaroxaban X-ray structure[58]. In contrast to our results using apixaban, the slightly smaller and more flexible rivaroxaban ligand was completely released into the solvent within 100 ns in three out of five simulations. In the two other trajectories, the P_4 moiety of rivaroxaban shifted into the S1′ pocket between residues F41, Q61, and Q192. These differential effects suggest that the binding stability of rivaroxaban is even more impacted upon F174 substitution compared to apixaban. Substitution of F174 for alanine or serine induces minor conformational modifications in the FXa active site, as shown by the reduced catalytic activity towards FXa-specific chromogenic substrates. However, plasma clotting and kinetic assays demonstrated that the conversion of the natural substrate prothrombin remained unaltered, suggesting that prothrombin does not engage in productive interactions with the S4 subsite of FXa. Alternatively, these results might suggest that exosites in FXa and prothrombin drive the proteolytic cleavage at the prothrombin activation residues R271 and R320[59,60]. Although our data does not provide any indication, it should be noted that the FXa-F174 variants might have potential off-target interactions that have not been uncovered by the *in vitro* experimental systems.

A limitation of our approach may be the use of a recombinant protein variant that could elicit an immunogenic response, thereby limiting the efficacy of repeated use. Since our FX variants comprise a single amino acid substitution, the risk for immunogenicity might be minimal. Thus far, neutralizing antibody responses against andexanet alfa have not been reported and neither have antibodies with cross-reactivity to factor X(a) been detected[17,61]. Non-neutralizing antibodies have been developed albeit with generally low antibody titers[61]. Importantly, only a few cases of patients with acquired inhibitors

against FX have been reported[62], suggesting that either FX or its derived variants have little immunogenic potential. It is also important to note that prohemostatic bypassing agents may significantly increase the risk for thrombotic complications and therefore require intensive evaluation in clinical practice. For safety purposes, we employed F174-substituted FX variants in an inactive zymogen form, which would prevent potential macromolecular interactions. Upon the initiation of secondary hemostasis, FX-F174 variants are activated through the intrinsic and extrinsic pathways in a similar manner as endogenous FX. As such, major disturbances that could fail to stop bleeding or otherwise induce pathological thrombosis might be prevented.

In conclusion, our findings show that via a single residue substitution we have created a FX variant that exhibits a decreased sensitivity for direct FXa inhibitors and is partially resistant to inhibition by TFPI. We further demonstrated the ability of F174-substituted FX variants to reverse the anticoagulant activity of apixaban and rivaroxaban in plasma of AF and VTE patients. As such, these variants have the potential to serve as a rapid-onset prohemostatic bypassing strategy to counteract life-threatening bleeding complications as a result of direct FXa inhibitors.

Acknowledgements

This work was financially supported by the Bayer Hemophilia Awards Program (Special Project Award) and Landsteiner Foundation for Blood Transfusion (LSBR, grant. no. 1451). The funding agencies had no role in the preparation, review, or approval of the manuscript.

Figures

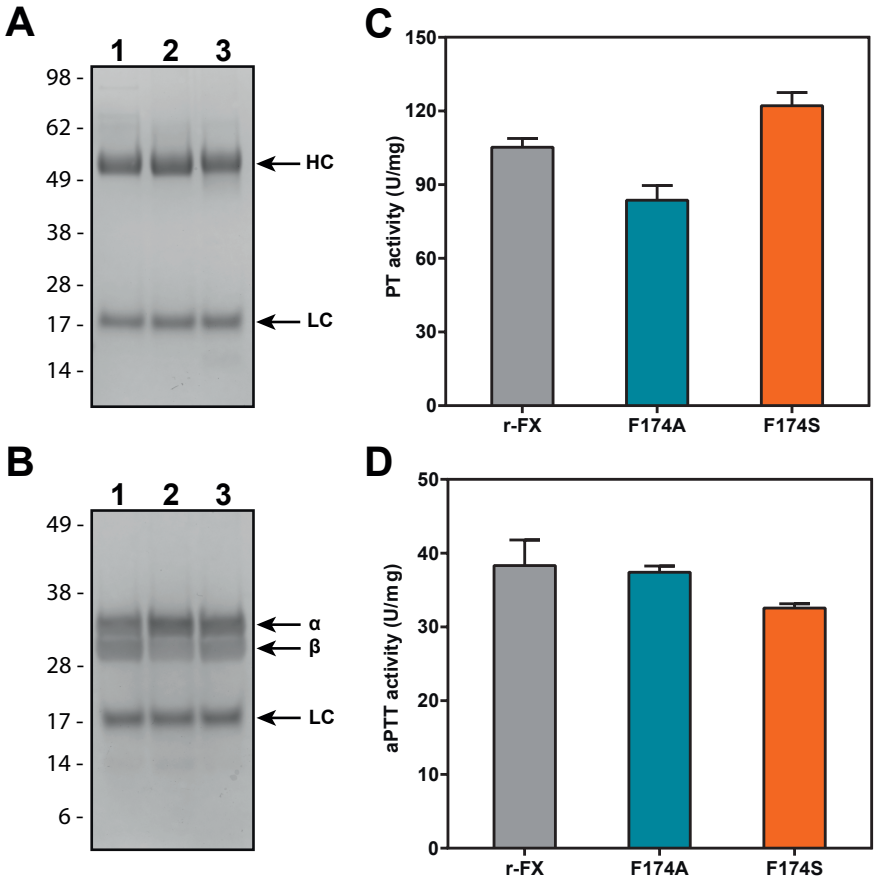


Figure 1. Characterization of F174-substituted factor X(a) variants. (A-B) SDS-PAGE analysis of purified recombinant FX **(A)** or FXa **(B)** variants (2 µg/lane) under reducing conditions and visualized by staining with Coomassie Brilliant Blue R-250. Lane 1, wild-type FX(a); lane 2, FX(a)-F174A; lane 3, FX(a)-F174S. The protein bands corresponding to the FX heavy chain (HC), the heavy chain derived from α or β FXa (α or β), the FX(a) light chain (LC), and the apparent molecular weights (kDa) of the standards are indicated. The purified FXa products migrate as a mixture of α and β FXa, with the latter resulting from autoproteolytic excision of the C-terminal portion of FXa-α (residues 436–447). Both α and β FXa isoforms are functionally similar with respect to prothrombinase assembly, prothrombin activation, antithrombin recognition, and peptidyl substrate conversion[63]. **(C-D)** The specific clotting activity of wild-type FX (r-FX), FX-F174A (F174A), or FX-F174S (F174S) initiated by the extrinsic **(C)** or intrinsic **(D)** pathway using a prothrombin time (PT)-based or activated partial thromboplastin time (aPTT)-based assay as described in 'Materials and Methods'. Mean values are given ± 1 S.D. Data are representative of three independent experiments.

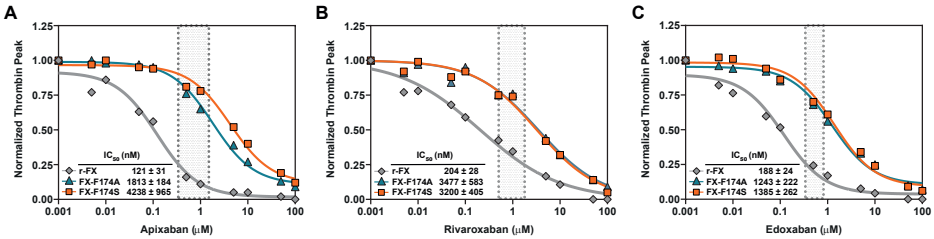


Figure 2. F174-substituted factor X variants facilitate thrombin generation in the presence of the direct factor Xa inhibitors. Thrombin generation was measured for 60 min at 37°C in normal pooled plasma supplemented with 30 µg/mL of r-FX (*grey diamonds*), FX-F174A (*blue triangles),* or FX-F174S (*orange squares*) and increasing concentrations (1 nM-100 µM) of apixaban **(A)**, rivaroxaban **(B),** or edoxaban **(C)**. Thrombin formation was triggered by the addition of 6 pM TF in the presence of 20 µM PCPS and initiated with $CaCl_2$ and a thrombin fluorogenic substrate as detailed in 'Materials and Methods'. The thrombin peak height was normalized to the peak height in the absence of inhibitor, and the lines were drawn by fitting the data to a three-parameter logistic function upon which the IC_{50} ± 1 standard deviation of the induced fit were obtained (**Table S1**), which are shown in the insert. The grey dotted areas represent therapeutic peak inhibitor levels (apixaban, 0.35-1.5 µM; rivaroxaban, 0.5-2 µM; edoxaban, 0.25-0.9 µM). Data are representative of three independent experiments.

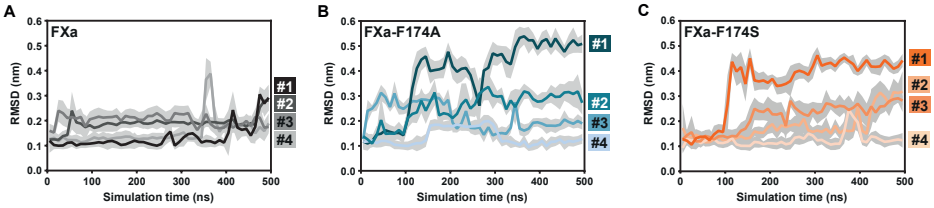


Figure 3. Molecular Dynamics of apixaban bound to factor Xa variants. MD simulations were performed using the X-ray structure of apixaban-bound factor Xa (PDB ID: 2P16)[5]. **(A, data from reference[32])**. Substitutions of phenylalanine 174 were modelled in order to generate FXa-F174A **(B)** or FXa-F174S **(C)** and were used here for respective simulations. Root-mean-square deviations (RMSDs, with respect to 2P16) of atomic positions of the apixaban ligand during four independent 500 ns simulations are presented as block averages over 10 ns intervals (#1-#4). The corresponding single standard deviation intervals are indicated (*gray density*).

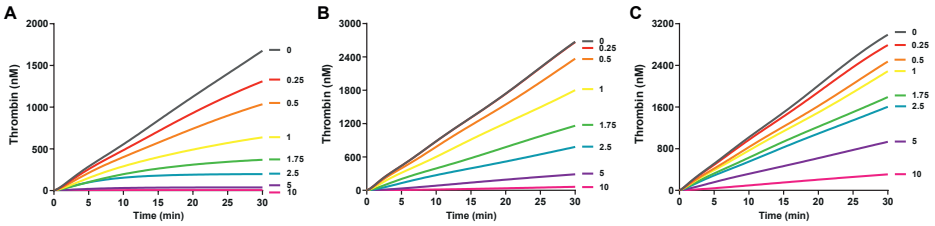


Figure 4. Inhibition of factor Xa variants by tissue factor pathway inhibitor (TFPI). The inhibition of factor Xa by TFPI was assessed by measuring the prothrombinase-dependent conversion of prothrombin. Reaction mixtures containing 1.4 μM prothrombin, 2 nM FV-810, 50 μM PCPS, 10 μM DAPA were initiated with 0.05 nM r-FXa **(A)**, FXa-F174A **(B)**, or FXa-F174S **(C)** in the presence of 0-10 nM TFPI. At selected time intervals, samples were removed and thrombin formation was assessed by S2238 (250 μM) conversion. The data was corrected for substrate consumption as described in 'Materials and Methods'. The data sets are representatives of two independent experiments.

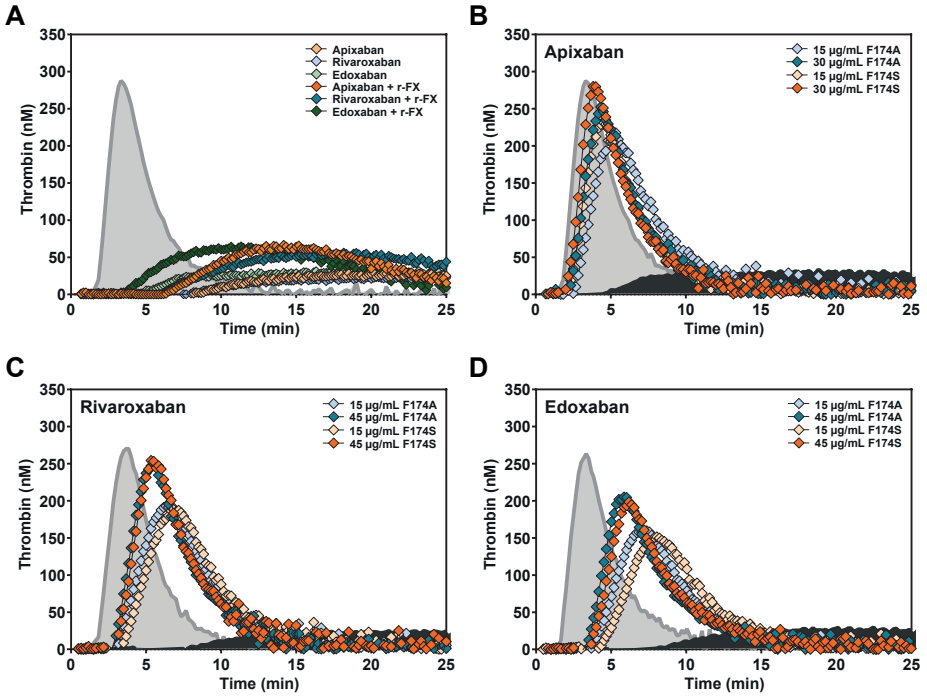


Figure 5. F174-substituted factor X variants restore thrombin generation in inhibitor-spiked plasma. Thrombin generation was measured for 60 min at 37°C in normal pooled plasma (NPP) supplemented with **(A)** 1 µM apixaban, rivaroxaban, or edoxaban in the absence (*yellow, light blue, or light green diamonds, respectively*) or with addition of 60 µg/mL r-FX (orange, dark blue or dark green, respectively), **(B)** 15-30 µg/mL FX-F174A (*light blue-dark blue diamonds*) or FX-F174S (*yellow-orange diamonds*) and apixaban (1 µM), or **(C-D)** 15-45 µg/mL FX-F174A (*light blue-dark blue diamonds*) or FX-F174S (*yellow-orange diamonds*) and 1 µM rivaroxaban **(C)** or edoxaban **(D)**. Thrombin formation was triggered by the addition of 6 pM TF in the presence of 20 µM PCPS and initiated with $CaCl_2$ and a thrombin fluorogenic substrate as detailed in 'Materials and Methods'. The thrombin generation curves of NPP in the absence **(A-D)** (light gray area under the curve) or presence **(B-D)** (dark gray area under the curve) of the inhibitors are shown. Data sets are representatives of three independent experiments.

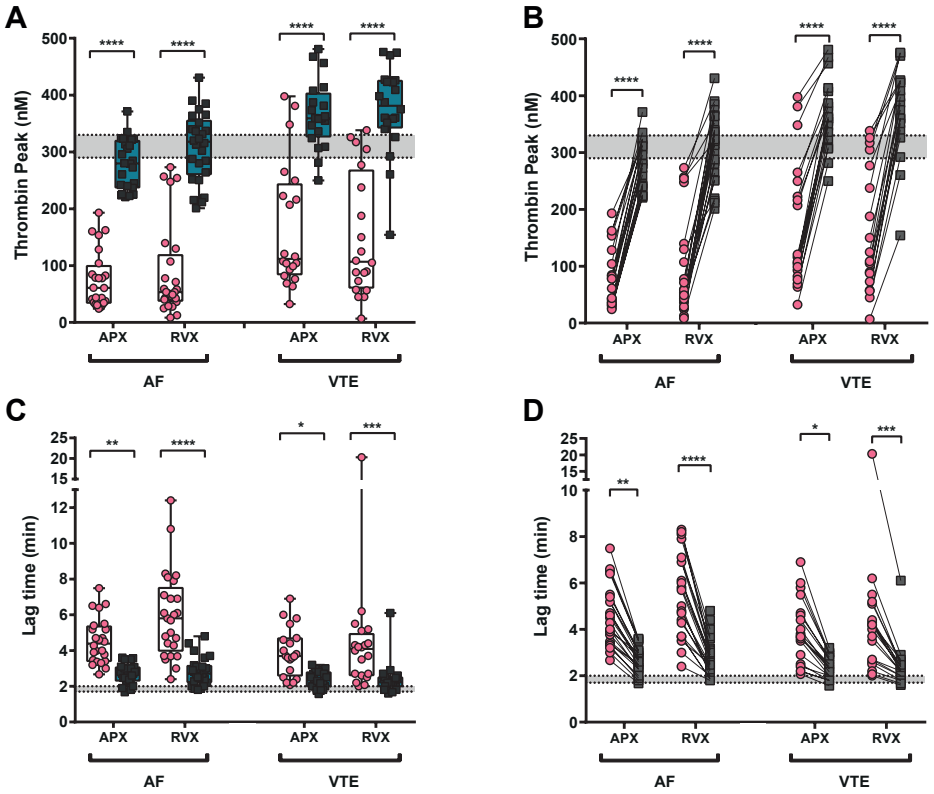


Figure 6. Reversal of the anticoagulant activity of apixaban or rivaroxaban in atrial fibrillation and venous thromboembolism patient plasma. Thrombin generation was measured for 60 min at 37°C in plasma from atrial fibrillation (AF) or venous thromboembolism (VTE) patients treated with apixaban (APX) or rivaroxaban (RVX) in the absence (*pink dots*) or supplemented (*grey squares*) with 30 µg/mL FX-F174A. Thrombin formation was triggered by the addition of 6 pM TF in the presence of 20 µM PCPS and initiated with CaCl2 and a thrombin fluorogenic substrate as detailed in 'Materials and Methods'. The thrombin peak height **(A-B)** and lag time **(C-D)** are shown. The thrombin peak height and lag time of individual patient plasma in the absence or supplemented with FX-F174A are shown by connected lines **(B, D)**. Bars represent the mean, grey dotted areas represent NPP values (n=13; thrombin peak, 290-330 nM; lag time, 1.7-2 min). *p<0.05, **p<0.01, ***p<0.001, ****p<0.0001 according one-way ANOVA. Each data point represents a single measurement performed for each patient sample.

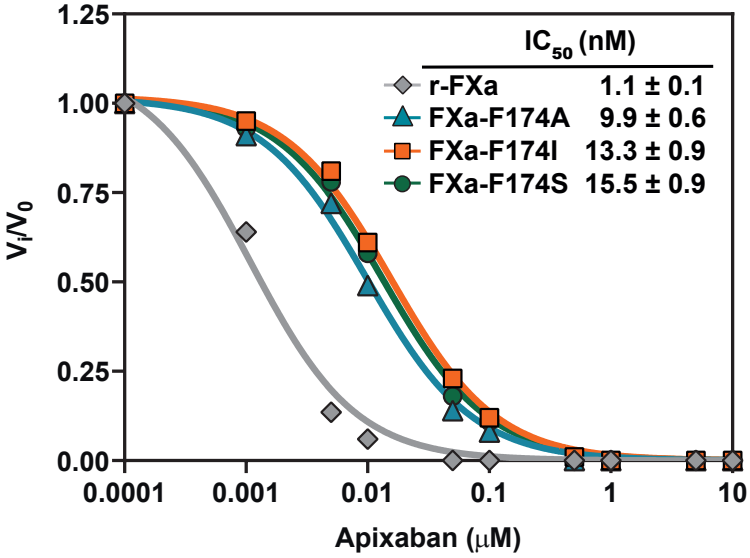
	Apixaban[a] IC_{50} (nM)	Rivaroxaban[a] IC_{50} (nM)	Edoxaban[a] IC_{50} (nM)	Apixaban[b] IC_{50} (nM)	Rivaroxaban[b] IC_{50} (nM)	Edoxaban[b] IC_{50} (nM)	Antithrombin[a] $k2$, uncatalyzed (M^{-1} S^{-1} x 10^3)	Antithrombin[a] $k2$, UFH (M^{-1} S^{-1} x 10^6)	TFPI[b] K_i (nM)
r-FXa	5.9 ± 0.3	2.5 ± 0.1	7.9 ± 0.2	9.2 ± 1.0	1.6 ± 0.2	5.3 ± 0.6	5.3 ± 0.1	2.0 ± 0.2	0.8 ± 0.04
FXa-F174A	24.6 ± 1.5	9.6 ± 0.3	16.5 ± 0.4	57.5 ± 7.4	12.1 ± 1.9	40.6 ± 4.3	4.7 ± 0.5	2.6 ± 0.1	1.3 ± 0.25
FXa-F174S	20.9 ± 1.1	14.3 ± 0.2	28.5 ± 0.4	55.6 ± 5.4	16.2 ± 1.7	24.2 ± 2.6	5.0 ± 0.5	3.8 ± 0.2	3.3 ± 0.48

Table 1. Kinetic constants for inhibition of free or prothrombinase-assembled factor Xa. The kinetic constants for free[a] or prothrombinase-assembled[b] factor Xa were obtained as described in 'Materials and Methods'. Fitted values ± 1 standard deviation of the induced fit are the means of two to three independent experiments.

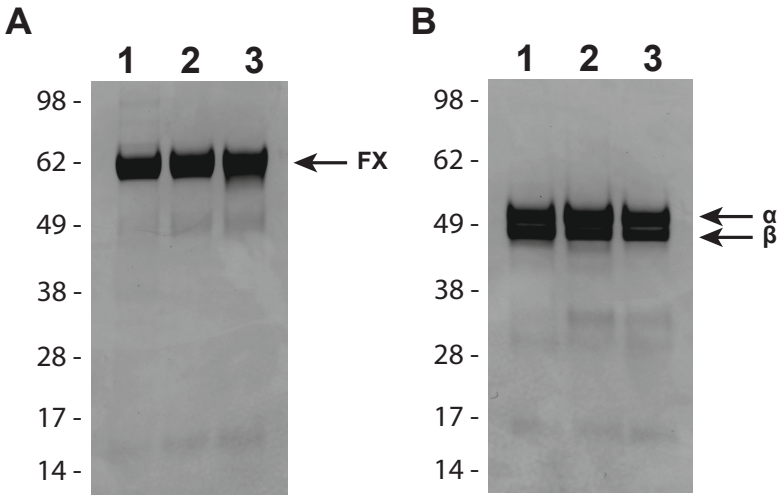
	SpecXa[1] K_m (μM)	SpecXa[1] k_{cat} (min^{-1})	S2765[1] K_m (μM)	S2765[1] k_{cat} (min^{-1})	Prothrombin[2] K_m (μM)	Prothrombin[2] k_{cat} (min^{-1})	Cofactor Va[2] $K_{d,\ app}$ (nM)
r-FXa	113 ± 9	23.9 ± 0.6	85 ± 10	34.3 ± 1.1	0.52 ± 0.10	960 ± 83	0.8 ± 0.2
FXa-F174A	251 ± 7	25.8 ± 0.3	360 ± 33	32.6 ± 1.2	0.70 ± 0.23	1041 ± 163	1.2 ± 0.1
FXa-F174S	186 ± 9	30.6 ± 0.6	217 ± 17	21.9 ± 0.6	0.69 ± 0.08	1152 ± 73	0.9 ± 0.2

Table 2. Kinetic parameters for peptidyl substrate and macromolecular conversion. The kinetic constants for free[(1)] or prothrombinase-assembled[(2)] factor Xa were obtained as described in 'Materials and Methods'. Fitted values ± 1 standard deviation of the induced fit are the means of two to three independent experiments.

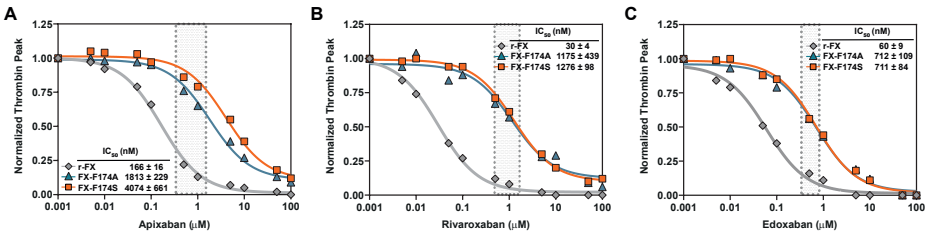
Supplementary Figures and Tables



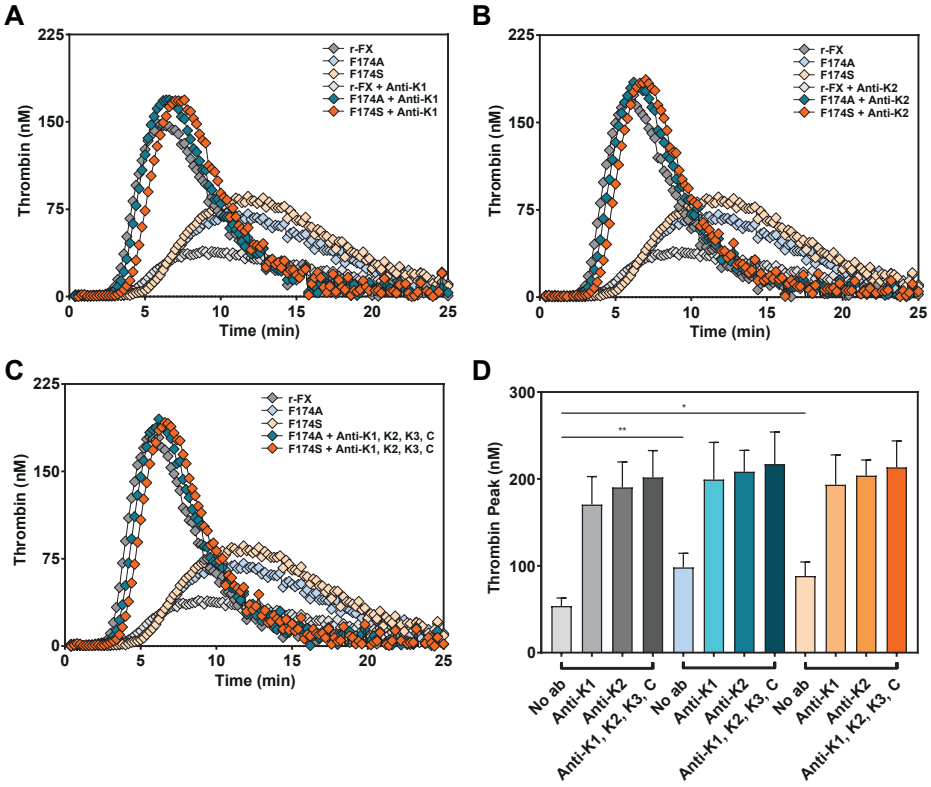
Supplementary figure 1. Apixaban inhibition of partially purified factor Xa variants. The rate of peptidyl substrate conversion (250 μM SpecXa) by 5 nM of RVV-X-activated r-FX (*grey diamonds*), FX-F174A (*blue triangles*), FX-F174I (*green circles*), or FX-F174S (*orange squares*) was determined in the absence (V_0) or presence (V_i) of increasing apixaban concentrations (0.1 nM–10 μM). The lines were drawn by fitting the data to a three-parameter logistic function, and the fitted parameters for IC_{50} ± 1 standard deviation of the induced fit are shown in the inset. Data are the means of two independent experiments.



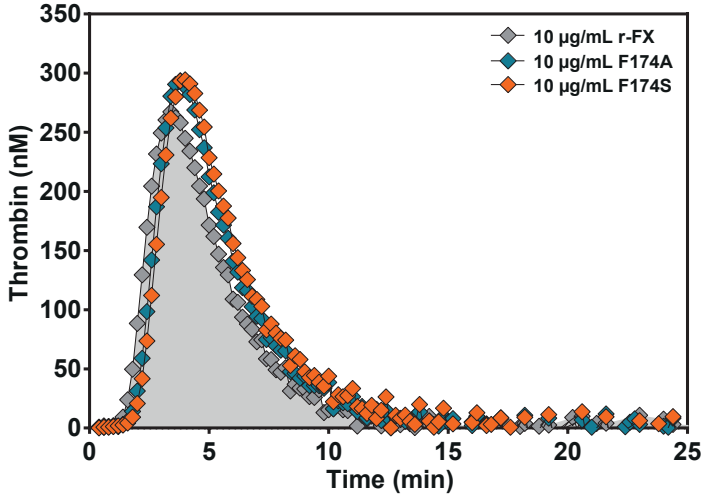
Supplementary figure 2. SDS-PAGE analysis of F174-substituted factor X(a) variants. SDS-PAGE analysis of purified recombinant FX **(A)** or FXa **(B)** variants (2 µg/lane) under non-reducing conditions and visualized by staining with Coomassie Brilliant Blue R-250. Lane 1, wild-type FX(a); lane 2, FX(a)-F174A; lane 3, FX(a)-F174S. The protein bands corresponding to full-length FX (FX), the full length α or β FXa (α or β), and the apparent molecular weights (kDa) of the standards are indicated. The purified FXa products migrate as a mixture of α and β FXa, with the latter resulting from autoproteolytic excision of the C-terminal portion of FXa-α (residues 436–447). Both α and β FXa isoforms are functionally similar with respect to prothrombinase assembly, prothrombin activation, antithrombin recognition, and peptidyl substrate conversion[63].



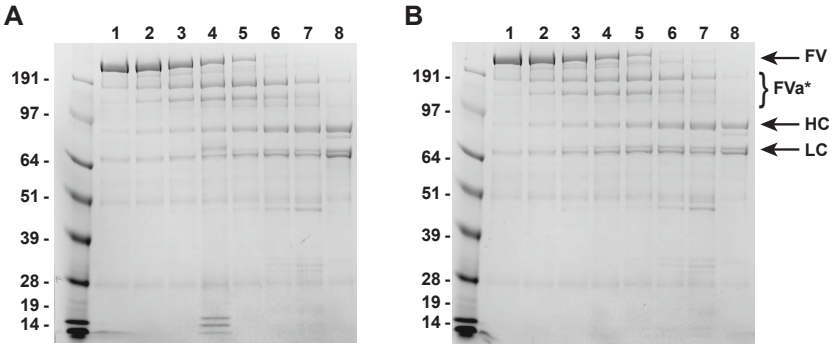
Supplementary figure 3. F174-substituted factor X variants facilitate thrombin generation in the presence of the direct factor Xa inhibitors following a low TF-trigger. (A-C) Thrombin generation was measured for 60 min at 37°C in normal pooled plasma supplemented with 30 µg/mL of r-FX (*grey diamonds*), FX-F174A (*blue triangles)* or FX-F174S (*orange squares*) and increasing concentrations (0.001-100 µM) of apixaban **(B)**, rivaroxaban **(C)** or edoxaban **(D)**. Thrombin formation was triggered by the addition of 2 pM TF in the presence of 20 µM PCPS and initiated with $CaCl_2$ and a thrombin fluorogenic substrate as detailed in 'Materials and Methods'. The thrombin peak height was normalized to the peak height in the absence of inhibitor, and the lines were drawn by fitting the data to a three-parameter logistic function upon which the IC_{50} ± 1 standard deviation of the induced fit were obtained (**Table S1**), which are shown in the insert. The grey dotted areas represent therapeutic peak inhibitor levels (apixaban, 0.35-1.5 µM; rivaroxaban, 0.5-2 µM; edoxaban, 0.25-0.9 µM). Data are representative of three independent experiments.



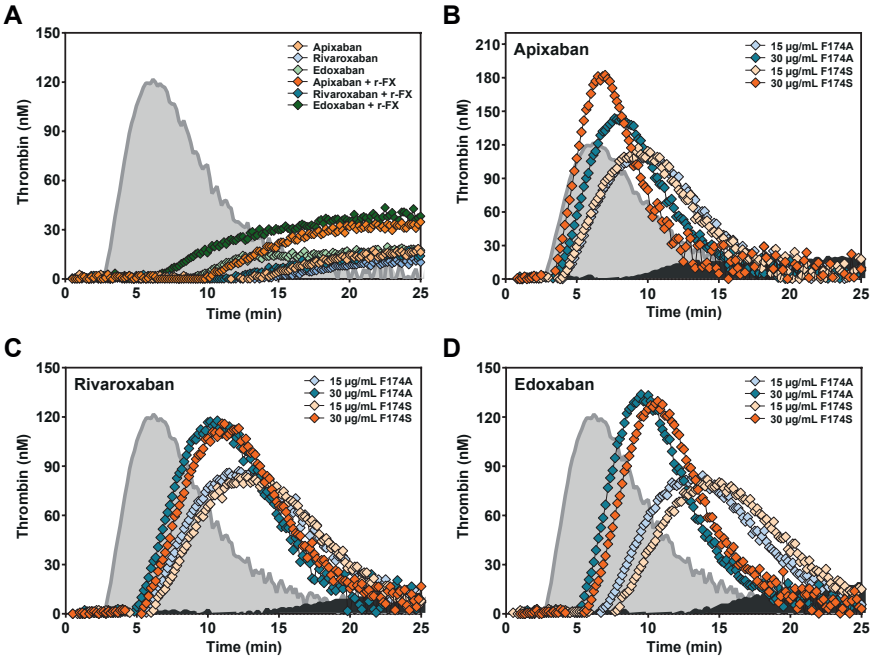
Supplementary figure 4. Blocking of tissue factor pathway inhibitor (TFPI) during thrombin generation by F174-substituted factor X variants. Thrombin generation was measured for 60 min at 37°C in FX-depleted plasma supplemented with 10 µg/mL r-FX, FX-F174A, or FX-F174S in the absence (*white, light blue,* and *yellow diamonds, respectively*) or presence (*grey, dark blue, and orange diamonds, respectively*) of TFPI blocking antibodies against the Kunitz 1 domain **(A,** 10 µg/mL**)**, the Kunitz 2 domain **(B,** 50 µg/mL**),** or the Kunitz 1 domain, Kunitz 2 domain, and C-terminus **(C,** 50 µg/mL**)**. **(D)** Thrombin peak height was plotted for each condition and the results are presented as mean ± SD (*grey: r-FX, blue: FX-F174A, orange: FX-F174S*). Ab indicates antibody; anti-K1, anti-K2, and anti-K1, K2, C indicate TFPI blocking antibodies against: Kunitz 1 domain; the Kunitz 2 domain; or the Kunitz 1 domain, Kunitz 2 domain and C-terminus, respectively. Thrombin formation was triggered by the addition of 1 pM TF in the presence of 20 µM PCPS and initiated with $CaCl_2$ and a thrombin fluorogenic substrate as detailed in 'Materials and Methods'. *p<0.05, **p<0.01, ***p<0.001, ****p<0.0001 according to one-way ANOVA. The statistically significant differences given are compared to the respective data in the absence of antibodies (no ab). Data sets are representatives of two to three independent experiments.



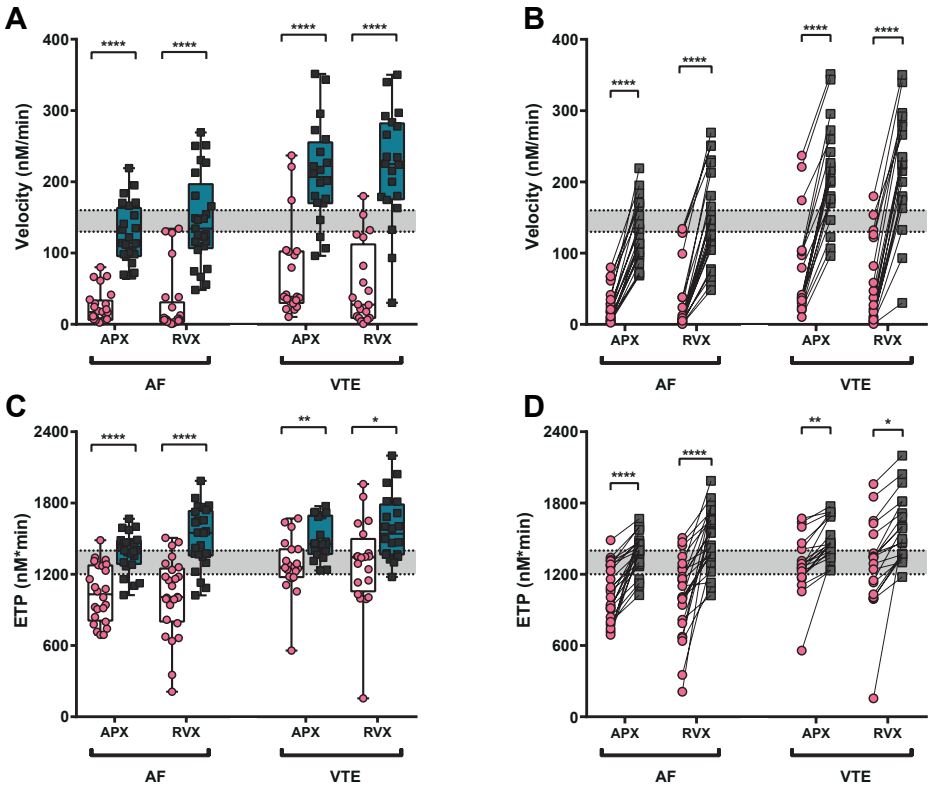
Supplementary figure 5. Thrombin generation in the absence of direct factor Xa inhibitors. Thrombin generation was measured for 30 min at 37°C in FX-deficient plasma supplemented with 10 µg/mL of r-FX (*grey diamonds; area under the curve*), FX-F174A (*blue diamonds)* or FX-F174S (*orange diamonds*). Thrombin formation was triggered by the addition of 6 pM TF in the presence of 20 µM PCPS and initiated with $CaCl_2$ and a thrombin fluorogenic substrate as detailed in 'Materials and Methods'.



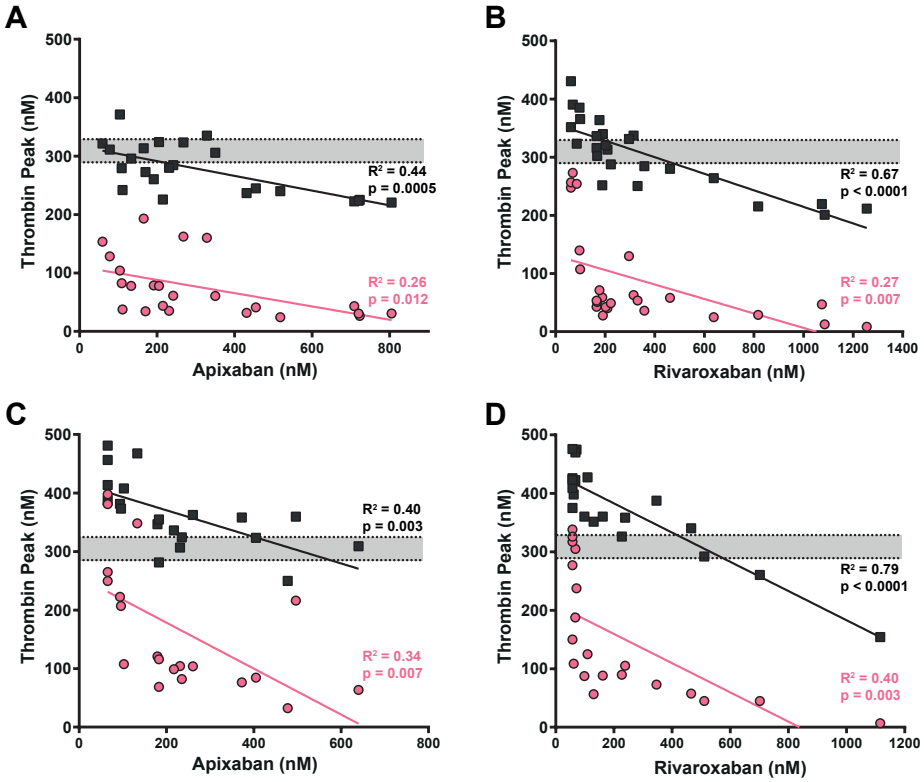
Supplementary figure 6. SDS-PAGE analysis of factor V activation by F174-substituted factor Xa variants. Plasma derived (pd)-FV (455 nM) was incubated for 10min at 25°C with increasing concentrations (0 – 100 nM) of **(A)** recombinant factor Xa (r-FXa) or **(B)** FXa-F174A in the presence of 50 µM PCPS. Samples (3 µg/lane) were subjected to SDS-PAGE under reducing conditions using the MOPS buffer system and visualized by staining with Coomassie Brilliant Blue. Lanes 1-7: pd-FV incubated with 0, 1, 5, 10, 20, 50, or 100 nM FXa; lane 8: thrombin-activated pd-FV (25 nM thrombin, 15min at 37°C). The protein bands corresponding to single chain uncleaved pd-FV (FV), partially activated FV (FVa*), FVa heavy chain (HC), FVa light chain (LC), and the apparent molecular weights of the standards (kDa) are indicated. The data represents a single experiment.



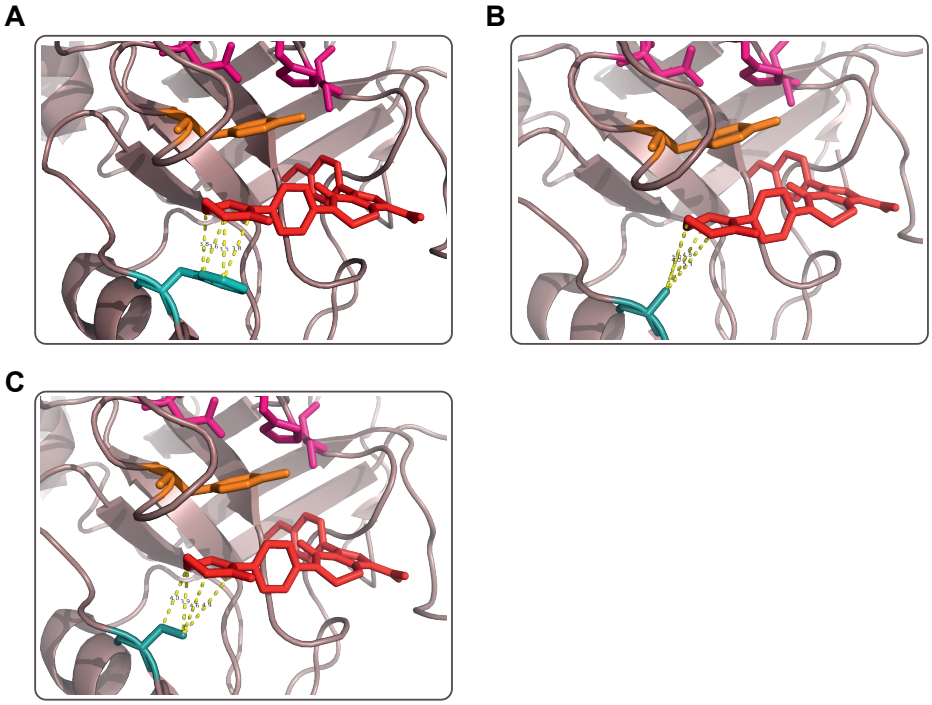
Supplementary figure 7. Correction of thrombin generation at a limited tissue factor concentration in the presence of the direct factor Xa inhibitors. Thrombin generation was measured for 60 min at 37°C in normal pooled plasma (NPP) supplemented with **(A)** 1 µM apixaban, rivaroxaban, or edoxaban in the absence (*yellow, light blue, or light green diamonds, respectively*) or with addition of 60 µg/mL r-FX (orange, dark blue or dark green, respectively), or **(B-D)** 15-30 µg/mL FX-F174A (*light blue-dark blue diamonds*) or FX-F174S (*yellow-orange diamonds*) and 1 µM apixaban **(B)**, rivaroxaban **(C)** or edoxaban **(D)**. Thrombin formation was triggered by the addition of 2 pM TF in the presence of 20 µM PCPS and initiated with $CaCl_2$ and a thrombin fluorogenic substrate as detailed in 'Materials and Methods'. The thrombin generation curves of NPP in the absence **(A-D)** (light gray area under the curve) or presence **(B-D)** (dark gray area under the curve) of the inhibitors are shown. Data sets are representatives of three independent experiments.



Supplementary figure 8. Velocity of thrombin generation and endogenous thrombin potential (ETP) in atrial fibrillation and venous thromboembolism patient plasma. Thrombin generation was measured for 60 min at 37°C in plasma from atrial fibrillation (AF) or venous thromboembolism (VTE) patients treated with either apixaban (APX) or rivaroxaban (RVX) in the absence (*pink dots*) or supplemented (*grey squares*) with 30 µg/mL FX-F174A. Thrombin formation was triggered by the addition of 6 pM TF in the presence of 20 µM PCPS and initiated with CaCl2 and a thrombin fluorogenic substrate as detailed in 'Materials and Methods'. The thrombin generation velocity **(A-B)** and ETP **(C-D)** are shown. Thrombin generation values of the individual patient plasma in the absence or supplemented with FX-F174A are shown by connected lines **(B, D)**. Bars represent the mean, grey dotted area represents NPP values (n=13; velocity, 130-160 nM/min; ETP, 1200-1400 nM*min). *p<0.05, **p<0.01, ***p<0.001, ****p<0.0001 according to one-way ANOVA. Each data point represents a single measurement performed for each patient sample.



Supplementary figure 9. Correlation between the thrombin peak height and factor Xa inhibitor plasma concentration in patients plasma. Thrombin generation was measured for 60 min at 37°C in plasma from atrial fibrillation **(A-B)** or venous thromboembolism **(C-D)** patients treated with either apixaban or rivaroxaban in the absence (*pink dots*) or presence (*grey squares*) of 30 µg/mL FX-F174A. Thrombin formation was triggered by the addition of 6 pM TF in the presence of 20 µM PCPS and initiated with $CaCl_2$ and a thrombin fluorogenic substrate as detailed in 'Materials and Methods'. The thrombin peak height is presented and lines represent the correlation drawn by fitting the data to a linear regression function upon which the coefficient of determination (R^2) and p-values of the linear regression were obtained; grey dotted area represents NPP values (n=13; thrombin peak, 290-330 nM). Each data point represents a single measurement performed for each patient sample.



Supplementary Figure 10. Phenylalanine 174 substitution in the factor Xa S4 subsite. (A) X-ray structure of apixaban bound to wild-type factor Xa (FXa; PDB 2P16)[5] shown in line configuration and the modelled structure of phenylalanine 174 substitution with alanine **(B;** FXa-F174A**)** or serine **(C;** FXa-F174S**)**. Interatomic distances between residue 174 and the P_4 moiety of apixaban are indicated by yellow dashed lines (wild-type FXa (3.5-3.8 Å), FXa-F174A (4.0-5.3 Å), FXa-F174S (3.9-4.9 Å)). Apixaban is shown in red. Tyrosine 99 (*orange stick*), residue 174 (*teal stick*) and the catalytic triad residues (His^{57}, Asp^{102}, and Ser^{195}; *magenta sticks*) are indicated. The figure was created using PyMol.

	Apixaban[a] IC_{50} (nM)	Rivaroxaban[a] IC_{50} (nM)	Edoxaban[a] IC_{50} (nM)	Apixaban[b] IC_{50} (nM)	Rivaroxaban[b] IC_{50} (nM)	Edoxaban[b] IC_{50} (nM)
r-FX	121 ± 31	204 ± 28	118 ± 24	166 ± 16	30 ± 4	60 ± 9
FX-F174A	1813 ± 184	3477 ± 583	1243 ± 222	1813 ± 229	1175 ± 439	712 ± 109
FX-F174S	4238 ± 965	3200 ± 405	1385 ± 262	4074 ± 661	1276 ± 98	711 ± 84

Supplementary Table 1. Half maximal inhibitory concentration (IC_{50}) of factor X variants in thrombin generation. IC_{50} values determined using thrombin generation in the presence of 6 pM[a] or 2 pM[b] tissue factor were obtained as described in 'Materials and Methods'. Fitted values ± 1 standard deviation of the induced fit are representative of three independent experiments.

	Intrinsic tenase K_M (μM)	Intrinsic tenase k_{cat} (min^{-1})	Extrinsic tenase K_M (μM)	Extrinsic tenase k_{cat} (min^{-1})
r-FX	275 ± 50	27.5 ± 1.6	502 ± 55	32.5 ± 1.3
FX-F174A	308 ± 51	27.3 ± 1.5	349 ± 54	32.7 ± 1.4
FX-F174S	345 ± 36	24.6 ± 0.9	320 ± 36	31.0 ± 1.1

Supplementary table 2. Kinetic parameters of factor X activation. The kinetic constants for the activation of the factor X variants by either the intrinsic or extrinsic tenase complexes were obtained as described in 'Materials and Methods'. Fitted values ± 1 standard deviation of the induced fit are representative of two to three independent experiments.

References

1 Wendelboe, A. M. & Raskob, G. E. Global Burden of Thrombosis: Epidemiologic Aspects. *Circ Res* **118**, 1340-1347, doi:10.1161/CIRCRESAHA.115.306841 (2016).

2 Zhang, P. *et al.* Discovery of betrixaban (PRT054021), N-(5-chloropyridin-2-yl)-2-(4-(N,N-dimethylcarbamimidoyl)benzamido)-5-methoxybenz amide, a highly potent, selective, and orally efficacious factor Xa inhibitor. *Bioorg Med Chem Lett* **19**, 2179-2185, doi:10.1016/j.bmcl.2009.02.111 (2009).

3 Furugohri, T. *et al.* DU-176b, a potent and orally active factor Xa inhibitor: in vitro and in vivo pharmacological profiles. *J Thromb Haemost* **6**, 1542-1549, doi:10.1111/j.1538-7836.2008.03064.x (2008).

4 Roehrig, S. *et al.* Discovery of the novel antithrombotic agent 5-chloro-N-({(5S)-2-oxo-3-[4-(3-oxomorpholin-4-yl)phenyl]-1,3-oxazolidin-5-yl}methyl)thiophene- 2-carboxamide (BAY 59-7939): an oral, direct factor Xa inhibitor. *J Med Chem* **48**, 5900-5908, doi:10.1021/jm050101d (2005).

5 Pinto, D. J. *et al.* Discovery of 1-(4-methoxyphenyl)-7-oxo-6-(4-(2-oxopiperidin-1-yl)phenyl)-4,5,6,7-tetrahydro-1H -pyrazolo[3,4-c]pyridine-3-carboxamide (apixaban, BMS-562247), a highly potent, selective, efficacious, and orally bioavailable inhibitor of blood coagulation factor Xa. *J Med Chem* **50**, 5339-5356, doi:10.1021/jm070245n (2007).

6 Hauel, N. H. *et al.* Structure-based design of novel potent nonpeptide thrombin inhibitors. *J Med Chem* **45**, 1757-1766, doi:10.1021/jm0109513 (2002).

7 Weitz, J. I. & Harenberg, J. New developments in anticoagulants: Past, present and future. *Thrombosis and haemostasis* **117**, 1283-1288, doi:10.1160/TH16-10-0807 (2017).

8 Connolly, S. J. *et al.* Dabigatran versus warfarin in patients with atrial fibrillation. *N Engl J Med* **361**, 1139-1151, doi:10.1056/NEJMoa0905561 (2009).

9 Patel, M. R. *et al.* Rivaroxaban versus warfarin in nonvalvular atrial fibrillation. *N Engl J Med* **365**, 883-891, doi:10.1056/NEJMoa1009638 (2011).

10 Agnelli, G. *et al.* Oral apixaban for the treatment of acute venous thromboembolism. *N Engl J Med* **369**, 799-808, doi:10.1056/NEJMoa1302507 (2013).

11 Deitelzweig, S. B., Johnson, B. H., Lin, J. & Schulman, K. L. Prevalence of clinical venous thromboembolism in the USA: current trends and future projections. *Am J Hematol* **86**, 217-220, doi:10.1002/ajh.21917 (2011).

12 Chugh, S. S. *et al.* Worldwide epidemiology of atrial fibrillation: a Global Burden of Disease 2010 Study. *Circulation* **129**, 837-847, doi:10.1161/CIRCULATIONAHA.113.005119 (2014).

13 Nazha, B. *et al.* Periprocedural Outcomes of Direct Oral Anticoagulants Versus Warfarin in Nonvalvular Atrial Fibrillation. *Circulation* **138**, 1402-1411, doi:10.1161/CIRCULATIONAHA.117.031457 (2018).

14 Sharma, M., Cornelius, V. R., Patel, J. P., Davies, J. G. & Molokhia, M. Efficacy and Harms of Direct Oral Anticoagulants in the Elderly for Stroke Prevention in Atrial Fibrillation and Secondary Prevention of Venous Thromboembolism: Systematic Review and Meta-Analysis. *Circulation* **132**, 194-204, doi:10.1161/CIRCULATIONAHA.114.013267 (2015).

15 Loo, S. Y., Dell'Aniello, S., Huiart, L. & Renoux, C. Trends in the prescription of novel oral anticoagulants in UK primary care. *Br J Clin Pharmacol* **83**, 2096-2106, doi:10.1111/bcp.13299 (2017).

16 Zhu, J., Alexander, G. C., Nazarian, S., Segal, J. B. & Wu, A. W. Trends and Variation in Oral Anticoagulant Choice in Patients with Atrial Fibrillation, 2010-2017. *Pharmacotherapy* **38**, 907-920, doi:10.1002/phar.2158 (2018).

17 Connolly, S. J. *et al.* Full Study Report of Andexanet Alfa for Bleeding Associated with Factor Xa Inhibitors. *N Engl J Med* **380**, 1326-1335, doi:10.1056/NEJMoa1814051 (2019).

18 January, C. T. *et al.* 2019 AHA/ACC/HRS Focused Update of the 2014 AHA/ACC/HRS Guideline for the Management of Patients With Atrial Fibrillation: A Report of the American College of Cardiology/American Heart Association Task Force on Clinical Practice Guidelines and the Heart Rhythm Society in Collaboration With the Society of Thoracic Surgeons. *Circulation* **140**, e125-e151, doi:10.1161/CIR.0000000000000665 (2019).
19 Christensen, H. *et al.* European Stroke Organisation Guideline on Reversal of Oral Anticoagulants in Acute Intracerebral Haemorrhage. *Eur Stroke J* **4**, 294-306, doi:10.1177/2396987319849763 (2019).
20 Lip, G. Y. H. *et al.* Antithrombotic Therapy for Atrial Fibrillation: CHEST Guideline and Expert Panel Report. *Chest* **154**, 1121-1201, doi:10.1016/j.chest.2018.07.040 (2018).
21 Kessler, C. M. & Goldstein, J. N. A New Strategy for Uncontrollable Bleeding After Treatment With Rivaroxaban or Apixaban. *Clinical Advances in Hematology & Oncology* **17**, 1-17 (2019).
22 Schreuder, M., Reitsma, P. H. & Bos, M. H. A. Reversal Agents for the Direct Factor Xa Inhibitors: Biochemical Mechanisms of Current and Newly Emerging Therapies. *Semin Thromb Hemost*, doi:10.1055/s-0040-1709134 (2020).
23 Bos, M. H. A., Van 't Veer, C. & Reitsma, P. H. Molecular biology and biochemistry of the coagulation factors and pathways of hemostasis. *Williams Hematology* **9th edn.**, 1915–1948 (2016).
24 Lu, G. *et al.* A specific antidote for reversal of anticoagulation by direct and indirect inhibitors of coagulation factor Xa. *Nat Med* **19**, 446-451, doi:10.1038/nm.3102 (2013).
25 Marlu, R. & Polack, B. Gla-domainless factor Xa: molecular bait to bypass a blocked tenase complex. *Haematologica* **97**, 1165-1172, doi:10.3324/haematol.2011.055699 (2012).
26 Ersayin, A. *et al.* Catalytically inactive Gla-domainless factor Xa binds to TFPI and restores ex vivo coagulation in hemophilia plasma. *Haematologica* **102**, e483-e485, doi:10.3324/haematol.2017.174037 (2017).
27 Schreuder, M., Reitsma, P. H. & Bos, M. H. A. Blood coagulation factor Va's key interactive residues and regions for prothrombinase assembly and prothrombin binding. *J Thromb Haemost* **17**, 1229-1239, doi:10.1111/jth.14487 (2019).
28 Huntington, J. A., Read, R. J. & Carrell, R. W. Structure of a serpin-protease complex shows inhibition by deformation. *Nature* **407**, 923-926, doi:10.1038/35038119 (2000).
29 Jourdi, G. *et al.* FXa-alpha2-Macroglobulin Complex Neutralizes Direct Oral Anticoagulants Targeting FXa In Vitro and In Vivo. *Thrombosis and haemostasis* **118**, 1535-1544, doi:10.1055/s-0038-1667014 (2018).
30 Thalji, N. K. *et al.* A rapid pro-hemostatic approach to overcome direct oral anticoagulants. *Nat Med* **22**, 924-932, doi:10.1038/nm.4149 (2016).
31 Toso, R., Zhu, H. & Camire, R. M. The conformational switch from the factor X zymogen to protease state mediates exosite expression and prothrombinase assembly. *J Biol Chem* **283**, 18627-18635, doi:10.1074/jbc.M802205200 (2008).
32 Verhoef, D. *et al.* Engineered factor Xa variants retain procoagulant activity independent of direct factor Xa inhibitors. *Nat Commun* **8**, 528, doi:10.1038/s41467-017-00647-9 (2017).
33 Higgins, D. L. & Mann, K. G. The interaction of bovine factor V and factor V-derived peptides with phospholipid vesicles. *J Biol Chem* **258**, 6503-6508 (1983).
34 Toso, R. & Camire, R. M. Removal of B-domain sequences from factor V rather than specific proteolysis underlies the mechanism by which cofactor function is realized. *J Biol Chem* **279**, 21643-21650, doi:10.1074/jbc.M402107200 (2004).
35 Camire, R. M., Larson, P. J., Stafford, D. W. & High, K. A. Enhanced gamma-carboxylation of recombinant factor X using a chimeric construct containing the prothrombin propeptide. *Biochemistry* **39**, 14322-14329, doi:10.1021/bi001074q (2000).

36 Krishnaswamy, S. & Walker, R. K. Contribution of the prothrombin fragment 2 domain to the function of factor Va in the prothrombinase complex. *Biochemistry* **36**, 3319-3330, doi:10.1021/bi9623993 (1997).
37 Bos, M. H. *et al.* Venom factor V from the common brown snake escapes hemostatic regulation through procoagulant adaptations. *Blood* **114**, 686-692, doi:10.1182/blood-2009-02-202663 (2009).
38 Peraramelli, S. *et al.* Role of exosite binding modulators in the inhibition of Fxa by TFPI. *Thrombosis and haemostasis* **115**, 580-590, doi:10.1160/TH15-04-0354 (2016).
39 Abraham, M. J. *et al.* GROMACS: High performance molecular simulations through multi-level parallelism from laptops to supercomputers. *SoftwareX* **1-2**, 19-25 (2015).
40 Lu, G., Broze, G. J., Jr. & Krishnaswamy, S. Formation of factors IXa and Xa by the extrinsic pathway: differential regulation by tissue factor pathway inhibitor and antithrombin III. *J Biol Chem* **279**, 17241-17249, doi:10.1074/jbc.M312827200 (2004).
41 Zur, M. & Nemerson, Y. Kinetics of factor IX activation via the extrinsic pathway. Dependence of Km on tissue factor. *J Biol Chem* **255**, 5703-5707 (1980).
42 Renatus, M. *et al.* Structural mapping of the active site specificity determinants of human tissue-type plasminogen activator. Implications for the design of low molecular weight substrates and inhibitors. *J Biol Chem* **272**, 21713-21719, doi:10.1074/jbc.272.35.21713 (1997).
43 Olson, S. T. *et al.* Accelerating ability of synthetic oligosaccharides on antithrombin inhibition of proteinases of the clotting and fibrinolytic systems. Comparison with heparin and low-molecular-weight heparin. *Thrombosis and haemostasis* **92**, 929-939, doi:10.1160/TH04-06-0384 (2004).
44 Camire, R. M. Prothrombinase assembly and S1 site occupation restore the catalytic activity of FXa impaired by mutation at the sodium-binding site. *J Biol Chem* **277**, 37863-37870, doi:10.1074/jbc.M203692200 (2002).
45 Li, W., Johnson, D. J., Esmon, C. T. & Huntington, J. A. Structure of the antithrombin-thrombin-heparin ternary complex reveals the antithrombotic mechanism of heparin. *Nat Struct Mol Biol* **11**, 857-862, doi:10.1038/nsmb811 (2004).
46 Johnson, D. J., Li, W., Adams, T. E. & Huntington, J. A. Antithrombin-S195A factor Xa-heparin structure reveals the allosteric mechanism of antithrombin activation. *EMBO J* **25**, 2029-2037, doi:10.1038/sj.emboj.7601089 (2006).
47 Parasrampuria, D. A. & Truitt, K. E. Pharmacokinetics and Pharmacodynamics of Edoxaban, a Non-Vitamin K Antagonist Oral Anticoagulant that Inhibits Clotting Factor Xa. *Clin Pharmacokinet* **55**, 641-655, doi:10.1007/s40262-015-0342-7 (2016).
48 Mueck, W., Stampfuss, J., Kubitza, D. & Becka, M. Clinical pharmacokinetic and pharmacodynamic profile of rivaroxaban. *Clin Pharmacokinet* **53**, 1-16, doi:10.1007/s40262-013-0100-7 (2014).
49 Byon, W., Garonzik, S., Boyd, R. A. & Frost, C. E. Apixaban: A Clinical Pharmacokinetic and Pharmacodynamic Review. *Clin Pharmacokinet* **58**, 1265-1279, doi:10.1007/s40262-019-00775-z (2019).
50 van Veen, J. J., Gatt, A. & Makris, M. Thrombin generation testing in routine clinical practice: are we there yet? *Br J Haematol* **142**, 889-903, doi:10.1111/j.1365-2141.2008.07267.x (2008).
51 Hertzberg, M. Biochemistry of factor X. *Blood Rev* **8**, 56-62, doi:10.1016/0268-960x(94)90007-8 (1994).
52 Schuijt, T. J. *et al.* Factor Xa activation of factor V is of paramount importance in initiating the coagulation system: lessons from a tick salivary protein. *Circulation* **128**, 254-266, doi:10.1161/CIRCULATIONAHA.113.003191 (2013).
53 Shapiro, A. D. *et al.* Subcutaneous concizumab prophylaxis in hemophilia A and hemophilia A/B with inhibitors: Phase 2 trial results. *Blood*, doi:10.1182/blood.2019001542 (2019).

54 Hilden, I. *et al.* Hemostatic effect of a monoclonal antibody mAb 2021 blocking the interaction between FXa and TFPI in a rabbit hemophilia model. *Blood* **119**, 5871-5878, doi:10.1182/blood-2012-01-401620 (2012).
55 Waters, E. K., Sigh, J., Friedrich, U., Hilden, I. & Sorensen, B. B. Concizumab, an anti-tissue factor pathway inhibitor antibody, induces increased thrombin generation in plasma from haemophilia patients and healthy subjects measured by the thrombin generation assay. *Haemophilia* **23**, 769-776, doi:10.1111/hae.13260 (2017).
56 Broze, G. J., Jr. & Girard, T. J. Tissue factor pathway inhibitor: structure-function. *Front Biosci (Landmark Ed)* **17**, 262-280, doi:10.2741/3926 (2012).
57 Wood, J. P., Ellery, P. E., Maroney, S. A. & Mast, A. E. Biology of tissue factor pathway inhibitor. *Blood* **123**, 2934-2943, doi:10.1182/blood-2013-11-512764 (2014).
58 Qu, S. Y. *et al.* An unexpected dynamic binding mode between coagulation factor X and Rivaroxaban reveals importance of flexibility in drug binding. *Chem Biol Drug Des* **94**, 1664-1671, doi:10.1111/cbdd.13568 (2019).
59 Krishnaswamy, S. Exosite-driven substrate specificity and function in coagulation. *J Thromb Haemost* **3**, 54-67, doi:10.1111/j.1538-7836.2004.01021.x (2005).
60 Schreuder, M. *et al.* Evolutionary adaptations in Pseudonaja textilis venom factor X induce zymogen activity and resistance to the intrinsic tenase complex. *Accepted in Thrombosis and Haemostasis* (2020).
61 Siegal, D. M. *et al.* Andexanet Alfa for the Reversal of Factor Xa Inhibitor Activity. *N Engl J Med* **373**, 2413-2424, doi:10.1056/NEJMoa1510991 (2015).
62 Menegatti, M. & Peyvandi, F. Factor X deficiency. *Semin Thromb Hemost* **35**, 407-415, doi:10.1055/s-0029-1225763 (2009).
63 Pryzdial, E. L. & Kessler, G. E. Kinetics of blood coagulation factor Xaalpha autoproteolytic conversion to factor Xabeta. Effect on inhibition by antithrombin, prothrombinase assembly, and enzyme activity. *J Biol Chem* **271**, 16621-16626, doi:10.1074/jbc.271.28.16621 (1996).

Chapter 8

General Discussion





General Discussion

Blood coagulation is a complex system consisting of several independent biochemical and cellular processes that prevent blood loss following vascular injury. Upon vascular damage, platelets bind to the site of injury and aggregate to form a platelet plug[1]. The coagulation cascade is initiated by the exposure of tissue factor[2] and blood clotting factors are activated on the negatively-charged surface of activated platelets and endothelial cells[3]. One of the key reactions in blood coagulation is the generation of thrombin by the prothrombinase complex that assembles on anionic membranes in the presence of calcium ions and consists of factor Va (FVa) and factor Xa (FXa)[3,4]. Thrombin catalyzes the activation of platelets and is responsible for the deposition of a stabilizing fibrin network. In addition, thrombin activates several positive feedback mechanisms that are required to generate a sufficient procoagulant response. Importantly, the anticoagulant pathway consists of several anticoagulant proteins that terminate the various stages of the procoagulant reaction to prevent excessive blood clotting[5,6]. In disease settings this hemostatic balance is disturbed. Deficiencies in coagulation factors may lead to bleeding disorders such as hemophilia, whereas mutations resulting in more procoagulant coagulation factors induce a hypercoagulant state. Intriguingly, the Australian Elapid family has exploited the coagulation cascade to gain a unique selective advantage. Several evolutionary adaptations in the factor V (FV) and factor X (FX) variants that are expressed in their venom have generated clotting factors with exceptional procoagulant enhancements[7,8]. Upon envenomation, these coagulation factors generate an explosive burst of thrombin that quickly results in the circulatory collapse of the prey animal[9-11].

The aim of the research in this thesis was to gain further insights into the remarkable procoagulant adaptations of *Pseudonaja textilis* venom-derived FV (ptFV) and FX (ptFX). To do so, we have generated a panel of recombinant chimeric FV and FX proteins and studied the structure-function relationships of various structural elements. This approach has allowed us to identify several regions that are at the basis of the procoagulant enhancements and potent toxicity of these venom proteins. In the current chapter, the main findings and implications are summarized and discussed in more detail and the perspectives for further research are outlined.

The Structural Integrity of ptFVa

Unique Structural Features of ptFV

The inactivation of mammalian FVa by activated protein C (APC) is one of the key reactions that downregulates the procoagulant response. Proteolytic cleavage at the

A2 domain residues Arg306, Arg506, and Arg679 results in the dissociation of the A2 domain and FVa inactivation[12]. In contrast, ptFVa is only cleaved by human APC at a position that is homologous to human Arg506 (Lys507)[7], and despite proteolysis this FVa variant retains full cofactor activity[8]. In **chapter 3** we aimed to unravel the functional APC resistance of ptFV. Our findings showed that the absence of a homologous Arg306 cleavage site and the presence of the unique ptFV disulfide bond are not responsible for the functional resistance to APC. This implies that ptFV comprises other structural elements that prevent the loss of cofactor activity. Interestingly, human-snake chimeric FVa variants generated by us maintained structural integrity following APC-catalyzed proteolysis, demonstrating the presence of robust non-covalent interactions between the ptFVa A2 domain and A1-A3 domains. Using *in silico* analysis we identified strong and stable interactions between the ptFVa A1 and A2 domains that significantly increase the A2 domain binding affinity. We further identified the so-called A2 domain loop2 as a structural element that seems to play a major role in the association of the A2 domain with the A1-A3 domains in ptFVa.

Activated Protein C Resistance of FVa

Unraveling at least part of the mechanistic principles that are responsible for the functional resistance to APC in ptFV has identified a new concept of APC resistance. To date, APC resistance has been described as a result of mutations that either prevent certain APC-mediated cleavages or decrease the sensitivity for APC. The most common FV mutation that results in APC resistance is $FV^{Leiden\ 13}$. The molecular basis of FV^{Leiden}-dependent APC resistance is derived from a point mutation that results in an Arg506Gln substitution, leading to a ten-fold slower APC inactivation rate relative to wild-type FVa[14]. Naturally occuring FV variants with mutations at the APC cleavage site Arg306 are $FV^{Hong\ Kong}$ (Arg306Gly) and $FV^{Cambridge}$ (Arg306Thr) which display a mild APC resistant phenotype[15], presumably due to the ability of protein S to stimulate Arg306 cleavage. In addition, the Ile359Thr ($FV^{Liverpool}$) mutation introduces a glycosylation site at Asn357 that impaires Arg306 cleavage, likely by steric hindrance[16]. The His1299Arg (FVR2) mutation that has been described to result in an APC resistant phenotype[17] seems to be inducing a quantitative FV deficiency owing to impaired expression of the mutant protein[18].

Mechanistic Principles of FVa Inactivation

Factor Va is inactivated via limited proteolysis at Arg306 and Arg506 resulting in the dissociation of the A2 domain. To date, the dissociation of the A2 domain following APC-catalysis has only been demonstrated in bovine FVa[12,19], with biochemical and structural data lacking for human FVa. Molecular Dynamics simulations using a complete human FVa model have previously suggested that APC cleavage results in the release of the A2 domain[20]. In our study, we have provided biochemical evidence

that human FVa is inactivated by APC in a similar fashion as compared to bovine FVa (**Figure 3, chapter 3**). Yet, the currently available data are unable to distinguish whether cleavage at Arg306 and Arg506 or the dissociation of the A2 domain serves as the major contributor to the loss of procoagulant activity. Using an engineered FVa mutant comprising an A2-A3 interdomain disulfide bond, Gale *et al.* showed that APC-induced cleavage markedly reduced the FVa cofactor activity while A2 domain dissociation was prevented[21]. This suggests that APC cleavage rather than A2 domain dissociation is responsible for the inactivation of FVa. In contrast, Molecular Dynamics simulations using a model for FVa^{Leiden} suggested that in the absence of the Arg506 cleavage, A2 domain dissociation occurs as a result of Arg306 proteolysis[20], implying that cleavage of the cofactor at Arg506 is not required for A2 domain dissociation but is rather required to facilitate cleavage at Arg306. Our findings using ptFV support the notion that A2 domain dissociation is the main determinant for FVa inactivation (**chapter 3**). Despite cleavage at Arg306 and Lys507, ptFVa retained structural integrity and full cofactor activity. Unfortunately, we were unable to determine whether release of the A2 domain would inactivate ptFVa. However, the human FVa A2 domain comprises essential FXa and prothrombin binding sites[4] . It seems therefore reasonable to assume that similar regions are present in the ptFV A2 domain, allowing us to speculate that the dissociation of the A2 domain will result in the inactivation of ptFVa.

A2 Domain Binding and Stability in the Homologous Cofactors FVIIIa and FVa

The residues that positively or negatively contribute to the FVa A2 domain binding affinity remain largely unknown. Characterization of the naturally occurring FV variants comprising an Ala221Val or Arg1698Trp mutation revealed a reduced FVa stability due to an increased dissociation rate of the heavy (A1-A2 domains) and light (A3-C1-C2 domains) chains[22,23]. Arg1698 was predicted to be located at the A2-A3 domain interface[22] and the Ala221Val mutation was found to induce structural changes toward the A2-A3 domain interface[23]. Using Molecular Dynamics simulations, we have identified the key hydrogen bond interaction pairs between the A2 domain and the A1 or A3 domain (**Figure 5, chapter 3**). Furthermore, we have shown that A2 domain dissociation upon APC cleavage is induced by a loss of A1-A2 domain affinity, indicating that the residues at the A1-A2 domain interface are crucial for A2 domain binding.

In contrast to FVa, the inactivation of the homologous factor VIIIa (FVIIIa) proceeds either via APC-mediated proteolysis[24,25] or via the spontaneous release of the A2 domain[26,27]. Whereas our understanding of the residues that contribute to productive interactions between the A2 and A1-A3 domains is lacking for FVa, biochemical and mutagenesis studies have identified multiple residues that support A2 domain binding in FVIIIa[28-35]. The FVIIIa A2 domain subunit weakly associates with the A1-A3 domains,

primarily through electrostatic interactions, and readily dissociates at physiologic pH wheareas FVIIIa stability is enhanced at pH 6.0[26]. The observation that increasing NaCl concentrations significantly and dose-dependently reduced the FVIIIa activity[27] could not be replicated for APC-proteolyzed ptFVa-h306-SS nor did we observe differences in the thermostability of our APC-treated ptFVa variants relative to wild-type ptFVa (**Figure S4, chapter 3**). Whether the unique interactions facilitated by the A2 domain loop2 in ptFVa could explain these differences remains to be determined by future biochemical studies that further characterize the functional consequences of the ptFV A2 domain loop2.

The Lipid Independent Activity and APC Resistance of ptFVa

Functional Role of the A2 Domain C-terminal Region

The FV A2 domain C-terminus (A2T) is a long, negatively charged region that is liberated upon release of the B-domain (**Figure S1, chapter 4**). Although X-ray structures have not been able to fully resolve the A2T, this structural element has been modelled as a highly flexible region with little if any conformational constraints[36,37]. From a functional perspective, the A2T has been implicated in the assembly of the prothrombinase complex and engagement of the substrate prothrombin[38-42]. However, its exact role remains poorly understood as contradictory results have been reported[43,44]. In **chapter 4** we studied the functional implications of the ptFV A2T that comprises a significant extended region relative to other known FV species. Our results revealed that the catalytic efficiency towards prothrombin was slighty reduced in FV variants comprising the ptFV A2T, indicating that the ptFV A2T engages prothrombin in a somewhat different manner. These observations are in accordance with previous reports suggesting that the FVa A2T does not provide major productive interactions with FXa and/or prothrombin, but rather plays a role in the positioning of the prothrombin activation sites towards the catalytic triad of FXa[39,42,44]. Collectively, the role of the A2T seems to be minimal in the presence of saturating amounts of phospholipid membranes, indicating that binding of FVa to FXa and prothrombin is mainly dependent on productive interactions facilitated by the regions surrounding Arg306, Arg506, and part of the A3 domain (reviewed in **chapter 2**).

The Lipid Independent Activity of ptFVa and ptFXa

Contrarily to our findings in the presence of anionic membranes, we demonstrated that the ptFV A2T plays a major functional role in the absence of membranes by facilitating prothrombin conversion via a lipid-independent mechanism. Interestingly, hFVa-ptA2T converted prethrombin-1, a prothrombin derivative that lacks the γ-carboxyglutamic

acid domain (GLA) domain and as such the membrane-binding ability, with similar rates relative to ptFVa (**Figure 4D, chapter 4**). Yet, this effect was only observed when hFV-ptA2T was complexed with ptFXa. This provides additional evidence that the lipid-independent activity of ptFV is entirely regulated by the A2T. Our findings further demonstrated that ptFXa comprises an essential element that is required to bypass the need for phospholipid binding. Currently, we can only speculate which unique region or regions are responsible. Our data excludes a role for the extended 99-loop in ptFXa, which extends towards, and possibly interacts with, FVa[45]. Another region of interest is the lipid-binding GLA domain. Binding of FXa to the lipid surface induces a conformational change that increases the affinity for FVa[46]. For ptFXa, structural differences in the GLA domain could potentially instigate similar conformational changes in the absence of anionic membrances and expose a FVa interactive site. Binding of FVa might promote further conformational changes that result in a functional FVa-ptFXa complex in solution. In our study, we used several peptides that comprise part of the ptFV A2T in an attempt to pinpoint the region that is responsible for the lipid-independent activity. These studies suggested a crucial role for the N-terminal region of the A2T (**Figure 4, S5, chapter 4**). The ptFV-ptFXa (Pseutarin C) X-ray structure revealed that this region interacts with the highly basic heparin binding site of ptFXa[45]. Based on these findings, we speculate that evolutionary changes in the ptFXa heparin binding site support the lipid-independent activity of the Pseutarin C complex. However, an initial comparison of the human ternary model and Pseutarin C structure did not reveal major structural differences[37,45]. Moreover, we can not exclude that our peptides interfere with prothrombinase activity in a non-specific manner nor can we conclude that the C-terminal region of the ptFV A2T is not involved in this procoagulant enhancement. To confirm our findings, new FV and FX variants would need to be generated and characterized that specifically substitute or truncate part of the ptFV A2T, or mutate potential important residues in the ptFXa A2T binding site, respectively.

Role of the ptFV A2T in the Functional Resistance to APC

Our findings further revealed that the ptFV A2T plays a major role in the functional resistance to APC. Substitution of the ptFV A2T for the corresponding human region significantly decreased the cofactor activity upon APC-mediated proteolysis. Intriguingly, the inactivation of ptFVa-hA2T was markedly slower compared to hFVa and retained ~25% cofactor activity following a two-hour incubation with APC (**Figure 5, chapter 4**). It is currently unclear whether prolonged incubations with APC would completely inactivate ptFVa-hA2T, but the residual cofactor activity might be explained by an enhanced stability of regions that are essential for the interaction with FXa and prothrombin. This is supported by our observation that the partial loss of ptFVa-hA2T cofactor activity was not a result of A2 domain dissociation (**Figure 6 chapter**

4). Moreover, a comparable loss of cofactor activity was observed when ptFVa was treated with the fibrinolytic serine protease plasmin (**Figure S5, chapter 3**). Similar to FVa^{leiden}, selective proteolysis of ptFVa could destabilize the interactions with ptFXa while cofactor activity is at least partially maintained by impeding A2 domain dissociation[14]. As described in previous sections, this could be the result of the increased A2 domain binding affinity facilitated by the productive interactions between the A2 domain loop2 and A1 domain. Taken together, our findings indicate that the conformational rigidity of loop2 together with the unique functional characteristics of the ptFV A2T provide a rationale for ptFVa's functional resistance to APC.

Unfortunately, we were unable to accurately determine the specific region of the A2T that contributes to the APC resistance. However, mutation of the Arg679 cleavage site in ptFVa-hA2T (**Figure S1, chapter 4**) resulted in a ptFVa variant that retained stable cofactor activity following an initial ~35% loss of activity (**Figure 5, chapter 4**). Considering the presumed high flexibility of the A2T[37,45,47], it is unlikely that cleavage at Arg679 significantly impairs FVa stability. Therefore, these results suggest that truncation of the A2T as a result of Arg679 cleavage decreases the ptFVa cofactor activity, providing evidence for a role of the A2T C-terminal region in the functional resistance to APC. In addition, the modest loss of ptFVa-hA2T-R679Q cofactor activity (~35%) following Arg679 mutation seems to indicate that the A2T N-terminal region is, besides its crucial role in the lipid-independent activity, also to some extent involved in the APC resistance of ptFV.

We further demonstrated that introduction of the ptFV A2T, the key structural element responsible for ptFVa's APC resistance (**chapter 4**), in human FVa would generate a human FVa variant with a similar gain-of-function. However, an additional mutation of the human Arg306 cleavage site was required, presumably to prevent the dissociation of the Asn307-Arg506 region. Furthermore, this hFVa-ptA2T-pt306 variant only retained full cofactor activity when in complex with ptFXa. This demonstrates that ptFXa comprises an essential element that is required for this gain-of-function feature, similar to that observed for the lipid-independent conversion of prothrombin. As discussed above, the ptFXa region that is responsible for these unique procoagulant enhancements is currently unknown, but likely involves a FVa interactive region. Collectively, our findings indicate that the ptFV A2T circumvents negative regulatory conditions by providing stable interactions with ptFXa and prothrombin in the absence of membranes or upon APC-mediated proteolysis.

Evolutionary Changes in the ptFX Activation Peptide

Role of the FX Activation Peptide in the Interaction with Intrinsic Tenase

The activation peptide of the venom-derived ptFX is remarkably shorter in amino acid length compared to that of various other FX species, including that of the liver-derived ptFX[48,49]. In **chapter 5** we aimed to unravel the functional implications of this evolutionairy adaptation by characterizing several chimeric FX variants. Assessment of the activation by the extrinsic tenase complex revealed identical kinetic constants between hFX and hFX-ptAP. This could suggest that the extrinsic tenase complex is able to interact with the venom-derived activation peptide in a similar manner as the human counterpart. Alternatively, it is possible that the FX activation peptide does not comprise a binding site for the extrinsic tenase complex. The latter is supported by previous studies revealing only modest alterations in kinetic parameters of extrinsic tenase-dependent FX activation following truncation of the activation peptide[50,51]. Our findings therefore provide further evidence that the substrate-specificity of the extrinsic tenase complex is completely dependent on the interactions with pro-exosite regions in FX. The exact interactive regions are not fully defined but previous studies have reported a tissue factor-factor VIIa binding site in the FX GLA[52,53], endothelial growth factor 1[53], and serine protease domain[54].

Somewhat surprising, kinetic analyses demonstrated that incorporation of the venom-derived activation peptide into human FX almost completely abrogated the activation by the intrinsic tenase complex. Furthermore, we showed that the variant hFX-ptAP is a poor competitor of FX activation by the intrinsic tenase complex relative to hFX-R15Q. Therefore our results indicate that activation by the intrinsic tenase complex is mainly dependent on the recognition and binding of the FX activation peptide, as has been suggested in earlier reports[51,55]. The evolutionairy advantage of the shortened activation peptide is unclear. It is possible that the venom-derived activation peptide has specifically evolved towards recognition by the intrinsic tenase complex of prey animals and may interact in a different manner relative to the human system. On the other hand, various reports have suggested that the intrinsic coagulation pathway may have only been fully evolved after the reptile lineage[56-60]. Although speculative, this could imply that the activation of FX by the intrinsic tenase complex does not play a significant role in the coagulation cascade of reptiles. Characterization of the liver-derived ptFX will gain more insight into the intrinsic tenase-mediated activation of ptFX and the role of the activation peptide.

The Zymogen Activity of ptFX

The evolutionary intermediate ptFX (isoform ptFX[49]) was reported to display zymogen activity towards the macromolecular substrate prothrombin when in complex with venom-derived ptFV[45]. In our study, we have unraveled the molecular basis for the zymogen activity of ptFX and identified that the venom-derived activation peptide is responsible for this remarkable procoagulant characteristic (**chapter 5**). Interestingly, substitution of the human activation peptide for that of ptFX generated a human chimeric FX variant with similar zymogen activity relative to ptFX. Furthermore, we observed that the zymogen activity is completely dependent on the presence of the cofactor, in contrast to previously reported data showing that human FV is not able to bind to zymogen FX[61]. This is in line with our kinetic data revealing that the apparent human FV-FX binding affinity could not be accurately assessed. In contrast, both venom ptFX and hFX-ptAP displayed a markedly increased apparent binding affinity for their respective cofactor, relative to human FX. Moreover, kinetic evaluation showed that the FX-cofactor complexes bind prothrombin with a similar affinity relative to prothrombinase-assembled FXa[62-65]. As such, our findings indicate that the venom-derived activation peptide allows exposure of a FVa binding site and formation of an initial FVa-FX complex. The productive interactions with FVa then facilitate conformational changes in the serine protease domain of FX that are required for catalytic activity.

Functionally Important Regions in the Venom-derived Activation Peptide

The exact structural features of the ptFX activation peptide that are responsible for the resistance to the intrinsic tenase complex or for the zymogen activity are currently unknown. Compared to various FX species, including the liver-expressed ptFX, the venom-derived activation peptide lacks the central acidic region[49]. Although no studies have reported a functional role for this region, our data might suggest that it comprises a binding site for the intrinsic tenase complex. Alternatively, the acidic region could prevent potential interactions with FVa in order to avoid catalytic activity of the FX zymogen. Other structural elements that play a role in FX activation are the carbohydrate chains that are present in the FX activation peptide[66]. Whereas the human FX activation peptide comprises two O-linked and two N-linked glycosylation sites, no experimental data is available on the glycosylation status of the venom FX activation peptide. Artificial mapping of glycosylation sites predicts that ptFX contains one N-linked and one O-linked carbohydrate[66,67]. In human FX, these O-linked carbohydrates have been shown to play a key role in the catalytic efficiency of the intrinsic tenase complex, indicating that both glycans make productive interactions with the complex[51,68-70]. In order to fully understand the mechanisms that are at the basis of these functional

characteristics, mutagenesis studies are required that specifically assess the role of the carbohydrates or the acidic region in the activation peptides.

Zymogenicity in Serine Proteases

Although serine proteases are kept in a zymogen state to prevent unwanted catalytic activity, substrate conversion has been reported by various zymogens. The 'molecular sexuality' principle relies on the insertion of a peptide that is sequentially similar to the strictly conserved Ile16 N-terminus into the preformed active site[71,72]. Such peptides have been shown to induce trypsinogen to trypsin transition[71]. In addition, bacterial proteins belonging to the zymogen-activator and adhesion proteins (ZAAP) family bind to serine proteases such as plasminogen[73] and prothrombin[74,75] and insert their N-terminus into the Ile16 pocket to form the characteristic salt bridge with Asp194. Formation of this salt bridge results in conformational changes of the activation domain and activation of the zymogen in a non-proteolytic manner.

Zymogen activity has also been reported in the absence of a cofactor. It is hypothesized that both zymogen and protease exist in different conformational states within a dynamic equilibrium[76-78]. In this case, zymogens may acquire a conformation that allows for some level of catalytic activity (protease-like), whereas proteases adopt conformations with limited activity (zymogen-like). The ratio between the activity of the mature protease and the activity of the zymogen is defined as the 'zymogenicity' of the protein. In general, the zymogenicity of serine proteases is high, which results in a minimal or absence of proteolytic activity in zymogens. Tissue-type plasminogen activator (tPA) is a unique exemption since its catalytic activity increases only 5-10-fold upon activation[79-81]. The low zymogenicity of tPA was shown to be the result of an intrinsic Lys156-Asp194 salt bridge which induced conformational changes leading to the maturation and stabilization of an active trypsin-like conformation[82,83]. More recently, the zymogen forms of prekallikrein and factor XII were shown to express physiological relevant activity[84,85]. Although their zymogen activity was several orders of magnitude lower than that of the activated proteases, non-cleavable forms of prekallikrein[84] and factor XII[85] were able to initiate the contact activation pathway. Our study has identified a novel mechanism by which the zymogenicity of a serine protease can be modified. However, the exact structural requirements to achieve zymogen activity remain unclear. It has previously been suggested that the residues surrounding Lys156 have a critical role in determining the potential formation of the Lys156-Asp194 salt bridge. For instance, in bovine trypsinogen Thr21 engages in a hydrogen bond with Lys156, effectively sequestering Lys156 from interacting with Asp194[86]. Similarly, in FXa and urokinase Lys156 interacts with Thr144 and Glu144, respectively[86]. In contrast, tPA comprises Phe21 and His144 that lack the potential

to sequester Lys156 and consequently allow Lys156-Asp194 interaction[86]. These observations led to the hypothesis that hydroxyl or acid groups at positions 21 and 144 interact with Lys156 to prevent formation of the Lys156-Asp194 salt bridge and stabilize an inactive conformation. Yet, the potential to form a Lys156-Asp198 salt bridge can not fully explain the zymogen activity of serine proteases since factor XII and prekalikrein display physiologically relevant catalytic activity despite comprising Glu156. In the case of factor XII, a crystal structure revealed a direct interaction between residues Arg73 and Asp194 which may act as an alternative salt bridge inducing catalytic activity[87]. Furthermore, productive interactions with macromolecular substrates might contribute to the stabilization of the protease state, provided that the substrate-binding exosites are exposed. In accordance to this hypothesis, the shortened venom FX activation peptide allows for productive interactions with the cofactor. As such, the zymogen activity of ptFX and hFX-ptAP could be a result of FVa binding that induces conformational changes in the protease domain allowing for Lys156-Asp194 salt bridge formation and active site maturation.

Procoagulant Enhancements of ptFV and ptFX

Collectively, our studies have uncovered several regions that are at the basis of the potent procoagulant effects of ptFV and ptFX. Previously, ptFV was shown to be synthesized in an constitutively active state as a result of the shortened B domain and the lack of the basic and acidic regions that keep human FV in an inactive procofactor state[8,88]. Here, we discovered two distinct mechanisms underlying the functional resistance to APC. First, our data indicate that stable hydrogen bond formation between the A1 and A2 domain of ptFV increases the A1-A2 domain binding affinity upon APC-mediated proteolysis which presumably prevents A2 domain dissociation. This increase in binding affinity was predominantly induced by the enhanced rigidity of the so-called A2 domain loop2 which supported stable interactions with the A1 domain. Following proteolysis, the extended ptFV A2T plays a pivotal role in the formation of the prothrombinase-like complex and conversion of prothrombin. In addition, we demonstrated that the A2T allows ptFV to circumvent the need for membrane binding. Based on the available data, we speculate that the A2T is able to provide productive interactions with ptFXa and prothrombin despite APC-mediated proteolysis or in the absence of anionic membranes. Our findings also revealed that the shortened activation peptide of ptFX induces zymogen activity and resistance to the intrinsic tenase complex. Although it remains to be determined whether venom ptFX is injected into the prey in a zymogen or protease form, the zymogen activity could elicit a procoagulant response by generating small amounts of thrombin to activate the feedback mechanisms of the coagulation cascade. Whether the resistance for

activation by the intrinsic tenase complex provides a selective advantage is unclear. Finally, a prior study revealed that the extended 99-loop in ptFX reduces the sensitivity of ptFXa for the active site inhibitors antithrombin and tissue factor pathway inhibitor (TFPI)[45,63]. Collectively, these unique structural elements provide the molecular basis for the procoagulant enhancements of ptFV and ptFX and are summarized by the schematic overview in **figure 1**.

Hemostatic System of the Elapid Snakes

Sequence analysis showed that liver-expressed and venom-expressed ptFV comprise ~96% sequence homology[89]. Intriguingly, functional characterization of the liver-expressed ptFV revealed that this FV form shares the enhanced procoagulant characteristics of venom-derived ptFV[90]. As such, these findings raise questions on the regulatory mechanisms of the coagulation cascade in Elapidae. Unfortunately, it is currently unclear whether elapidae express protein C. However, it would be of interest to evaluate the effects of snake protein C on ptFV. In our study, we observed that plasmin significantly reduced the cofactor activity of ptFVa. This might suggest that plasmin plays a physiological role in the regulation of liver-expressed ptFVa. The putative plasmin-mediated inactivation of ptFVa may occur in a later stage of hemostasis relative to the action of APC. Moreover, it has been suggested that reptiles have a primitive contact activation pathway[56-60]. We therefore speculate that FV plays a more procoagulant role in the coagulation cascade of elapidae relative to the mammalian hemostatic system in order to generate sufficient amounts of thrombin.

Liver- and venom-expressed ptFX comprise ~76% sequence homology[49], which could indicate that venom ptFX underwent evolutionary adaptations in order to circumvent negative regulatory mechanisms. This is supported by functional studies demonstrating that the extended 99-loop, unique to venom and isoform FX species in Elapidae, reduces the inhibition of FXa by antithrombin and TFPI[45,63], although inhibition experiments have not yet been performed with liver-expressed ptFX. It is possible that the activity of the liver-expressed ptFVa-ptFXa complex is mainly regulated by inhibition of ptFXa via inhibitors such as antithrombin, α2-macroglobulin, or TFPI. Furthermore, the observation that liver ptFV shares the procoagulant properties of venom ptFV[90] suggests that the activity of the liver-expressed ptFVa-ptFXa complex is confined to anionic membranes via the membrane binding requirement of liver ptFXa. As such, we hypothesize that in Elapidae, FV plays a more procoagulant role in order to overcome the premature and inefficient contact activation pathway. However, the enhanced procoagulant functions of FV might in part be averted by the regulation of liver ptFXa activity and the requirement of liver ptFXa for membrane binding.

Potential Therapeutic Implications

Our studies have at least in part uncovered the molecular mechanisms that enhance the activity of ptFV. The responsible functional regions could be implemented in novel FV variants for potential therapeutic use in bleeding disorders such as hemophilia. Hemophilia A and B are the result of a congenital defect in blood coagulation FVIII or factor IX (FIX), respectively. These bleeding discorders are effectively treated by protein replacement therapy. Unfortunately, replacement therapy may induce neutralizing inhibitory antibodies against the administered product, rendering therapy ineffective and increasing the risk of severe hemorrhagic events[91]. Disease management of inhibitor patients therefore includes the use of hemostatic bypassing agents[92]. The most commonly used bypassing agents used to treat major bleeding in hemophilia A patients with inhibitors include recombinant factors or plasma concentrates (i.e. activated prothrombin complex concentrate and recombinant activated factor VII). However, in the last decade a new class of subcutaneous non-factor products have emerged that are longer-acting relative to conventional bypassing agents[93]. Of these novel agents emicizumab has recently been approved for routine prophylaxis in hemophilia A patients with or without FVIII inhibitors[94,95]. Emicizumab is a humanized bispecific antibody that binds to both FIX(a) and FX(a) to promote FX activation in a FVIIIa-independent manner[96]. As an alternative strategy, we hypothesize that procoagulant enhancement of FV could generate novel variants that may significantly stimulate coagulation. In **chapter 3**, we demonstrated that the ptFV A2 domain loop2 engages in stable interactions with the A1 domain following APC-mediated proteolysis. As such, substitution of human loop2 for the corresponding ptFV loop2 might generate a human FV variant in which A2 domain dissociation is prevented. Previous *in vitro* and *in vivo* studies have provided evidence for a disease-modifier effect of APC-resistant FV mutations in hemophilia[97-100]. For instance, FV^{Leiden} and $FV^{Cambridge}$ showed enhanced thrombin generation in hemophilic plasma compared with wild-type FV[101,102], and FV^{leiden} was found to improve hemostasis in a murine hemophilia model[100]. Furthermore, an engineered FVa variant (^{super}FVa) comprising an A2-A3 domain disulfide bond and mutations at the APC cleavage sites Arg306, Arg506, and Arg697 was able to reduce hemophilia-related bleeding[97-99].

The ptFV A2T is an other structural element that might enhance the procoagulant activity of novel therapeutic FV variants. We demonstrated that this region is responsible for the lipid independent activity of ptFV and plays a major role in the functional resistance to APC. Importantly, these remarkable characteristics could be translated to human FV. However, the procoagulant enhancements relied on the presence of ptFXa, which likely limits the potential therapeutic use of the ptFV A2T. Alternatively,

targeting the ptFV A2T could be a viable strategy to inhibit the extreme procoagulant effects of the ptFVa-ptFXa complex upon envenomation. This would generate the first specific antidote for envenomation by brown snakes[103]. Venom-induced consumptive coagulopathy (VICC) is the most commonly observed clinical envenoming phenotype in Australia and is characterized by the activation and consumption of various coagulation factors, resulting in a markedly increased risk for bleeding[104-107]. Novel antidotes that specifically target the venom-induced procoagulant response could have a significantly enhanced potency compared to the conventional non-specific antidotes.

A potential therapeutic application for the venom-derived activation peptide is currently uncertain. Although the zymogen activity of our FX variants is several orders of magnitude lower than that of FXa, the kinetics for prothrombin conversion demonstrated that the catalytic activity can generate significant amounts of thrombin. The generation of thrombin can in turn elicit a procoagulant response by activating the feedback mechanisms of coagulation. In this way, the FX variants act in a similar fashion as factor XII and prekalikrein, which initiate the contact activation pathway in zymogen state[84,85]. Based on this principle, our chimeric FX variant could potentially be used as bypassing agent in the treatment of bleeding-related disorders. Unfortunately, the efficacy is hampered by the resistance to activation by the intrinsic tenase complex, which nullifies crucial amplication loops. Future studies could focus on the modification of the venom-derived activation peptide in order to allow intrinsic tenase-mediated FX activation while maintaining the unique zymogen activity.

Phe174-substituted FX Variants as Bypassing agent for the Direct FXa Inhibitors

Mechanistic Principles of Phe174-substituted FX Variants

In **chapter 7**, we presented Phe174-substituted FX variants that are able to counteract the anticoagulant effects of the direct FXa inhibitors. We observed that disruption of the S4 subsite significantly affected the FXa binding affinity for the inhibitors. In accordance with previous reports[63,108,109], this study confirmed the important regulatory role of the FXa S4 subsite in inhibitor binding. The crystal structure of FXa in complex with apixaban or rivaroxaban demonstrated that the P4 ring of apixaban and the morpholinone ring of rivaroxaban are sandwiched between the S4 subsite residues Tyr99 and Phe174[108,109]. These residues were shown to be crucial for the high affinity interaction and inhibitor binding stability. Furthermore, we recently demonstrated that specific modification of the S4 subsite disrupts the high affinity binding of apixaban[63]. In concordance, our kinetic data and Molecular Dynamics simulations provided additional evidence that the bypassing effect of FXa-F174 variants is mediated by a

disrupted inhibitor binding stability. Substitution of the large hydrophobic Phe174 for the smaller alanine or serine enlarges the S4 subpocket and provides a rationale for the increased inhibitor mobility. Further support for our observations comes from the Molecular Dynamics simulations performed by Qu *et al*. on the FXa-rivaroxaban X-ray structure using a modelled Phe174Ala FXa variant[110]. These Molecular Dynamics simulations revealed that the binding of rivaroxaban was affected to a greater extent by the Phe174 substitution compared to similar simulations using the FXa-apixaban structure[110]. However, in our study kinetic assessment did not reveal any differences in FXa-F174 inhibition between apixaban or rivaroxaban. This might be explained by the alternative binding mode of rivaroxaban that may occur upon disruption of the S4 subsite. In this binding mode, the morpholinone moiety of rivaroxaban shifts into the shallow S1′ pocket and forms strong interactions with Phe41, Gln61, and Gln192[110]. As a consequence, rivaroxaban occupies the essential S1 subsite in a relatively stable manner. These different rivaroxaban binding modes may ultimately result in a loss of FXa sensitivity that is similar to that observed for apixaban.

Interestingly, we observed that the ability of the FX-F174 variants to overcome the anticoagulant effects of the direct FXa inhibitors was enhanced in plasma. Our findings demonstrated that these additional effects were mediated by a decreased sensitivity for TFPI. As such, the Phe174-substituted FX variants bypass the direct FXa inhibitors via two independent mechanisms, i.e. a disrupted inhibitor binding and in part via resistance to TFPI. These results also indicate that the FXa S4 subsite is an important regulator for TFPI binding, supporting earlier reports suggesting that the hydrophobic Kunitz 2 residues Ile13 and Leu39 engage the S4 subsite residues Tyr99 and Phe174[111].

Therapeutic Potential and Comparison of Reversal Agents

Rapid reversal of the anticoagulant DOAC activity may be required in case of life-threatening hemorrhage, major trauma, emergency surgery, or DOAC overdose. Over the last years, several specific reversal agents have been generated that either act as stoichiometric bait antidotes or initiate coagulation via a bypassing mechanism. To date, andexanet alfa (andexanet) is the only FDA- and EMA-approved specific reversal agent for major bleeding events induced by the direct FXa inhibitors. Other specific reversal agents, summarized in **chapter 6**, are still in clinical or preclinical development.

A major advantage of the FX-F174 variants resides in the limited amount of protein that is needed to correct inhibitor-induced bleeding relative to the bait antidotes. Based on an average individual, 880-1760 mg andexanet is required to restore hemostasis compared to an estimated 40-130 mg of the FX-F174 variant, a 14-22-fold lower dose. This can be explained as follows. First, the mechanism of bait antidotes relies on the

sequesteration of inhibitors in order to generate free endogenous FXa. In theory, the bait antidotes sequester the inhibitors in a stoichiometric manner. However, the binding between the direct FXa inhibitors and bait antidotes is reversible and the affinity of bait antidotes for the inhibitors is usually similar, if not slightly weaker, relative to endogenous FXa. This creates an equilibrium between inhibitor-bound antidote, free inhibitor, and inhibitor-bound endogenous FXa, resulting in a persistant pool of free FXa inhibitor and inhibitor-bound FXa. As a consequence, an increased ratio between antidote and inhibitor may be required to sufficiently restore hemostasis. Conversely, the prohemostatic agents do not rely on the activity of endogenous FXa, but rather intiate coagulation in the presence of the inhibitors via a bypassing mechanism. Therefore only small amounts of inhibitor-resistant FXa would be required to restore hemostasis. Secondly, an antidote should ideally neutralize and clear the inhibitor from the circulation. Pharmacokinetics studies revealed that andexanet exhibits a terminal elimination half-life of 4 to 8 hours[112]. The relatively slow clearance of andexanet-inhibitor complexes might potentially explain the necessity for a continuous infusion of andexanet in addition to the initial bolus injection.

The prohemostatic bypassing agents that are currently in preclinical development are recombinantly-generated variants of endogenous coagulation factors. As such, these factor-based products could potentially elicit an immune response which would limit their efficacy of repeated use. However, the immunogenic potential of FXa-I16L and the FX-F174 variants might be minimal since they comprise only a single amino acid substitution. In contrast, FX-C contains an unique nine-residue insertion and substitution of surrounding residues derived from the *P. textilis* isoform FX[63] that could potentially be targeted by the immune response. Whether these variants would elicit an immune response upon administration is unpredictable. Thus far, non-neutralizing antibodies against andexanet have been detected in patients albeit with low antibody titers[113,114]. Importantly, neutralizing antibody responses against andexanet have not been reported and neither have antibodies with cross-reactivity to factor X(a) been detected[114]. Moreover, only a few patients with acquired inhibitors against FX have been reported[115], which might suggest that the immunogenic potential of FX is low.

Thrombotic complications associated with FXa inhibitor reversal remain a major concern in clinical practice. Thrombotic events occurred in approximately 10% of the patients within 30 days following andexanet treatment[113]. This is relatively high compared to the percentage of thrombotic events observed during idarucizumab-mediated reversal of dabigatran (4.8%)[116] or other anticoagulant reversal studies (3.9-7%)[117,118]. The relatively high incidence of thrombosis might be explained by the interaction of andexanet with the natural anticoagulant TFPI. Previous reports have shown that andexanet binds to

TFPI with high affinity and dose-dependently increases the thrombin peak height in normal and hemophilic plasma[119-121]. Whether andexanet is able to interact with TFPI when andexanet is bound to the direct FXa inhibitors is unlikely. However, considering the high administrated dose of andexanet, we speculate that significant amounts of the antidote circulate in free form and thus could interact with TFPI. Additionally, due to their reversible binding nature, the direct FXa inhibitors and TFPI compete for binding to andexenet and establish an equilibrium between andexanet-inhibitor and andexanet-TFPI complexes. Since the inhibitory constants of the FXa inhibitors are similar to that of TFPI[63,122,123], significant amounts of andexanet might circulate in complex with TFPI. Jourdi *et al.* circumvented these potential macromolecular interactions by generating a GLA-domainless FXa in complex with α2-macroglobulin[63,124]. Although this antidote could potentially be safer, it might prove difficult to large-scale purify or recombinantly produce α2-macroglobulin for therapeutic use.

Even though clinical data for the prohemostatic bypassing agents remain to be obtained, these agents may potentially induce thrombotic complications. Patients could be at risk for overdosis since it might prove difficult to determine adequate dosing as a consequence of individual variation in blood clotting. In addition, the therapeutic window of these reversal agents is likely narrow because small differences in dosing may significantly impact the hemostatic outcome. From a safety perspective, FXa-I16L requires FVa to induce catalytic activity towards prothrombin[62,125]. Furthermore, FXa-I16L is unlikely to interact appreciably with plasma proteins, most notably the endogenous protease inhibitors, due to its disordered active site[125] which could limit the risk for reversal agent-induced thromboembolisms. In our studies, we have generated FX variants in zymogen form. When coagulation is triggered, these factors will be activated through the intrinsic and extrinsic pathways in a similar manner as endogenous FX. Moreover, by making use of the zymogen form of FX-F174 variants, productive interactions or sequesteration by plasma proteins might be prevented. As such, these reversal agents have the potential to restore hemostasis in case of life-threatening bleeding events that are induced by the direct FXa inhibitors and might minimize the risk for thrombotic complications.

Concluding Remarks

The aim of the research in this thesis was to gain further insights into the remarkable procoagulant adaptations of *Pseudonaja textilis* venom-derived FV and FX. To achieve this goal we examined the structure-function relationships of several structural elements unique to ptFV and ptFX. A better understanding of the procoagulant enhancements of ptFV and ptFX could provide significant opportunities for the generation of novel

therapeutic agents. The FX-C and FX-F174 variants originated from research on the extended 99-loop in ptFX and provide important examples of how unique structural elements can be used for therapeutic purposes or how the exceptional functionalities increase our knowledge of important physiological processes.

Our findings in **chapters 3** and **4** strongly suggest that the ptFV A2 domain loop2 and the uniquely extended ptFV A2T are responsible for the functional resistance of ptFV to APC. Furthermore, we revealed that the ptFV A2T facilitates prothrombin conversion in the absence of membranes by enabling productive interactions with ptFXa and prothrombin. By making use of the ptFX activation peptide we showed in **chapter 5** that the human FX activation peptide comprises an essential binding site for the intrinsic tenase complex. In addition, the venom-derived activation peptide allows FVa binding, inducing structural rearrangements that allow for the maturation of the active site and thereby enable catalytic activity while in zymogen state. Finally, in **chapter 7** we generated FX variants that have the potential to serve as rescue therapeutic agents to overcome the effect of the direct FXa-inhibitors. Collectively, these studies have identified the mechanistic principles by which ptFV and ptFX have circumvented the normal regulatory mechanisms of blood clotting. Translation of these procoagulant enhancements to human coagulation proteins might provide unique opportunities towards the generation of novel therapeutic agents for bleeding disorders.

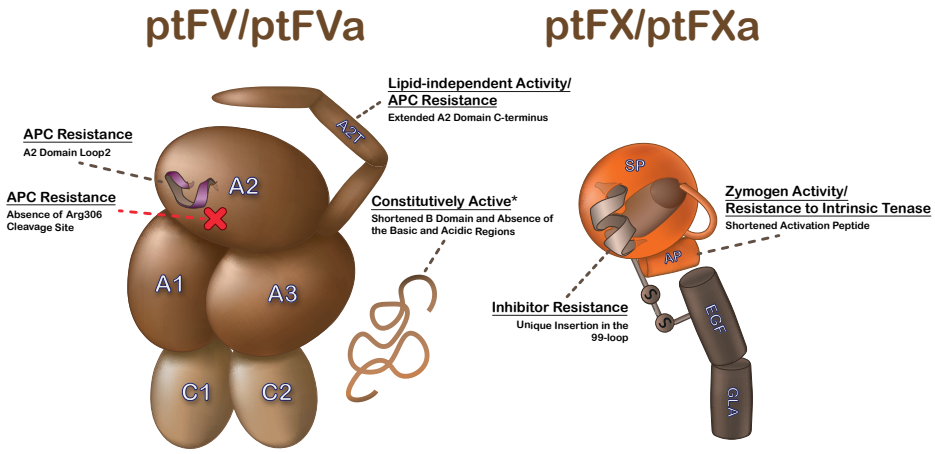


Figure 1. Schematic summary of the unique procoagulant enhancements of venom-derived ptFV and ptFX. Venom-expressed ptFV comprises several unique structural modifications that are responsible for ptFV's constitutive cofactor activity, the functional resistance to APC, and the lipid-independent cofactor activity. Furthermore, venom-expressed ptFX comprises a shortened activation peptide and insertion in the 99-loop that facilitate zymogen activity and resistance to activation by the human intrinsic tenase complex, and a reduced sensitivity for active site inhibitors, respectively. *Upon activation to ptFVa, the ptFV B domain that covalently connects the C-terminal A2 domain (A2T) with the N-terminal A3 domain is proteolyically removed. Abbreviations: A2T, A2 domain C-terminus; GLA, γ-carboxyglutamic acid domain; EGF, endothelial growth factor 1 and 2 domains; AP, activation peptide; SP, serine protease domain. S-S indicates the disulfide bond covalently linking the EGF-2 and serine protease domains.

References

1 Broos, K., Feys, H. B., De Meyer, S. F., Vanhoorelbeke, K. & Deckmyn, H. Platelets at work in primary hemostasis. *Blood Rev* **25**, 155-167, doi:10.1016/j.blre.2011.03.002 (2011).
2 Versteeg, H. H., Heemskerk, J. W., Levi, M. & Reitsma, P. H. New fundamentals in hemostasis. *Physiol Rev* **93**, 327-358, doi:10.1152/physrev.00016.2011 (2013).
3 Mann, K. G., Nesheim, M. E., Church, W. R., Haley, P. & Krishnaswamy, S. Surface-dependent reactions of the vitamin K-dependent enzyme complexes. *Blood* **76**, 1-16 (1990).
4 Schreuder, M., Reitsma, P. H. & Bos, M. H. A. Blood coagulation factor Va's key interactive residues and regions for prothrombinase assembly and prothrombin binding. *J Thromb Haemost* **17**, 1229-1239, doi:10.1111/jth.14487 (2019).
5 Dahlback, B. & Villoutreix, B. O. The anticoagulant protein C pathway. *FEBS Lett* **579**, 3310-3316, doi:10.1016/j.febslet.2005.03.001 (2005).
6 Mast, A. E. Tissue Factor Pathway Inhibitor: Multiple Anticoagulant Activities for a Single Protein. *Arterioscler Thromb Vasc Biol* **36**, 9-14, doi:10.1161/ATVBAHA.115.305996 (2016).
7 Rao, V. S., Swarup, S. & Kini, R. M. The nonenzymatic subunit of pseutarin C, a prothrombin activator from eastern brown snake (Pseudonaja textilis) venom, shows structural similarity to mammalian coagulation factor V. *Blood* **102**, 1347-1354, doi:10.1182/blood-2002-12-3839 (2003).
8 Bos, M. H. *et al.* Venom factor V from the common brown snake escapes hemostatic regulation through procoagulant adaptations. *Blood* **114**, 686-692, doi:10.1182/blood-2009-02-202663 (2009).
9 Fry, B. G. Structure-function properties of venom components from Australian elapids. *Toxicon* **37**, 11-32, doi:10.1016/s0041-0101(98)00125-1 (1999).
10 Rao, V. S. & Kini, R. M. Pseutarin C, a prothrombin activator from Pseudonaja textilis venom: its structural and functional similarity to mammalian coagulation factor Xa-Va complex. *Thrombosis and haemostasis* **88**, 611-619 (2002).
11 Kini, R. M. The intriguing world of prothrombin activators from snake venom. *Toxicon* **45**, 1133-1145, doi:10.1016/j.toxicon.2005.02.019 (2005).
12 Mann, K. G., Hockin, M. F., Begin, K. J. & Kalafatis, M. Activated protein C cleavage of factor Va leads to dissociation of the A2 domain. *J Biol Chem* **272**, 20678-20683 (1997).
13 Bertina, R. M. *et al.* Mutation in blood coagulation factor V associated with resistance to activated protein C. *Nature* **369**, 64-67, doi:10.1038/369064a0 (1994).
14 Griffin, J. H. *et al.* Activated protein C resistance: molecular mechanisms. *Thrombosis and haemostasis* **74**, 444-448 (1995).
15 Norstrom, E., Thorelli, E. & Dahlback, B. Functional characterization of recombinant FV Hong Kong and FV Cambridge. *Blood* **100**, 524-530, doi:10.1182/blood-2002-02-0343 (2002).
16 Steen, M. *et al.* Functional characterization of factor V-Ile359Thr: a novel mutation associated with thrombosis. *Blood* **103**, 3381-3387, doi:10.1182/blood-2003-06-2092 (2004).
17 Castaman, G., Lunghi, B., Missiaglia, E., Bernardi, F. & Rodeghiero, F. Phenotypic homozygous activated protein C resistance associated with compound heterozygosity for Arg506Gln (factor V Leiden) and His1299Arg substitutions in factor V. *Br J Haematol* **99**, 257-261, doi:10.1046/j.1365-2141.1997.3993213.x (1997).
18 Yamazaki, T., Nicolaes, G. A., Sorensen, K. W. & Dahlback, B. Molecular basis of quantitative factor V deficiency associated with factor V R2 haplotype. *Blood* **100**, 2515-2521, doi:10.1182/blood.V100.7.2515 (2002).
19 Adams, T. E., Hockin, M. F., Mann, K. G. & Everse, S. J. The crystal structure of activated protein C-inactivated bovine factor Va: Implications for cofactor function. *Proc Natl Acad Sci U S A* **101**, 8918-8923, doi:10.1073/pnas.0403072101 (2004).

20 Orban, T., Kalafatis, M. & Gogonea, V. Completed three-dimensional model of human coagulation factor va. Molecular dynamics simulations and structural analyses. *Biochemistry* **44**, 13082-13090, doi:10.1021/bi050891t (2005).
21 Gale, A. J., Xu, X., Pellequer, J. L., Getzoff, E. D. & Griffin, J. H. Interdomain engineered disulfide bond permitting elucidation of mechanisms of inactivation of coagulation factor Va by activated protein C. *Protein Sci* **11**, 2091-2101, doi:10.1110/ps.0210002 (2002).
22 Calzavarini, S. *et al.* Molecular basis of coagulation factor V deficiency caused by the R1698W inter-domain mutation. *Thrombosis and haemostasis* **110**, 31-38, doi:10.1160/TH12-10-0780 (2013).
23 Steen, M., Miteva, M., Villoutreix, B. O., Yamazaki, T. & Dahlback, B. Factor V New Brunswick: Ala221Val associated with FV deficiency reproduced in vitro and functionally characterized. *Blood* **102**, 1316-1322, doi:10.1182/blood-2003-01-0116 (2003).
24 Wilhelm, A. R. *et al.* Activated Protein C has a Regulatory Role in Factor VIII Function. *Blood* **137**, 2532-2543, doi:10.1182/blood.2020007562 (2021).
25 Fay, P. J., Smudzin, T. M. & Walker, F. J. Activated protein C-catalyzed inactivation of human factor VIII and factor VIIIa. Identification of cleavage sites and correlation of proteolysis with cofactor activity. *J Biol Chem* **266**, 20139-20145 (1991).
26 Lollar, P. & Parker, C. G. pH-dependent denaturation of thrombin-activated porcine factor VIII. *J Biol Chem* **265**, 1688-1692 (1990).
27 Fay, P. J., Haidaris, P. J. & Smudzin, T. M. Human factor VIIIa subunit structure. Reconstruction of factor VIIIa from the isolated A1/A3-C1-C2 dimer and A2 subunit. *J Biol Chem* **266**, 8957-8962 (1991).
28 Bloem, E. *et al.* Mass spectrometry-assisted study reveals that lysine residues 1967 and 1968 have opposite contribution to stability of activated factor VIII. *J Biol Chem* **287**, 5775-5783, doi:10.1074/jbc.M111.308627 (2012).
29 Wakabayashi, H., Monaghan, M. & Fay, P. J. Cofactor activity in factor VIIIa of the blood clotting pathway is stabilized by an interdomain bond between His281 and Ser524 formed in factor VIII. *J Biol Chem* **289**, 14020-14029, doi:10.1074/jbc.M114.550566 (2014).
30 Wakabayashi, H., Griffiths, A. E. & Fay, P. J. Combining mutations of charged residues at the A2 domain interface enhances factor VIII stability over single point mutations. *J Thromb Haemost* **7**, 438-444, doi:10.1111/j.1538-7836.2008.03256.x (2009).
31 Monaghan, M., Wakabayashi, H., Griffiths, A., Wintermute, J. & Fay, P. J. Enhanced factor VIIIa stability of A2 domain interface variants results from an increased apparent affinity for the A2 subunit. Results from an increased apparent affinity for the A2 subunit. *Thrombosis and haemostasis* **112**, 495-502, doi:10.1160/TH14-01-0086 (2014).
32 Celie, P. H. *et al.* Substitution of Arg527 and Arg531 in factor VIII associated with mild haemophilia A: characterization in terms of subunit interaction and cofactor function. *Br J Haematol* **106**, 792-800, doi:10.1046/j.1365-2141.1999.01590.x (1999).
33 Monaghan, M., Wakabayashi, H., Griffiths, A. E. & Fay, P. J. Stabilizing interactions between D666-S1787 and T657-Y1792 at the A2-A3 interface support factor VIIIa stability in the blood clotting pathway. *J Thromb Haemost* **14**, 1021-1030, doi:10.1111/jth.13292 (2016).
34 Pipe, S. W., Saenko, E. L., Eickhorst, A. N., Kemball-Cook, G. & Kaufman, R. J. Hemophilia A mutations associated with 1-stage/2-stage activity discrepancy disrupt protein-protein interactions within the triplicated A domains of thrombin-activated factor VIIIa. *Blood* **97**, 685-691, doi:10.1182/blood.v97.3.685 (2001).
35 Bloem, E., Meems, H., van den Biggelaar, M., Mertens, K. & Meijer, A. B. A3 domain region 1803-1818 contributes to the stability of activated factor VIII and includes a binding site for activated factor IX. *J Biol Chem* **288**, 26105-26111, doi:10.1074/jbc.M113.500884 (2013).

36 Pomowski, A., Ustok, F. I. & Huntington, J. A. Homology model of human prothrombinase based on the crystal structure of Pseutarin C. *Biological chemistry* **395**, 1233-1241, doi:10.1515/hsz-2014-0165 (2014).
37 Shim, J. Y., Lee, C. J., Wu, S. & Pedersen, L. G. A model for the unique role of factor Va A2 domain extension in the human ternary thrombin-generating complex. *Biophysical chemistry* **199**, 46-50, doi:10.1016/j.bpc.2015.02.003 (2015).
38 Kalafatis, M., Beck, D. O. & Mann, K. G. Structural requirements for expression of factor Va activity. *J Biol Chem* **278**, 33550-33561, doi:10.1074/jbc.M303153200 (2003).
39 Hirbawi, J., Bukys, M. A., Barhoover, M. A., Erdogan, E. & Kalafatis, M. Role of the acidic hirudin-like COOH-terminal amino acid region of factor Va heavy chain in the enhanced function of prothrombinase. *Biochemistry* **47**, 7963-7974, doi:10.1021/bi800593k (2008).
40 Bukys, M. A., Kim, P. Y., Nesheim, M. E. & Kalafatis, M. A control switch for prothrombinase: characterization of a hirudin-like pentapeptide from the COOH terminus of factor Va heavy chain that regulates the rate and pathway for prothrombin activation. *J Biol Chem* **281**, 39194-39204, doi:10.1074/jbc.M604482200 (2006).
41 Beck, D. O., Bukys, M. A., Singh, L. S., Szabo, K. A. & Kalafatis, M. The contribution of amino acid region ASP695-TYR698 of factor V to procofactor activation and factor Va function. *J Biol Chem* **279**, 3084-3095, doi:10.1074/jbc.M306850200 (2004).
42 Bakker, H. M. *et al.* Functional properties of human factor Va lacking the Asp683-Arg709 domain of the heavy chain. *J Biol Chem* **269**, 20662-20667 (1994).
43 Kalafatis, M. & Mann, K. G. The role of the membrane in the inactivation of factor va by plasmin. Amino acid region 307-348 of factor V plays a critical role in factor Va cofactor function. *J Biol Chem* **276**, 18614-18623, doi:10.1074/jbc.M007134200 (2001).
44 Toso, R. & Camire, R. M. Role of Hirudin-like factor Va heavy chain sequences in prothrombinase function. *J Biol Chem* **281**, 8773-8779, doi:10.1074/jbc.M511419200 (2006).
45 Lechtenberg, B. C. *et al.* Crystal structure of the prothrombinase complex from the venom of Pseudonaja textilis. *Blood* **122**, 2777-2783, doi:10.1182/blood-2013-06-511733 (2013).
46 Qureshi, S. H., Yang, L., Manithody, C. & Rezaie, A. R. Membrane-dependent interaction of factor Xa and prothrombin with factor Va in the prothrombinase complex. *Biochemistry* **48**, 5034-5041, doi:10.1021/bi900240g (2009).
47 Corral-Rodriguez, M. A., Bock, P. E., Hernandez-Carvajal, E., Gutierrez-Gallego, R. & Fuentes-Prior, P. Structural basis of thrombin-mediated factor V activation: the Glu666-Glu672 sequence is critical for processing at the heavy chain-B domain junction. *Blood* **117**, 7164-7173, doi:10.1182/blood-2010-10-315309 (2011).
48 Rao, V. S., Swarup, S. & Manjunatha Kini, R. The catalytic subunit of pseutarin C, a group C prothrombin activator from the venom of Pseudonaja textilis, is structurally similar to mammalian blood coagulation factor Xa. *Thrombosis and haemostasis* **92**, 509-521, doi:10.1160/TH04-03-0144 (2004).
49 Reza, M. A., Minh Le, T. N., Swarup, S. & Manjunatha Kini, R. Molecular evolution caught in action: gene duplication and evolution of molecular isoforms of prothrombin activators in Pseudonaja textilis (brown snake). *J Thromb Haemost* **4**, 1346-1353, doi:10.1111/j.1538-7836.2006.01969.x (2006).
50 Baugh, R. J. & Krishnaswamy, S. Role of the activation peptide domain in human factor X activation by the extrinsic Xase complex. *J Biol Chem* **271**, 16126-16134, doi:10.1074/jbc.271.27.16126 (1996).
51 Yang, L., Manithody, C. & Rezaie, A. R. Functional role of O-linked and N-linked glycosylation sites present on the activation peptide of factor X. *J Thromb Haemost* **7**, 1696-1702, doi:10.1111/j.1538-7836.2009.03578.x (2009).

52 Pinotti, M. *et al.* Reduced activation of the Gla19Ala FX variant via the extrinsic coagulation pathway results in symptomatic CRMred FX deficiency. *Thrombosis and haemostasis* **88**, 236-241 (2002).
53 Thiec, F., Cherel, G. & Christophe, O. D. Role of the Gla and first epidermal growth factor-like domains of factor X in the prothrombinase and tissue factor-factor VIIa complexes. *J Biol Chem* **278**, 10393-10399, doi:10.1074/jbc.M212144200 (2003).
54 Chattopadhyay, A. & Fair, D. S. Molecular recognition in the activation of human blood coagulation factor X. *J Biol Chem* **264**, 11035-11043 (1989).
55 Duffy, E. J. & Lollar, P. Intrinsic pathway activation of factor X and its activation peptide-deficient derivative, factor Xdes-143-191. *J Biol Chem* **267**, 7821-7827 (1992).
56 Doolittle, R. F. & Feng, D. F. Reconstructing the evolution of vertebrate blood coagulation from a consideration of the amino acid sequences of clotting proteins. *Cold Spring Harb Symp Quant Biol* **52**, 869-874 (1987).
57 Jiang, Y. & Doolittle, R. F. The evolution of vertebrate blood coagulation as viewed from a comparison of puffer fish and sea squirt genomes. *Proc Natl Acad Sci U S A* **100**, 7527-7532, doi:10.1073/pnas.0932632100 (2003).
58 Ponczek, M. B., Gailani, D. & Doolittle, R. F. Evolution of the contact phase of vertebrate blood coagulation. *J Thromb Haemost* **6**, 1876-1883, doi:10.1111/j.1538-7836.2008.03143.x (2008).
59 Davidson, C. J., Tuddenham, E. G. & McVey, J. H. 450 million years of hemostasis. *J Thromb Haemost* **1**, 1487-1494 (2003).
60 Joseph, J. S., Chung, M. C., Mirtschin, P. J. & Kini, R. M. Effect of snake venom procoagulants on snake plasma: implications for the coagulation cascade of snakes. *Toxicon* **40**, 175-183 (2002).
61 Guinto, E. R. & Esmon, C. T. Loss of prothrombin and of factor Xa-factor Va interactions upon inactivation of factor Va by activated protein C. *J Biol Chem* **259**, 13986-13992 (1984).
62 Toso, R., Zhu, H. & Camire, R. M. The conformational switch from the factor X zymogen to protease state mediates exosite expression and prothrombinase assembly. *J Biol Chem* **283**, 18627-18635, doi:10.1074/jbc.M802205200 (2008).
63 Verhoef, D. *et al.* Engineered factor Xa variants retain procoagulant activity independent of direct factor Xa inhibitors. *Nat Commun* **8**, 528, doi:10.1038/s41467-017-00647-9 (2017).
64 Pozzi, N., Chen, Z., Pelc, L. A., Shropshire, D. B. & Di Cera, E. The linker connecting the two kringles plays a key role in prothrombin activation. *Proc Natl Acad Sci U S A* **111**, 7630-7635, doi:10.1073/pnas.1403779111 (2014).
65 Ahnstrom, J., Gierula, M., Temenu, J., Laffan, M. A. & Lane, D. A. Partial rescue of naturally occurring active site factor X variants through decreased inhibition by tissue factor pathway inhibitor and antithrombin. *J Thromb Haemost* **18**, 136-150, doi:10.1111/jth.14627 (2020).
66 Gupta, R., Jung, E. & Brunak, S. Prediction of N-glycosylation Sites in Human Proteins. **Available online: http://www.cbs.dtu.dk/services/NetNGlyc/ (accessed on April 2018).** (2004).
67 Steentoft, C. *et al.* Precision mapping of the human O-GalNAc glycoproteome through SimpleCell technology. *EMBO J* **32**, 1478-1488, doi:10.1038/emboj.2013.79 (2013).
68 Iino, M. *et al.* The role of human factor X activation peptide in activation of factor X by factor IXa. *J Biochem* **116**, 335-340, doi:10.1093/oxfordjournals.jbchem.a124528 (1994).
69 Inoue, K. & Morita, T. Identification of O-linked oligosaccharide chains in the activation peptides of blood coagulation factor X. The role of the carbohydrate moieties in the activation of factor X. *Eur J Biochem* **218**, 153-163 (1993).
70 Sinha, U. & Wolf, D. L. Carbohydrate residues modulate the activation of coagulation factor X. *J Biol Chem* **268**, 3048-3051 (1993).
71 Bode, W. & Huber, R. Induction of the bovine trypsinogen-trypsin transition by peptides sequentially similar to the N-terminus of trypsin. *FEBS Lett* **68**, 231-236, doi:10.1016/0014-5793(76)80443-7 (1976).

72 Bode, W. The transition of bovine trypsinogen to a trypsin-like state upon strong ligand binding. II. The binding of the pancreatic trypsin inhibitor and of isoleucine-valine and of sequentially related peptides to trypsinogen and to p-guanidinobenzoate-trypsinogen. *J Mol Biol* **127**, 357-374, doi:10.1016/0022-2836(79)90227-4 (1979).
73 Verhamme, I. M., Panizzi, P. R. & Bock, P. E. Pathogen activators of plasminogen. *J Thromb Haemost* **13 Suppl 1**, S106-114, doi:10.1111/jth.12939 (2015).
74 Friedrich, R. *et al.* Staphylocoagulase is a prototype for the mechanism of cofactor-induced zymogen activation. *Nature* **425**, 535-539, doi:10.1038/nature01962 (2003).
75 Kroh, H. K., Panizzi, P. & Bock, P. E. Von Willebrand factor-binding protein is a hysteretic conformational activator of prothrombin. *Proc Natl Acad Sci U S A* **106**, 7786-7791, doi:10.1073/pnas.0811750106 (2009).
76 Huber, R. & Bode, W. Structural Basis of the Activation and Action of Trypsin. *Accounts of Chemical Research* **11**, 114-122 (1978).
77 Pozzi, N., Vogt, A. D., Gohara, D. W. & Di Cera, E. Conformational selection in trypsin-like proteases. *Curr Opin Struct Biol* **22**, 421-431, doi:10.1016/j.sbi.2012.05.006 (2012).
78 Chakraborty, P., Acquasaliente, L., Pelc, L. A. & Di Cera, E. Interplay between conformational selection and zymogen activation. *Sci Rep* **8**, 4080, doi:10.1038/s41598-018-21728-9 (2018).
79 Ranby, M. Studies on the kinetics of plasminogen activation by tissue plasminogen activator. *Biochim Biophys Acta* **704**, 461-469, doi:10.1016/0167-4838(82)90068-1 (1982).
80 Tate, K. M. *et al.* Functional role of proteolytic cleavage at arginine-275 of human tissue plasminogen activator as assessed by site-directed mutagenesis. *Biochemistry* **26**, 338-343, doi:10.1021/bi00376a002 (1987).
81 Ranby, M., Bergsdorf, N. & Nilsson, T. Enzymatic properties of the one- and two-chain form of tissue plasminogen activator. *Thromb Res* **27**, 175-183, doi:10.1016/0049-3848(82)90197-9 (1982).
82 Tachias, K. & Madison, E. L. Converting tissue type plasminogen activator into a zymogen. Important role of Lys156. *J Biol Chem* **272**, 28-31, doi:10.1074/jbc.272.1.28 (1997).
83 Renatus, M. *et al.* Lysine 156 promotes the anomalous proenzyme activity of tPA: X-ray crystal structure of single-chain human tPA. *EMBO J* **16**, 4797-4805, doi:10.1093/emboj/16.16.4797 (1997).
84 Ivanov, I. *et al.* Protease activity in single-chain prekallikrein. *Blood* **135**, 558-567, doi:10.1182/blood.2019002224 (2020).
85 Ivanov, I. *et al.* Proteolytic properties of single-chain factor XII: a mechanism for triggering contact activation. *Blood* **129**, 1527-1537, doi:10.1182/blood-2016-10-744110 (2017).
86 Stubbs, M. T., Renatus, M. & Bode, W. An active zymogen: unravelling the mystery of tissue-type plasminogen activator. *Biological chemistry* **379**, 95-103, doi:10.1515/bchm.1998.379.2.95 (1998).
87 Pathak, M. *et al.* Coagulation factor XII protease domain crystal structure. *J Thromb Haemost* **13**, 580-591, doi:10.1111/jth.12849 (2015).
88 Bos, M. H. & Camire, R. M. A bipartite autoinhibitory region within the B-domain suppresses function in factor V. *J Biol Chem* **287**, 26342-26351, doi:10.1074/jbc.M112.377168 (2012).
89 Minh Le, T. N., Reza, M. A., Swarup, S. & Kini, R. M. Gene duplication of coagulation factor V and origin of venom prothrombin activator in Pseudonaja textilis snake. *Thrombosis and haemostasis* **93**, 420-429, doi:10.1160/TH04-11-0707 (2005).
90 Verhoef, D. *et al.* Functional implications of the unique disulfide bond in venom factor V from the Australian common brown snake Pseudonaja textilis. *Toxin Reviews* **33**, 37-41, doi:10.3109/15569543.2013.844712 (2014).
91 Wight, J. & Paisley, S. The epidemiology of inhibitors in haemophilia A: a systematic review. *Haemophilia* **9**, 418-435, doi:10.1046/j.1365-2516.2003.00780.x (2003).

92 Shapiro, A. D., Mitchell, I. S. & Nasr, S. The future of bypassing agents for hemophilia with inhibitors in the era of novel agents. *J Thromb Haemost* **16**, 2362-2374, doi:10.1111/jth.14296 (2018).
93 Nogami, K. & Shima, M. New therapies using nonfactor products for patients with hemophilia and inhibitors. *Blood* **133**, 399-406, doi:10.1182/blood-2018-07-820712 (2019).
94 Oldenburg, J. *et al.* Emicizumab Prophylaxis in Hemophilia A with Inhibitors. *N Engl J Med* **377**, 809-818, doi:10.1056/NEJMoa1703068 (2017).
95 Mahlangu, J. *et al.* Emicizumab Prophylaxis in Patients Who Have Hemophilia A without Inhibitors. *N Engl J Med* **379**, 811-822, doi:10.1056/NEJMoa1803550 (2018).
96 Kitazawa, T. *et al.* Factor VIIIa-mimetic cofactor activity of a bispecific antibody to factors IX/IXa and X/Xa, emicizumab, depends on its ability to bridge the antigens. *Thrombosis and haemostasis* **117**, 1348-1357, doi:10.1160/TH17-01-0030 (2017).
97 von Drygalski, A. *et al.* An engineered factor Va prevents bleeding induced by anticoagulant wt activated protein C. *PLoS One* **9**, e104304, doi:10.1371/journal.pone.0104304 (2014).
98 von Drygalski, A. *et al.* Improved hemostasis in hemophilia mice by means of an engineered factor Va mutant. *J Thromb Haemost* **12**, 363-372, doi:10.1111/jth.12489 (2014).
99 Bhat, V., von Drygalski, A., Gale, A. J., Griffin, J. H. & Mosnier, L. O. Improved coagulation and haemostasis in haemophilia with inhibitors by combinations of superFactor Va and Factor VIIa. *Thrombosis and haemostasis* **115**, 551-561, doi:10.1160/TH15-07-0525 (2016).
100 Schlachterman, A. *et al.* Factor V Leiden improves in vivo hemostasis in murine hemophilia models. *J Thromb Haemost* **3**, 2730-2737, doi:10.1111/j.1538-7836.2005.01639.x (2005).
101 Bos, M. H., Meijerman, D. W., van der Zwaan, C. & Mertens, K. Does activated protein C-resistant factor V contribute to thrombin generation in hemophilic plasma? *J Thromb Haemost* **3**, 522-530, doi:10.1111/j.1538-7836.2005.01181.x (2005).
102 van 't Veer, C. *et al.* An in vitro analysis of the combination of hemophilia A and factor V(LEIDEN). *Blood* **90**, 3067-3072 (1997).
103 Zdenek, C. N. *et al.* Coagulotoxic effects by brown snake (Pseudonaja) and taipan (Oxyuranus) venoms, and the efficacy of a new antivenom. *Toxicol In Vitro* **58**, 97-109, doi:10.1016/j.tiv.2019.03.031 (2019).
104 Berling, I. & Isbister, G. K. Hematologic effects and complications of snake envenoming. *Transfus Med Rev* **29**, 82-89, doi:10.1016/j.tmrv.2014.09.005 (2015).
105 Isbister, G. K. Procoagulant snake toxins: laboratory studies, diagnosis, and understanding snakebite coagulopathy. *Semin Thromb Hemost* **35**, 93-103, doi:10.1055/s-0029-1214152 (2009).
106 Johnston, C. I. *et al.* The Australian Snakebite Project, 2005-2015 (ASP-20). *Med J Aust* **207**, 119-125, doi:10.5694/mja17.00094 (2017).
107 Masci, P. P., Rowe, E. A., Whitaker, A. N. & de Jersey, J. Fibrinolysis as a feature of disseminated intravascular coagulation (DIC) after Pseudonaja textilis textilis envenomation. *Thromb Res* **59**, 859-870, doi:10.1016/0049-3848(90)90399-w (1990).
108 Pinto, D. J. *et al.* Discovery of 1-(4-methoxyphenyl)-7-oxo-6-(4-(2-oxopiperidin-1-yl)phenyl)-4,5,6,7-tetrahydro-1H -pyrazolo[3,4-c]pyridine-3-carboxamide (apixaban, BMS-562247), a highly potent, selective, efficacious, and orally bioavailable inhibitor of blood coagulation factor Xa. *J Med Chem* **50**, 5339-5356, doi:10.1021/jm070245n (2007).
109 Roehrig, S. *et al.* Discovery of the novel antithrombotic agent 5-chloro-N-({(5S)-2-oxo-3-[4-(3-oxomorpholin-4-yl)phenyl]-1,3-oxazolidin-5-yl}methyl)thiophene- 2-carboxamide (BAY 59-7939): an oral, direct factor Xa inhibitor. *J Med Chem* **48**, 5900-5908, doi:10.1021/jm050101d (2005).
110 Qu, S. Y. *et al.* An unexpected dynamic binding mode between coagulation factor X and Rivaroxaban reveals importance of flexibility in drug binding. *Chem Biol Drug Des* **94**, 1664-1671, doi:10.1111/cbdd.13568 (2019).

111 Burgering, M. J. *et al.* The second Kunitz domain of human tissue factor pathway inhibitor: cloning, structure determination and interaction with factor Xa. *J Mol Biol* **269**, 395-407, doi:10.1006/jmbi.1997.1029 (1997).
112 Siegal, D. *et al.* Safety, pharmacokinetics, and reversal of apixaban anticoagulation with andexanet alfa. *Blood Adv* **1**, 1827-1838, doi:10.1182/bloodadvances.2017007112 (2017).
113 Connolly, S. J. *et al.* Full Study Report of Andexanet Alfa for Bleeding Associated with Factor Xa Inhibitors. *N Engl J Med* **380**, 1326-1335, doi:10.1056/NEJMoa1814051 (2019).
114 Siegal, D. M. *et al.* Andexanet Alfa for the Reversal of Factor Xa Inhibitor Activity. *N Engl J Med* **373**, 2413-2424, doi:10.1056/NEJMoa1510991 (2015).
115 Menegatti, M. & Peyvandi, F. Factor X deficiency. *Semin Thromb Hemost* **35**, 407-415, doi:10.1055/s-0029-1225763 (2009).
116 Pollack, C. V., Jr. *et al.* Idarucizumab for Dabigatran Reversal - Full Cohort Analysis. *N Engl J Med* **377**, 431-441, doi:10.1056/NEJMoa1707278 (2017).
117 Sarode, R. *et al.* Efficacy and safety of a 4-factor prothrombin complex concentrate in patients on vitamin K antagonists presenting with major bleeding: a randomized, plasma-controlled, phase IIIb study. *Circulation* **128**, 1234-1243, doi:10.1161/CIRCULATIONAHA.113.002283 (2013).
118 Goldstein, J. N. *et al.* Four-factor prothrombin complex concentrate versus plasma for rapid vitamin K antagonist reversal in patients needing urgent surgical or invasive interventions: a phase 3b, open-label, non-inferiority, randomised trial. *Lancet* **385**, 2077-2087, doi:10.1016/S0140-6736(14)61685-8 (2015).
119 Ersayin, A. *et al.* Catalytically inactive Gla-domainless factor Xa binds to TFPI and restores ex vivo coagulation in hemophilia plasma. *Haematologica* **102**, e483-e485, doi:10.3324/haematol.2017.174037 (2017).
120 Marlu, R. & Polack, B. Gla-domainless factor Xa: molecular bait to bypass a blocked tenase complex. *Haematologica* **97**, 1165-1172, doi:10.3324/haematol.2011.055699 (2012).
121 Lu, G., Lin, J. P., Curnutte, J. T. & Conley, P. B. Abstract: Effect of Andexanet-TFPI Interaction on in Vitro Thrombin Formation and Coagulation Markers in the TF-Pathway. *Blood* **130**, 629 (2017).
122 Huang, Z. F., Wun, T. C. & Broze, G. J., Jr. Kinetics of factor Xa inhibition by tissue factor pathway inhibitor. *J Biol Chem* **268**, 26950-26955 (1993).
123 Hackeng, T. M., Maurissen, L. F., Castoldi, E. & Rosing, J. Regulation of TFPI function by protein S. *J Thromb Haemost* **7 Suppl 1**, 165-168, doi:10.1111/j.1538-7836.2009.03363.x (2009).
124 Jourdi, G. *et al.* FXa-alpha2-Macroglobulin Complex Neutralizes Direct Oral Anticoagulants Targeting FXa In Vitro and In Vivo. *Thrombosis and haemostasis* **118**, 1535-1544, doi:10.1055/s-0038-1667014 (2018).
125 Bunce, M. W., Toso, R. & Camire, R. M. Zymogen-like factor Xa variants restore thrombin generation and effectively bypass the intrinsic pathway in vitro. *Blood* **117**, 290-298, doi:10.1182/blood-2010-08-300756 (2011).

Chapter 9

Nederlandse Samenvatting





Nederlandse Samenvatting

De stollingscascade speelt een belangrijke rol in de vorming van een bloedstolsel om bloedverlies te beperken na vasculaire schade. Wanneer het stollingsysteem geactiveerd wordt, wordt er via een serie van enzymatische reacties een sterk fibrine netwerk aangelegd. Dit fibrine netwerk stabiliseert het initiele bloedstolsel dat gevormd wordt door de aggregratie van bloedsplaatjes en dat het gat in het bloedvat als eerste afdicht. Centraal in de stollingscascade staan de plasma-eiwitten factor V (FV) en factor X (FX) die na activatie worden aangeduid als factor Va (FVa) en factor Xa (FXa). In de stolling functioneert FVa als cofactor van het enzym FXa en samen vormen deze eiwitten het zogenaamde protrombinase complex dat verantwoordelijk is voor de omzetting van protrombine naar het essentiele stollingsenzym trombine. Om ongewenste stolling te voorkomen kan dit complex alleen gevormd worden in de aanwezigheid van calcium en een negatief-geladen membraan dat voornamelijk aangeleverd wordt door de geactiveerde bloedplaatjes die zich op de plek van de wond bevinden. Wanneer er genoeg trombine en fibrine aangemaakt is zorgen specifieke antistollingsfactoren ervoor dat er niet teveel bloedstolling plaatsvindt door de procoagulante factoren te inactiveren. De inactivatie van FVa speelt een belangrijke rol in het stopzetten van de bloedstolling en wordt gereguleerd door geactiveerd proteïne C (APC). APC knipt FVa op drie verschillende plekken in het FVa A2 domein wat leidt tot dissociatie van het A2 domein. Doordat het A2 domein belangrijke bindingsplekken voor FXa en protrombine bevat kan het protrombinase complex na dissociate niet meer gevormd worden en verliest dit complex zijn activiteit. Daarnaast wordt het enzym FXa door verschillende antistollingsfactoren geinactiveerd, waarvan tissue factor pathway inhibitor (TFPI) en antitrombine de belangrijkste zijn. Deze antistollingsfactoren binden in de actieve centrum van FXa en blokkeren daarmee de toegang voor het substraat protrombine.

Afwijkingen in stollings- of antistollingsfactoren kunnen de regulatie van de bloedstolling verstoren en resulteren in bloedingscomplicaties of overmatige bloedstolling, ook wel trombose genoemd. Een belangrijke afwijking in FV is de R506Q mutatie (FV Leiden) die ervoor zorgt dat APC FVa in mindere mate kan inactiveren met als gevolg een zevenvoudig verhoogd risico op trombose. Het verstoren van de bloedstolling kan echter ook een krachtig instrument zijn. Slangen die tot de meest giftige ter wereld behoren gebruiken uniek gemodificeerde stollingseiwitten om het bloed ongecontroleerd te laten stollen. De gif geinduceerde stolsels resulteren in een hart- en/of herseninfarct waardoor het prooidier geïmmobiliseerd raakt. Het gif van dergelijke slangen heeft zo'n desastreus effect op de bloedstolling doordat het speciale FV- en FX-achtige eiwitten bevat. Onderzoek aan een van deze slangen, *Pseudonaja textilis*, heeft aangetoond dat het in het gif aanwezige FV (ptFV) en FX (ptFX) unieke eigenschappen hebben die

de normale regulering van deze eiwitten omzeilen. Waar het humane FV in plasma circuleert als een inactieve procofactor en geactiveerd wordt via proteolyse op een aantal specifieke knipplekken, is ptFV van nature al actief als cofactor voor geactiveerd ptFX (ptFXa). Een zuur en basisch gedeelte van het FV B domein voorkomt in humaan FV dat het ongeactiveerde FV als cofactor kan dienen voor FXa. In ptFV is echter een groot deel van het B domein afwezig, waaronder de essentiele zure en basische onderdelen. Daarnaast is aangetoond dat ptFV resistent is tegen APC, ondanks dat ptFV geknipt wordt door APC in het A2 domein. Verder is het ptFV-ptFXa complex actief in afwezigheid van een negatief-geladen membraan en het kan daardoor potentieel overal in de bloedbaan de bloedstolling stimuleren. De mechanismen die verantwoordelijk zijn voor de APC resistentie of voor de activiteit van het ptFVa-ptFXa complex in de afwezigheid van een normaal essentiële membraan zijn tot nu toe niet bekend. In dit proefschrift is getracht om de mechanismen van deze unieke eigenschappen te ontrafelen door de functie van enkele bijzondere structurele elementen in ptFV en ptFX te bestuderen. We hebben dit geprobeerd te doen door enkele chimere eiwitten te maken waarbij deze structurele elementen uitgewisseld zijn tussen humaan en *P. textilis* FV/FX en vervolgens zijn de functionele consequenties onderzocht.

De interactie die eiwitten met elkaar aangaan zijn doorgaans van cruciaal belang voor hun functie. Een suboptimale binding tussen FVa en FXa kan bijvoorbeeld de omzetting van protrombine verminderen en ervoor zorgen dat er te weinig bloedstolling plaatsvindt. Karakterisering van de bindingsplekken kan daarmee niet alleen belangrijke informatie verschaffen over het werkingsmechanisme van de eiwitten, maar biedt ook de mogelijkheid om de interactie te beinvloeden voor therapeutische doeleinden. In **hoofdstuk 2** bespreken we de huidige literatuur die ingaat op de interactie van FVa met FXa en protrombine en proberen we specifieke bindingsplekken te identificeren. Dit overzicht geeft een richtlijn voor vervolgonderzoeken met doelgerichte experimenten die bindingsplekken verder kunnen karakteriseren.

In **hoofdstuk 3** proberen we het mechanisme dat aan de basis ligt van ptFV's functionele resistentie voor APC te ontrafelen. APC knipt humaan FVa in het A2 domain op de plekken R306, R506, en R679. De knip op R506 resulteert in een intermediair FVa eiwit met ~50% cofactor activiteit. De R306 positie wordt veel langzamer geknipt dan de R506 positie, maar deze knip is essentieel om FVa volledig te kunnen inactiveren. Het doel van de R679 plek is niet geheel duidelijk. Eerdere studies hebben laten zien dat ptFV door APC op K507 wordt geknipt, een vergelijkbare positie als R506 in het humane FVa. Echter in tegenstelling tot humaan FVa wordt ptFV niet op een vergelijkbare R306 positie geknipt. Omdat deze knipplek essentieel is voor de inactivering van humaan FVa zou de afwezigheid van een R306 knipplek mogelijk de resistentie van ptFV voor APC kunnen

verklaren. Daarnaast bevat ptFV een unieke disulfide brug die het A2 domein met het A3 domein verbind. Deze covalente verbinding zou potentieel de A2 domein dissociatie kunnen voorkomen. In **hoofdstuk 3** hebben we FV varianten gegenereerd waarbij de R306 regio is uitgewisseld tussen humaan FV en ptFV. Daarnaast hebben we een ptFV variant gecreëerd waarbij we eveneens de disulfide brug hebben verwijderd middels mutagenese. Door deze FV varianten via functionele experimenten te karakteriseren hebben we aangetoond dat deze elementen de resistentie voor APC niet kunnen verklaren. Echter een belangrijke observatie in onze studie was dat incorporatie van de R306 knipplek niet leidde tot dissociatie van het A2 domein na de behandeling met APC. Dit impliceert dat het ptFV A2 domein via sterke non-covalente interacties gelinkt is aan de A1-A3 domeinen. In vervolgexperimenten hebben we getracht om deze interacties te identificeren. Via 'Moleculaire Dynamische' simulaties konden we aantonen dat de A2 domein dissociatie in humaan FVa geinduceerd wordt door verlies aan bindingsaffiniteit tussen het A1 en A2 domein. Daarentegen bevat ptFV een sterke bindingsinteractie die gefaciliteerd wordt door een specifieke A2 domein loop, de zogenaamde A2 domein loop2, met het A1 domein. Deze stabiele interactie voorkomt mogelijk de A2 domein dissociatie en zou dus een belangrijke oorzaak kunnen zijn van de APC resistentie.

In **hoofdstuk 4** hebben we de functionele rol van de verlengde A2 domein C-terminus (A2T) in ptFV onderzocht. Na activering bestaat FVa uit een zware keten (A1 en A2 domeinen) en een lichte keten (A3, C1, en C2 domeinen) die non-covalent met elkaar verbonden zijn. Het A2T vormt een lange keten van aminozuren welke interacties aangaat met FXa en protrombine. De exacte functie van deze regio is niet geheel duidelijk. Hoewel tegenstrijdige resultaten gepubliceerd zijn duiden eerdere studies op een rol in de vorming van het protrombinase complex of de binding van protrombine. Sequentie analyses tonen aan dat de lengte van het FV A2T relatief gelijk is gebleven tijdens de evolutie. Het is daarom opvallend dat, vergeleken met het humane A2T, het A2T verlengd is met 31 aminozuren in het gif FV van de *Elapidae* slangen. Om de rol van het verlengde A2T in ptFV te ontrafelen hebben we FV varianten gegenereerd waarin het A2T uitgewisseld is tussen humaan FV en ptFV. Protrombinase experimenten toonden aan dat het ptFV A2T niet significant beter of slechter aan (pt)FXa of protrombine bindt in de aanwezigheid van negatief-geladen fosfolipiden. Daarentegen vonden we tot onze verassing dat de FV varianten met het ptFV A2T significant meer activiteit vertoonden in vergelijkbare experimenten waarin deze fosfolipiden afwezig waren. Bovendien was de fosfolipide-onafhankelijke activiteit van een ptFV eiwit met het humane A2T vrijwel volledig verdwenen. Experimenten waarbij gebruik werd gemaakt van fosfolipase C om eventuele lipiden die zich als onzuiverheid in de eiwit preparaten bevinden te verwijderen bevestigden onze waarneming dat het ptFV A2T verantwoordelijk is voor de cofactor activiteit in de afwezigheid van fosfolipiden. De fosfolipide-onafhankelijke

activiteit was echter alleen waarneembaar in de aanwezigheid van ptFXa en dit geeft aan dat ptFXa een essentieel element bevat dat deze reactie mogelijk maakt. Welk structureel element in ptFXa hiervoor verantwoordelijk is, is niet bekend.

Onze uitkomsten lieten daarnaast ook zien dat het ptFV A2T een belangrijk element is welke ptFV in staat stelt om protrombine om te zetten na proteolyse door APC. Vervanging van het ptFV A2T voor de overeenkomstige humane regio verminderde de cofactor activiteit aanzienlijk na behandeling met APC. Dit suggereert dat het ptFV A2T een substantiële rol speelt in de APC-resistentie en vermoedelijk mogelijk gemaakt wordt door productieve interacties aan te gaan met ptFXa en/of protrombine. Deze suggestie werd verder ondersteund door onze waarneming dat de afname van cofactor activiteit geen gevolg was van de A2 domein dissociatie. Samengevat hebben we substantieel bewijs gevonden dat evolutie van het FV A2T een cruciale bijdrage heeft geleverd aan de extreme procoagulante eigenschappen van ptFV. De in dit hoofdstuk verkregen resultaten impliceren dat het ptFV A2T stabiele interacties aan kan gaan met ptFXa en protrombine in condities waarin dit normaal niet mogelijk is, namelijk in de afwezigheid van negatief-geladen fosfolipiden of na proteolyse door de natuurlijke remmer APC.

Naast de exceptionele mechanismen die ptFV in staat stellen om de bloedstolling ongecontroleerd te stimuleren bevat ptFX ook verschillende elementen die op unieke wijze zijn aangepast tijdens de evolutie. Een van deze elementen is een opzienbarende verkorting van het activatie peptide. Hoewel het activatie peptide van alle FX-homologen uit tenminste 40 residuen bestaat, waaronder het ptFX dat tot expressie komt in de lever, is het activatie peptide van het gif ptFX slechts 27 residuen lang. In **hoofdstuk 5** hebben we de consequenties van deze verkorting op de activering en activiteit van FX bestudeerd. Afhankelijk van de stimulus waarmee de stolling geïnitieerd is wordt FX geactiveerd door het intrinsieke (factor VIIIa-factor IXa) of extrinsieke (tissue factor-factor VIIa) tenase complex. Met behulp van FX varianten waarin het activatie peptide is uitgewisseld tussen humaan FX en ptFX hebben we laten zien dat de FX activatie via het extrinsieke tenase complex onafhankelijk van het activatie peptide verloopt. Dit is in overeenstemming met eerdere studies die erop wezen dat het activatie peptide geen rol speelt in de FX activatie uitgevoerd door dit complex. Daarentegen was de activatie door het intrinsieke tenase complex vrijwel volledig geremd in onze FX variant met het ptFX activatie peptide (hFX-ptAP). Competitie studies demonstreerden verder dat het humane activatie peptide van FX een belangrijke bindingsplek herbergt voor het intrinsieke tenase complex. Onze waarnemingen geven daarmee aan dat het ptFX activatie peptide resistentie tegen het intrinsieke tenase complex induceert doordat

een belangrijke bindingsplek voor dit complex niet aanwezig is in het ptFX activatie peptide.

Daarnaast hebben we bestudeerd of de zymogeniciteit van FX is veranderd als gevolg van de uitwisseling van het activatie peptide. Resultaten uit een eerdere studie suggereerden dat ptFX actief is in zymogene, niet geactiveerde, vorm. Uit onze kinetische data blijkt dat het gif activatie peptide hiervoor verantwoordelijk is. De protrombine conversie door onze chimere ptFX en humaan FX varianten was namelijk sterk verminderd of verhoogd, respectievelijk, ten opzichte van hun wild-type tegenhangers. De zymogene activiteit bleek volledig afhankelijk te zijn van FVa. Verassend genoeg bleek daarnaast dat actieve centrum remmers zoals antitrombine, TFPI, en de directe FXa remmer apixaban niet binden aan hFX-ptAP. Deze data suggereren dat het verkorte gif-FX activatie peptide cofactor binding en vorming van een prematuur protrombinase-complex mogelijk maakt. De FVa-FX interactie induceert vervolgens structurele veranderingen in het enzym die het katalytisch centrum beschikbaar maken en FX in staat stellen om zijn natuurlijke substraat om te zetten. Hoe het gif activatie peptide de resistentie voor het intrinsieke tenase complex of de verhoogde zymogene activiteit precies mogelijk maakt is niet bekend. Wellicht zou de afwezigheid van een zuur/hydrofoob gebied dat verwijderd is uit het gif activatie peptide en/of N- of O-gebonden glycanen deze observatie kunnen verklaren.

De mechanismen die verantwoordelijk zijn voor de unieke eigenschappen van ptFV en ptFX zouden wellicht vertaald kunnen worden naar humane stollingsfactoren om zodoende eiwitvarianten te genereren met de potentie om bloedingscomplicaties of bloedingsziekten te behandelen. Eerder onderzoek in ons laboratorium heeft aangetoond dat humane FX varianten die een structureel element bevatten afkomstig uit slangengif FX een sterk verminderde sensitiviteit hebben voor de directe FXa remmers. Deze FXa remmers worden als antistollingsmiddel voorgeschreven aan patienten voor de behandeling en preventie van veneuze trombose of een beroerte. Helaas kunnen als gevolg van het gebruik van deze middelen ernstige bloedingscomplicaties optreden als bijwerking. Een van deze FX varianten, FX-C, had het vermogen om de trombine generatie in plasma geremd door de directe FXa remmers te herstellen. Als zodanig heeft deze variant de potentie om bloedingscomplicaties als gevolg van de directe FXa remmers tegen te gaan. In **hoofdstuk 6** hebben we de tot nu toe ontwikkelde middelen beschreven die de potentie hebben om het effect van de directe FXa remmers op te heffen. Dit overzicht toont de verschillende strategieën die zijn toegepast om de directe FXa remmers weg te vangen of om de bloedstolling te stimuleren in de aanwezigheid van deze antistollingsmiddelen.

In silico simulaties en inhibitie experimenten uit een vorige studie van ons laboratorium toonden aan dat aminozuur substituties in de zogenaamde S4 subsite van FXa's actieve centrum de binding van de directe FXa remmers verminderde. Substitutie van de S4 subsite residue Y99 resulteerde echter in een FX variant met een sterk verlaagd stollingspotentieel. In tegenstelling hiermee behield een FX-variant met een F174-substitutie de stollingsactiviteit. Deze variant zou daarmee mogelijk de directe FXa remmers kunnen omzeilen door de stolling te stimuleren in de aanwezigheid van deze remmers. In **hoofdstuk 7** hebben we het therapeutische potentieel van de FX varianten met een F174 substitutie onderzocht. FXa varianten met de aanpassingen F174A, F174S, of F174I vertoonden een vergelijkbare verlaging in de gevoeligheid voor de directe FXa remmer apixaban. Het omzeilingsmechanisme van de FX-F174A en FX-F174S varianten werd vervolgens uitgebreid gekarakteriseerd. Middels trombine generatie experimenten konden we demonstreren dat onze varianten beschikken over een 10- tot 35-voudige verlaging in de gevoeligheid voor de directe FXa remmers apixaban, rivaroxaban, en edoxaban. Deze waarnemingen wezen erop dat FX varianten met een F174 substititie de stolling kunnen stimuleren in de aanwezigheid van een fysiologische concentratie FXa remmer. Dit effect bleek een gevolg te zijn van enerzijds een verandering in de S4 subsite waardoor de FXa remmers niet meer stabiel in het actieve centrum konden binden en anderzijds door een verminderde sensitiviteit voor de natuurlijke antistollingseiwit TFPI. Het vermogen om de directe FXa-remmers te omzeilen en de hemostase te herstellen werd vervolgens gevalideerd in plasma afkomstig van patiënten met atriumfibrilleren of veneuze trombose die werden behandeld met apixaban of rivaroxaban. Deze experimenten bevestigden de procoagulante werking van onze FX varianten in de aanwezigheid van de directe FXa remmers. Samengevat hebben deze varianten de potentie om als prohemostatische omzeilingsstrategie te dienen en levensbedreigende bloedingscomplicaties tegen te gaan.

In **hoofdstuk 8** worden de belangrijkste vindingen van het promotieonderzoek samengevat. In dit hoofdstuk worden ook de inzichten, moleculaire mechanismen, en implicaties in meer detail bediscussieërd.

Nederlandse Samenvatting voor Leken

Het hart en de bloedvaten vormen een essentieel systeem waarmee zuurstof en belangrijke bouwstenen worden getransporteerd naar de organen en cellen in het lichaam en waarmee tegelijkertijd afvalstoffen worden afgevoerd. Wanneer er sprake is van schade aan de bloedvaten, bijvoorbeeld in het geval van een verwonding, zorgt het bloedstollingsysteem voor de vorming van een bloedstolsel om de wond te dichten en het bloedverlies te beperken. In eerste instantie zullen bloedplaatjes zich aan de open wond hechten om zo het bloedvat te dichten. Bloedplaatjes zijn kleine celfragmenten die als de EHBO'ers van het bloed kunnen worden beschouwd. Het stolsel dat op deze manier gevormd wordt is echter niet sterk genoeg. Om het stolsel te verstevigen worden er zogenaamde fibrinedraaden gevormd door het stollingssysteem. Deze fibrinedraden vormen een een kleverig net om de bloedplaatjes stevig bij elkaar te houden. Het stollingssysteem, ook wel coagulatie genoemd, vormt een balans tussen eiwitten die zorgen voor bloedstolling (pro-coagulanten) en eiwitten die de bloedstolling tegengaan (anti-coagulanten).

Eiwitten zijn de miniscule werkers van het lichaam. Vrijwel elk proces in het menselijke lichaam wordt uitgevoerd door eiwitten die opgebouwd zijn uit aminozuren en bestaan in allerlei soorten en maten. De eiwitten die een rol spelen in de bloedstolling worden ook wel stollingsfactoren genoemd. Centraal in de bloedstolling staan de stollingsfactoren genaamd factor V en factor X. Wanneer er schade aan een bloedvat ontstaat worden deze stollingsfactoren geactiveerd en vormen ze samen het zogenaamde protrombinase enzymcomplex. Dit complex is verantwoordelijk voor de activering van het inactieve protrombine tot het actieve eiwit trombine en vormt een erg belangrijke stap in de vorming van een bloedstolsel. Trombine zorgt namelijk voor de vorming van de fibrinedraden die het bloedstolsel verstevigen. Maar nog belangrijker, trombine activeert allerlei stollingsfactoren via verschillende terugkoppelings-mechanismen. Op deze manier wordt er nog veel meer factor Va, factor Xa, en trombine gevormd wat nodig is om genoeg fibrinedraaden te maken. De vorming van trombine wordt daarmee ook wel als een drempel beschouwt; wanneer er eenmaal een bepaalde hoeveelheid trombine gemaakt is zal er een stevig bloedstolsel gevormd worden. Na de vorming van het stevige bloedstolsel worden de anti-coagulante stollingseiwitten geactiveerd. Deze anti-stollingsfactoren inactiveren de pro-coagulante eiwitten om ervoor te zorgen dat het stolsel niet te groot wordt en het bloedvat volledig geblokkeerd wordt.

De balans tussen pro-coagulante en anti-coagulante stollingsfactoren is erg belangrijk en zorgt ervoor dat er niet te weinig of teveel bloedstolling plaatsvindt. Genmutaties

en omgevingsfactoren kunnen deze balans echter beïnvloeden met ernstige gevolgen. Op het moment dat het bloed niet of te weinig stolt kan een wond blijven bloeden en ontstaat er schade aan omliggende weefsels, zoals bijvoorbeeld in het geval van een hersenbloeding. Aan de andere kant, wanneer er een stolsel wordt gevormd op een plek waar dat niet nodig is kunnen bloedvaten verstopt raken en bijvoorbeeld een hartinfarct veroorzaken. Het evenwicht in het stollingssysteem is dus cruciaal om te voorkomen dat er trombose ontstaat of bloedingen optreden.

Hoewel een disbalans in het stollingsysteem nadelige gevolgen kan hebben, zijn er verschillende dieren die via hun gif gebruik maken van de bloedstolling om prooidieren te vangen. Met behulp van speciale gifeiwitten, zogenaamde coagulotoxines, verstoren zij de balans om interne bloedingen te induceren (anti-coagulant gif) of vele stolsels in de bloedbaan te vormen (pro-coagulant gif). In beide gevallen probeert het roofdier schade aan te richten aan het hart en/of de hersenen zodat het prooidier niet kan ontsnappen. De coagulotoxines komen met name in slangen voor, waarvan de meest giftige slangensoorten uit Australië afkomstig zijn. Een van deze gifslangen is de *Pseudonaja textilis*, ook wel de Oosterse bruine slang genoemd. Deze slang komt uit de familie koraalslangachtigen (*Elapidae*) en deze soort geldt als de op één na giftigste slang ter wereld. Wanneer deze slang zijn gif injecteert zorgen speciale gifstollingseiwitten dat het bloed in rap tempo stolt, waardoor er hart- en herseninfacten kunnen ontstaan. Onderzoek heeft aangetoond dat de gif-geinduceerde bloedstolling wordt veroorzaakt door de stollingseiwitten die erg lijken op de menselijke stollingsfactoren factor V en factor X. Deze slangengif factor V en factor X eiwitten zijn echter geëvolueerd in specifieke gifeiwitten waardoor ze de bloedstolling oncontroleerbaar kunnen stimuleren.

In dit onderzoek hebben we de werking van factor V en factor X uit het slangengif nader onderzocht. In hoofdstuk 2 bestudeerden we de interactie tussen de menselijke geactiveerde factor V en factor X die samen het protrombinase complex vormen. Wanneer we een beter inzicht hebben in hoe deze eiwitten aan elkaar binden en hoe dit complex vervolgens een interactie aangaat met protrombine, komen we meer te weten over hoe deze eiwitten precies werken en welke delen van de eiwitten belangrijk zijn. Dit kan waardevolle informatie opleveren voor patienten bij wie de bloedstolling niet goed werkt door een defect in één van deze eiwitten. In de hoofdstukken 3 en 4 hebben we onderzocht hoe het kan dat het slangengif factor V zo extreem actief is en niet geïnactiveerd wordt na de vorming van een bloedstolsel. Onze onderzoeksresultaten hebben aangetoond dat twee delen van het slangengif factor V zo geëvolueerd zijn dat het de stabiliteit van het eiwit sterk verhoogd. In hoofdstuk 5 hebben we laten zien dat ongeactiveerd slangengif factor X al op redelijke schaal trombine kan vormen, terwijl dit

niet of vrijwel niet gebeurd met het menselijke factor X. Dit zou mogelijk een belangrijke werking van het gif kunnen zijn aangezien het factor X op deze manier bloedstolsels kan vormen op plekken waar geen verwondingen zijn, zoals in de hartvaten. Met de kennis die we vergaard hebben door de werking van het slangengif te bestuderen kunnen we wellicht nieuwe geneesmiddelen ontwikkelen ter behandeling van patienten met een bloedingsziekte of bloedingscomplicaties als gevolg van een chirurgische ingreep of bloedverdunners. In de hoofdstukken 6 en 7 worden zulke nieuwe geneesmiddelen beschreven die deels voortkomen uit het onderzoek naar slangengif. Deze nieuwe geneesmiddelen hebben de potentie om bloedingscomplicaties als gevolg van bloedverdunners tegen te gaan, maar verder onderzoek is nodig om hun werking te testen in de patienten.

Samengevat kan onderzoek naar gifsoorten dus een belangrijke bijdrage leveren aan de kennis van het menselijke lichaam en aan de ontwikkeling van nieuwe geneesmiddelen die de behandeling van allerlei ziektes kunnen verbeteren. In ons onderzoek hebben we dit getracht te doen met de stollingsfactoren uit het gif van de Australische slang *Pseudonaja texilis*. Onze resultaten hebben nieuwe structurele elementen geïdentificeerd in ptFV en ptFX die verantwoordelijk zijn voor de unieke stollingsactiviteit van deze gifeiwitten. Daarnaast heeft de informatie uit gifonderzoek geleid tot de generatie van een nieuw potentieel therapeutisch middel dat gebruikt kan worden als behandelingsmethode wanneer patiënten bloedingscomplicaties krijgen ten gevolge van specifieke antistollingsmiddelen.

Appendix

Curriculum Vitae
Scientific Publications
Dankwoord





Curriculum Vitae

Mark Schreuder was born on the 20th of April 1990 in Amersfoort, The Netherlands. He completed his pre-university education in 2008 at the public school De Amersfoortse Berg, Amersfoort with an interest in the Science and Health discipline. In September 2008, Mark started a Bachelor study in Biomedical Sciences at the University of Utrecht. Following completion of the Bachelor in 2011, he pursued a Master in Biomedical Sciences (the track of Biology of Disease) with a strong focus on cardiovascular research. In his first internship, he was studying the role of complement factor C5a receptor in myocardial ischemia-reperfusion injury under supervision of Dr. Vince de Hoog and Prof. Dr. Dominique de Kleijn. In 2013, Mark moved to Sydney, Australia to start his second internship in the laboratory of Dr. Andrew Hoy at the University of Sydney, focussing on the role of obese adipocytes in the progression of prostate cancer. He graduated in July 2014.

In January 2015, Mark started his doctoral research at the department of Internal Medicine, division of Thrombosis and Hemostasis under supervision of Prof. Dr. Pieter Reitsma and Dr. Mettine Bos. In his projects, Mark aimed to identify and characterize several unique procoagulant modifications of coagulation factor V and factor X from the venom of the Australian snake Pseudonaja textilis. With the obtained findings he aimed to develop novel protein-based agents to counteract bleeding complications. Since January 2019 Mark moved again to Sydney, Australia to continue his academic career in the group of Prof. Dr. Philip Hogg at the University of Sydney.

Scientific Publications

Schreuder M, Xiaosong L, Cheung KL, Reitsma PH, Nicolaes GAF, Bos MHA. *Pseudonaja textilis* factor Va retains structural integrity and cofactor function following proteolysis by activated protein C. *Arteriosclerosis, Thrombosis, and Vascular Biology* 2021; 41:2263-2276.

Schreuder M, Poenou G, Cheung KL, Reitsma PH, Bos MHA. The shortened activation peptide of *Pseudonaja textilis* venom FX confers zymogenicity and resistance to factor VIIIa-IXa activation. *Thrombosis and Haemostasis* 2020; 120:1512-1523.

Schreuder M, Reitsma PH, Bos MHA. Antidotes for the direct factor Xa inhibitors: the biochemical mechanisms of current and newly emerging therapies. *Seminars in Thrombosis and Hemostasis* 2020; 46:986-998, invited review.

Schreuder M, Reitsma PH, Bos MHA. Blood coagulation factor Va's key interactive residues and regions for prothrombinase assembly and prothrombin binding. *Journal of Thrombosis and Haemostasis* 2019; 00:1–11.

Ho Shon I, Kumar D, **Schreuder M** *et al.* Preclinical assessment of [68Ga]Ga-Cell Death Indicator (CDI): a novel hsp90 ligand for positron emission tomography of cell death. *Current Radiopharmaceuticals* 2021; online ahead of print.

Balaban S, Nassar ZD, Zhang A, Hosseini-Beheshti E, Centenera M, **Schreuder M** *et al.* Extracellular Fatty Acids are the Major Contributor to Lipid Synthesis in Prostate Cancer. *Molecular Cancer Research* 2019; 17:949-962.

Rietveld IM, **Schreuder M,** Reitsma PH, Bos MHA. Elevated coagulation factor levels affect the tissue factor-threshold in thrombin generation. *Thrombosis Research* 2018; 172:104-109.

Balaban S*, Lee LS*, **Schreuder M*** and Hoy AJ. Obesity and Cancer Progression: Is There a Role of Fatty Acid Metabolism? *Biomed Research International* 2015; 2015:1-17 *Equal first author (Invited review).

Balaban S, Shearer R, Lee LS, Geldermalsen M, **Schreuder M** *et al.* Adipocyte lipolysis links obesity to breast cancer growth: adipocyte-derived fatty acids drive breast cancer cell proliferation and migration. *Cancer & Metabolism* 2017; 5:1-14.

Wang Q, Hardie R, Hoy AJ, van Geldermalsen M, Ladan F, Wong JJ, Gao D, Balaban S, **Schreuder M** *et al.* Targeting ASCT2-mediated glutamine uptake blocks prostate cancer growth and tumour development. *The Journal of Pathology* 2015; 236:278-289.

In Preparation

Schreuder M, Verhoef D, Cheung KL, Visscher KM, Geerke DP, Reitsma PH, Bos MHA. Targeted substitution at the S4 subsite of human factor X infers resistance to the direct factor Xa inhibitors Phe174. (Manuscript in preparation).

Schreuder M, Cheung KL, Reitsma PH, Bos MHA. The *Pseudonaja textilis* factor V A2 domain C-terminus mediates lipid-independent cofactor activity and functional activated protein C resistance. (Manuscript in preparation).

Dankwoord

Nu het einde van dit proefschrift en mijn promotietraject nadert rest mij de laatste en belangrijke taak om iedereen te bedanken die direct of indirect hebben bijgedragen aan de totstandkoming van mijn promotieonderzoek. Ik heb het geluk gehad dat ik veel steun en hulp heb mogen ontvangen, mooie kansen heb gekregen, en een ontzettend leuke tijd heb gehad.

Mettine, waar menig met zwoegen en steunen de eindstreep halen heb ik altijd met veel plezier en zonder veel stress het hele traject doorlopen. Ik ben erg dankbaar dat ik onder je begeleiding heb mogen werken en had me geen betere co-promotor kunnen wensen.

Pieter, bedankt voor de rol die je als promotor hebt vervuld. Ik heb veel geleerd van onze werkbesprekingen.

Kelley, we hebben veel samen op het lab gezeten en ontelbare experimenten gedaan, maar het was vooral ook een tijd van gezelligheid. Ontzettend bedankt voor al het werk dat je hebt verricht maar vooral ook voor de persoon die je bent en de sfeer die je in de groep brengt.

Aat, bedankt dat ik naast je heb mogen werken en de humor die je op het lab bracht. Ik hoop dat je van je pensioen aan het genieten bent.

De rest van team Snakesss, Daniel en Viola, het doen van je promotieonderzoek is niets zonder een leuke groep om je heen. Bedankt voor de dingen die ik van jullie geleerd heb, jullie bijdrages aan mijn proefschrift, en natuurlijk ook de leuke tijd. Ook alle studenten uit ons team, met name Charlotte, Veerle, Geraldine, en Lynn, bedankt voor jullie inzet en positieve energie die jullie op ons lab brachten.

Natuurlijk wil ik ook graag alle promovendi en post-docs op het Einthoven Lab bedanken voor de leuke samenwerkingen en de tijd die we samen doorgebracht hebben na werktijd.

Daarnaast wil ik ook alle analisten binnen de trombose en hemostase en het Einthoven lab bedanken voor alle hulp en gezelligheid. Jullie hebben de soms lastige taak om ons in het gareel te houden maar jullie zijn ook essentieel om de leuke sfeer op het lab te behouden.

Seher, ook al was je een groot gedeelte van mijn promotietijd aan de andere kant van de wereld, je bent altijd een grote steun geweest en hebt me geholpen waar je kon. Ik ben zeer dankbaar voor het feit dat je ook een lab achtergrond hebt en dus begrijpt wanneer ik s 'avonds of in het weekend moet werken. Ik ben ontzettend blij dat we inmiddels samen onze tijd kunnen doorbrengen en kijk uit naar nog vele jaren samen.

Als laatste wil ik graag mijn familie bedanken. Denise, ik ben ontzettend trots op je dat je voor je droom bent gegaan en nu op de plek zit die je altijd voor ogen had. Mijn oma's, ik kijk uit om nog vele jaren op visite te komen. En als laatste natuurlijk Paps en Mams voor de onvoorwaardelijke steun. Jullie hebben altijd ontzettend veel geholpen en geïnvesteerd in een zo goed mogelijke opleiding en ik ben daar heel erg dankbaar voor. Ik heb enorm veel geluk dat ik jullie mijn ouders mag noemen.